

M.Sc. thesis

## Experimental research on dynamic dredge overflow plumes

Name: Erik van Eekelen  
Student nr: 1091549

Graduation committee:

prof.dr.ir. G.S. Stelling (TU Delft - Environmental fluid mechanics section)

dr.ir. J.C. Winterwerp (TU Delft - Env. fluid mechanics section & WL Delft hydraulics)

ir. W.G. Dirks (Van Oord Dredging and Marine contractors bv)

ir. G.L.M. van der Schrieck (TU Delft - Hydraulic engineering section)

ir. J.G. Boon (WL Delft hydraulics)





## Preface

This thesis concludes the Master of Science programme in Civil Engineering, at Delft University of Technology at the Environmental Fluid Mechanics section. It describes all facets of my study on dynamic dredge overflow plumes. The study was initiated by the Engineering department of Van Oord Dredging and Marine Contractors bv and the experiments have been carried out at the Fluid Mechanics Laboratory of the Faculty of Civil Engineering and Geosciences at Delft University of Technology.

I would like to thank all people involved in this graduation project. First of all I would like to thank my graduation committee for their supervision, support and interest during the whole graduation project. Next to that I would like the people at the Fluid Mechanics Laboratory for making my experiments possible and my colleagues at Van Oord for their support during the writing of my thesis.

In particular I would like to thank Wim, Sander, Hans, Jaap and Arie at the Fluid Mechanics Laboratory for their morale support during my long stay in the laboratory, Wouter Dirks at Van Oord and Han Winterwerp at TU Delft for keeping me focussed during the whole graduation project, Wouter Ockeloen for all the fruitful discussions and Annica and my brother Ronald for their valuable comments on my writings. Finally I would to thank my parents, family and girlfriend Ellen for their everlasting morale support.

Leiden, 22<sup>nd</sup> of October 2007



## Abstract

The overflow mixture of hopper dredgers contains fine sediment which when released in the environment forms a so-called plume. The spreading of this sediment and the related turbidity increase and sedimentation pattern can be of environmental importance. Understanding the behaviour of these plumes is therefore important.

The first phase of the plume is called dynamic. It is characterized by the rapid descent of a dense mixture under influence of its initial momentum and buoyancy. The dynamic phase is followed by the passive phase that is governed by the settling behaviour of the particles. The behaviour and fate of the dynamic phase is depending on several properties and is therefore more difficult to model than the passive phase. This M.Sc. thesis is focused on getting more insight in some of these influences. Also the implementation of these influences in dynamic plume models is investigated.

A preliminary study was carried out to investigate both theory and modelling of dynamic plumes in order to define the knowledge gaps present. The possibilities to fill these knowledge gaps were studied which resulted in carrying out experiments on two properties of the dynamic plume: stripping and vortex divergence.

Stripping is defined as the removal of material from a dynamic plume by the cross flow. Its process is not well understood and the few quantifications presented in literature were found to have no proper base. To obtain more information laboratory experiments were performed at a 1:100 distorted Richardson scale. The experiments were partly hindered by the limited flume dimensions of the experimental setup, but the tests yielded interesting observations. Stripping was hardly occurring in the created continuous overflow plumes and was not caused by the hypothesized process. Stripping appeared to be counteracted by the dynamic plume influences. The creation of passive clouds of material outside the dynamic plume was caused by other processes like internal irregularities, moving of the outflow pipe and density differences within the discharged material. As no significant stripping was observed in the experiments the possibilities to implement stripping in dynamic plume models were not further investigated.

Vortex divergence is depending on the strength of the vortex pair that is formed when a plume is bent over by a cross flow. In homogenous surroundings the plume does not bifurcate, but the vortices of the vortex pair are diverging at a near constant rate. This divergence was already observed in the stripping experiments and was further investigated in specialized experiments. Next to that the need and possibility for an extension of the CORMIX model to include this divergence was investigated. The experiments did only provide limited results suitable for the quantification of the process. The plumes did not bifurcate, but the divergence rate was considerable but fell within the range described in literature. As no bifurcation was observed in the experiments it is considered unimportant for overflow plumes. That also seems true for vortex divergence, but that could not be proved. The investigation of CORMIX yielded that although the profile is approximated with a Gaussian profile for simplicity, the extra mixing due to the vortex pair creation is taken into account. For modelling overflow plumes this delivers acceptable results. Describing the actual concentration cross profile in the model would harm its simplicity and functionality and is therefore considered undesirable.



## Samenvatting

Het overvloeimengsel van sleeppopperzuigers bevat fijn sediment dat wanneer het geloosd wordt in het omgevingswater een zogenaamde pluim vormt. De verspreiding van dit fijne sediment en de troebelheid die ermee gepaard gaat zijn vaak belangrijk voor het milieu. Het verkrijgen van inzicht in pluimgedrag is daarom belangrijk.

De eerste fase van een pluim wordt dynamisch genoemd en wordt gekenmerkt door het snelle zinkproces van een zwaar mengsel onder de invloed van het meegekregen momentum en dichtheidsverschil. De volgende fase wordt passief genoemd en wordt beheerst door het bezinkingsgedrag van de individuele deeltjes. Het gedrag en einde van de dynamische fase hangt van veel verschillende invloeden af en deze is daarom moeilijker te modelleren dan de passieve fase. Deze afstudeerscriptie probeert daarom meer inzicht te verschaffen in sommige van deze invloeden en de mogelijke implementatie daarvan in dynamische pluim modellen.

Een inleidende studie is uitgevoerd om zowel de theorie als het modelleren van dynamische pluimen te onderzoeken op kennishiaten. De mogelijkheden om deze hiaten te vullen met experimenteel onderzoek zijn bekeken en er is gekozen om twee invloeden op dynamische pluimen verder te onderzoeken: stripping en vortex divergentie.

Stripping is gedefinieerd als het verwijderen van materiaal uit de dynamische pluim door de dwarsstroom. Het proces achter stripping is niet bekend en ook van de hoeveelheid materiaal dat gestript wordt is niets bekend aangezien de weinige kwantificaties in de literatuur geen juiste achtergrond bleken te hebben. Om meer inzicht te krijgen zijn experimenten uitgevoerd op een verstoorde 1:100 Richardson schaal. Deze experimenten werden deels gehinderd door de kleine dimensies van de gootopstelling, maar de testen hebben interessante observaties opgeleverd. Er was bijna geen stripping in de opgewekte continue overvloeipluimen en stripping was niet veroorzaakt door het proces dat gedacht was het te veroorzaken. Stripping blijkt te worden tegengegaan door dynamische pluiminvloeden. Het ontstaan van passieve wolken van sediment buiten de dynamische pluim wordt veroorzaakt door andere processen zoals interne onregelmatigheden, het bewegen van de uitstroompip of een dichtheidsverschil in het gedumpte materiaal. Aangezien er geen significante stripping is waargenomen in de experimenten zijn de mogelijkheden om stripping te implementeren in dynamische pluimmodellen niet verder onderzocht.

Vortex divergentie is afhankelijk van de sterkte van het gevormde vortex paar dat ontstaat wanneer een pluim omgebogen wordt door de dwarsstroom. In homogeen omgevingswater zal de pluim niet splitsen, maar de vortexen zullen divergeren met een constante hoek. Deze divergentie was al gezien gedurende de stripping experimenten en was verder onderzocht met een serie experimenten die hier speciaal op gericht waren. Daarnaast waren de noodzaak en mogelijkheden om het CORMIX model uit te breiden om deze divergentie mee te nemen onderzocht. Deze nieuwe experimenten gaven weinig resultaten die bruikbaar waren voor kwantificatie van het proces. De pluimen in de experimenten splitsten niet, maar de divergentie

---

was aanzienlijk maar binnen de grenzen die worden aangegeven in de literatuur. Aangezien de pluimen in het experiment niet splitsen is gedacht dat dit niet belangrijk is voor overvloeipluimen. Ook voor divergentie lijkt dit het geval, maar dat kunnen de experimenten niet met zekerheid vaststellen.

Het onderzoek naar het gebruik van CORMIX gaf aan dat ondanks dat CORMIX het dwarsprofiel voor de eenvoud benaderd met een Gaussiaans profiel, het extra mixgedrag dat veroorzaakt wordt door het gevormde vortex-paar toch wordt meegenomen. Voor het modelleren van overvloeipluimen geeft dit acceptabele resultaten. Als de werkelijke (concentratie)dwarsprofielen moesten worden weergegeven in het model dan zou de eenvoud en daarmee de functionaliteit van het model aangetast worden, hetgeen onwenselijk is.

# Contents

Preface.....	iii
Abstract .....	v
Samenvatting.....	vii
Contents.....	ix
<b>Chapter 1: Introduction.....</b>	<b>1</b>
1.1 Reasons for studying overflow plumes	2
1.1.1 Environmental aspects of dredging	2
1.1.2 The sediment loss assessment	3
1.1.3 Sediment source terms	5
1.1.4 Dynamic plume behaviour	7
1.2 General problem definition	9
1.3 Evaluation of M.Sc. thesis research	10
1.4 Outline of the report	11
<i>Part 1: Preliminary study</i>	
<b>Chapter 2: Theory on plumes .....</b>	<b>17</b>
2.1 General buoyant jet description	17
2.1.1 Governing parameters	17
2.1.2 Zone of Flow Establishment	17
2.1.3 Zone of Established Flow	19
2.2 Plume processes	24
2.2.1 Inventory of processes	24
2.2.2 Entrainment process	26
2.2.3 Vortex pair creation, divergence and bifurcation	29
2.2.4 Stripping	34
2.3 Theoretical behaviour of overflow plumes	35
2.3.1 Typical parameter values for overflow plumes	35
2.3.2 Categorization of overflow plumes	36
2.3.3 Description of the typical behaviour of the overflow plume	38
2.3.4 Entrainment of overflow plumes	40
2.3.5 Other phenomena influencing overflow plumes	41
<b>Chapter 3: Modelling of plumes.....</b>	<b>45</b>
3.1 Approaching modelling of plumes	45
3.1.1 Main modelling categories	45
3.1.2 Jet-integral models	46
3.1.3 Numerical (field) models	47
3.1.4 Length scale models	48
3.2 Improvements and extensions in modelling	49
3.2.1 Jet-integral model improvements	49
3.2.2 Numerical model improvements	49
3.2.3 Length-scale model improvements	50
3.3 The CORMIX model	51
3.3.1 Working of the CORMIX program	51
3.3.2 Formulations for overflow plumes (flow class IV1)	56

<b>Chapter 4: Experimental research needed</b> .....	<b>61</b>
4.1 Identification of knowledge gaps	61
4.1.1 Knowledge gaps in current literature	61
4.1.2 Information need in modelling	63
4.2 Experimental possibilities	64
4.2.1 Feasibility of laboratory experiments	64
4.2.2 Some ideas for experiments	66
<b>Chapter 5: Definition of M.Sc. thesis research work</b> .....	<b>69</b>
5.1 Choice for experiments to implement	69
5.1.1 Stripping experiment	69
5.1.2 Vortex divergence experiment	70
5.2 Objectives of the research work	71
5.2.1 Objectives of stripping research	71
5.2.2 Objectives of vortex divergence research	71

*Part 2: Stripping*

<b>Chapter 6: Stripping experiment</b> .....	<b>75</b>
6.1 Basic idea of the experiment	75
6.1.1 Objectives of experiment	75
6.1.2 Hypotheses	75
6.1.3 Measurements needed	76
6.2 Experimental setup	77
6.2.1 Scaling	77
6.2.2 Dimensions	77
6.2.3 Controlling the parameters	78
6.3 Measuring plan	79
<b>Chapter 7: Stripping experiment results</b> .....	<b>81</b>
7.1 Measurements	81
7.2 Main observations	81
<b>Chapter 8: Discussion of stripping</b> .....	<b>89</b>

*Part 3: Vortex divergence*

<b>Chapter 9: Vortex divergence experiment</b> .....	<b>93</b>
9.1 Basic idea of the experiment	93
9.1.1 Objectives	93
9.1.2 Hypotheses	93
9.1.3 Measurements needed	94
9.2 Experimental setup	95
9.2.1 Scaling	95
9.2.2 Dimensions	95
9.2.3 Controlling the parameters	96
9.3 Measuring plan	97
<b>Chapter 10: Vortex divergence experiment results</b> .....	<b>99</b>
10.1 Measurements	99
10.2 Cross profiles of every plume	100
10.3 Vortex divergence rate	103
10.4 Plume paths of tested plumes	104
10.5 Entrainment and dilution	104

<b>Chapter 11: CORMIX model results .....</b>	<b>107</b>
11.1 Results for the tested plumes .....	107
11.2 Comparison with test results .....	108
<b>Chapter 12: Discussion of vortex divergence .....</b>	<b>115</b>
12.1 Discussion of vortex divergence experiment .....	115
12.2 Discussion on CORMIX applicability .....	116

*Part 4: Conclusions & recommendations*

<b>Chapter 13: Conclusions.....</b>	<b>121</b>
13.1 Conclusions on stripping .....	121
13.2 Conclusions on vortex divergence .....	121
13.3 Conclusions on the experimental setup .....	122
<b>Chapter 14: Recommendations for further research.....</b>	<b>123</b>
14.1 Recommendations for overflow plume research .....	123
14.1.1 General overflow plume research .....	123
14.1.2 Stripping research .....	124
14.1.3 Vortex divergence research .....	124
14.2 Advice for further research with the experimental setup .....	126
14.2.1 Plume research in the experimental setup .....	126
14.2.2 Other research in the experimental setup .....	127
<b>References .....</b>	<b>129</b>
<b>List of used symbols.....</b>	<b>133</b>
<b>List of figures and tables.....</b>	<b>135</b>

*Appendices*

<b>Appendix A: Deduction of asymptotic results .....</b>	<b>143</b>
<b>Appendix B: All combinations of parameter values.....</b>	<b>149</b>
<b>Appendix C: Parameter study for scaling.....</b>	<b>151</b>
<b>Appendix D: Measuring plan stripping experiment .....</b>	<b>155</b>
<b>Appendix E: Working and use experimental setup.....</b>	<b>157</b>
<b>Appendix F: Instruments used in experimental setup .....</b>	<b>165</b>
<b>Appendix G: Siphons used in experimental setup.....</b>	<b>174</b>
<b>Appendix H: Velocity deviations in the flume .....</b>	<b>180</b>
<b>Appendix I: Development history of exp. setup.....</b>	<b>187</b>
<b>Appendix J: Course of experiments .....</b>	<b>195</b>
<b>Appendix K: Raw results of vortex divergence exp.....</b>	<b>200</b>
<b>Appendix L: CORMIX input data .....</b>	<b>204</b>
<b>Appendix M: Head fall calculation waste water pipe.....</b>	<b>205</b>
<b>Appendix N: OPCON calibration curves.....</b>	<b>207</b>
<b>Appendix O: OSLIM calibration curves .....</b>	<b>212</b>
<b>Appendix P: Siphon calibration graphs.....</b>	<b>214</b>



## Chapter 1: Introduction

*This M.Sc. thesis discusses laboratory experimental research that has been carried out on dynamic dredge overflow plumes. This introduction chapter tries to explain what (dynamic) dredge overflow plumes are, why they are relevant and what the problems concerning overflow plumes are.*

*Figure 1.1 presents an overflow plume in practice to give the reader a first impression what a plume is. The first paragraph of this chapter familiarises the reader further with the reasons for interest in plume research and the background of plumes. The second paragraph defines the general problem tackled in this thesis. The development of the M.Sc. thesis research is shortly discussed in the third paragraph and the chapter is concluded with a reading guide for this thesis.*



Figure 1.1: Picture of an overflow plume in practice  
(Hong Kong East Lamma Marine Borrow Area, December 2000)

## 1.1 Reasons for studying overflow plumes

*The subject of overflow plumes has its background in environmental aspects of dredging. Those aspects are discussed first. One major item of these environmental impacts is sediment loss causing turbidity. The assessment of sediment loss is therefore dealt with in the second section. Important therein is the determination of source terms discussed in the third section. The influence on these source terms by the dynamic plume behaviour is dealt with in the final section of this paragraph.*

### 1.1.1 Environmental aspects of dredging

By its nature dredging has an impact on the environment. Dredging is the excavation of material from a sea, river or lake bed and the relocation of the excavated material elsewhere. Removal of natural resources and a possible destruction of habitats at the dredging site as well as at the disposal site are unavoidable consequences. However, those impacts directly related to the relocation of material should be weighted against the benefits gained by executing the projects (Smits, 1998).

Another major environmental impact of dredging is the resuspension of sediment in the water column during dredging operation, transport or disposal. These impacts are often secondary to the abovementioned aspect. Nevertheless the focus in assessments and regulations is often on this resuspension and its far field effects. That is mainly due to the idea that these effects may to some extent be avoided, reduced or mitigated, depending on the circumstances (Nieuwaal, 2001).

The physical impacts of sediment resuspension are an increase of turbidity of the surrounding waters and/or sedimentation at possible vulnerable places. Both physical impacts may have in turn adverse impacts on the biological and ecological environment.

There are many speculations on the extent of those impacts that are not backed by research (Burt and Hayes, 2005). However, making an Environmental Impact Assessment (EIA) of the dredging works is required in most regulations concerning dredging projects. In some occasions dredging is even prohibited unless it is demonstrated that the environmental impact is acceptable.

To demonstrate this is however difficult, since physical processes and the resulting biological impacts are very difficult to quantify. Burt and Hayes (2005) state that the greatest priority in improving environmental assessments is to be able to measure and predict how much sediment is actually released and where that sediment goes.

The extent of the physical impact of this sediment loss needs to be known before biological and ecological impacts can be assessed.

The sediment loss assessment therefore needs separate attention when the environmental aspects of dredging are reviewed. That assessment is therefore worked out in the next part.

### 1.1.2 The sediment loss assessment

Sediment losses, sometimes also referred to as sediment resuspension, can be described/assessed in different ways. John *et al.* (2000) determined four different ways of quantification:

- 1) Sediment concentration increases in the vicinity of dredging (mg/l).
- 2) The rate of release of sediment into the water column per unit of time (kg/s).
- 3) Via the S-factor approach, in which the total mass of sediment put into suspension is expressed relative to the quantity of material that is dredged ( $\text{kg/m}^3$ ).
- 4) Via the sediment flux method which describes the net sediment flow through the boundaries of a designated area within which the dredger is working.

Ad. 1) Bray *et al.* (1997) proposes to measure the suspended sediment concentration increase as a mean to assess the effects of sediment resuspension. These concentration increases are however highly site specific. That generates large variances for exactly the same operation. Therefore this method has a weak basis for the comparison of different dredging methods, operations, hydrodynamic conditions and materials.

Ad. 2) The rate of release of sediment seems to be more promising in an overall sediment resuspension assessment (John *et al.*, 2000). The measured or estimated release rates can be used as a source term in any type of far-field (plume) model (Whiteside *et al.*, 1995). The problem with this method lies in the translation of release rate to a source term for a model. Not every kg/s sediment released generates the same amount of 'source' for the far field. It is depending on the way of release, the kind of material released and the corresponding near field behaviour.

Ad. 3) Blokland (1988) states that the environmental effects can best be compared making use of the ratio between resuspended material and the amount of soil removed, thus relating the cause (production) to the consequence (sediment resuspension). This ratio is called the S-factor and is depending on the soil class, type of dredger and the ambient conditions present. The S-factor can be a useful first estimate for situations where there is no site-specific information. Pennekamp *et al.* (1996) states that the S-factor (or in their paper S-parameter) is determined not so much by the dredging technique but rather by the way in which this technique is used. For future dredging works it is therefore advisable to carefully investigate whether previously calculated S-factors might be used again.

Ad. 4) The sediment flux method is used in the Øresund link project and is a measuring method rather than a sediment resuspension description. The sediment loss was called spill and was defined as "... soil particles (...) brought in suspension by the dredging works, leaving the workzone defined around the area of dredging..." (Jansen, 1999: p 176). The flux of sediment leaving the work area can be calculated by multiplying the velocity by the sediment load at the boundary of the work area. The velocity can be measured directly, the sediment load has to be determined via turbidity measurements and a validated conversion. In this way near real-time information can be obtained. At the Øresund project the gathered information was

directly used in the management of the dredging operation. In that way the spill was not only measured but also controlled (Jansen, 1999). The systems used at a measuring vessel to determine the spill are presented in figure 1.2. Such an extensive measuring setup is indispensable in the sediment flux method.

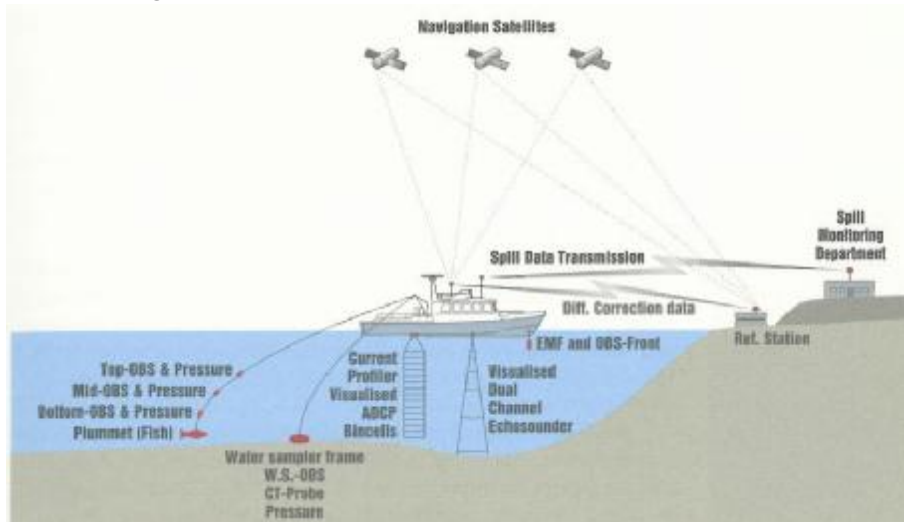


Figure 1.2: Monitoring setup at Øresund link project (Jansen, 1999)

According to John *et al.* the sediment flux method "... can be more relevant in terms of environmental evaluation but it ignores everything that happens between the dredger and the point of measurement." (2000: p 52). Other objections against this way of determining resuspended material are the high costs and the (labour) intensive measurement program associated with it. Moreover it must be stated that the sediment flux method as a measuring method for sediment resuspension might be useful when operating a dredging project, but that the method lacks the ability to produce effective long-term predictions of sediment resuspension before any field data is collected.

The rate of release of sediment therefore seems to be the most promising approach in assessing sediment resuspension problems. It is therefore studied more often than the other approaches. The returning difficulty in the method however is defining the source term. Gerritsen *et al.* (2005) describes the feasibility of a new method for monitoring turbidity which combines operational dredging data, remote sensing data, modelling of sediment transport and in-situ data. The method can give hindcasts, nowcasts and in the future possibly short period forecasts. Again the need for reliable source terms came forward; the released material can be measured or predicted with the new method but the translation to a sediment source term is still required. The combination of the several data sources delivers more insight in the conditions under which the release takes place and might make this translation easier. The sediment release approach was also deployed by Whiteside *et al.* (1995), involving plume tests with the HAM 310 in Hong Kong. There field measurements were used to estimate a 'source' concentration for a particle tracking hydrodynamic model. Again the conclusion is that more research is needed in the determination of the source for sediment resuspension in the far field. Therefore the sediment source terms are discussed in the next part.

### 1.1.3 Sediment source terms

The source for sediment resuspension differs per dredger type and dredging operation. John *et al.* (2000) reviews most types of dredgers and list the possible causes of sediment release. Apart from hydrodynamic dredgers, all dredging equipment generates three main sources for sediment resuspension:

- Disturbance of the bed by draghead, cutter, grab, buckets or otherwise.
- Overflow or other material removal from the barge like screening or Light (or Lean) Material Over Board (LMOB).
- Leakage losses from pipes, buckets, grabs as well as dripping and splashing.

This M.Sc. thesis focuses only on the overflow discharge because it is thought to be a prominent source. Screened material and LMOB occur less frequently and might be treated similarly. Leakage losses are considered to be smaller or better manageable. Disturbance of the seabed is another prominent source but since it is acting at the bottom it is considered somewhat less important for far field resuspension.

Overflow is the excess water from the dredging process which is spilled. The Trailing Suction Hopper Dredger (TSHD) is the most common equipment that uses overflow, therefore this M.Sc. thesis mainly considers overflow of TSHD's. The water/sand mixture which is pumped up remains only for a short time in the hopper-well before the water is overflowed. Fine sediment with a long settling time will be released through the overflow. To estimate the amount of released material Van Rhee (2002) developed a simple 1DV model and a more extensive 2DV model. Badloo (1998) discussed possibilities to minimize the amount of released material. The amount of sediment released and the properties of the sediment in the overflow will be boundary conditions for this M.Sc. thesis.

The sediment released in the water column will form a so-called plume and it is this plume that is the main subject of this M.Sc. thesis. Lee and Chu gave a more strict definition of a plume: "Plumes are fluid motions that are produced by continuous sources of buoyancy" (2003: p 55). When the source is not only buoyant but also contains momentum, which is the case in overflow discharges, the plume should be classed as forced plume or buoyant jet (Rodi, 1982; Lee and Chu, 2003). As in most literature the buoyant jet caused by the overflow discharge will here be referred to as plume or dredging (spill) plume.

The first stage of the plume is called the dynamic phase. Herein the plume behaves as a density current that rapidly descends the water column and entrains water meanwhile (Whiteside *et al.*, 1995). After this dynamic phase a passive phase follows in which the plume decays by settling of the particles under the influence of advective and diffusive processes in the ambient water. Generally this passive phase is modelled in practice, so the source terms needed are determined by the end of the dynamic phase. The end of the dynamic phase is then defined as the moment the plume stops acting as a dense mixture and the particles start to settle separately. An overall view of an overflow plume including some relevant processes that influence the dynamic phase is sketched in figure 1.3. The transition from dynamic to passive phase is also indicated. The relevant processes are further worked out in later chapters.

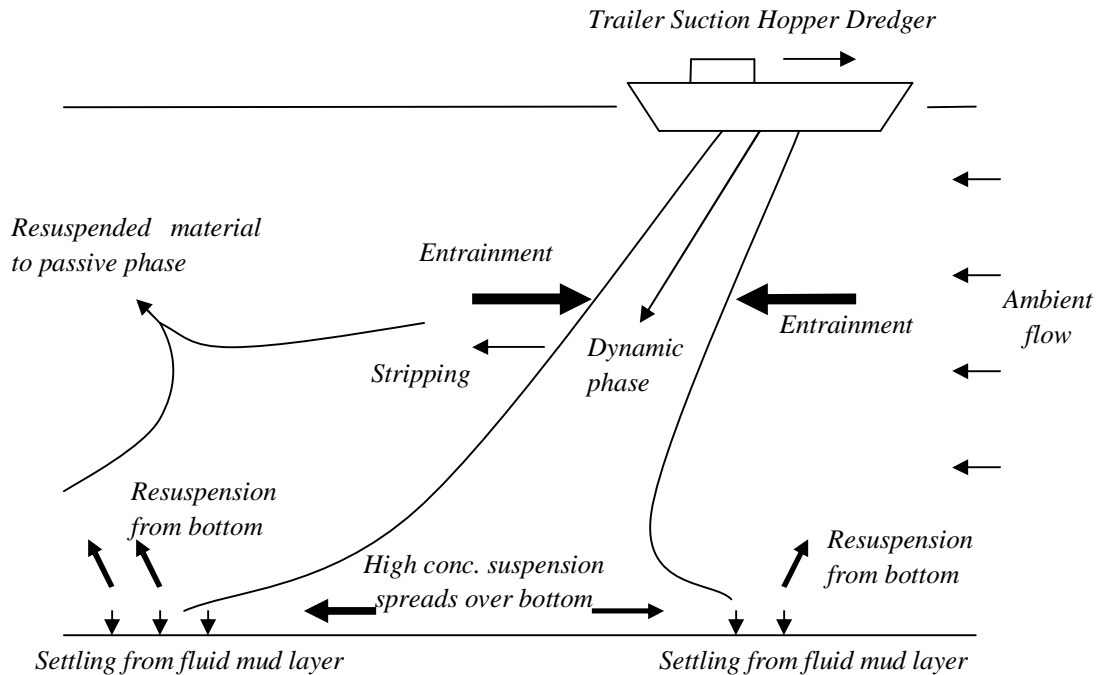


Figure 1.3: Sketch of dredge plume including processes.  
(free after: Baird, 2004)

Dankers (2002) uses another classification of overflow plumes, which is also used in other research works (Winterwerp, 2002; Boot, 2000). Here dynamic plumes are classified as plumes which descend rapidly towards the seabed and after impingement on the seabed spread radially outward as a density current. Passive plumes mix directly with the ambient water. The plume sketched in figure 1.3 is typically a dynamic plume; a passive plume is sketched in figure 1.4. In the terminology of the preceding part a plume with a dynamic phase that exceeds bottom impingement is called dynamic. A plume which is taken over by mixing processes before the bottom is reached is called passive.

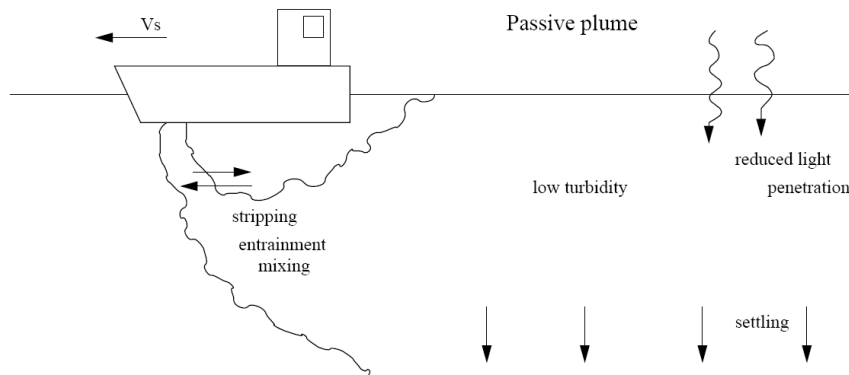


Figure 1.4: Sketch of a passive plume with relevant processes  
(Dankers, 2002)

Passive plumes will be mixed rapidly and entirely with the surrounding water. This makes modelling with a rate of release approach quite easily possible since all released material will settle with its own settling velocity under the influence of the hydrodynamic conditions. The input for the models can then simply be averaging the released material over the water column. For dynamic plumes it is far more difficult to come to source terms for far-field modelling since it is not predefined how much material will enter the passive phase at what position. Therefore a lot of research and modelling efforts were focussed on gaining more insight in dynamic plume behaviour. In the next section more is explained about dynamic plumes.

### 1.1.4 Dynamic plume behaviour

Research on the behaviour of the dynamic phase of a plume has for a long time been focussed on buoyant jets arising from cooling water or wastewater releases in open water or on gas plumes released in the atmosphere (Delvigne, 1977; Fischer *et al.*, 1979; Wood *et al.*, 1993; Fannelöp, 1994).

Winterwerp (2002) analysed experiments by Boot (2000) on the near field of dredge overflow plumes. Objective was to determine whether an overflow plume is expected to be dynamic or passive. It showed that the behaviour of the plume is determined by two parameters: a bulk Richardson number ( $Ri$ ) and a velocity ratio ( $\zeta$ ) which are defined by:

$$Ri = \frac{\epsilon g D_{pipe}}{W_0^2} \quad (1.1)$$

$$\zeta = \frac{U}{W_0} \quad (1.2)$$

in which  $\epsilon$  is the relative excess density of the dredging plume,  $g$  is the acceleration of gravity,  $D_{pipe}$  is the diameter of the overflow pipe,  $U$  is the velocity of the ambient water relative to the ship and  $W_0$  is the outflow velocity of the plume.

The experiments showed that low  $\zeta$  values and high  $Ri$  values yield that the plume is dynamic, while high  $\zeta$  values and low  $Ri$  values result in a passive plume. In between a transitional zone exists. Here both the dynamic plume processes, mainly being density currents, and the passive plume processes, mainly being mixing processes, are important and could not be distinguished. The relation found in the tests between  $Ri$  and  $\zeta$  and the corresponding zones for dynamic plumes (density currents), transition and passive plumes (mixing zone) are presented in figure 1.5. Important notice is the fact that the exact shape of the transition might be different for other water depths. Furthermore the role of air entrained in the plume and ship propeller effects are discussed. Van der Salm (1998) already discussed the importance of the level of turbulence in the ambient water, especially in the mid- and far-field. Perhaps even more parameters or conditions contribute to the behaviour of the plume's mixing and settling properties.

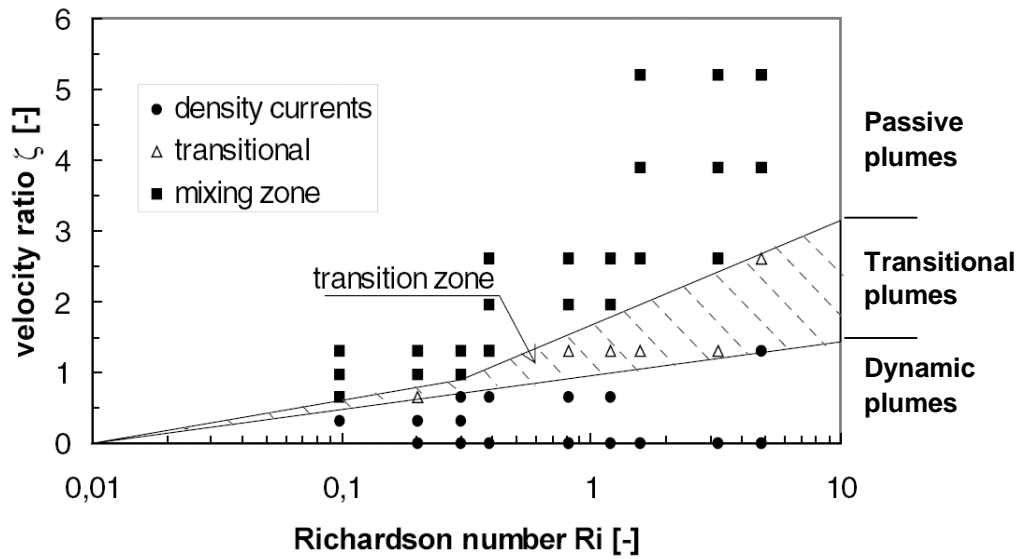


Figure 1.5: Classification of overflow plumes in shallow water (Winterwerp, 2002)

In the last decades several efforts were undertaken to model the behaviour of the dynamic phase. The main problem these models encounter is validation. More unified information from plume monitoring measurements is required to enhance the possibilities to validate models (Whiteside *et al.*, 1995; John *et al.*, 2000; Burt and Hayes, 2005).

## 1.2 General problem definition

The main interest in overflow plume research is to be able to determine what the source is for (passive) far-field spreading of resuspended sediment. For this determination, one has to know not only whether a plume is dynamic or passive but also what the behaviour in the dynamic phase is.

The dynamic plume behaviour is influenced by several processes and phenomena that have to be taken into account in this determination of source terms. For several processes this influence is known and implemented in dynamic plume models. Other influences, mostly more typical for overflow plumes, are only qualitatively described or not known at all. Carrying out laboratory experiments that specifically focus on these influences is one of the possible approaches in improving the current knowledge on this. This M.Sc. thesis followed this approach and therefore aimed at carrying out such laboratory experiments focussing on one or more important influences. The general goal of this thesis is therefore formulated as:

*Improving insights in one or more influences determining the behaviour of overflow plumes in their dynamic phase, using laboratory experiments, to improve the quantification of the source of fines for numerical sediment resuspension models that describe the environmental impact of dredging.*

This general goal already specifies that this M.Sc. thesis, due to limited time and size, is only able to carry out experiments focussing on one or more influences. The determination of these influences has to be based on the current knowledge available. Therefore first the theory and modelling practice of dynamic overflow plumes is investigated and the knowledge gaps in these fields are determined and evaluated. After that more specific objectives for this M.Sc. thesis are formulated based on the chosen processes. This is completed before any experiments started and is therefore referred to as 'Preliminary study'.

After the preliminary study the actual research work of this M.Sc. thesis is started. Experiments are carried out and the possibilities to implement the gathered knowledge in (dynamic) plume models are tested. Furthermore the results are interpreted and discussed showing to what extent the goal of improving source term determination for (far-field) suspension models are fulfilled. Finally also the need and possibilities further research are pointed out.

### 1.3 Evaluation of M.Sc. thesis research

As indicated in the previous paragraph the thesis work was started with a preliminary study. As a result of that preliminary study several ideas for experimental research were opted, but an experiment focussing on the process called stripping was thought to be the most promising. As the process of stripping is barely understood, focussing on this process yielded a good possibility to improve current knowledge.

In order to carry out these experiments on stripping an experimental setup had to be built in the Fluid Mechanics Laboratory at Delft University of Technology. The designing, building and calibration of this experimental setup were a major undertaking. Not only large constructions had to be built, also several practical problems were faced. Most striking were the velocity deviations observed in the flume, the development of the siphons and the calibration and implementation of several measurement devices. Much of the time and effort of this M.Sc. thesis had to be put in building and testing this experimental setup.

Several experiments on stripping were carried out. Although the limited dimensions of the flume put limitation on the amount and quality of the experiments carried out, several interesting observations could be made. Most important was that stripping was not significant in the experiment. For that reason it was not needed to extensively investigate the dependency of stripping on several parameters and the stripping research was stopped after several tests.

At that point it was chosen to implement another experiment, to make use of the possibilities created with the experimental setup. Since vortex divergence was already observed in the stripping experiments, it was chosen to further investigate that process with experiments. As the scale and the focus of the experiments had changed the experimental setup had to be adjusted. The use of this adjusted setup raised other practical problems which limited the quantity and quality of the measurements on vortex divergence.

Next to the experiments the CORMIX model was investigated and used to make comparison of the model predictions with the measurements. However the lack of high-quality measurements made it impossible to base any conclusions on this comparison.

This thesis work therefore consists out of two experimental research works and the design, building and calibration of the experimental setup. In order to keep the report readable, it was chosen that in the main text the two research works would be described separately and that the issues concerning the experimental setup would be described in the appendices. The discussion of the two research works are split into two parts that could be read independently.

## 1.4 Outline of the report

*In the preceding paragraph the research work carried out was described and some comments on the contents of the report were presented. In this paragraph this structure of the report is further worked out to give an overview of the contents described in every part and chapter.*

*The outline of the report is discussed first before the paragraph is concluded with a diagram, figure 1.6, that schematically recapitulates the structure of the report.*

### **Part 1: Preliminary study**

After this introductory chapter first the results of the preliminary study are presented. The theory of overflow plumes is presented in Chapter 2. The general buoyant jet theory is first discussed, followed by typical plume processes. The chapter is concluded with a theoretical description of overflow plumes and several typical overflow plume phenomena. In Chapter 3 the several approaches to model the dynamic plume are discussed and some comments on possible improvements are mentioned, furthermore the CORMIX model is looked at in detail. The knowledge gaps persisting in theory and modelling are presented in Chapter 4. Also the feasibility to fill these knowledge gaps by carrying out experiments is presented, concluded by proposing some possible experiments. The preliminary study is ended with the discussion of the research works adopted in this M.Sc. thesis in Chapter 5. Not only the choice for the experiments to be carried out is clarified, but also the concrete objectives related to these experiments are stated.

As stated in the previous paragraph the two different research works were looking into the processes of stripping and vortex divergence respectively and both research works are treated independently in a separate part of the report.

### **Part 2: Stripping**

The part on the stripping research is treated first. The experiment that is carried out is described in the first chapter, Chapter 6, followed by the results in Chapter 7. Since the results did not yield possibilities to improve or test any modelling with respect to stripping the stripping research is concluded with a discussion on stripping in Chapter 8.

### **Part 3: Vortex divergence**

In the third part of this thesis the vortex divergence research is discussed. First the experiment that is carried out is described in Chapter 9, followed by the experiment results in Chapter 10. The investigation of the CORMIX model, especially looking into the treatment of vortex divergence, is described in Chapter 11. Also the part on vortex divergence is finished off with a discussion; Chapter 12.

### **Part 4: Conclusion and recommendations**

The last part of this thesis presents the conclusions and recommendations of this research. In Chapter 13, the conclusions found in both research works as well as in the preparation of the experimental setup are listed. Chapter 14 concludes with a summary of further research needs and possibilities.

---

## Appendices

After the main text the appendices are presented. In the text the reader is referred to the appendices several times. In the appendices, amongst others, the exact working of the experimental setup is discussed as well as the problems faced during the design and building of the setup. The sequence of the appendices is based on the appearance of the subjects in the main text.

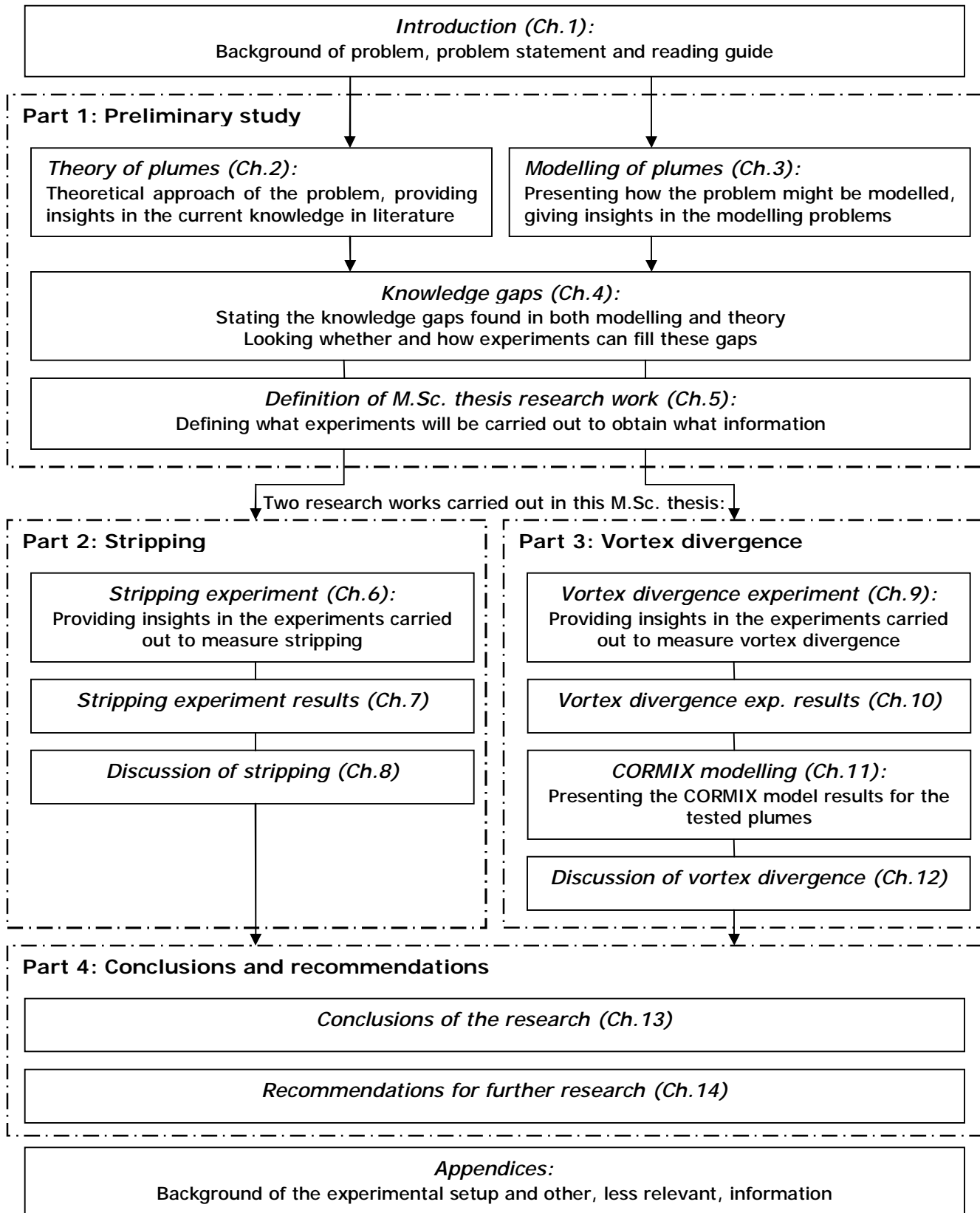


Figure 1.6: Diagram of the outline of the report.



## **Part 1: Preliminary study**



## Chapter 2: Theory on plumes

*A literature study was carried out to acquire more knowledge on plumes and their processes. This chapter describes the results of that study. Focus is laid on giving a clear description of the material, not on reviewing the literature. In the introduction it is discussed that overflow plumes are specific examples of buoyant jets. Therefore first the main characteristics of buoyant jets in general are discussed. After that several plume processes that are considered important in overflow plumes are studied. Finally the overflow plume is discussed in detail.*

### 2.1 General buoyant jet description

*A buoyant jet can be divided in two parts. It starts with the Zone of Flow Establishment (ZFE) and continues with the Zone of Established Flow (ZEF) as can be seen in figure 2.1. The length of these zones and the behaviour of the buoyant jet in each of these zones are determined by multiple parameters. These parameters can be reduced to three governing parameters. First the formulation of these governing parameters is presented. After that the ZFE and ZEF are treated sequentially.*

#### 2.1.1 Governing parameters

The parameters involved in describing buoyant jets are categorized in three classes by Fischer *et al.* (1979): jet parameters, environmental parameters and geometrical parameters. However, mostly the relative influence of these parameters is of importance. Therefore some of those parameters are grouped to form a more meaningful parameter. The description of buoyant jets uses three of these governing parameters, being the volume flux ( $Q$ ), the specific (meaning divided by the density of the discharged fluid) momentum flux ( $M$ ) and the specific buoyancy flux ( $B$ ). Their initial values are given by the following formulae:

$$Q_0 = \frac{1}{4} \rho D_{pipe}^2 W_0 \quad (2.1)$$

$$M_0 = \frac{1}{4} \rho D_{pipe}^2 W_0^2 \quad (2.2)$$

$$B_0 = g \frac{(r_{mix} - r_{amb})}{r_{amb}} Q_0 \quad (2.3)$$

In which  $D_{pipe}$  is the pipe diameter,  $W_0$  is the initial jet velocity,  $\rho_{mix}$  is the density of the discharged fluid,  $\rho_{amb}$  is the ambient density and  $g$  is the acceleration of gravity.

#### 2.1.2 Zone of Flow Establishment

The first zone after the release of a buoyant jet is called the ZFE. It is determined by the changing velocity profile from the pipe velocity distribution to a jet like velocity distribution, which is, if averaged over time, approximated by a Gaussian distribution (Wood *et al.*, 1993). Water is entrained in the jet, but the central part of it, mostly called the potential core, is not mixed. The mixing layer in between the core and the edge of the buoyant jet is increasing in width because of entrainment and turbulent mixing action at the core edge. Finally the potential core is consumed by the mixing layer and the jet like flow distribution is fully developed. There the ZFE ends and the

ZEF starts. Most important property of the ZFE is its length. First the ZFE without crossflow is investigated, after that buoyant jets in a crossflow are analysed.

#### Excluding ambient crossflow

In a standing ambient fluid the self-preserving Gaussian form of the velocity profile is created in a distance of a few pipeline diameters (Fännelop, 1994). Fischer *et al.* (1979) states that buoyant jets released in still water the ZFE length is about 7 pipe diameters and that the dilution and widening of the plume is about 2 at the end of the ZFE. For a vertical released buoyant jet figure 2.1 shows the principal components and length scales of the ZFE without ambient crossflow.

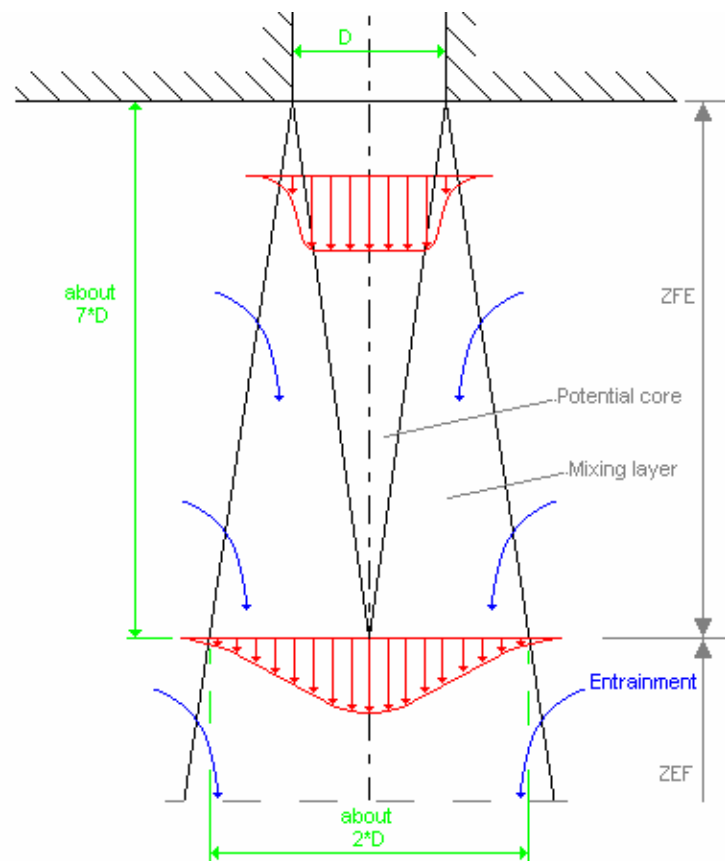


Figure 2.1: Sketch of a vertical downward released negatively buoyant jet in a stagnant fluid (free after: Fannelöp. 1994)

#### Including ambient crossflow

When overflow plumes are investigated the ambient crossflow cannot be excluded. The crossflow changes the shape and length of the ZFE. This influence must be considered against other properties of the buoyant jet such the initial velocity and the density differences. Lee and Chu (2003) state that the potential core length, or ZFE length, is depending on the combination of density differences, initial orientation and relative ambient crossflow magnitude. When a vertically released jet in a crossflow is considered Wood *et al.* (1993) gives a formula that estimates the vertical length of the ZFE ( $Z_{ZFE}$ ) based on experiments by Keffer and Baines (1963) and Rajaratnam (1976):

$$Z_{ZFE} = 7D_{pipe} \left( 1 - \frac{0.86}{0.03 \left( \frac{W_0}{U} \right)^{1.5} + 1} \right) \quad (2.4)$$

In which  $U$  is the ambient velocity.

Whether this formula can also be used for buoyant jets is unknown, since not a lot of research has focused on the applicability of this formula. Also for further analysis of the ZFE the result of this formula is not applicable, since it has no further physical meaning. Therefore most buoyant jet calculations rather make use of a length scale  $l_Q$  given by the following formula (Fischer *et al.*, 1979; Rodi, 1982):

$$l_Q = \frac{Q}{\sqrt{M}} \quad (2.5)$$

For  $z \gg l_Q$  the flow is fully developed and for  $z \approx l_Q$  the flow is still controlled by the exit geometry (Fischer *et al.*, 1979). Using this formula does not provide a clear length of the transition from the ZFE to the ZEF, but the parameter  $l_Q$  turns out to be more useful for descriptions of behaviour in the ZEF.

In a later part the exact magnitude of  $l_Q$  for overflow plumes is calculated. Here it is already stated that the ZFE in overflow plumes is usually relatively small. Therefore it is considered unnecessary to look in more detail to processes that play a role in the ZFE such as turbulent action around the potential core, the widening rate of the initial mixing zone, etc.

### 2.1.3 Zone of Established Flow

After the ZFE the Zone of Established Flow (ZEF) starts. The behaviour here can be either more like a jet or more like a plume, depending on the magnitude of the initial momentum and the momentum created by the buoyancy effects (Rodi, 1982). If the momentum created by the buoyancy effects is larger then the initial momentum, the buoyant jet behaves more like a plume, otherwise it behaves more like a jet. This implies that in the long run, when possible, every buoyant jet will behave like a plume, since buoyancy will continuously be transferred into momentum.

To start the description of the ZEF the parameters that determine this behaviour are investigated, first for the case without ambient crossflow, then for the case including a crossflow. After that the properties of both jetlike and plumelike behaviour are discussed more in detail.

#### Without ambient crossflow

In a situation without ambient crossflow the transition from jetlike to plumelike behaviour can be represented using a characteristic length scale  $l_M$ , which describes the relative importance of momentum and buoyancy fluxes (Papanicolaou and List, 1988; Fischer *et al.*, 1979). It is defined by the following formula:

$$l_M = \frac{M^{\frac{3}{4}}}{\sqrt{B}} \quad (2.6)$$

The buoyant jet behaves jetlike if  $z \ll l_M$  and plumelike if  $z \gg l_M$ . Another way of representing this behaviour is a comparison between the aforementioned  $l_Q$  and the  $l_M$  just obtained. The ratio between the two is recognizable as a Richardson number, which is referred to as the jet Richardson number ( $Ri_{jet}$ ) (Rodi, 1982):

$$\frac{l_Q}{l_M} = \frac{QB^2}{M^{\frac{5}{4}}} = Ri_{jet} \tag{2.7}$$

This jet Richardson number also indicates whether the flow is jet-like, since then the  $Ri_{jet}$  is very small, or plumelike, since  $Ri_{jet}$  is then close to unity already in the beginning of the ZEF (Papanicolaou and List, 1988).

**Including ambient crossflow**

When the buoyant jet is exposed to an ambient crossflow it will tend to bend over in the direction of the crossflow. Whether or not a buoyant jet bends over is determined by a characteristic vertical length scale  $z_M$  or  $z_B$ . Which one of those two has to be used is depending whether the buoyant jet is jetlike ( $z_M$ ) or plumelike ( $z_B$ ). Their magnitude is given by (Fischer *et al.*, 1979; Rodi, 1982; Lee and Chu, 1993):

$$z_M = \frac{\sqrt{M}}{U} \tag{2.8}$$

$$z_B = \frac{B}{U^3} \tag{2.9}$$

The buoyant jet always starts as a vertical jet and will finally behave as a bent-over plume. What happens in between is depending on the relative magnitude of  $z_M$  and  $z_B$ . If  $z_M > z_B$  the buoyant jet will first behave jetlike after a length of about  $l_M$ . After that it will behave plumelike, almost the same as in the case without crossflow. After a height of about  $z_B$  the buoyant jet will bend over and behaves as a bent-over plume. If  $z_M < z_B$  the buoyant jet will first behave jetlike until it bends over at a height of  $z_M$  and behaves as a bent-over jet. Later the behaviour also changes to bent-over plume. The vertical height where that takes place is given by  $z_C$ , which can be calculated by:

$$z_C = \left( \frac{M^2}{UB} \right)^{\frac{1}{3}} = z_M \left( \frac{z_M}{z_B} \right)^{\frac{1}{3}} \tag{2.10}$$

Figure 2.2 is a schematic figure that demonstrates what transition takes place at what height for each case.

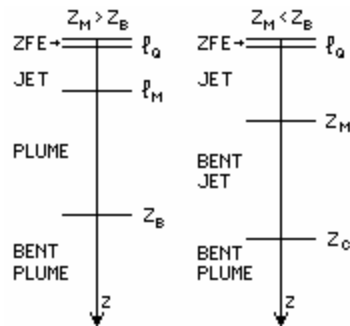


Figure 2.2: Schematic figure of the transitions in behaviour of the buoyant jet.

### Jet and plumelike behaviour in the ZEF

An established buoyant jet is well defined by two outer boundaries. Water is entrained over these boundaries and mixing takes place between ambient fluid and jet fluid. This mixing is highly turbulent and dynamic, which causes instantaneous measurements in buoyant jets to show large differences in jet fluid concentration in time and place. However, if the jet fluid concentration is averaged over time a concentration profile shows up, which can be approximated by a Gaussian concentration profile (Fischer *et al.*, 1979; Wood *et al.*, 1993; Fannelöp, 1994).

For that reason the behaviour of the buoyant jet can be described by only three parameters: i) the centreline trajectory, ii) a measure for the vertical jet velocity (in relation to the ambient velocity for example) and iii) a combination of a width and a concentration or dilution at each point of the centreline.

A crossflow on the buoyant jet will create pressure drag and make the plume start to bend over. Due to turbulent mixing and entrainment the edges of the buoyant jet will lose more vertical momentum and gain more horizontal momentum than its centre. That causes the edges to deflect more easily. As a result the buoyant jet acquires a cross-profile consisting of a pair of counter-rotating vortices. This typical profile is called the vortex(-pair) profile or sometimes kidney shape profile (Rajaratnam, 1976; Lee and Chu, 1993). The formation of this profile is schematically shown in figure 2.3; a more extensive discussion on the formation of the vortex-pair profile will follow later this chapter.

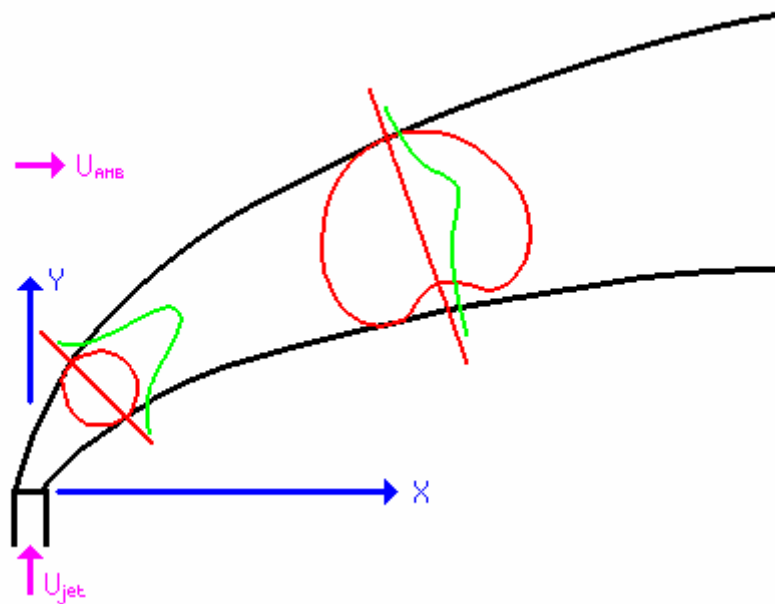


Figure 2.3: The transition from a Gaussian profile (near field) to a vortex-pair profile (far field) of a buoyant jet in a crossflow (Lee and Chu, 1993)

Most descriptions in the vortex-pair profile region however still make only use of the same three parameters as in the Gaussian profile region. The action of the vortices is only taken into account in the (higher) mixing parameters (Lee and Chu, 1993).

For a general overview of buoyant jets asymptotic forms of the jet trajectory are used. The formulations for these asymptotic forms can be deduced by applying conservation of momentum and assuming self-similarity on sections across the jet. The development of those formulations is described in Appendix A. The resulting relationships for the vertical velocity (compared to the ambient velocity), the buoyant jet trajectory (in x-direction) and the dilution for every limiting case are presented in table 2.1 (Fischer *et al.*, 1979; Rodi, 1982). In the formulation of the dilution is  $\mu$  the local specific mass flux and  $C$  the local mean concentration.

Limiting case	Vertical velocity $\frac{W}{U}$	Buoyant jet trajectory $\frac{z}{z_M}$	Dilution $\frac{mU}{M} = \frac{UB}{MgC}$
$z \ll z_M$ jetlike	$z_M/z$	$C_1(x/z_M)^{\frac{1}{2}}$	$D_1(z/z_M)$
$z \gg z_M$ bent jet	$(z_M/z)^2$	$C_2(x/z_M)^{\frac{1}{3}}$	$D_2(z/z_M)^2$
$z \ll z_B$ plumelike	$(z_B/z)^{\frac{1}{3}}$	$(z_B/z_M)C_3(x/z_B)^{\frac{3}{4}}$	$\frac{1}{(z_M/z_B)^2}D_3(z/z_B)^{\frac{5}{3}}$
$z \gg z_B$ bent plume	$(z_B/z)^{\frac{1}{2}}$	$(z_B/z_M)C_4(x/z_B)^{\frac{2}{3}}$	$\frac{1}{(z_M/z_B)^2}D_4(z/z_B)^2$

Table 2.1: Vertical velocity, buoyant jet trajectory and dilution formulations for the four limiting cases of a buoyant jet.

Together with the vertical transition lengths for the behaviour given in figure 2.2, the normalized buoyant jet trajectory can be drawn in a separate graph for both  $z_M < z_B$  and  $z_M > z_B$ . The figures 2.4 and 2.5 show these graphs, using normalization around the first transition point.

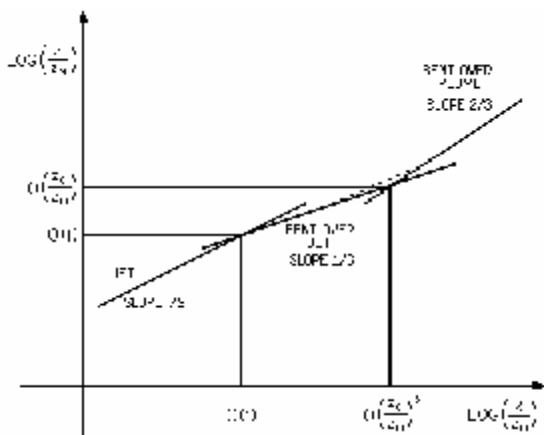


Figure 2.4: Normalized jet trajectory when  $z_M < z_B$  (Fischer *et al.*, 1979)

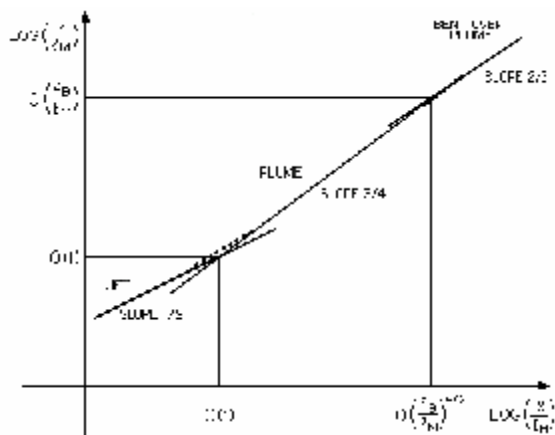


Figure 2.5: Normalized jet trajectory when  $z_M > z_B$  (Fischer *et al.*, 1979)

The coefficients in the formulations of the asymptotic results are determined by experiments. For the asymptotic results these coefficients turn out to be constants. However the investigations show that there is some spread in the values to be adopted. Therefore the term ‘constant’ must be treated with care and the term ‘coefficient’ is rather used. Table 2.2 lists the results of various investigators as brought together by both Fischer *et al.* (1979) and Rodi (1982).

Investigator	Coefficient $C_1$
Hoult, Fay and Forney (1969)	1.8-2.5
Wright (1977)	1.8-2.3
	<b>Coefficient <math>C_2</math></b>
Briggs* (1975)	1.8-2.1
Wright (1977)	1.6-2.1
Chu and Goldberg (1974)	1.44
	<b>Coefficient <math>C_3</math></b>
Wright (1977)	1.4-1.8
	<b>Coefficient <math>C_4</math></b>
Briggs* (1975)	0.85-1.3
Wright (1977)	0.85-1.4 $(z_M/z_B)^2$
Chu and Goldberg (1974)	1.14
	<b>Coefficients <math>D_1</math>-<math>D_4</math></b>
Wright (1977)	~2.4
* Summary of 14 investigations	

Table 2.2: Experimentally determined coefficients used in asymptotic trajectory and dilution formulations. (Fischer *et al.*, 1979)

The formulations above create the possibility to model a buoyant jet. The results should however be treated with care. The results of modelling using asymptotic results only provide order of magnitude estimates for the trajectories and dilutions (Fischer *et al.* 1979). In reality there will be factors that are not accounted for in asymptotic theory. Also the differences in local or instantaneous values compared to long-term averages make the application of these results delicate. The validity of this kind of approach changes for every different ambient situation (Fannelöp, 1994).

Another major drawback of the formulations above is the oversimplification of the problem. Already earlier it was mentioned that the three parameters do not correctly prescribe the (time-averaged) momentum and concentration distribution present in the cross profile of buoyant jets in a crossflow. The formulations presented here are therefore unable to describe the influences of the processes that create those distributions. Furthermore time-averaging makes that the description presented here is not complete in describing all (overflow) plume processes. Information on these processes is therefore treated separately. That is done in the second paragraph of this chapter.

## 2.2 Plume processes

*In the introduction it was said the behaviour of overflow plumes is determined by sediment driven density currents and mixing processes. Here these processes are further investigated. The three processes considered most important, entrainment, vortex behaviour and stripping, are described in more detail. In those sections not only information about these process is discussed, also modelling possibilities are reviewed.*

### 2.2.1 Inventory of processes

A dynamic overflow plume widens, dilutes and bends over during its descent in water with an ambient crossflow. The characteristic behaviour is changing along this descent upon bottom impingement.

Main cause of the widening and the dilution is the entrainment process. Ambient fluid, with a lower concentration and a lower turbulence level than the plume fluid, is entrained by turbulent vortices at the interface between the plume and the ambient fluid. The entrained fluid is further spread along the plume via turbulent diffusion (Delvigne, 1977). The combination of these two processes starts directly beyond the pipe opening and creates a shear layer that will reshape the time averaged velocity profile into one that can be approximated by a Gaussian profile (Fischer *et al.*, 1979). It will continue to stabilize that profile while the plume gets more diluted. When the plume is getting more diluted, the turbulent diffusion (the process that redistributes the momentum and concentration within the plume) becomes more important compared to entrainment (the process that encloses ambient fluid in the plume) (Delvigne, 1977). However, in most descriptions the influence of turbulent diffusion and entrainment processes are not treated separately, but the whole concept of entraining ambient fluid and spreading it over the total plume is called entrainment.

Since entrainment of ambient water is an important process in determining the dilution and other features of dynamic overflow plumes, this process is treated in a separate section in more detail.

When a vertical released buoyant jet descends further from the outlet, the ambient current gets more influence on its behaviour. Horizontal momentum is entrained and drag forces are exerted on the plume causing the plume to bend over. The advection of the plume by the current mostly takes place at the outer layers of the plume. This is caused by the fact that the outer part loses vertical momentum and gains horizontal momentum earlier than the plume centre (Rajaratnam, 1976). The time-averaged cross-profile of momentum gets therewith reshaped to the vortex-pair shape. The two vortices are counter rotating and are diverging. Eventually they might even bifurcate, especially when a boundary layer is approached.

Since the vortex-pair profile is a component of a far-field bent over buoyant jet, it is thought that its creation is important in overflow plumes. Also the influence of vortex divergence on the spreading of overflow plumes and existence of vortex bifurcation in overflow plumes might be worth investigating. Therefore these subjects are worked out further in a later section.

Another interaction between the dynamic dredge overflow plume and the moving ambient fluid is the process called stripping. It comprehends all removal of material from the descending plume by the ambient flow (Thevenot *et al.*, 1992; Baird, 2004). This means that stripped material will be the source term for a passive (far-field) plume model, since it is no longer under the influence of the dynamic plume. It is not clear whether this stripping is a separate process that acts independently or a result of the aforementioned turbulent interactions between the plume edge and the ambient fluid.

Since the material that is removed from the dynamic plume by stripping is a significant source term for far-field modelling, stripping will be treated in a separate section.

The overflow mixture consists of water and sediment. Therefore processes that influence the settlement of (fine) materials such as segregation, hindered settling and convective settling also play a role. However, in the dynamic phase the comparison between the characteristics (momentum and buoyancy) of the overflow mixture and the ambient fluid determines the behaviour whereas the settling behaviour of the individual sediment particles is not a factor of importance (Winterwerp, 2002). Overflow mixture is said to be a single phase fluid. As a result the buoyant jet processes determine the behaviour of the plume and not the sediments where it consists of (Dankers, 2002).

Since the importance is small, sediment settling processes are not further worked out in this M.Sc. thesis.

## 2.2.2 Entrainment process

In most common discussions only the effects of entrainment are discussed. If the process itself is discussed in detail, it is normally split up in only two parts, being turbulent interaction at the plume edge that encloses ambient fluid and dispersion that spreads out the fluid and creates the typical distribution (Fannelöp, 1994; Wood *et al.*, 1993). Modelling entrainment is however based on assumptions that combine both effects. In this section a more refined description of the entrainment process is given before the modelling assumptions are given.

### Process description

The origin of entrainment lies in the difference of turbulence level of the waters within and outside the buoyant jet. The higher turbulence level within the jet creates turbulent shear between the buoyant jet and the ambient fluid. This leads to the establishment of vortices, that are sometimes also called eddies. These vortices are recognizable in all jets and plumes and are shown in the flow visualization of a jet in figure 2.6.



Figure 2.6: Flow visualization of an axi-symmetric turbulent jet.  
(Kurima *et al.*, 1983)

As can be seen in figure 2.6, the created vortices entrap or engulf ambient fluid with lower turbulence level in rolling eddies of jet fluid with higher turbulence level. This is the first step in the entrainment process. It is known as the induction phase, is kinematic by nature and acts on a reasonably large scale known as the turbulent eddy scale (Sreenivas and Prasad, 2000). The induced fluid has not yet acquired any vorticity of its own, but does participate in the large scale structures of the vortical fluid in the jet (Dimotakis, 1986). After the induction phase turbulent straining reduces the spatial scale of the fluid element until it is small enough to come within the reach of the (viscous) diffusive process. This stage is called diastrophy. During this phase viscosity brings vorticity in the fluid as the scale cascades down to the viscous (Kolmogorov) scale (Dimotakis, 1986). In a final phase the (viscous) diffusion process takes over and mixes the induced fluid at the molecular level with the turbulent jet flow (Sreenivas and Prasad, 2000). This final phase is called infusion.

When a buoyant jet is released in a crossflow another process will enhance entrainment. Interactions of the ambient current with the plume edge changes the (time-averaged) cross-profile of the plume and its centreline direction. These interactions consist of deceleration of incoming ambient flow and deflection around the plume. This deflection is comparable to the flow around a rigid structure, but the

boundaries of the plume are compliant and entraining (Moussa *et al.*, 1977). The result is the creation of the vortex-pair shape and enhanced entrainment. The enhanced entrainment is caused by the differences in the normal direction of the velocity, whereas the abovementioned ‘three step’ entrainment process handles about velocity differences in the axial direction (Fannelöp, 1994). Since velocity differences in axial direction results in turbulent shear, the ‘three step’ entrainment process is called shear entrainment. The entrainment process caused by the interaction of the crossflow is called forced entrainment. The two different types are illustrated in figure 2.7.

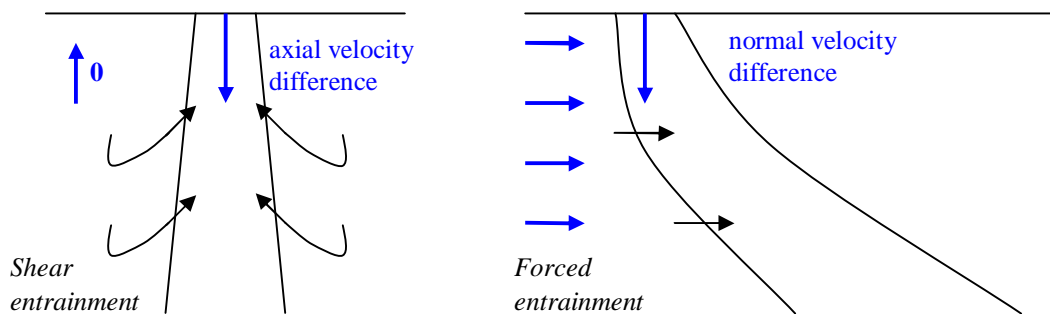


Figure 2.7: Illustration of different types of entrainment

### Entrainment assumptions

For engineering purposes it is not necessary to look into all these phases and corresponding processes in detail. However modelling of plumes requires an understanding of entrainment and its (turbulent) processes. Entrainment ( $E$ ) determines the increase in volume flux ( $Q$ ) per unit plume length ( $s$ ). It is the only factor in the continuity equation of the plume. A formulation for entrainment is needed to close the set of momentum equations and should be based on some assumption on the entrainment processes.

Mostly a (simple) empirical relation for the entrainment rate is used instead of a complex turbulence model (Fannelöp, 1994). Morton, Taylor and Turner (1956) proposed that the shear entrainment velocity is proportional to a local jet velocity scale. When the mean jet velocity is taken as the velocity scale, the formulation for shear entrainment becomes:

$$E_{shear} = 2pbaw \tag{2.11}$$

in which  $b$  is the half width of the plume and  $W$  is the local jet velocity. The factor  $a$  is determined by experiments, and turns out to be different for jets and for plumes. For buoyant jets a transition formulation is needed, since they can behave more jetlike and plumelike. Classically this is done taking the Richardson number as the depending factor (Fischer *et al.*, 1979). More recent results take also the wake-forming characteristics induced by the crossflow into account (Jirka, 2004). The way this is done varies with the modelling technique used. Several shear entrainment formulations are presented in table 2.3 in which  $\sigma$  is the horizontal angle and  $\theta$  the vertical angle with the horizontal plane,  $Ri$  is the (jet) Richardson number and  $Fr$  the corresponding (jet) Froude number and  $U$  is the ambient velocity (Fischer *et al.*, 1979; Rodi, 1982; Lee and Cheung, 1990; Jirka, 2004).

Model	(Shear) Entrainment results
Morton, Taylor and Turner (1956)	$a_{jet} = 0.0535 \pm 0.0025$ $a_{plume} = 0.0833 \pm 0.0042$
Priestley and Ball (1955)	$a = a_{jet} - (a_{jet} - a_{plume}) \left( \frac{Ri}{0.557} \right)^2$
JETLAG (Lee & Cheung, 1990)	$a = \sqrt{2} \frac{\left( 0.057 + \frac{0.554 \sin q}{Fr^2} \right)}{\left( 1 + 5 \frac{U \cos q \cos s}{ W - U \cos q \cos s } \right)}$
CorJet (Jirka, 2004)	$a = \left( a_1 + a_2 \frac{\sin q}{Fr^2} + a_3 \frac{U \cos q \cos s}{W + U} \right)$

 Table 2.3: Model formulations for the shear entrainment factor  $\alpha$ 

In recent modelling also the forced entrainment by ambient crossflow is taken into account. Similarly to shear entrainment the approach connects entrainment to a velocity scale, in this case the ambient crossflow velocity. The general formulation of forced entrainment becomes then:

$$E_{forced} = 2pbU \quad (2.12)$$

The values for  $\beta$  follow from experiments, and also here several formulations for it can be found in different modelling approaches. Table 2.4 gives an overview (Lee and Cheung, 1990; Jirka, 2004).

Model	Forced entrainment results
JETLAG (Lee & Cheung, 1990)	$b = 2\sqrt{\sin^2 q + \sin^2 s - (\sin q \sin s)^2} + p \frac{\Delta b}{\Delta s} \cos q \cos s$ $+ \frac{p}{2} b \frac{(\cos q \cos s - \cos q_{k-1} \cos s_{k-1})}{\Delta s}$
CorJet (Jirka, 2004)	$b = \sqrt{1 - \cos^2 q \cos^2 s} \cdot a_4  \cos q \cos s $

 Table 2.4: Model formulations for the forced entrainment factor  $\beta$ 

In this chapter the effects of the separate modelling formulations are not further discussed, since this chapter aimed at giving an insight in entrainment and the way it is treated in engineering practice. Discussions on the effects of the modelling formulations are, when necessary, put forward in the chapter on the modelling of plumes. An overview of the entrainment results for overflow plumes is presented later in this chapter in paragraph 2.3 where the properties of overflow plumes will be discussed.

### 2.2.3 Vortex pair creation, divergence and bifurcation

A typical feature of a buoyant jet in a crossflow is the formation of the counter-rotating vortex pair in the deflected phase. After formation, the vortices of the vortex pair are continuously diverging. In some cases the vortex pair even bifurcates. To discuss all vortex-related processes properly the source of vorticity for the vortex pair is treated first, followed by vortex divergence and bifurcation. Finally vortex behaviour at bottom impingement is discussed as an example of a boundary approach that might cause bifurcation.

#### Source and creation of counter-rotating vortex pair

Earlier the creation of the counter-rotating vortex-pair (CVP) distribution was explained by the fact that material at the plume edge does deflect more easily than the centre of the jet, since near the edge more ambient momentum is entrained and the drag force exerts most pressure. While simple and correct, it does not comprise a reason to create two separate counter-rotating vortices, since it does not describe any source of vorticity.

A most simple principle for the creation of vorticity is based on the idea that torque is exerted by some sort of shear force exerted by the surrounding flow. Furthermore pressure gradients are introduced. The idea is sketched in figure 2.8. In the green coloured area most shear force is exerted on the plume edge with its centre of rotation somewhere in the indicated yellow circle. As a result rotation around the yellow centres will develop as indicated in red. Finally the cross-section will reshape to the double vortex-shape.

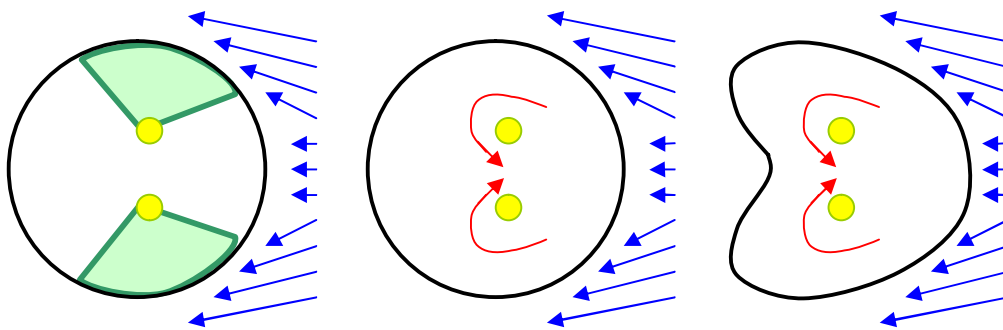


Figure 2.8: Development of vortex pair cross section due to shear forcing at the plume edge and its resulting torque.

Discussion of this principle is not described in great detail in literature. Occasionally a similar shear process called azimuthal shear is mentioned to be the cause of the creation of the CVP (Jirka, 2004), but the exact creation of vorticity is not described in detail. This azimuthal shear process is analogue to the process that creates vortex pairs in thermals as described by Richards (1963), but also Richards (1963) does not present an exact reason for the creation of vorticity. A sketch of the mechanism of azimuthal shear is presented in figure 2.9.

In other discussions of the CVP in literature the source of vorticity is attributed to the vorticity issuing from the nozzle. The CVP is then formed by the thin shear layer

which emanates from the pipe (Kelso *et al.*, 1996; Cortelezzi and Karagozian, 2001). Fric (1990) compared the flux of vorticity from the nozzle with the flux of vorticity in the fully developed CVP and concluded that it is possible for the CVP to evolve from the vorticity emitted from the jet nozzle within the near field. Morton and Ibetson (1996) are opposed to this assumption and state that vorticity cannot be created in the jet nozzle due to the absence of a solid boundary.

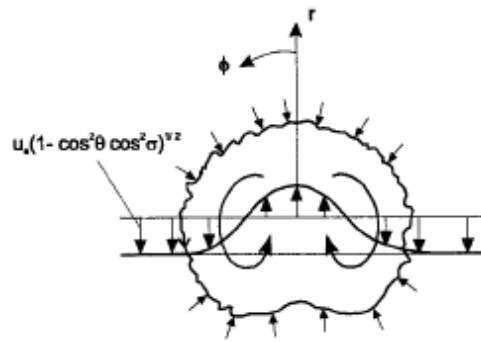


Figure 2.9: Mechanism of azimuthal shear (Jirka, 2004)

All authors do agree on the fact that the CVP and its creation have interactions with other vortex systems created in the near field of the deflected jet. These interactions result mostly in the transfer of vorticity. For further details on these vortex systems and their influence on vortex pair creation in buoyant jets the reader is referred to the research works of Fric (1990), Kelso *et al.* (1996), Morton and Ibetson (1996) and Cortelezzi and Karagozian (2001).

### Vortex divergence

The two concentration centres of the vortex pair cross profile created in the bent over phase of a buoyant jet diverge. Under the influence of the vortex flow the concentration centres are constantly moving out of each other while the profile stays united. The amount of divergence in a plume depends on the relative magnitude of the circulation flow created by buoyancy and momentum flux compared to the turbulent mixing (Lee and Chu, 2003). This results in concentration cross profiles ranging from near Gaussian with one concentration peak via the kidney shape to near-bifurcated plumes.

Cheung (1991) also investigated the divergence of buoyant jets in a cross current. He defined a statistical parameter  $L$ , measuring the degree of concentration separation, to indicate the effect of the vortex flow on the concentration distribution. The result on the concentration distribution showed that  $L$  depended very much on the relative magnitudes of momentum, buoyancy and ambient current. To characterize the relative vortex strength a comparison is made between the ambient velocity and the vectorial velocity  $\hat{u}$  which is defined as:

$$\hat{u} = \frac{U}{4r^2} (z_M^2 + z_B x) \quad (2.13)$$

In which  $x$  is the downstream distance,  $z_M$  and  $z_B$  are the momentum and buoyancy characteristic length scales respectively and  $\hat{r}$  represents the characteristic width which is depending on the downstream stream distance following:

$$\frac{\mathbf{r}}{r} \sim \left( z_M^2 x + \frac{1}{2} z_B x^2 \right) \quad (2.14)$$

The determination of  $L$  on the relative vortex strength could not be presented by a function due to the statistical character of  $L$ , but the dependency is demonstrated graphically by Cheung (1991). The diagram is reproduced as figure 2.10.

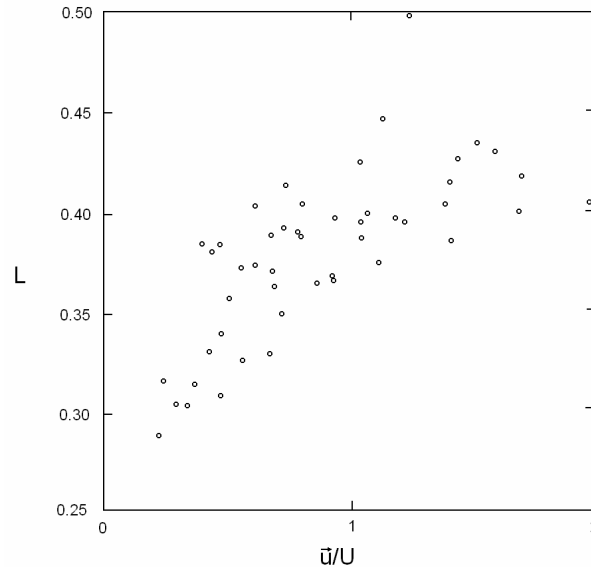


Figure 2.10: Correlation of  $L$  with  $\frac{u'}{U}$  (Cheung, 1991)

A slightly different definition of the process was used by Fischer *et al.* (1979) who also investigated the divergence of buoyant jets, but denominated it bifurcation. They found that the bifurcation angle (that in the nomenclature of this M.Sc. thesis better is called divergence angle) is near constant at 8-10°.

The observation that the concentration centres are only diverging at a near constant rate could be explained by assuming that the vortices of the velocity cross-profile do diverge with a constant rate but that the divergence of the concentration centres is depending on the relative vortex strength. The local situation determines to what extent the concentration profile will follow the divergence of the velocity vortices or will be held together by turbulent diffusion influences.

### Vortex bifurcation

Unlike Fischer *et al.* (1979) vortex bifurcation is defined here as the extremity of vortex divergence where the concentration peaks are so much separated that clean, unmixed ambient fluid enters the centreline and the plume is split into two separate elements. Usually bifurcation only occurs when the (buoyant) jet approaches a boundary, as there the divergence rate increases. That boundary might either be the bottom in negatively buoyant jets released vertically downwards, the water surface for vertically upwards released positively buoyant jets or density stratification for either of the types (Hodgson *et al.*, 1999; Jirka and Fong, 1981; Abdelwahed and Chu, 1978; Scorer, 1959).

It can be visualized that in homogeneous condition the diverging rate of the vortices is only small (and constant) so that turbulent diffusion will be strong enough to keep the profile complete, whereas at a boundary approach the diverging rate will differ and increase, and the diffusion can no longer make sure that no ambient water enters the centre of the plume, so that the plume gets bifurcated. This idea is sketched in figure 2.11.

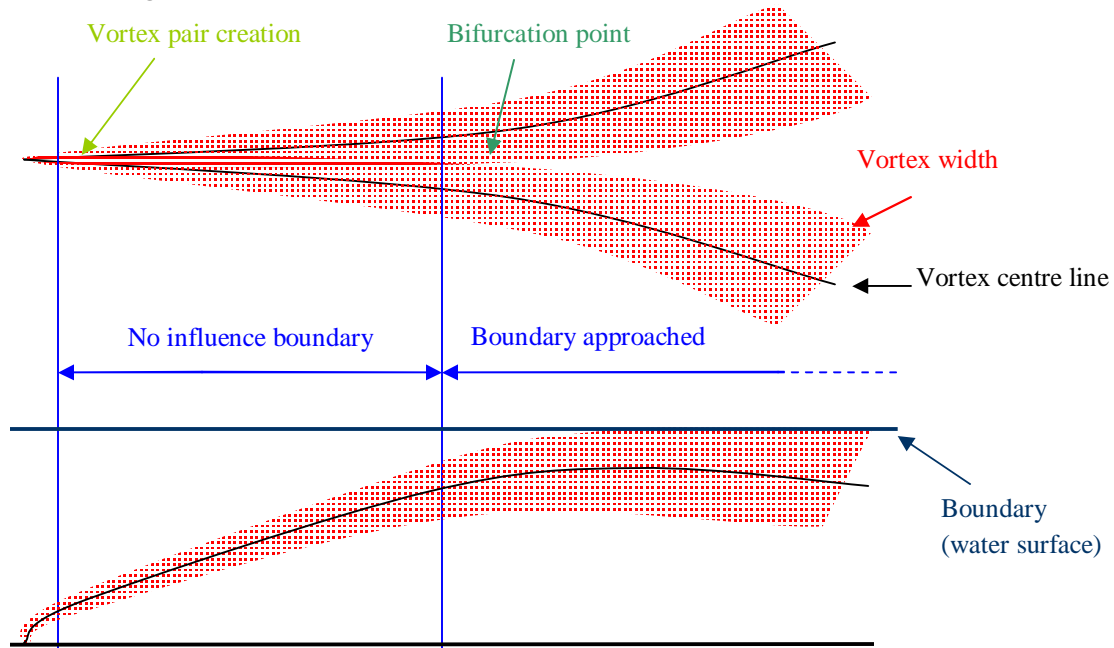


Figure 2.11: Top and side view of vortex bifurcation due to influence boundary (in this case water surface approach)

Hodgson *et al.* (1999) investigated vertically upward released non-buoyant jets in shallow water and related bifurcation to the relative depth, since water surface approach would be the forcing mechanism. The relative depth is defined as  $\zeta D_{pipe}/h$ , in which  $\zeta$  is the velocity scale,  $D_{pipe}$  is the initial jet diameter and  $h$  is the channel depth. It turned out that for  $\zeta D_{pipe}/h > 0.42$  the jets all bifurcated, if the data by Abdelwahed and Chu (1978) was also used even for  $\zeta D_{pipe}/h > 0.34$ . For buoyant jets it is discussed that this value might be smaller. What this means for downward released negatively buoyant jets such as the overflow is not discussed.

Jirka and Fong (1981) formulated a bifurcation criterion based on local properties of the buoyant jet. Bifurcation occurs when the external forcing, the repulsive force due to boundary approach, becomes larger than the binding force of the plume. This binding force is determined from the turbulence level, based on Lilly (1964) who stated that the level of internal turbulence determines whether a vortex element holds together or splits under the influence of an external forcing. To keep the formulation simple, the so-called repulsive force induced spreading rate is used and compared with the turbulent growth rate.

For detailed formulation of their total model including bifurcation the reader is referred to Jirka and Fong (1981), but again no details about implementing vortex behaviour at bottom impingement of overflow plumes are presented here.

**Vortex behaviour at bottom impingement**

An interesting boundary approach for overflow plumes is bottom impingement. As in homogeneous surroundings the overflow plume is not likely to bifurcate, bottom approach or impingement is the boundary approach in overflow plumes that might give reason to bifurcation. Although the bottom indeed can be seen as a boundary that could create bifurcation on the one hand, on the other hand the properties of the bottom might create objections to (vortex) circulations and therewith oppose bifurcation and even create convergence. Both ideas are sketched in figure 2.13.

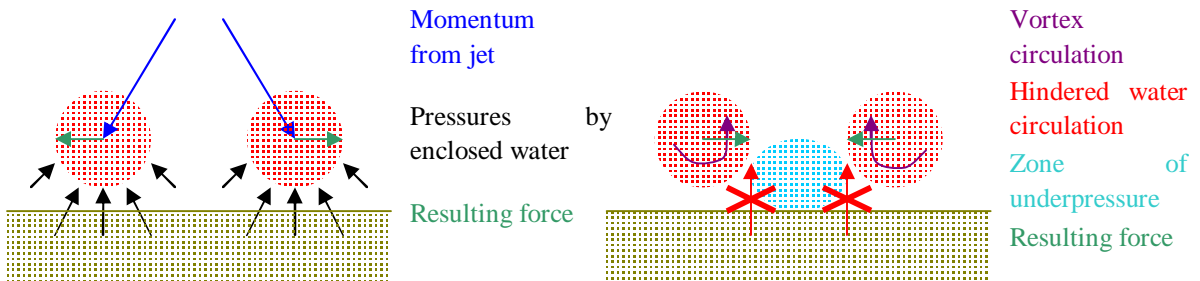


Figure 2.13: Sketch of bottom influences possible (left: bifurcation, right convergence)

## 2.2.4 Stripping

Unlike the entrainment process and the processes related to the vortex behaviour the processes causing stripping are not clearly defined. In fact there is even not a clear definition of stripping. The process has never been investigated separately.

Sometimes stripping is referred to as the result of entrainment and other turbulent processes (Dankers, 2002) while in other cases it is treated as an advection process by ambient currents (Thevenot *et al.*, 1992; John *et al.*, 2000). In this M.Sc. thesis stripping is defined as the removal of material from the dynamic plume into the ambient fluid caused by the interaction between the plume and the (continuous) crossflow. In this definition the exact processes of stripping are left undefined as are the influencing parameters.

From more general reviews of dredge overflow plumes it becomes clear that stripping must consist of (at least) two mechanisms: exchange of material over the plume boundary and advection by the crossflow. The need for an advection process is clear, since material must be removed from the plume edge but the exchange mechanism over that plume edge is more peculiar. On the one hand it would seem plausible that this mechanism is connected to the vortices or eddies created by the shear at the plume edge, since these are highly dynamic and irregular. On the other hand stripping by the use of these eddies is contradicted by the one-way movement of ambient water into the plume that causes entrainment (Baird, 2004). Possibly stripping is caused by the break up of some of the vortices that normally entrain water into the plume.

Also quantitatively not much is known about stripping. In some earlier work (Van der Salm, 1998; Boot, 2000) the loss of sediment by stripping is estimated at 3-5% of the total amount of sediment making use of the results by Gunter *et al.* (1964). However, that report does not mention stripping at all and discusses only the effects of disposal of dredged material in Chesapeake Bay. The paraphrase referred to states that "... the total fine sediment that will be resuspended in the water will amount to only about 3 to 5 per cent of the sediment brought into the bays by the rivers every day." (Gunter *et al.*, 1964). The estimation of stripping by Van der Salm (1998) and Boot (2000) is therefore thought to be incorrect. Also other references do not provide numerical estimates for the stripped material but conclude only that the amount of stripped material is small compared to the total plume (Thevenot *et al.*, 1992; Demas, 1995).

## 2.3 Theoretical behaviour of overflow plumes

In the previous paragraphs the main features of buoyant jets and plume behaviour were presented. In this paragraph the results are combined to give a description of the theoretical behaviour of typical overflow plumes. Hereto first some typical values and dimensions for overflow plumes are determined followed by a categorization based on the results by Winterwerp (2002) and on other relevant parameters. After that each type of behaviour is discussed separately. Finally some remarks are made about other phenomena that influence overflow plumes, such as ships movements, air in the overflow mixture and ships propeller disturbance.

### 2.3.1 Typical parameter values for overflow plumes

Numerical values for all parameters are needed in order to know something about the behaviour of overflow plumes. Therefore the range of possibilities for each parameter in practice needs to be known. In table 2.5 that range is presented for each parameter with a short explanation.

Parameter	Value/range	Unit	Explanation
$D_{pipe}$	1.5 – 4.0	m	Estimates based on overflow pipes in ships of Van Oord
$W_o$	0.5 – 1.5	m/s	Estimates based on production and pipe diameter figures
$g$	9.81	m/s <sup>2</sup>	Constant
$\rho_{mix}$	1040 - 1090	kg/m <sup>3</sup>	Estimates based on stage in production process
$\rho_{amb}$	1020 - 1030	kg/m <sup>3</sup>	Near-constant, depending on temperature and salinity
$U$	0 - 4.0	m/s	Estimates based on ship speeds
$h$	5 – 45 (100)	m	Known depth limits for hopper dredgers

Table 2.5: Typical value range for parameters in overflow plumes

The overflow pipe diameter is typical for the ship. Looking at ships in the fleet of Van Oord it can be seen that in small (inland) hoppers overflow pipes are installed with diameter as small as 1.5 m. But large, sea-going hoppers can have overflow pipe diameters up to 3.8 m. The typical overflow diameter of a large sea-going vessel considered here is about 3 m.

The vertical jet velocity is determined by the overflow discharge and the overflow diameter. The overflow discharge is by definition the same as the discharge with which material is sucked up by the suction pipes. That discharge differs for every hopper, as variation in loading time is usually small at about 20-90 minutes (Bray *et al.*, 1997). The discharge varies between 1 m<sup>3</sup>/s for very small ships (capacity about 1000 m<sup>3</sup>) and 15 m<sup>3</sup>/s for very large ships (capacity about 18000 m<sup>3</sup>). Taken into account the fact that small ships have small overflow pipes the variance in overflow velocity is somewhat smaller than the variance in the discharge. For small ships 0.5 m/s gives an estimation, for large ships about 1.5 m/s can occur. The typical value for the jet velocity of a normal hopper (capacity about 7500 m<sup>3</sup>) with a 7.5 m<sup>3</sup>/s discharge through an overflow pipe with a diameter of 3 m is about 1.0 m/s.

The density of the overflow mixture is depending on the concentration of the mixture of sand and water sucked up by the suction pipes, the particle size distribution of the

dredged material and the density of the sediment. Van der Schrieck (2000) indicates that the mixture concentration that is sucked up is usually about 20-25% and that the overflow is about 5-15% of the material in that mixture in normal conditions. With a sediment density of  $2650 \text{ kg/m}^3$  and a seawater density of  $1025 \text{ kg/m}^3$  the corresponding overflow densities can be calculated. The minimum is estimated at about  $1040 \text{ m}^3/\text{s}$  and the maximum at about  $1090 \text{ m}^3/\text{s}$ . It must be stated that the amount of overflow can increase when dredging is continued when the hopper is already full. Then the concentration can even be far higher. The typical value is thought to be  $1060 \text{ kg/m}^3$ .

The density of the ambient water is the density of seawater. The density of seawater varies with the temperature of the water and the salinity. The normal range is about  $1020\text{-}1030 \text{ kg/m}^3$  but  $1025 \text{ kg/m}^3$  is considered the normal and constant value.

The velocity of the ambient water relative to the ship is the superposition of the ships velocity and the ambient current. For the ships velocity with respect to the bottom Bray *et al.* (1997) proposes 1-5 knots. Because an ambient current of about  $1.5 \text{ m/s}$  is still considered workable, the variation of the ambient water velocity ranges from  $0 \text{ m/s}$  to about  $4 \text{ m/s}$ . A common relative ambient velocity of the water is estimated to be about  $1 \text{ m/s}$ , since the direction of the ambient current and the ships velocity not necessarily have to coincide.

Bray *et al.* (1997) gives the boundary conditions where trailing suction hopper dredgers can still operate. Minimum water depth for small hoppers is about  $4 \text{ m}$ , maximum water depth about  $45 \text{ m}$ . With a few very large hoppers this might be increased to even  $100 \text{ m}$ . The economic depth for a hopper is about  $35 \text{ m}$ . Another relevant depth for the Dutch situation is the water depth at the North Sea, which is about  $20 \text{ m}$ .

### 2.3.2 Categorization of overflow plumes

The data collected in the paragraph above is used to define three cases: the minimum, the maximum and the typical case. For each of them the corresponding relevant parameters are presented in table 2.6.

Case	Minimum	Typical	Maximum
Initial volume flux ( $Q_0$ )	$0.88 \text{ m}^3/\text{s}$	$7.07 \text{ m}^3/\text{s}$	$18.85 \text{ m}^3/\text{s}$
Initial specific momentum flux ( $M_0$ )	$0.44 \text{ m}^4/\text{s}^2$	$7.07 \text{ m}^4/\text{s}^2$	$28.27 \text{ m}^4/\text{s}^2$
Initial specific buoyancy flux ( $B_0$ )	$0.13 \text{ m}^4/\text{s}^3$	$2.37 \text{ m}^4/\text{s}^3$	$11.73 \text{ m}^4/\text{s}^3$
Jet Richardson number ( $Ri$ )	0.86	1.00	1.11
Velocity scale ( $\zeta$ )	0.00	1.00	2.67

Table 2.6: Values for relevant parameters in three cases.

However, when four main variables are considered ( $D_{pipe}$ ,  $W$ ,  $U$  and  $\rho_{mix}$ ) there are more (81) combinations possible. They are listed with their corresponding parameter values in appendix B. Although some of these combinations are not likely to occur the list does show what overflow plumes are possible. To discuss the extremities in parameter values possible the range of results is presented in table 2.7.

Parameter	Range of results	Unit
Initial volume flux ( $Q_0$ )	0.88-18.85	$m^3/s$
Initial specific momentum flux ( $M_0$ )	0.44-28.27	$m^4/s^2$
Initial specific buoyancy flux ( $B_0$ )	0.13-11.76	$m^4/s^3$
Characteristic length scale $l_Q$	1.33-3.54	m
Characteristic length scale $l_M$	0.73-7.45	m
Characteristic length scale $z_M$	0.17-5.32	m
Characteristic length scale $z_B$	0.00-11.73	m
Jet Richardson number ( $Ri$ )	0.10-9.95	-
Velocity scale ( $\zeta$ )	0.00-8.00	-

Table 2.7: Range of values for governing parameters in overflow plumes.

Striking are the large differences in range between the characteristic length scales indicating the existence of overflow plumes that show plumelike behaviour before they are fully established ( $l_M < l_Q$ ) or even bent over before the ZFE ends ( $z_B$  or  $z_M < l_Q$ ). The result is that four types of behaviour are possible after the ZFE, being jetlike, plumelike, bent jetlike and bent plumelike. Which type of behaviour is possible is depending on the combination of length scale magnitudes. Figure 2.14 schematically shows which combination delivers which behaviour.

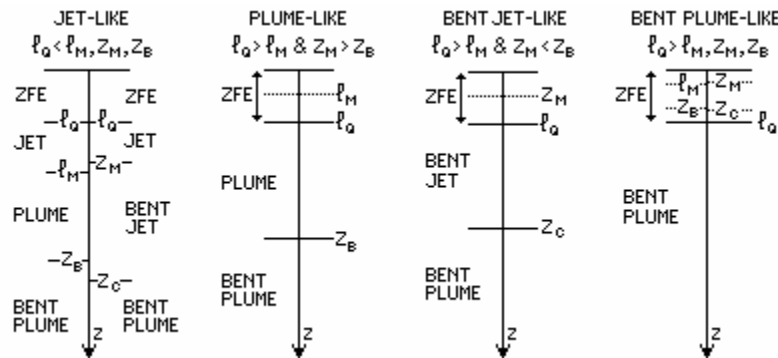


Figure 2.14: Relative magnitude of length scales determines the behaviour type

The large range in both Richardson number and velocity scale in table 2.7 shows that both passive and dynamic plumes can be expected. To show whether a plume is dynamic or passive, the classification by Winterwerp (2002) is used, keeping in mind that the transition zone might be different because of the effects of different depths. In figure 2.15 the Richardson numbers and velocity scales of all data points are plotted. The type of behaviour directly after the ZFE, based on the length scale combination as described above, is also indicated using different colours to mark the different behaviour types. Next to that the classification of plumes by Winterwerp (2002) is also shown in figure 2.15.

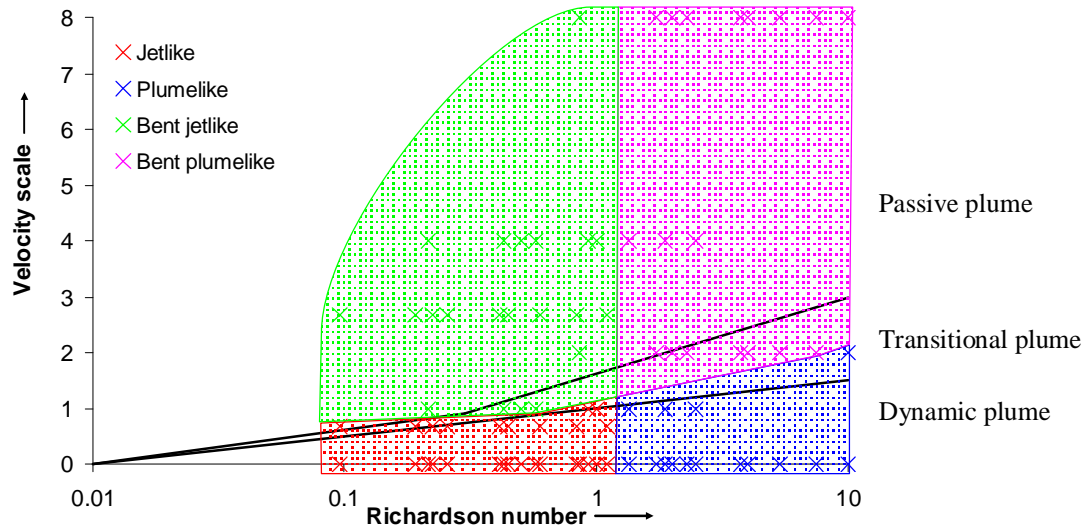


Figure 2.15: Plot of Richardson numbers and velocity scales of data points.

The results obtained must be treated with care. Since the approach with length scales is used only asymptotic behaviour is investigated, so the transitions indicated are in reality smoother. Furthermore, in many cases the length scales of the transitions in behaviour are smaller than the length scale of the ZFE. What that means for the behaviour of the transition and the resulting plume is not described in common literature. The graph of figure 2.15 is created by assuming that those transitions take place completely within the ZFE and that the behaviour of the plume after the ZFE is the one corresponding to the last length scale passed, just as shown in the schematic picture of figure 2.14.

Despite those comments, figure 2.15 provides very useful information. Overflow plumes, with low Richardson numbers are more jetlike, while higher Richardson numbers yield more plumelike behaviour. A low velocity scale indicates unbent behaviour, whereas overflow plumes discharged into stronger ambient currents will show bent-over behaviour. The four plume types described can therefore be treated as the extremities of the overflow plume behaviour. The visual concurrence that might be observed between the transition between dynamic and passive overflow plumes and the length scale transition to bending over within the ZFE length is thought to be coincidental. These phenomena are completely different and there is no theoretical background for the existence of any link between them. The two classifications should therefore be treated separately as is done in the next section.

### 2.3.3 Description of the typical behaviour of the overflow plume

Only for the jetlike case detailed information is present in literature. In literature descriptions that use the same length scales approach as put forward here only state that the method loses its validity in cases where the buoyant jet is not jetlike directly after the ZFE. This makes the definition of the behaviour of the other three types quite difficult. However, by combining information on the 'established' variant of these types and information gathered in other approaches a workable description can be obtained.

**The jetlike type**

An overflow plume with a low velocity ratio and a low Richardson number is established similarly to a jet. In the (short) ZFE the overflow plume stays nearly vertical and the initial vertical momentum dominates the behaviour. However in the ZEF the vertical momentum generated by the buoyancy increases and also horizontal momentum is acquainted by the entrainment of ambient fluid and by the drag force exerted by the crossflow. Depending on the relative magnitude of the buoyancy to the ambient horizontal momentum the overflow plume first bends over and then changes to a plume or the other way around. The time averaged concentration profile is in the beginning nearly a Gaussian profile but changes slowly to the vortex-pair profile when it is bent over and changed into a plume. Eventually these vortices might bifurcate when the bottom is approached. Either way the overflow plume does not show extended mixture over the whole water column.

**The bent jetlike type**

An overflow plume with a high velocity ratio and low Richardson number is influenced by the horizontal momentum of the ambient current at the moment it leaves the orifice. The material at the plume edges is taken up by the ambient current first. That makes that the creation of the vortex-pair profile takes place as the flow establishes. Since the plume is at the end of the ZFE already bent over there is a long trajectory needed before the plume reaches the bottom. In this long trajectory significant dilution can take place. Also the strong ambient current enhances (turbulent) mixing. This makes that this overflow plume can be treated as passive and that the concentration profile gets vague. Finally the material is mixed over the whole water column.

**The plumelike type**

An overflow plume which is of the plumelike type has a relatively small initial momentum. Since the ambient current is also relatively small the overflow plume does not bend over in the ZFE but establishes as a plume. The trajectory will be more horizontal than the jetlike type, but the time averaged concentration profile will be comparative to the Gaussian profile. After some time, depending on the initial momentum and the magnitude of the crossflow the plume starts to bend over. Similarly as in other behaviour types the vortex-pair profile is created when the plume is bent over. The plume does not spread widely before impinging the bottom, but vortex bifurcation is possible.

**The bent plumelike type**

An overflow mixture discharged at a high Richardson number in a strong ambient current will behave plume like and bend over while the flow is still establishing. This establishing will be quite irregular and most material will be removed at the plume edges. At the end of the ZFE (if a ZFE can be indicated) the vortex-pair shape will be formed more or less. However mixing processes mainly determine the behaviour of the plume, so the plume will result soon in a passive plume which is mixed entirely over the water column.

**Dynamic vs. passive**

Of the four types described above, two result in more dynamic plumes and two in more passive ones. The difference within dynamic or passive plumes, being more jetlike or plumelike behaviour, is very small in practice. The transition between the

two is smooth and overflow plumes are mostly in that transition zone. That makes the distinction quite academic. Most research on overflow plumes in particular does therefore merely focus on the dynamic or passive behaviour. A sketch of a dynamic overflow plume is given in figure 2.16.

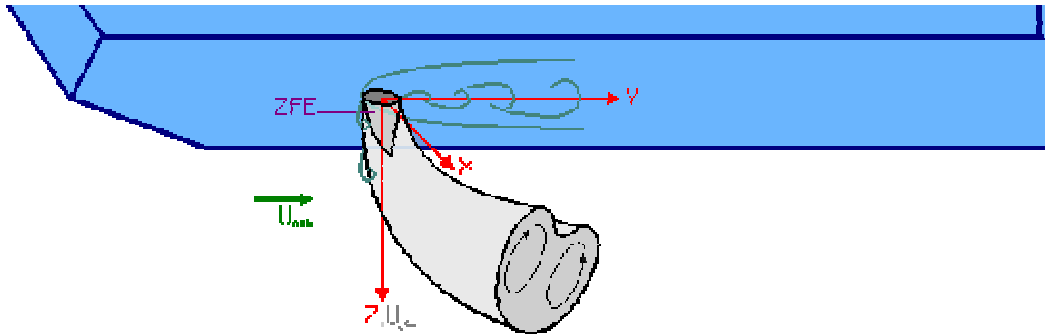


Figure 2.16: Sketch of a dynamic overflow plume (free after: Su and Mungal, 2006)

### 2.3.4 Entrainment of overflow plumes

In the second paragraph of this chapter, entrainment was discussed as an important process that is typical for the behaviour of the plume. Several methods to estimate the amount of ambient fluid entrained per meter plume were presented. Here the entrainment of overflow plume is discussed followed by the presentation of some numerical estimates on the amount of fluid entrained by overflow plumes based on model predictions for the typical overflow plume that is discussed in section 2.3.1.

The entrainment of overflow plumes is not different from entrainment of any other buoyant jet: it is determined by the turbulence level within the plume (hence the local velocity) and the surface area of the plume/ambient water interface (John *et al.*, 2000). The magnitude of the ambient current might also be of (secondary) influence, since also forced entrainment has to be taken into account.

Numerical estimates for overflow plumes are usually calculated for a small part of the plume, since the magnitude of the entrainment is depending on local parameters that are continuously changing. To give an idea about the order of magnitude of entrainment in overflow plumes the 'typical' overflow plume is modelled with CORMIX software (using the CorJet model) and for each presented point of the plume the entrainment is calculated using the CorJet entrainment formulations presented in table 2.3 and 2.4 by filling in all local parameter values. To compare the entrainment rate the specific volume flux at each point is presented too. The results are presented in table 2.8.

The entrainment thus calculated is somewhat smaller than one would derive from the specific volume flux increases (since entrainment is the only factor in the continuity equation the volume flux increase per unit plume length should be exactly the same as the entrainment). This is due to the fact the method developed here is crude. Every calculation step presented in each row in table 2.8 consists of 50 timesteps in the model and the plume centreline angles could only be calculated by taking the

average angle of these 50 timesteps. Still, table 2.8 provides a useful first assessment for the order of magnitude of entrainment. More details on the calculation of entrainment in CorJet will be treated in chapter 3, paragraph 3.3.

$X$ (m)	$Y$ (m)	$Z$ (m)	$S$ (-)	$b$ (m)	$E$ (m <sup>2</sup> /s)	$Q$ (m <sup>3</sup> /s)
0,00	0,00	41,00	1,0	1,50	-	7,07
0,00	0,00	41,00	1,0	1,50	5,46	10,00
13,30	0,00	32,58	6,5	3,04	3,93	65,32
25,69	0,00	27,77	12,7	4,27	4,09	127,55
38,31	0,00	23,59	19,9	5,38	4,26	200,11
51,05	0,00	19,80	28,0	6,40	4,48	280,31
63,86	0,00	16,28	36,7	7,35	4,59	367,26
76,74	0,00	12,96	46,1	8,26	4,74	460,71
89,65	0,00	9,81	56,0	9,12	4,88	558,56
102,60	0,00	6,79	66,4	9,94	4,97	661,17
115,57	0,00	3,88	77,2	10,74	5,16	768,61
128,56	0,00	1,08	88,4	11,51	5,15	880,55

Table 2.8: CorJet model prediction of typical overflow plume extended with entrainment and specific volume flux.

### 2.3.5 Other phenomena influencing overflow plumes

The descriptions above did not take into account typical phenomena that influence overflow plumes released from a sailing ship on the sea. Here the effects of ship movements, entrapped air, propeller induced turbulence, density stratification and wave action are shortly discussed.

#### Ship movement

Mainly due to waves ships continuously move. There are six degrees of freedom a ship experiences: three translations and three rotations. The translations are heave (vertical), sway (lateral) and surge (longitudinal). The rotations are roll (around the longitudinal axis), pitch (around the transverse axis) and yaw (around the vertical axis). They are visualized in figure 2.17.

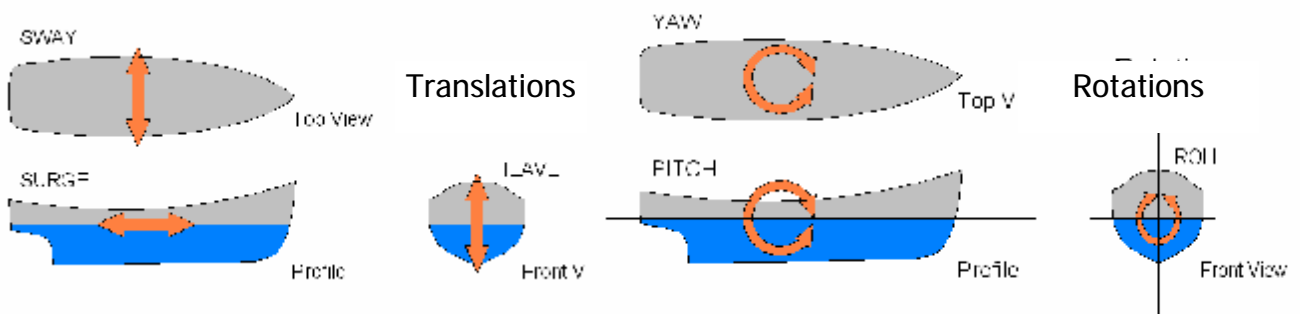


Figure 2.17: Visualizations of degrees of freedom of ships.

Due to the ship movements the direction and magnitude of the overflow discharge is far from continuous. However, since the variation is considered small with respect to the magnitude of the ship length or water depth for instance, these effects on the discharge are usually neglected.

An effect of ship movements and the resulting discontinuous overflow discharge is the possibility of air entrapment in the overflow pipe. This phenomenon does have significant influence and is more often discussed in literature. Therefore it is discussed separately.

### Entrapped air

The presence of air makes the overflow mixture less dense or even positively buoyant. The result is a weaker density current and therefore a shorter dynamic phase, its spreading will occur by advection and mixing only (Winterwerp, 2002). Due to the irregular behaviour of air entrapment the overflow plume is no longer continuous but behaves as different clouds of sediment, water and air bubbles as can be seen in figure 2.18 (Dankers, 2002). Overflow plumes which contain air will suspend more material at the water surface as a result (John *et al.*, 2000).

To reduce the entrapment (or entrainment) of air bubbles a hopper dredger can be equipped with an Anti Turbidity Valve (ATV) in the overflow pipe. With the ATV the head loss in the overflow pipe and therewith the water level at the overflow intake can be regulated. The water level should be kept large enough to make sure that the overflow intake behaves as a submerged spillway, so that no air can be entrapped (Van der Schrieck, 2000).

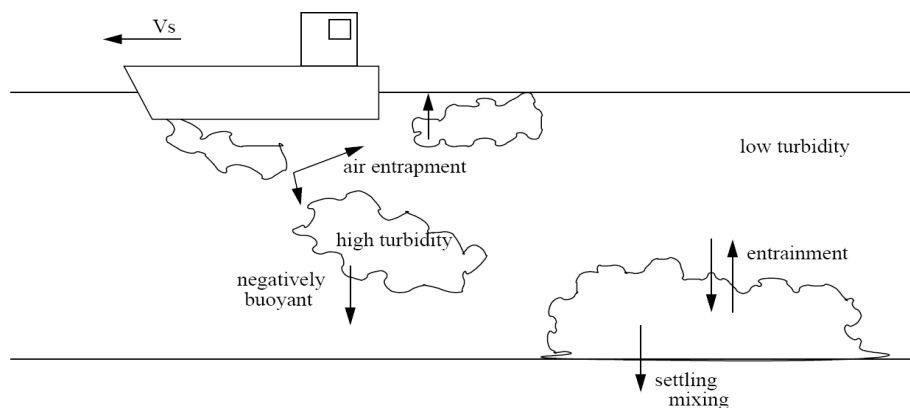


Figure 2.18: Cloud formation in overflow plumes containing air (Dankers, 2002)

In this M.Sc. thesis the effect of air entrapment is not taken into account, as it is known to be too difficult to simulate on scale. The overflow plumes considered in this thesis are continuous dynamic or passive plumes.

### Propeller induced turbulence

The propeller of a hopper dredger produces a wake behind the ship. In that wake turbulence is higher and higher mixing and entrainment might take place. The overflow plume can be influenced by these mixing and entraining effects. An idea of the effect of this phenomenon is sketched in figure 2.19.

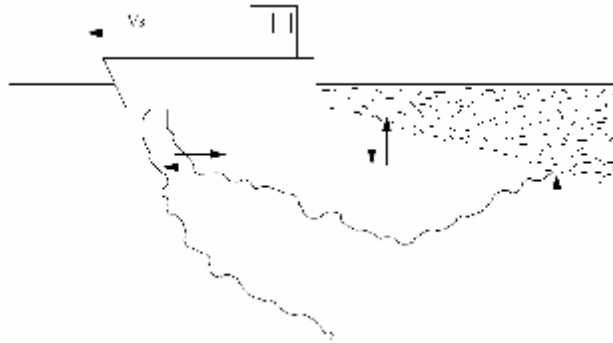


Figure 2.19: Influence of ship's propeller mixing effects (free after: Dankers, 2002)

The propeller may increase the overall mixing but it does not affect the classification diagram which distinguishes between the importance of mixing and density currents (Winterwerp, 2002). Since propeller action takes place well behind the ship, its induced turbulence might rather be treated as a mid-field process affecting the (passive) plume rests. In this M.Sc. thesis propeller induced mixing effects are not considered.

### Density stratification

In the ocean temperature and salinity variations exist over depth creating density differences. Usually the density increases with depth. As a result, plumes will sink continuously slower due to the reduced buoyancy difference and can even stop sinking at a so called terminal height of rise where the buoyancy difference is zero. In literature the buoyant jet in a crossflow with density stratification is well known and described. In this M.Sc. thesis however it is not taken into account.

### Wave action

The presence of waves in the ocean can influence the dispersive properties of the overflow plume. Since (ocean surface) waves create orbital motion which decreases with depth, more dispersion might take place near the surface when compared to a situation without waves. Usually this process is referred to as differential advection by wave motion. Mostly the effects of wave action are taken into account in higher diffusion rates in far-field computations. For (dynamic) near-field effects, wave action is normally considered a secondary effect. That is also done in this M.Sc. thesis.



## Chapter 3: Modelling of plumes

*In engineering practice, the theoretical behaviour of plumes is not described in detail, but a numerical approximation is made with the use of models. The principals of these models are discussed in this chapter. First the several approaches of modelling present are discussed, followed by some comments on the possibilities and need to improve and extend these different approaches. Finally, to present an example of a model, the working of the CORMIX model is explained.*

### 3.1 Approaching modelling of plumes

*The mathematical modelling of overflow plumes or buoyant jets in general faces difficulties with the complexity of the problem and large number of influencing parameters. The theoretical influences of these parameters are discussed in chapter 2. Simple calculation models cannot take every detail of these influences into account. The amount of details captured and the complexity of the model is depending on the modelling approach used. The first section shows that three categories of approach can be distinguished, the following sections deal with the separate categories.*

#### 3.1.1 Main modelling categories

The difficulty of modelling buoyant jets in general and dynamic overflow plumes in particular is that its behaviour is depending on a large number of influencing parameters. Several approaches to take these parameters into account are possible and usually they are categorized in three categories: jet-integral models, three-dimensional numerical (field) models and length-scale (or flow class) models (Jones *et al.*, 1996).

##### Jet-integral models

Jet-integral models approach the problem by looking at the plume as a whole. The cross-profile distribution of the velocity and concentration is thought to be self-similar for the whole buoyant jet. This reduces the set of partial differential equations into a set of ordinary differential equations. The result is that relatively simple numerical schemes can be used to determine the development of jet properties in time.

##### Numerical field models

Numerical (field) models determine the velocity components, local density and concentration for each point in the flow field. No assumptions are made on the behaviour of the plume, and the partial differential equations are solved numerically. Difficulties herein are the formulation of turbulent transport terms and the correct specification of boundary conditions.

##### Length scale models

Length scale or flow class models approach the buoyant jet in a similar way as the jet-integral approach, but divide the buoyant jet in different compartments. The compartment boundaries are determined by characteristic length scales (hence the name length scale models). For each compartment the buoyant jet is classed (hence

the name flow class models) differently and uses another (empirical) formulation for the development of the jet properties.

### 3.1.2 Jet-integral models

There are different jet-integral models. This paragraph provides similarities between these models as well as some points of distinction between them. The philosophy behind jet-integral modelling is provided, not the formulation of typical jet models. For typical formulations of jet-integral models the reader is referred to Jirka (2004) and Lee and Chu (2003).

One of the main characteristics of plume modelling with a jet-integral model is the a priori specification of the concentration, density and velocity distribution in the cross profile. That specification makes jet-integral models a simplified approximation for a general buoyant jet which develops these profiles depending on the ambient conditions. Taken into account that those distributions must be valid for the whole buoyant jet, the Gaussian profiles that are commonly used seem to be the most reasonable.

Jet-integral models can be formulated either in a Lagrangian framework or an Eulerian one. In a Lagrangian framework one jet element is followed and its development is described. It is advected with the local velocity along the trajectory and during that advection the element is transformed by several processes. In an Eulerian framework the evolution of the jet is given with respect to a global coordinate system. The framework adopted is a main point of distinction between jet-integral models. Generally, a Lagrangian formulation is more convenient in the final stage of buoyant jets. Eulerian formulations are usually simpler for the initial jet stages. The decision on which framework has to be adopted is usually based on the importance of the near-field or the far-field effects.

Jet-integral models usually describe the development of the integral quantities of the plume being the total volume flux  $Q$ , axial momentum flux  $M$  and buoyancy flux  $B$ . The starting values of these integral quantities were given by equations (2.1), (2.2) and (2.3) in the previous chapter. Since the whole plume is looked at, the integral quantities are usually conserved and only change by interactions over the boundary of the plume.

Examples of important interactions present between the plume and its surrounding are the turbulent entrainment of ambient fluid and the drag force exerted by the ambient crossflow. For these (turbulent) processes empirical assumptions are needed. For entrainment those assumptions were presented in the previous chapter section 2.2.2. For the drag force assumptions can be made in a similar way. The definition of these assumptions is a typical point of distinction between several integral models and there is a large variety between them.

The applicability of the jet-integral method is a major point of discussion. In order to be applicable for buoyant jets in general any jet-integral approach should as a minimum be consistent with the asymptotic cases as described in chapter 2 and presented in table 2.1. In these cases the buoyant jet indeed behaves as a self-

similar flow. The formulation of the transitions between these cases is arbitrary and should be formulated in order to obtain good data fit (Jirka, 2004). Jet-integral models are not longer applicable when strong spreading or curvature makes that the jet-type character (i.e. the self-similarity of the cross-profiles) of the buoyant jet gets lost. The ZFE is an example of a region where this is the case and the jet-integral models are normally not able to correctly describe this ZFE. However, since the ZFE is usually short compared to the region of interest, an empirical formulation is appropriate to take the ZFE into account.

As the concentration cross profile is predefined, any changes therein are not taken into account in jet-integral models. As most models choose for a Gaussian cross profile, the formation of the vortex-pair cross profile and the divergence or bifurcation of these vortices cannot be taken into account.

The applicability of jet-integral models always ends within some spatial restrictions. Beyond these limits, which are specific for every jet model, the outcome of the model is nonsensical. This especially holds when physical boundaries, such as the bottom, are approached (Jirka, 2004).

### 3.1.3 Numerical (field) models

Numerical models start the analysis of the buoyant jet in crossflow from general conservation laws stated in partial differential equation form (Demuren, 1994). By doing that, no prerequisites are laid on the behaviour of the plume. That creates potential for wide generality and applicability.

For the velocity field the Navier-Stokes equations are used and corresponding concentration equations are used for the concentration field. However, for modelling the overall quantities of the buoyant jet, time-averaged forms of these equations must be used. The process of time-averaging introduces a closure problem due to non-linear correlations between turbulent velocity and concentration field. For that closure a turbulence model has to be used. In this turbulence model the empirical input required for this type of modelling shows up (Rodi, 1982).

The turbulence model that is employed determines to a large extent the performance of the numerical model. Normally the simplicity of the turbulence model used determines to a large extent its suitability and accuracy. Very simple turbulence models such as the Prandtl mixing length hypothesis are unlikely to yield better results than the complex full Reynolds-stress models. Demuren (1994) determined that the  $k$ - $\varepsilon$ -model, a widely used relatively simple two-equation model, describes the mean flow of plumes just as adequate as a more complex full Reynolds-stress model. If the turbulence field is required, for example for mixing predictions, a Reynolds-stress model delivers better results.

The success of numerical models is next to the turbulence model used also influenced largely by the boundary conditions applied. For the specification of these boundary conditions detailed knowledge is needed on the effects on the accuracy of the outcomes. The same holds for the grid resolution to be applied. Since these are

complicated matters, the user of numerical models needs quite some modelling skills, which hinders widespread use and general applicability of these models.

### 3.1.4 Length scale models

The theoretical approach of the buoyant jet which was adopted in chapter 2 discussed the limiting cases of the buoyant jet to describe the behavioural possibilities. A similar approach is adopted in a so-called length-scale model. The buoyant jet is divided into different limiting cases (also called classes, regimes or zones) that are dominated by particular flow properties such as initial momentum, buoyancy or ambient crossflow. Within each case, the flow is approximated with simple asymptotic relationships in which only the most significant properties are accounted for. If needed, several sub-cases (or (sub-)regimes, (sub-)zones or (sub-)classes) can be introduced in which perturbations are added that take lesser effects into account. The extent of each regime is delineated by the use of specific length scales.

Length-scale models are extremely suitable for application in a computer program. Such computer programs are mostly referred to as expert systems. A knowledge data base is needed for data input and flow classification as well as 'model' selection. 'Model' can then refer to the description to be used for a case or sub-case, but expert systems can also include several models with different modelling approaches. Next to the data base, hydrodynamic prediction models are needed for each of the cases and sub-cases (Doneker and Jirka, 1991).

The advantage of using a length-scale model or expert system is its ease in use. This is caused by the fact that per definition the correct descriptions are used, assuring that the model is properly chosen for the given physical situation. The boundaries beyond which the model results in nonsensical outcomes are also automatically indicated. Finally expert systems are generally easier in maintenance and extension than other more comprehensive models (Doneker and Jirka, 1991). The main objection raised against expert systems is also this ease in use, which makes that the models might be used as 'black box model' that does not provide the modeller with any feeling on the actual plume mixing processes.

The best known length-scale model and expert system is the CORMIX package. More information on the working of that package is provided in the paragraph 3.3.

### 3.2 Improvements and extensions in modelling

*To discuss the need and possibilities to improve and extend overflow plume modelling the different modelling approaches as described in the preceding paragraph are investigated. For every modelling approach remarks are made on drawbacks to be improved and extensions for more general applicability.*

*Independent of the modelling approach, every improvement proposed will require experimental and/or practical data for verification purposes.*

#### 3.2.1 Jet-integral model improvements

Main drawback of the jet-integral model approach is the fact that the cross-sectional distribution and behaviour of the buoyant jet is predefined by the model. Not only will this yield that modelled cross-section of the plume is different compared to the real cross-section, but also typical influences on the behaviour of the plume will be left out. An improvement can be made by including more typical aspects of the plume behaviour, for example by improving entrainment and drag force function. This improvement process has already started, but further extension will give better results. Another possibility is to define new assumptions for the cross-sectional distributions that are depending on both jet and ambient conditions. However, the complexity of the models will then further increase, which will make that the main advantage of jet-integral models, their simplicity, might be undone.

Other improvements of jet-integral models needed include the extension of the applicability, since jet-integral models predefine the plume behaviour, this cannot hold for several types of plume, this can be improved by setting up different jet-integral models for different types of plumes. By doing so, the jet-integral approach is left and the system of models becomes comparable to a length scale model.

Typical overflow plume processes are also not embedded in jet-integral models. Ship movements, stripping and vortex behaviour are totally ignored since they are too typical and case-specific. If enough information is present about those typical (overflow) plume processes it is possible to develop a jet-integral model that does include these processes. In general these sorts of extensions need extra data for verification.

#### 3.2.2 Numerical model improvements

The applicability of numerical models was discussed to be dependent on the turbulence model used and the definition of boundary conditions and grid resolutions. The continuous improvement of turbulence models makes that numerical models for buoyant jets are also improving. Current turbulence models are thought to be sufficiently detailed to give reasonable numerical model results for mean flow characteristics (Demuren, 1994; Rodi, 1993).

Therefore improving numerical models should rather focus on the simplification of modelling specific cases. For the definition of boundary conditions and grid resolution in current models the user needs to have a considerable amount of modelling skills. Also the general accuracy of the model is depending on the skills of the model users.

This makes that numerical models of buoyant jets are not ready to use in general applications. Concrete proposals to improve this are however difficult to state.

In numerical models typical overflow plume processes are not readily implemented. Some features like ship movements might be introduced by modelling a moving input of material and defining the correct boundary conditions, whatever those might be. Other processes like stripping require other sorts of interactions between cells to be included. What these interactions should be and how they should be formulated requires more information on these processes and extra (experimental) data to verify the correctness of the implementations.

### 3.2.3 Length-scale model improvements

The length-scale models are addressed to predetermine the behaviour of the plume for separate parts depending on the classification by different length scales. The comprehensiveness of these length-scale models depends on the amount of different classes and zones. In reality the plume changes gradually from one behaviour to the other, and length-scale models by definition make these transitions stepwise (by changing from one class to the other). Introducing more intermediate classes, the magnitudes of these steps might be decreased.

Next to the amount of classes the amount of detail of the descriptions of the flow used for each class determines the correctness of the model prediction. As in the jet-integral models, the amount of typical aspects of the plume behaviour included should be increased to improve the description of the plume. At this moment the state of the art in jet-integral and length scale modelling is at a same level. The two approaches are however facing the same difficulty: their power of simplicity is fading when more (complex) behaviour is implemented.

Typical overflow plume processes are not included in the current length-scale models. This might be improved by introducing new classes (for modelling moving overflow pipes for instance) or by the implementation of typical processes (like stripping and vortex pair creation) in the current description of several flow classes. Despite the difficulties mentioned this is for example carried out for settling processes in the far-field prediction in the sediment version of CORMIX (Doneker and Jirka, 1997). Also the experiences with that improvement show that the amount of data needed to verify such extensions is considerable.

### 3.3 The CORMIX model

To give an example of a dynamic plume model, the working of the CORMIX model is discussed here. CORMIX is an expert system applying a length scale model and is therefore rather a software packet than a calculation model. Here the working of this software packet is discussed first before the model formulations applied for dynamic overflow plumes are treated.

#### 3.3.1 Working of the CORMIX program

As the conceptual model layout presented in figure 3.1 shows, the CORMIX program elements are the Graphic User Interface (GUI), the Mixing Zone Process Knowledge Base (Rulebased expert system), the Hydrodynamic Simulation Models, and the Outfall Design/System Documentation Tools.

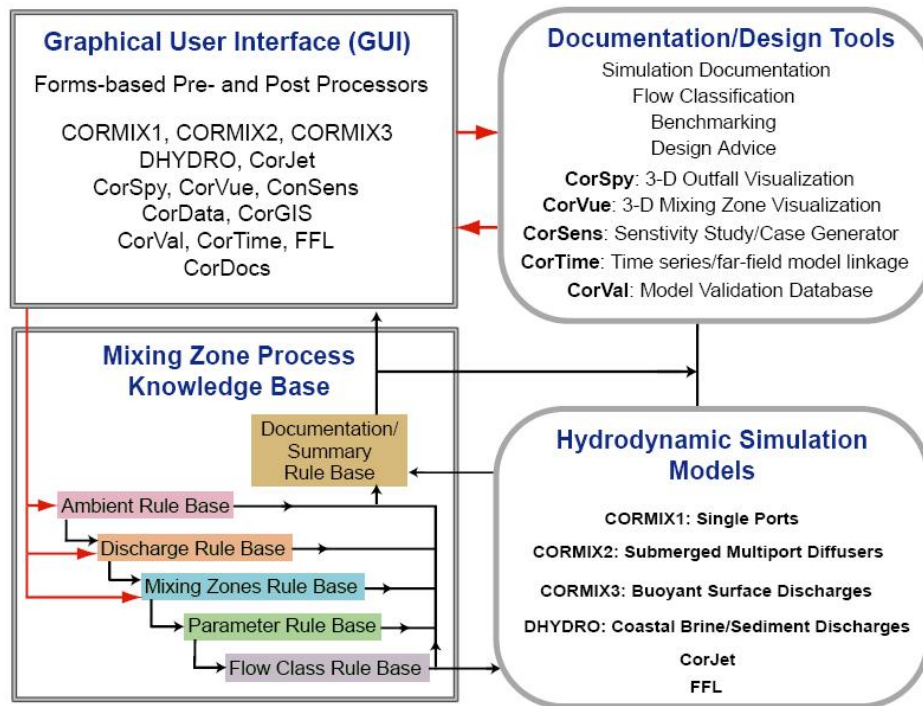


Figure 3.1: CORMIX elements and conceptual linkages

The user interacts with the GUI which is used for data input and initialization of program elements. The Mixing Zone Process Knowledge Base checks the input data for data consistency with model assumptions and computes a number of important physical parameters and length scales. Here also the hydrodynamic classification of the situation into one of the possible flow configurations takes place. After flow classification, the appropriate hydrodynamic model from the Hydraulic Simulation Models is selected and the numerical prediction of the effluent plume characteristics is performed. Finally, summary rule base summarizes the results from the classification and prediction and interprets them as regards mixing zone regulations. Documentation presents the results and gives the possibilities for post-processing.

The outlook of the GUI is presented in figure 3.2. The user inputs data by completing each data entry from on every 'tab'. Each 'tab' represents a different data group such as effluent properties, ambient conditions, discharge conditions etc. Next to data input the validation and simulation can be initialized in the GUI as well as pre- and post processor tools such as CorVue for visualizations of the plume, CorSpy for visual design of outfall, CorSens for sensitivity analysis, CorTime for further far field modelling and CorVal for online validation. These tools are not further discussed here.

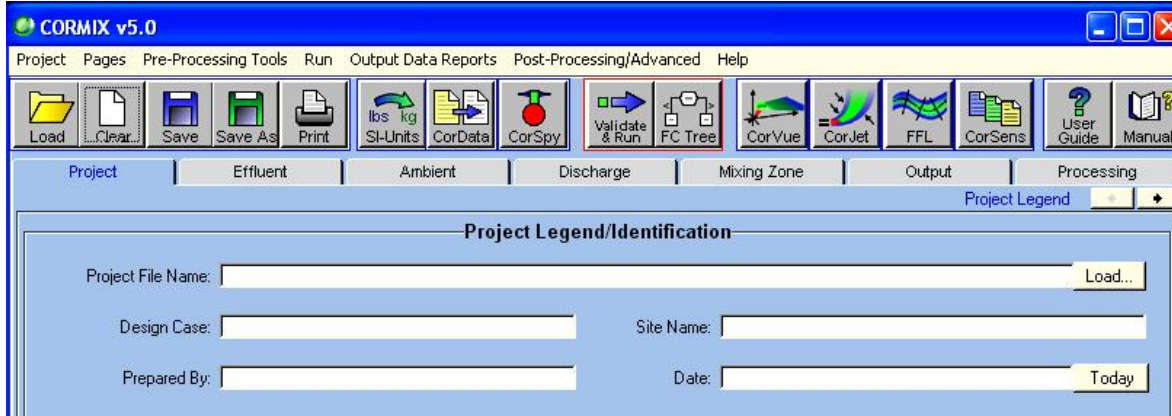


Figure 3.2: Overview of CORMIX GUI

The Mixing Zone Process Knowledge Base contains rule-bases that use the input data to check for data consistency with model assumptions. After that the physical parameters and length scales are computed. These parameters and length scales are used in the preceding hydrodynamic classification of the given discharge situation into one of the generic flow configurations present in the model. The relevant length scales used in the classification of overflow plumes are listed and explained in table 3.1 in which  $\epsilon$  is the ambient density gradient.

Length scale	Formulation	Description
Jet to plume transition scale	$L_M = M_0^{3/4} / B_0^{1/2}$	Distance at which the transition takes place from jet to plume behaviour
Jet penetration in crossflow scale	$L_m = M_0^{1/2} / U$	The distance of the transverse jet penetration beyond which the jet is deflected
Plume penetration in crossflow scale	$L_b = B_0 / U^3$	The flotation distance beyond which a plume becomes strongly advected
Jet to stratification scale	$L_m' = M_0^{1/4} / \epsilon^{1/4}$	Distance at which a jet becomes strongly affected by the (linear) stratification
Plume to stratification scale	$L_b' = B_0^{1/4} / \epsilon^{3/8}$	Distance at which a plume becomes strongly affected by the (linear) stratification

Table 3.1: Length scales used in CORMIX relevant for overflow plumes

The flow classification forms the heart of the CORMIX model and is contained in the classification rule base. It provides a “rigorous and robust expert knowledge base” (Doneker *et al.*, 2007) that determines which of the many possible flow patterns is most appropriate in the current situation. The criteria are based on the same, though extended, theoretical principles as discussed in chapter 2. The classification uses several classification schemes, whose difference is caused by the placement and orientation of the outlet as well as the existence of density stratification. The classification procedure is verified by the developers through testing and data comparison to optimise the actual criteria adopted (Doneker *et al.* 2007). As an example of classification schemes, the scheme needed for overflow plumes, the vertical part of the scheme for negative buoyant jets released near the surface of a homogeneous ambient, is presented in figure 3.3.

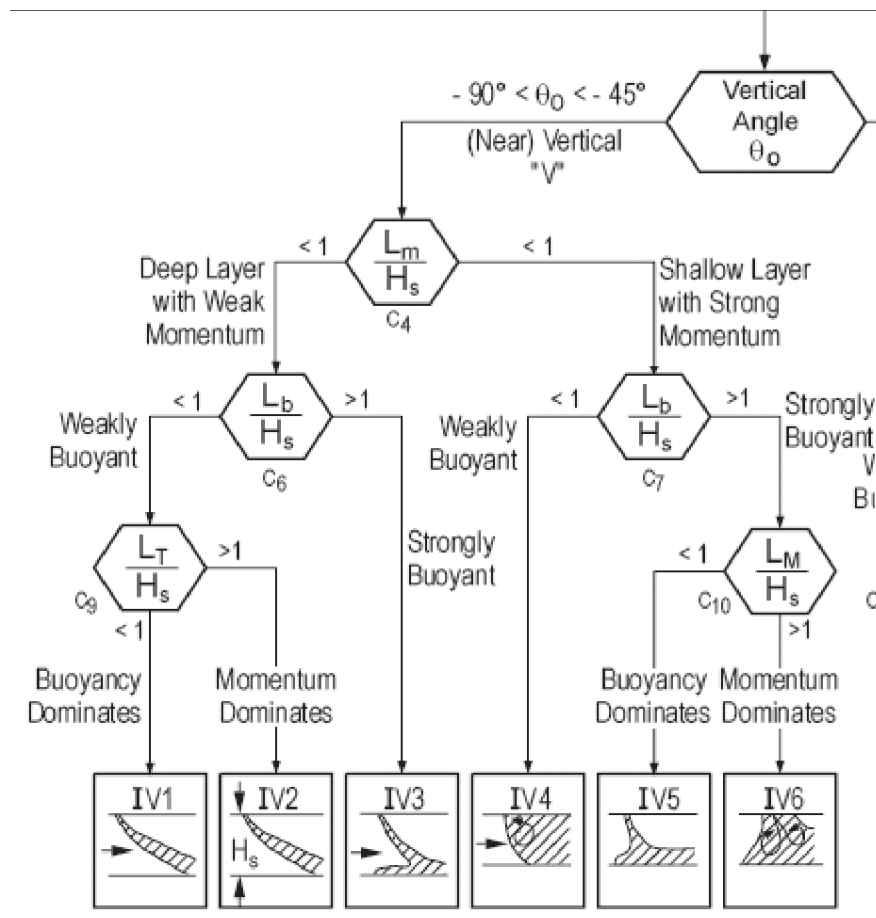


Figure 3.3: Vertical part of flow classification diagram for negative buoyant jets released in a homogenous ambient.

For each class a qualitative description of the behaviour is present in CORMIX to give the model user some insight in the mixing process. Next to that a sequence of appropriate simulation models are assembled and executed depending on this flow class. For overflow plumes the flow class used is mostly flow class IV1. The simulation model used for overflow plumes upon bottom impingement is the CorJet integral model. As the formulation of this model determines the accuracy of the

---

CORMIX prediction for overflow plume spreading, it is presented separately in the next part. The qualitative flow class description of flow class IV1 is reproduced in box 3.1 to give an indication of the insights in physical mixing processes CORMIX tries to give its user.

For further information of the CORMIX software package, the reader is referred to Doneker *et al.* (2007).

```

***** FLOW CLASS DESCRIPTION *****
The following description of flow class IV1 applies to the FULL WATER
DEPTH at the discharge site.
FLOW_CLASS_IV1
A slightly submerged buoyant effluent issues vertically or near-
vertically from the discharge port.
The discharge configuration is hydrodynamically "stable", that is the
discharge strength (measured by its momentum flux) is weak in
relation to the layer depth and in relation to the stabilizing effect
of the discharge buoyancy (measured by its buoyancy flux).
The following flow zones exist:
1) Weakly deflected jet in crossflow: The flow is initially dominated
   by the effluent momentum (jet-like) and is weakly deflected by the
   ambient current.
2) Weakly deflected plume in crossflow: After some distance the
   discharge buoyancy becomes the dominating factor (plume-like). The
   plume deflection by the ambient current is still weak.
Alternate possibility: Depending on the ratio of the jet to crossflow
length scale to the plume to crossflow length scale the above zone
may be replaced by a strongly deflected jet in crossflow:
2) Strongly deflected jet in crossflow: The jet has become strongly
   deflected by the ambient current.
3) Strongly deflected plume in crossflow: The plume has been strongly
   deflected by the current and is slowly descending towards the
   bottom.
4) Layer boundary approach: The bent-over submerged jet/plume
   approaches the layer boundary (bottom or pycnocline). Within a
   short distance the concentration distribution becomes relatively
   uniform across the plume width and thickness.
*** The zones listed above constitute the NEAR-FIELD REGION in which
strong initial mixing takes place.
5) Buoyant spreading at layer boundary: The plume spreads laterally
   along the layer boundary (bottom or pycnocline) while it is being
   advected by the ambient current. The plume thickness may decrease
   during this phase. The mixing rate is relatively small. The plume
   may interact with a nearby bank or shoreline.
6) Passive ambient mixing: After some distance the background
   turbulence in the ambient shear flow becomes the dominating mixing
   mechanism. The passive plume is growing in depth and in width. The
   plume may interact with the channel bottom and/or banks.
*** Predictions will be terminated in zone 5 or 6 depending on the
definitions of the REGULATORY MIXING ZONE or the REGION OF INTEREST.
***** END OF FLOW CLASS DESCRIPTION *****

```

Box 3.1: CORMIX flow class description of flow class IV1

### 3.3.2 Formulations for overflow plumes (flow class IV1)

As stated in the previous section, the hydrodynamic simulation model CORMIX uses for modelling the overflow plumes is the CorJet model. This is a jet integral model and its functioning is extensively described by Jirka (2004). In this section the model formulations are reproduced and comments are given on the way the theoretical influences of several processes described in chapter 2 are taken into account.

Being a jet integral model, CorJet predefines the cross profile of the plume. The distribution function for the local velocity  $u$ , the local buoyancy  $g'$ , the local excess state parameter value  $X_i$  and the local concentration  $c$  are predefined to be:

$$u = W_c e^{-r^2/b^2} + u_a \cos S \cos q \quad (3.1)$$

$$g' = g'_c e^{-r^2/(lb)^2} \quad (3.2)$$

$$X_i = X_{i,c} e^{-r^2/(lb)^2} + X_{i,a}(z) \quad (3.3)$$

$$c = c_c e^{-r^2/(lb)^2} \quad (3.4)$$

in which  $W_c$  is the (excess) axial velocity,  $r$  is the radius and  $g'_c$  is the buoyancy given by:

$$g'_c = \frac{(r_a(z) - r_c)}{r_{ref}} g \quad (3.5)$$

$\rho_c$  is the density,  $X_{i,c}$  is the excess value of the state parameter and  $c_c$  the concentration, all on the centreline as indicated with subscript  $c$ .  $\lambda$  is the dispersion coefficient to include the effect that the scalar distributions are wider than the velocity distribution. The standard value for this coefficient in CorJet is 1,20.  $X_{i,a}$  and  $\rho_a$  are the ambient values of state parameter and density respectively which can both be depending on  $z$ .

As the first step for the modelling the integral quantities of the plumes are obtained through cross sectional integration. These parameters include the total volume flux ( $Q$ ), the axial momentum flux ( $M$ ), the buoyancy flux ( $B$ ), the flux of excess state parameter ( $Q_{X_i}$ ) and tracer mass flux ( $Q_c$ ) and are given by:

$$Q = 2p \int_0^{R_j} u r dr = pb^2 (W_c + 2U \cos q \cos S) \quad (3.6)$$

$$M = 2p \int_0^{R_j} u^2 r dr = \frac{1}{2} pb^2 (W_c + 2U \cos q \cos S)^2 \quad (3.7)$$

$$B = 2p \int_0^{R_j} u g' r dr = pb^2 \left( W_c \frac{I^2}{1+I^2} + I^2 U \cos q \cos S \right) g'_c \quad (3.8)$$

$$Q_{X_i} = 2p \int_0^{R_j} u (X_i - X_{i,a}) r dr = pb^2 \left( W_c \frac{I^2}{1+I^2} + I^2 U \cos q \cos S \right) X_{i,c} \quad (3.9)$$

$$Q_c = 2p \int_0^{R_j} u c r dr = pb^2 \left( W_c \frac{I^2}{1+I^2} + I^2 U \cos q \cos S \right) c_c \quad (3.10)$$

The integration limit  $R_j$  is usually taken as  $R_j \rightarrow \infty$ , as the cross profiles (defined in 3.1 to 3.4) are unbounded, however as an approximation a jet radius of  $\sqrt{2}b$  is sometimes used for crossflow contributions (since those do not converge when  $R_j \rightarrow \infty$ ). From equations (3.1) to (3.4) it can be seen that  $R_j = \sqrt{2}b$  defines a local velocity excess of 14% and scalar value of 25% of the centreline values. This definition  $R_j$  concurs with the visual analysis of plumes.

For the integral (flux) quantities of the plume defined by equation (3.6) to (3.10) conservation equations are formulated for a jet element of length  $ds$  centred on the trajectory. The conservation of volume (continuity), of momentum components in the global directions  $x$ ,  $y$  and  $z$  and of scalar mass are described by:

$$\frac{dQ}{ds} = E \quad (3.11)$$

$$\frac{d}{ds}(M \cos q \cos S) = EU + F_D \sqrt{1 - \cos^2 q \cos^2 S} \quad (3.12)$$

$$\frac{d}{ds}(M \cos q \sin S) = -F_D \frac{\cos^2 q \sin S \cos S}{\sqrt{1 - \cos^2 q \cos^2 S}} \quad (3.13)$$

$$\frac{d}{ds}(M \sin q) = \rho l^2 b^2 g'_c - F_D \frac{\sin q \cos q \cos S}{\sqrt{1 - \cos^2 q \cos^2 S}} \quad (3.14)$$

$$\frac{dQ_{x_i}}{ds} = -Q \frac{dX_{i,a}}{dz} \sin q \quad (3.15)$$

$$\frac{dQ_c}{ds} = 0 \quad (3.16)$$

in which  $E$  is the entrainment rate and  $F_D$  is the ambient drag force, which will both be further specified later. As said in chapter 2, part 2.2.2 the only factor in the continuity equation is the entrainment of ambient fluid. The term  $EU$  in (3.12) represents the entrainment of ambient momentum in the jet, whereas the first right hand term in (3.14) represents the momentum created by the buoyancy force. The right hand terms in (3.15) represent the influence of the (density) stratification of the ambient.

The geometry of the trajectory is defined by:

$$\frac{dx}{ds} = \cos q \cos S \quad (3.17)$$

$$\frac{dy}{ds} = \cos q \sin S \quad (3.18)$$

$$\frac{dz}{ds} = \sin q \quad (3.19)$$

The entrainment rate  $E$  consists of the summation of four different streamwise and azimuthal shear mechanisms that lead to the entrainment of ambient fluid into the jet. In chapter 2, part 2.2.2 entrainment was discussed and the streamwise mechanisms were there called 'shear' mechanism and presented in table 2.3, the

azimuthal mechanisms were called 'forced' mechanism and presented in table 2.4. The complete definition in CorJet is given by:

$$E = 2pbW_c \left( a_1 + a_2 \frac{\sin q}{Fr^2} + a_3 \frac{U \cos q \cos s}{W + U} \right) + 2pbU \sqrt{1 - \cos^2 q + \cos^2 s} \cdot a_4 |\cos q \cos s| \quad (3.20)$$

As explained in part 2.2.2 the streamwise entrainment is proportional to the centre line velocity and composed by the additive contributions of the pure jet, pure plume and the pure wake. The pure plume contribution is depending on the buoyancy present expressed by the local densimetric Froude number  $Fr$  which is given by:

$$Fr = \frac{W_c}{\sqrt{g'_c b}} \quad (3.21)$$

Furthermore the plume influence depends on the vertical angle  $\theta$ . As said in part 2.2.2 such transition is common use. The influence of the wake is less commonly taken into account, but the relative wake strength is well expressed with the wake parameter  $U/(W+U)$ . The azimuthal contribution is applied to take into account the influence of the crossflow on the entrainment rate. Both the influence of cross flowing water colliding the plume as the extra entrainment possible due to the vortex pair cross profile created by the influence of the crossflow are taken into account. The magnitude of both influences is determined by the ambient velocity component transverse to the jet; the deviation of the jet element axis from the direction of the ambient crossflow is taken into account by the last factor of the formulation. The entrainment coefficients are determined based on experimental data fit. The values adopted in CorJet are presented in table 3.2.

Coefficient	Value
$a_1$	0.055
$a_2$	0.3
$a_3$	0.055
$a_4$	0.5

Table 3.2: Standard values entrainment coefficients used in CorJet

The jet drag force  $F_D$  is parameterized by using the quadratic of the transverse velocity component:

$$F_D = c_D 2\sqrt{2}b \frac{U^2 (1 - \cos^2 q \cos^2 s)}{2} \quad (3.22)$$

in which  $c_D$  is the drag coefficient and  $2\sqrt{2}b$  represents the full jet diameter. The drag force is thus specified using a quadratic law. It is described analogous to the flow around a rigid cylindrical body, but the effects of the non-rigidness, being jet entrainment and jet deflection, are taken into account by the coefficient choice. Based on experimental data fit a value of 1.3 for  $c_D$  is applied in CorJet as a standard.

As the model includes the very start of a plume the Zone of Flow Establishment (ZFE), in which the transition from uniform efflux to self similar profile takes place, is also prescribed. Including this transition process would be highly complex if successful and is thought unnecessary in view of the limited extent of the ZFE.

To overcome the problem of the ZFE the inputted initial data values should be 'translated' to initial conditions for the self-similar regime that is calculated by the jet equations. For that reason first the ZFE length and its final transverse angle is defined by:

$$L_{ZFE} = 5.0D(1 - 3.22 \sin g_0 / R) \left(1 - e^{-2.0 Fr_0 / Fr_{plume}}\right) \quad (3.23)$$

$$g_{ZFE} = \tan^{-1} \left( \frac{\sin g_0}{\cos g_0 - (\sqrt{2} - 1) / R} \right) \quad (3.24)$$

in which  $\gamma_0$  is the transverse discharge angle relative to the ambient current direction, given by:

$$g_0 = \sin^{-1} \left( \sqrt{1 - \cos^2 q_0 \sin^2 S_0} \right) \quad (3.25)$$

The crossflow parameter  $R = W_0/U$  is used to define the initial relative crossflow strength.  $Fr_0$  is the initial Froude number (inverse of the square root of the bulk Richardson number) and  $Fr_{plume}$  is the asymptotic value for the local densimetric Froude number of a pure plume, having an approximate value of 4.67 (calculated by applying the coefficient values mentioned above).

Using this ZFE length and its transverse angle, the initial conditions used in the jet equations for the geometry can be calculated by:

$$q_e = \sin^{-1} (\sin g_{ZFE} \sin d_0) \quad (3.26)$$

$$S_e = \tan^{-1} (\sin g_{ZFE} \cos d_0 / \cos g_{ZFE}) \quad (3.27)$$

$$x_e = L_{ZFE} \cos q_{average} \cos S_{average} \quad (3.28)$$

$$y_e = L_{ZFE} \cos q_{average} \sin S_{average} \quad (3.29)$$

$$z_e = h_0 + L_{ZFE} \sin q_{average} \quad (3.30)$$

in which  $\delta_0$  is the projection of the transverse discharge angle onto the x-y plane, given by:

$$d_0 = \tan^{-1} (\tan q_0 / \sin S_0) \quad (3.31)$$

The average angles  $\theta_{average}$  and  $\sigma_{average}$  are determined by simply averaging the  $\theta_0$  and  $\theta_e$  as well as  $\sigma_0$  and  $\sigma_e$  respectively. The fluxes of the integral quantities at the end of the ZFE are equal to the initial fluxes excepted for the volume flux at the end of the ZFE which is determined by:

$$Q_e = \sqrt{2} Q_0 \quad (3.32)$$

Further comments on the formulation of the CorJet integral model can be found in Jirka (2004).



## Chapter 4: Experimental research needed

*To get more insights in the dynamic overflow plume behaviour experimental research was proposed. This chapter presents the possibilities for experiments to extend current knowledge in overflow plume theory and modelling. First the information needed in both theory and modelling efforts is discussed followed by the experimental possibilities to fulfil the identified information need.*

### 4.1 Identification of knowledge gaps

*The previous chapters discussed the theory and modelling of overflow plumes. This paragraph investigates the possibilities to make those descriptions of overflow plume theory and modelling more complete and correct. The knowledge gaps in current theory are identified as well as the extra information needed to model overflow plumes.*

#### 4.1.1 Knowledge gaps in current literature

As shown in chapter 2, the theoretical descriptions of overflow plumes in specific are limited. Mostly general buoyant jet theory is extended with some specific overflow plume processes and phenomena. An exception forms the work of Winterwerp (2002) which gives the classification between passive and dynamic overflow plumes. Extending theoretical knowledge of overflow plumes can for that reason be based on several approaches:

- 1) Demonstrating the degree of correspondence between general buoyant jet theory and overflow plumes.
- 2) Obtaining more information on specific (overflow) plume processes.
- 3) Estimating the influence of typical overflow phenomena on plume behaviour.
- 4) Extending/improving the work of Winterwerp (2002).

Ad 1) Creating overflow plumes in practice is needed to demonstrate whether the dynamic phase of the plume indeed behaves as a buoyant jet. ZFE length, behaviour and dilution predicted by the theory can be checked for validity with measurement results. The typical behaviour in the ZEF like vortex pair formation and overall dilution can be measured and compared to theory.

Ad 2) Typical processes such as entrainment, stripping, vortex pair formation and bifurcation can be isolated in (physical) models to obtain more information. Entrainment and vortex pair formation and divergence have been studied quite often, so further research should be in line with those investigations. The stripping process has not yet been studied in detail.

Ad 3) The effects on plume behaviour of typical operational and environmental phenomena such as ship movements, the existence of air bubbles in the overflow, density stratification effects and wave effects can also be investigated separately. Including these phenomena in model tests can yield (quantifiable) information on the effects of these phenomena on overflow plumes. Furthermore it provides possibilities to obtain more insights in the processes involved with these phenomena.

Ad 4) To make the results of Winterwerp (2002) more practically applicable, the research can be extended/improved with more quantitative information, including the influences of other parameters and clarifying its underlying assumptions. In that way more possibilities to generalize its results are created. The prediction whether an overflow plume will be dynamic or passive can then be better founded.

Using these four approaches, many knowledge gaps can be identified. The different approaches might pinpoint the same gap of knowledge. As an example research on the stripping process will yield information not only on the process (2), but also to whether overflow plumes will show (dilution) behaviour that is non-typical for buoyant jets (1) and show whether the transition proposed by Winterwerp (2002) might be accounted for by an increase in stripping (4). The fact that this knowledge gap is pinpointed by several approaches demonstrates that it is important.

To reduce the amount of information only knowledge gaps relevant for two or more different approaches are mentioned in table 4.1 with some comments.

Knowledge gap	Comment
Influence of entrapped air	Mentioned by Winterwerp (2002) to influence the nature of a plume, important phenomenon, not investigated in earlier experimental research
Influence of waves	Influences mixing properties in the ambient fluid and therewith dilution, creates ship movements, not accounted for in earlier research
Influence of mixture grading/segregation	Important process in the passive phase of overflow plumes, typical for overflow plumes, mixture in dynamic phase is assumed to be single phase fluid
Standing ship assumption	Assumption made by Winterwerp (2002) and others that allows to model overflow with standing pipe in moving fluid, especially near bottom effects are interesting
Stripping of overflow plumes	Possible process in overflow plumes which is completely unknown, perhaps linked with the dynamic or passive nature of an overflow plume
Entrainment of overflow plumes	Entrainment of overflow plumes might be different in passive or dynamic situations, possibly linked with stripping processes
Influence of ships propeller	Mentioned by several authors but never investigated phenomenon around overflow plumes, might be a reason for extra dilution in the far field
Vortex pair creation	Process which is not well understood for sediment containing plumes, details of influence of ZFE, source of vorticity still under discussion in literature
Vortex bifurcation	Process only well understood for upward released jets, influence of negative buoyancy and bottom impingement unknown.
Influence of density stratification	Well known in general buoyant jet theory, but unknown for overflow plumes
ZFE behaviour in overflow plumes	Behavioural changes of overflow plumes already within ZFE, the effect on main plume characteristics not well described in common literature

Table 4.1: List of important knowledge gaps in theory with comments

### 4.1.2 Information need in modelling

As discussed in chapter 3 any improvement of the modelling of overflow plumes will need more data. Some existing general buoyant jet models are well calibrated with data, but lack specific overflow plume behaviour descriptions. The approach for obtaining better modelling results can therefore only be based on two principles:

- 1) Obtaining more data for the verification of (new) overflow plume models.
- 2) Generating data streams of plumes containing one or more typical overflow processes or phenomena in order to compare those with general buoyant jet models.

Unlike the theoretical approaches, these two approaches are difficult to combine. The importance of the different need for information is therefore given by the practical importance of the 'knowledge gap' present in the models. The information needs that are considered important in this M.Sc. thesis are listed in table 4.2 with some comments.

Information need	Comment
Data for TASS software calibration	A new model called Turbidity ASsesment Software (TASS) is currently under development by SSB and aims at becoming the new standard in predicting source terms; for calibration and verification of this model extra data is necessary
Data on air influence for buoyant jet models	The influence of air is large and typical for overflow plumes but is included in buoyant jet modelling. To make the models more suitable for overflow modelling this process should be included, which requires (experimental) data
Data of ships propeller influence on buoyant jet models	Typical overflow plume phenomenon, not included in general buoyant jet models, data needed about extent of different mixing properties of ambient fluid
Data on stripping of overflow plumes	The process of stripping might be influencing overflow plumes and be important in environmental impact assessment. If stripping is significant it should be included in any overflow plume model
Data on vortex-pair profile for buoyant jet models	Existence of vortex-pair profile enhances mixing, process not included in buoyant jet models, need to obtain data about the formation of the profile
Data on vortex bifurcation for buoyant jet models	Vortex divergence might alter dynamic plume density distribution, not included in general buoyant jet model, data needed on criterion and description of bifurcated jets.

Table 4.2: List of important information needs in modelling with comments

## 4.2 Experimental possibilities

*The knowledge gaps and information needs for theory and modelling considered in this M.Sc. thesis are described in the preceding paragraph. Now the possibilities to fill in these gaps and obtain the information needed with laboratory experiments are investigated. First the feasibility of laboratory experiments is discussed followed by some feasible experimental possibilities.*

### 4.2.1 Feasibility of laboratory experiments

The feasibility of filling in the considered knowledge gaps by laboratory (scale) experiments is discussed here for every knowledge gap. This is done by separately looking at the type of information need, the possibility to scale the process down and the possibilities to create the desired circumstances in the laboratory. If possible, theoretical knowledge gaps and modelling information needs that have overlap are treated collectively.

#### 1) Influence of air entrainment.

To obtain some theoretical knowledge and data for modelling purposes it would be useful to develop laboratory experiments of plumes containing air bubbles. However scaling of air bubbles is very difficult, since a minimum bubble size exists and there is no reason why bubbles in reality would not already be approaching that size. Making a scale model seems therefore impossible within the framework of this M.Sc. thesis work.

#### 2) Influence of waves.

The influence of waves on an overflow plume can be measured in a laboratory experiment without problems. An experiment should be set up in a flume that is able to generate both flow and waves. The scale of the experiment can be varied depending on the dimensions of that flume.

#### 3) Influence of mixture grading/segregation.

Though difficult in small scale experiments it should be possible to conduct experiments that compare plumes of material with different particle size distributions. Looking at the passive phase in detail (which might be needed for segregation effects) requires quite a large flume or a very small scale.

#### 4) Standing ship assumption.

In most experiments the pipe releasing the buoyant jet is standing and the water is moving, in overflow plumes, it is partially the other way around. The effects of that, especially in the near-bottom region, might be investigated by carrying out experiments with a moving source. Perhaps this might be possible in a towing tank or by mounting a moving ship on a (large) flume.

#### 5) Entrainment of overflow plumes.

Depending on the amount of information to be gathered it is possible in a laboratory experiment to measure the amount of entrainment of overflow plumes. If however all typical phenomena also have to be included it might be wiser to set up measurements in the field. Also because entrainment has already been investigated in laboratory conditions, further focussing on entrainment of overflow plumes is better carried out in field measurements.

- 6) Stripping of overflow plumes.  
The possibilities to measure stripping in a laboratory experiment are depending on the amount of phenomena that are reviewed. Since stripping is barely known as a process, a more simplified laboratory model to look what the origin of the stripping process is seems a possible approach in gaining more knowledge on this phenomenon.
- 7) Influence of ships propeller.  
Creating plumes in an ambient fluid in which the wake of a ships propeller is present is possible. The effects of a ships propeller are discussed in literature not to happen in the near-field of the plume so quite a large research facility is needed to investigate the effects in enough detail.
- 8) Vortex pair creation.  
Already quite some researchers have investigated the vortex pair creation of small scale buoyant jets in the laboratory. Therefore it is possible to do the same for overflow plumes. To obtain more, 'new' insights the extent of scaling errors should be reduced. For that reason the spatial scale of this experiment should become larger then other experiments.
- 9) Vortex divergence and bifurcation.  
Vortex divergence and bifurcation are previously studied in laboratory experiments. Obtaining more information in new laboratory research seems to cause no problems.
- 10) Influence of density stratification.  
Also the influence of density stratification on buoyant jets has already been studied in laboratory experiments. Creating an experimental setup which corresponds to overflow plumes should be possible. Since far-field effects are important here, the facility should be sufficiently large or the scale should be sufficiently small.
- 11) ZFE behaviour in overflow plumes.  
Within the ZFE of overflow plumes several transitions in behaviour take place. To investigate what happens in detail, the ZFE has to be investigated visually. For that reason the scale of the experiment should be large. The apparatus needed should therefore also be very large.
- 12) Extra data for TASS software calibration.  
Since the data need for TASS also includes data from the dredge process and since the approach should contain as much information on the practice of overflow plumes as possible, field data collection is more advantageous than experimental research.

For several knowledge gaps it is in principle possible to obtain the needed information by laboratory experiments, but problems are foreseen with scales. For mid-field and far-field effects, the spatial extent of a physical model can become quite large, or the scale must be very small. In this M.Sc. thesis these experiments cannot be conducted due to the limited dimensions of the facilities in the Fluid Mechanics Laboratory of Delft University of Technology or due to the lack of available time. For these knowledge gaps the experimental research possibilities of this M.Sc. thesis are not sufficient to make it feasible in filling in these gaps.

## 4.2.2 Some ideas for experiments

With the elimination of knowledge gaps that cannot be filled by the experimental research of this M.Sc. thesis the remainder of experimental possibilities have to be worked out to ideas for experimental setups. For all remaining knowledge gaps some possible ideas are presented in this section, discussing main issues concerning it and, if possible, giving a sketch of the main idea of the experiment. As this section contains ideas and possibilities for experiments, the list is not thought to be complete, but to give an insight of possibilities thought of.

### Influence of waves (2)

The influence of waves on the overflow plume can be investigated in an experimental flume which is able to create both flow and waves. A ship model should be prepared that has the same degrees of freedom as a normal ship and can be attached to the flume. Since spreading of the plume over the bottom of the flume is incorporated in the research, a relatively wide flume is needed.

Due to the ship's movement irregular overflow in both quantity and direction might be possible. That makes the comparison of different runs difficult. A solution can be found in making several runs with the same characteristics to improve statistics. That is however time consuming and costly.

A sketch of the experimental idea is presented in figure 4.1.

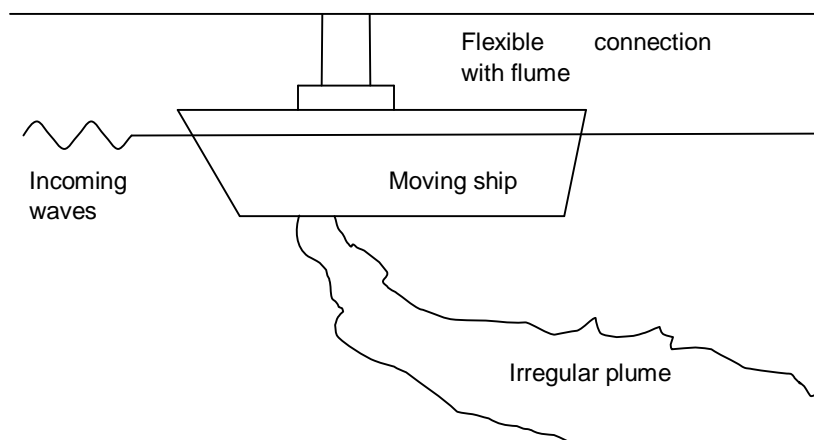


Figure 4.1: Sketch of wave influence experimental setup

### Influence of grading mixture (3)

When a scale experiment is carried out that has to represent overflow, the particle size distribution of the mixture might be varied during the tests enabling the investigation of the influence of the mixture grading. Any experiment could be extended with a few tests with mixtures with a different particle size distribution to investigate its influence.

Focussing specifically on the process differences caused by different particle size distributions of the mixture has to take place in a non-scaled experiment, but as already mentioned earlier, then the spatial extent becomes too large.

#### Standing ship assumption (4)

In a wide flume with only flow, the overflow plumes of standing ships can be compared with a moving ship. It would be most advantageous if the flume used by Boot (2000) might be adapted so that a ship can move over the flume. The plumes of the previous research by Boot (2000) can then be compared with the plumes in the new setup.

Important in this research is the placement of the measuring points, this should be done in such a way that each point measures in the same 'stage' of the plume for each measurement. Therefore one could think of a measuring frame that is moving with the ship. Another option is to provide a measuring frame that can measure the development of the plume.

A sketch of the setup with the moving measurement frame is presented in figure 4.2, to give an idea of the possibilities.

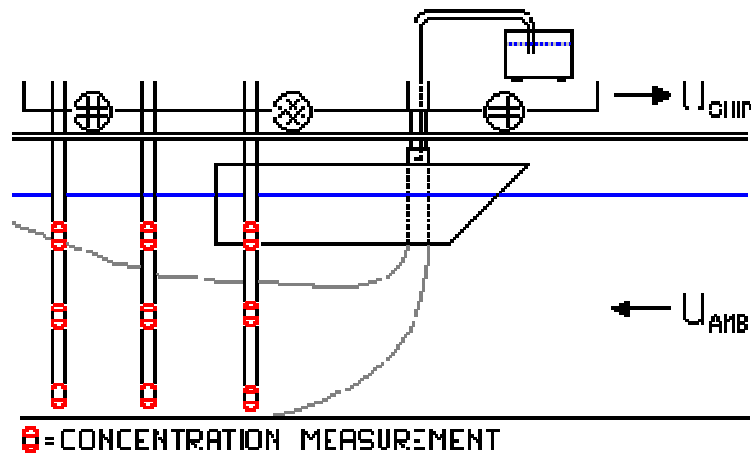


Figure 4.2: Sketch of the moving measurement frame method applied in a moving ship experimental setup

#### Stripping of overflow plumes (6)

To investigate stripping plumes might be created in a flowing flume. The final parts of the dynamic plume, which are influenced by bottom effects, could be captured under a plate separating lower and upper water column. The concentration increase between the upper water column above the plate and the water in front of the plume is solely due to stripping.

The largest difficulties in this approach would be the influence of the plate. Firstly in the dynamic phase of the plume, the whole plume has to descend under that plate and the splitting must not hinder sediment to move under it.

An exaggerated sketch of the principal of the experimental setup is presented in figure 4.3.

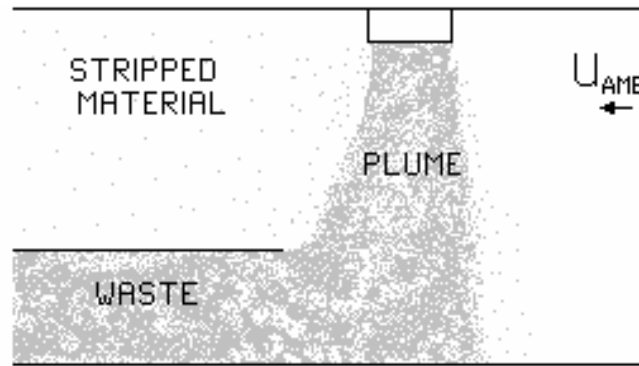


Figure 4.3: Principal of stripping experiment.

**Vortex divergence (9)**

In a flume for only flow a plume might be created and the divergence process might be investigated by taking density profiles of the plume at several (downstream) distances from the release point. In this way it can be seen whether the plume really bifurcates or whether the vortices are only diverging and the plume stays complete. Next to that the diverging angle of the two vortices can be measured. As an idea, the top view of the experimental setup in the flume is presented in figure 4.4.

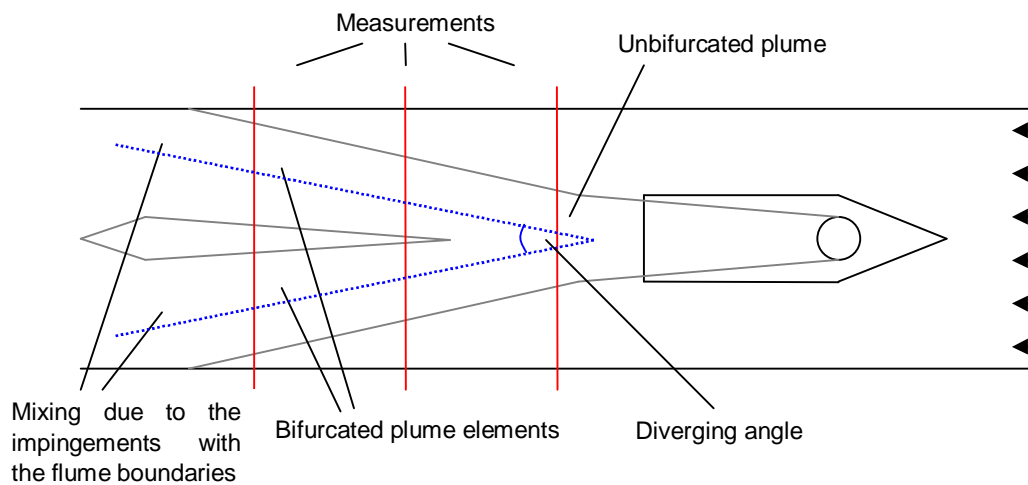


Figure 4.4: Top view of the vortex divergence experimental idea

## Chapter 5: Definition of M.Sc. thesis research work

*The possibilities to do experimental research to fill current knowledge gaps in plume theory and modelling were presented in the preceding chapter. From this information, which was founded on the analysis of the theory and models in chapters 2 and 3, the objectives for this M.Sc. thesis research works can be extracted, since the research work will include carrying out one or more of the experimental ideas mentioned. First it is decided which experiments are implemented followed by a discussion of the objectives of the research connected to these experiments.*

### **5.1 Choice for experiments to implement**

*Two of the five experiments presented in paragraph 4.2 are chosen for implementation. This choice is mainly based on practical feasibility weighted against the opportunity to make theoretical progress i.e. the relative importance of the knowledge gap. The stripping experiment and vortex divergence experiment are the implemented experiments. Here some comments and further explanations on this choice are presented.*

#### **5.1.1 Stripping experiment**

The main reason for choosing to implement the stripping experiment is the presumed but unknown influence on overflow plumes. In the dynamic phase of the plume, relatively near to the surface, material will be stripped and directly enter the passive phase. Other transitions from dynamic to passive behaviour, like bottom impingement and resuspension from the fluid mud layer, take place at greater depth. Stripped material is therefore more likely to stay in the water column for a long time, which makes it more relevant from an environmental point of view (John *et al.*, 2000).

Despite of its importance in overflow plumes, no research has spent much effort on the description of the stripping process. For that reason it is not exactly known why and how much material is stripped. The laboratory experiment proposed might result in the first step in obtaining this information. On the one hand it means that all sorts of results from this experiment will be useful as long as they provide some information on the process. On the other hand, since it is the first experiment that will aim at investigating the stripping process, the risks might be larger than in other experimental ideas listed above.

The possibilities to make an experimental setup to measure the stripping process in the Fluid Mechanics Laboratory were reasonable. A long tilting flume was available for quite some time to build the specific setup with the dividing plate. The depth was limited to 0.40 m, which would be sufficient for a 1:100 scale. The width was also limited to 0.40 m, which is relatively small. However, since the widening of the plume in the descent to the bottom is small, this was not thought to be problematic.

### 5.1.2 Vortex divergence experiment

After the stripping experiment the vortex divergence experiment was carried out. Main reason was the availability of the flume and the good possibilities to carry out the measurements. During the stripping experiments it was seen that the vortices of the vortex pair were diverging, but it was uncertain whether these plumes were completely bifurcating. In literature the occurrence of bifurcation in homogeneous environments is not described and also the difference between bifurcation and vortex divergence is not commonly discussed, as it is a matter of definition only. Investigations on plumes in the laboratory focussing on this process could possibly illustrate and clarify the differences. The results should also indicate whether vortex divergence is an issue in overflow plumes.

Another reason for interest in vortex divergence and bifurcation is the representation of these phenomena in plume modelling. Simple models such as jet-integral and length scale models do commonly not take the creation of the vortex pair concentration cross profile into account let alone the divergence or bifurcation. Carrying out the vortex divergence experiment is thought to provide a data set with which it can be checked to what extent these models need improvements on that matter.

As vortex divergence was seen in the stripping experiment, it was known that the possibilities to build this vortex divergence experiment in the flume available in the Fluid Mechanics Laboratory were good. In the stripping experiment it was seen that the dimensions of the flume were not sufficient for a 1:100 scale, so the scale had to be adapted. Also several other minor changes had to be made to the setup, but the adaptation of the stripping setup to a working divergence measurement experimental setup was easily accomplished.

## 5.2 Objectives of the research work

*In paragraph 5.1 the choice for the implemented experiments was explained. However, the exact objectives for these experiments were not determined. In paragraph 1.2 the general goal for this thesis was stated. Here this general goal is reformulated in more concrete objectives for the stripping and vortex divergence research that accompanies the chosen experiments.*

### 5.2.1 Objectives of stripping research

Stripping is, as said in section 2.2.4, a feature of overflow plumes which is barely understood. The processes causing stripping are not described in literature and are also not defined in the definition used in this M.Sc. thesis. Next to that there is no idea about the quantities of material stripped. In order to be able to provide better input for far-field sediment resuspension modelling, stripping should, if significant, also be included in the treatment of the dynamic phase of a plume by models. To do so mostly information on the process and the quantification of stripping is needed.

The objectives of the stripping research therefore consist firstly of providing more information on this process and secondly of measuring the amount of stripped material. Also the dependency of stripping on several parameters has to be investigated, to obtain a complete perspective. Finally the implementation of stripping in dynamic plume models has to be investigated too.

### 5.2.2 Objectives of vortex divergence research

In section 2.2.3 vortex bifurcation was mentioned to be an extremity of the diverging process of the vortices of the vortex pair. Bifurcation occurs when the vortex strength of the vortex pair created is large compared to the turbulent diffusion. It was said that this always holds when a boundary is approached but it is not excluded that plumes discharged in homogeneous environments bifurcate too. For far-field sediment resuspension predictions it is interesting to know whether overflow plumes do bifurcate or, if they do not, what the rate of diverging of overflow plume vortices globally is. It is also important to know what these results mean for the applicability of integral and length-scale plume models that commonly not represent the vortex pair cross profile formation.

The objectives for the vortex divergence research therefore not only include the acquisition of (quantifiable) results on the diverging rate of the vortices in the vortex pair, but also determination of the existence of bifurcation in the modelled plumes. Furthermore CORMIX has to be studied as a representative of integral and length-scale plume models. The formulations of CORMIX are investigated for the influence of the vortex pair cross profile and the model predictions are to be compared with the measurements. Finally possible approaches to extend the model might, if needed and if possible, be proposed.



## Part 2: Stripping



## Chapter 6: Stripping experiment

*The most important parts of the stripping research are the experiments that have been carried out. In this chapter these experiments are further explained. In separate paragraphs the basic idea, the experimental setup and the plan of measurements is discussed.*

### 6.1 Basic idea of the experiment

*The basic idea of the experiment is presented by discussing the objectives of the experiment, the hypotheses on the outcomes and the measurements needed in the experiment.*

#### 6.1.1 Objectives of experiment

Most important objectives of the stripping research were providing more information on the process of stripping and giving a quantification of stripping. The experiment on stripping was designed to fulfil these objectives. Visual observations were needed to obtain information on the stripping process; especially observations around the plume edge would be very useful for that. To determine the amount of material stripped it was needed to measure the concentration of ambient waters before and after the plume. Several plumes with several varied parameters would be investigated to gain more insights on the dependency of stripping on these parameters. The varied parameters would be the same parameters as mentioned in paragraph 2.3:

- ambient velocity
- overflow velocity
- overflow pipe diameter
- density difference
- water depth
- grading of material

The experiment results should also contain global indications what the influence of the abovementioned six parameters is on stripping.

#### 6.1.2 Hypotheses

The process that causes stripping is expected to consist of breaking of vortices at the plume edge and subsequent advection. The vortices or eddies created at the plume edge normally cause the entrainment of ambient fluid by engulfing ambient fluid in these eddies and bring it into the plume. It might be possible that during this vortex interaction some of the vortices are not able to entrain the cross flowing ambient fluid and break up as a result. These broken vortices are then removed from the plume by advection forces of the ambient flow.

The quantity of material stripped from a typical overflow plume is unknown.

### 6.1.3 Measurements needed

Gaining insights in the process of stripping is difficult to carry out by measuring. Visual observations are thought best in defining what exactly happens with the plume. To be able to study one plume for several times in detail video recordings of the plume were made.

For the quantification of stripping the total amount of material that leaves the plume during its descent to the bottom has to be measured. To be able to do this in a flume the plume is confined in the lower part of the water column by placing a dividing plate that separates the upper part of the water column from the lower part. The concentration increase in the upper part of the water column after passing the plume will be measured. To assess the loss of material by stripping this concentration increase is converted to a volume by multiplying by time, flume velocity and projected surface. The idea is sketched in figure 6.1.

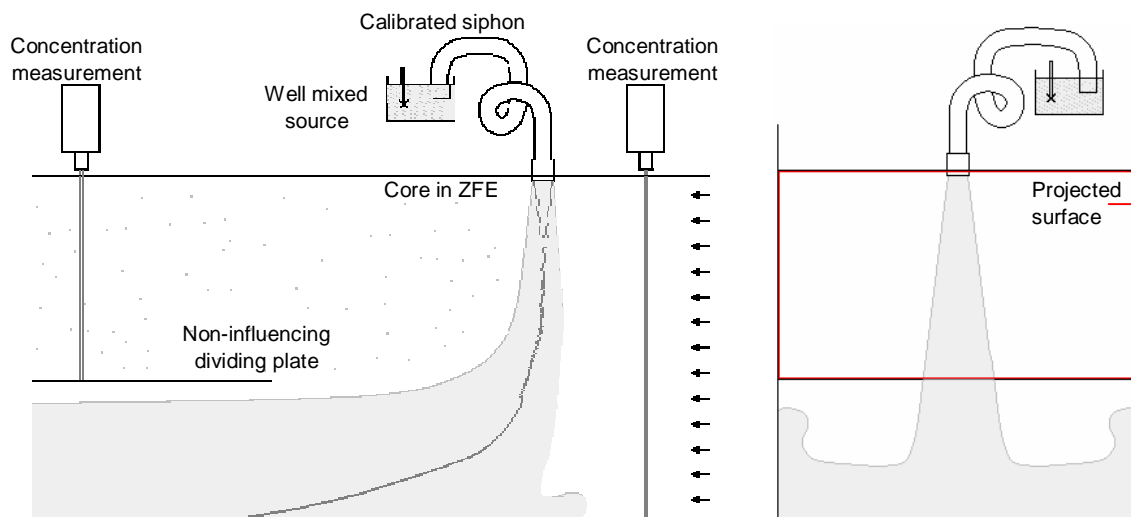


Figure 6.1: Sketch of the measuring plan for stripping.  
(Left: side view, Right: frontal view with projected surface marked)

For the concentration measurements it is needed to define a range of measurable concentrations. As these concentrations are depending on the amount of stripped material an estimation on the amount of stripping had to be made. It was decided that the minimum concentration measurable should correspond to 1% stripping or less, whereas the maximum concentration measurable should at least correspond to 5% stripping.

## 6.2 Experimental setup

*This paragraph presents how the basic idea described above is worked out to an experimental setup. First the scaling and dimensions are discussed, after that it is shown how the several parameters that influence the plume behaviour are controlled. The exact working and use of the experimental setup is further explained in Appendix E whereas more detailed information on several parts of the setup is presented in Appendix F, G, and H. Appendix I presents the development history of the setup.*

### 6.2.1 Scaling

A parameter study, which is presented in Appendix C, yielded that the experiment is scaled correctly if both the (internal) Froude number (or the Richardson number) and Reynolds number are the same for model and reality. Fulfilling both requirements is only possible if the process is not scaled at all, therefore usually only one of them is fulfilled. It is generally accepted that the requirement for the Reynolds number can be dropped if the process in reality and in the model is turbulent. The minimum Reynolds numbers should be in the order of 4000 to 10000 (Ettema *et al.*, 2000).

For the stripping experiment a Richardson scaling of 1:100 was used. This means that all length scales are 100 times smaller than in reality while all velocity scales are  $\sqrt{100} = 10$  times smaller than in reality. There are two potential problems in applying that scale: the grain size of the sediment has to be considered and the overflow pipe dimensions might cause the jet Reynolds number to become too low.

- Scaling of the overflow material.  
Since the material in reality is already fine, applying scaling would mean that non-existing small material should be used. However, the overflow plume is a single phase fluid, meaning that the fluid properties rather than the sediment properties determine the behaviour of the plume. If sufficiently small material is used the plume created in the experiment will also be a single phase fluid and the scaling is not hindered.
- Scaling of the overflow pipe dimensions.  
If the overflow pipe dimensions are scaled correctly, the jet Reynolds number within the overflow pipe will become too small. For that reason it is thought to distort the scale by keeping the overflow pipe diameter larger.  
Later experiments with smaller overflow pipes will be undertaken, which will investigate the influence of the low Reynolds number. As long as the material leaving the overflow shows turbulent behaviour in the ZFE it is thought that the low jet Reynolds number within the overflow pipe is not hindering the experiment.

### 6.2.2 Dimensions

The typical values for parameters concerning overflow in practice are presented in chapter 2. With the scaling rules presented above the dimensions for the experimental setup can be determined. The dimensions needed to be optimized to come to a workable experimental setup in which the concentrations are still measurable. These optimization calculations presented in Appendix J, since they

determined the development of the experimental setup to great extent. Table 6.1 presents both the typical parameter values in practice (here called prototype) and the parameter values finally adopted in the experiment.

Parameter	Prototype	Experiment	Unit
$\rho$	1025	1000	kg/m <sup>3</sup>
$\rho_{\text{mix}}$	1040-1060-1090	1020-1035-1050	kg/m <sup>3</sup>
$u_{\text{amb}}$	0-1-4	(0.00)-0.05-0.10-0.15	m/s
$h$	20-35-80	0.20-0.30-0.40	m
$D_{\text{pipe}}$	1-3-4	(0.03)-0.04-0.05-0.06	m
$u_{\text{jet}}$	0.5-1.0-1.5	0.07-0.11-0.15	m/s
$g$	9.81	9.81	m/s <sup>2</sup>

Table 6.1: Dimensions of parameters in experiment

For the overflow material kaolinite (sometimes also called China Clay) is used. This very fine material ( $d = 1-10 \mu\text{m}$ ) has the advantage to be white. It is commonly used in plume experiments (Boot, 2000).

### 6.2.3 Controlling the parameters

Paragraph 6.1 discussed the influences of several parameters on stripping to be investigated. These parameters were therefore controlled for every experimental run. Here for every parameter the method of control is discussed shortly. For the exact working of the experiment the reader is referred to the appendices.

- The ambient velocity is the velocity to be set in the flume. It is determined by the discharges going in and out of the flume. For every combination of water depth and the incoming and outgoing discharge the velocity was calculated exactly. Since only a few predefined settings were to be made, the discharges needed to be set to several distinct values. To control the discharge the frequency of the pump was adjusted and the discharge was checked by measuring it with a pipe discharge meter. During the building of the setup the flume velocity suffered from significant deviations. The cause and solutions for these deviations are discussed in Appendix H.
- The overflow velocity is controlled by adjusting the height difference over the siphon. The relation between the height difference and the resulting velocity was determined in calibration tests for each different siphon. The actual height difference was measured for every run.
- The overflow pipe diameter is varied by using several different siphons.
- The density of the mixture is created by adding kaolinite to clean water. The amounts of kaolinite and water needed were weighted to create the mixture with the required properties.
- The water depth in the flume is regulated by a weir at the end of the plume. Using weir overflow functions the water height above the weir can be calculated for the planned discharged. To set the wanted total water depth the weir height should be adjusted properly. The water depth is checked by a water height meter.
- The grading of material can be measured before the mixture is prepared.

### 6.3 Measuring plan

The measuring plan that defines which parameter combinations are tested is discussed in this paragraph. In the stripping experiment, a multitude of parameter combinations were possible. Since the amount of runs had to be limited and the reproducibility and statistical reliability had to be guaranteed not all combinations were tested, while others were tested frequently.

To improve reproducibility and statistical reliability a 'base case' was introduced towards which all experiments were linked. Every series of runs would investigate the effect of one or more variables and contain this 'base case'. This means that the 'base case' would be tested several times (to assess reproducibility) so that time-dependent influences could be traced by comparing several 'base cases'.

The measuring plan would consist of:

- One single 'base case' test.
- Five series of three tests single parameter variation around the 'base case", to investigate the influence of one of the five parameters varied ( $\rho$ ,  $D$ ,  $W$ ,  $U$  and  $h$ ).
- Three tests with high  $Ri$  and high  $\zeta$  followed by a 'base case' for comparison.
- Three tests with high  $Ri$  and halved  $\zeta$  followed by a 'base case' for comparison.
- Three tests with low  $Ri$  and low  $\zeta$  followed by a 'base case' for comparison.
- Three tests with low  $Ri$  and doubled  $\zeta$  followed by a 'base case' for comparison.
- Four tests with a smaller overflow pipe to check the influence of a lower Reynolds number, followed by a 'base case' for comparison.
- Three tests with a different grading.

The resulting measuring plan with the parameter values indicated is shown in appendix D. The tests can also be presented graphically through the  $Ri$ - $\zeta$  diagram used by Winterwerp (2002), this is done in figure 6.3.

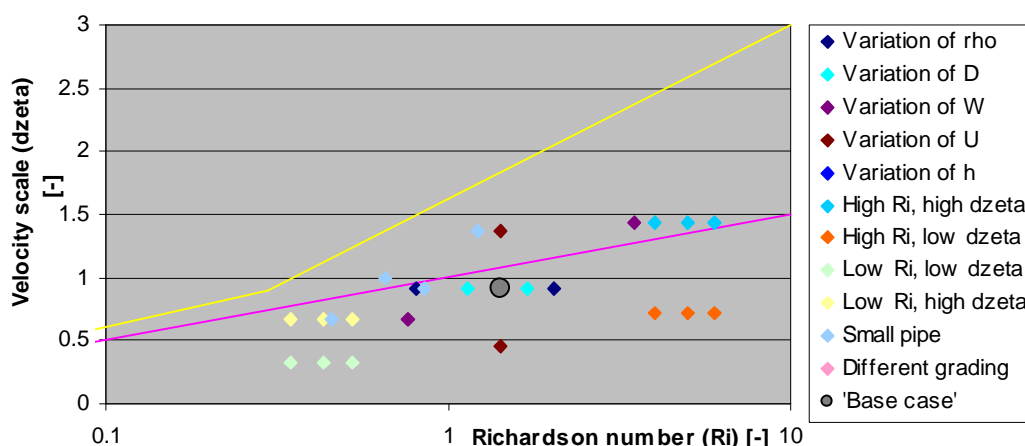


Figure 6.3: Graphical presentation of measuring plan



## Chapter 7: Stripping experiment results

*In this chapter the results of the stripping experiment are presented. As not all tests on stripping aimed for were carried out, the plume tests that have been carried out are presented in the first paragraph. After that the main observations made during these experiments are listed in the second paragraph.*

### 7.1 Measurements

The inadequate dimensions of the flume prevented that quantitative measurements could be obtained during the stripping experiments. For that reason almost every test from the measuring plan was dropped and only several tests were carried out, determining the influence of stripping qualitatively. Table 7.1 summarizes the test runs that were carried out. Details of the development of the experiment into this resulting list of measurements are given in Appendix J.

Run nr	$\rho$ (kg/m <sup>3</sup> )	$D$ (m)	$W$ (m/s)	$U$ (m/s)	Comments	$Ri$ (-)	$\zeta$ (-)
1	1035	0.05	0.11	0.10	Base case	1.42	0.91
2	1050	0.05	0.11	0.05	Velocity halved, density increased	2.03	0.45
3	1050	0.04	0.11	0.05	As (2) but smaller pipe	1.62	0.45
4	1050	0.03	0.11	0.05	Smallest pipe used	1.22	0.45
5	1050	0.012	0.11	0.05	New smaller pipe made	0.49	0.45
6	1030 – 1070	0.012	0.10 – 0.15	0.04 – 0.10	Trying to stop circulation	0.30 – 0.80	0.25 – 1.00
7	varying	0.01	varying	0.05	Varying input to stimulate stripping	-	-

Table 7.1: Stripping tests carried out in the experimental setup

All plumes except run (2) have been recorded on video and were examined visually for several times. In run (6) and (7) next to the visual observations an OPCON concentration measurement device was used several times to monitor the concentration just downstream of the descending dynamic plume.

### 7.2 Main observations

The observed features concerning stripping of the overflow plumes modelled in the tests are discussed in this paragraph. The discussion focuses on observations valid for all plume tests, although some observations typical for separate individual tests are also mentioned. For every observation striking pictures are presented to illustrate the features.

### Clear surrounding water

One of the most important observations was that the surrounding water just downstream of the plume was quite clear. As can be seen in figure 7.1, visually no material could be detected just next to the descending plume.

To check whether the concentration indeed was negligible the OPCON concentration meter was placed just downstream of the visually identified plume edge. In the resulting measurements the concentration normally did not differ from that of the ambient fluid. In some occasions concentration increases were measured, but only during irregularities in the overflow, such as movement of the pipe, changing the jet velocity, etc. During these irregularities it was also seen that the concentration of the surrounding water was increased. This means that it is possible to observe any significant concentration increase visually.

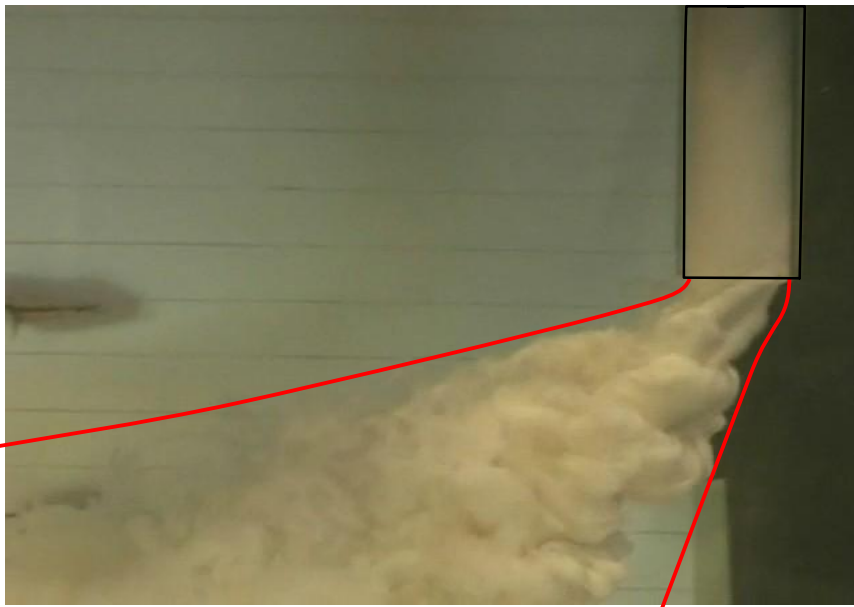


Figure 7.1: No material found outside the plume edges.

### Rare breaking of vortices

A rarely observed feature of the overflow plume was the breaking of vortices which was expected to be the main process of stripping. Sometimes a vortex seemed to overstretch itself, and got placed partly outside the plume. Via advection the loose vortex is removed from the plume, while diffusing in the ambient flow. The vortex breaking occurred only incidentally and turned out to be an irreproducible feature.

To illustrate the vortex breaking process a series of pictures is presented in figure 7.2 which shows a vortex that got overstretched, cut loose from the plume and subsequently advected by the ambient current.



Figure 7.2: Series of subsequent pictures showing a vortex breaking from a plume

#### **Influence of discontinuities**

In the steady, continuous overflow plumes modelled, the plume stayed closely together and the surrounding waters were quite clear except for some rarely occurring breaking of vortices. However, after discontinuities the plume looks very different. Discontinuities present in the tests were starting of the overflow, displacement of the overflow pipe and abrupt changes of density (due to settling effects in the siphon).

When the overflow was started, the plume front entered clean water. While the plume front was descending to the bottom some material was advected more by the ambient flow than the rest of the plume. Subsequently, at the moment of bottom impingement one or more clouds of material were formed downstream of the plume. Those clouds show passive behaviour and are advected and diffused by the ambient flow in the flume. Figure 7.3 gives an impression of these clouds.



Figure 7.3: Clouds formed directly downstream of a starting plume

When the place of the overflow pipe was displaced in upstream or downstream direction the plume got cut into two pieces and showed a different behaviour. The part of the plume belonging to the 'original' position got partially advected by the ambient flow. For small movements the effects were too small and could not be isolated. For large movements (several pipe diameters) the effects were more easily seen. Figure 7.4 presents a series of pictures of a pipe displacement to give the reader an idea of what was happening.



Figure 7.4: Series of subsequent pictures showing the results of a pipe displacement

Due to the fact that the siphon through which the overflow was released in the experiment was shut for some time density differences occurred within the siphon fluid. In the vertical parts of the siphon kaolinite tended to settle. As a result the start of the plume consists of subsequent parts of higher and lower density. This starting phase normally lasted for about one minute, but did incidentally last for about five minutes. Main parameter determining the influence of these irregularities was the time the kaolinite was given to settle.

When the density differences were small, the change in plume behaviour was small and smooth, however if the density differences were large, as in figure 7.5 for example, the difference in behaviour was very large. In figure 7.5 the development of a dynamic plume of dense material within the rests of the passive plume of a very light starting fluid is shown.



Figure 7.5: Development of a dynamic plume of heavy material in the passive plume rests of preceding lighter mixture.

#### Tests with varying overflow properties

To enhance the creation of passive clouds of material the last test series (number 7 in table 7.1) was carried out with an overflow with discontinuous jet velocity and density. To be able to create variability a new overflow pipe was constructed by mounting a funnel on a pipe. The overflow fluid should be poured into the funnel and the water level in the funnel determines the jet velocity. Figure 7.6 shows a picture of this overflow pipe.



Figure 7.6: Overflow pipe with funnel constructed for variable overflow creation

The results of these tests were similar to the results of earlier tests. The surrounding water near the plume stayed quite clear and vortices only rarely broke up. In fact no clear example of vortex breaking could be obtained from the tests that were carried out.

The discontinuities generated in these tests were smaller than the discontinuities due to movements and starting effects described earlier. The density of the overflow material was varied between  $1030 \text{ kg/m}^3$  and  $1070 \text{ kg/m}^3$ . The variance of the velocity was caused by a variation of 10 cm, which is about 20% of the total height difference.

The plume turned out to be irregular. Especially when heavier material was mixed into lighter material the plume showed an irregular, puffy behaviour. When light material was used and the jet velocity was also low, the plume sometimes showed a more passive behaviour. Tests carried out with parameters in that region show particularly interesting behaviour as the plume seems to consist of different clouds and puffs. An example of that is presented in figure 7.7.



Figure 7.7: Plumes with varying overflow parameters behaving as separate clouds and puffs.

Directly downstream of the plume the concentration was measured with the OPCON concentration meter. The concentration turned out to be barely measurable. The water was not continuously clear, but the concentration peaks were not very high and were spotted only occasionally. Since the plume dimensions were much smaller in this series, the relative amount of material that was removed from the plume and advected passively was higher than in continuous plumes. It is however more likely that this caused by the presence of the passive clouds and puffs described above than by the process of stripping. This idea is strengthened by the observation that these concentration peaks occurred more often in plumes with lower density and lower jet velocity. For these plumes the increase in the number of passive clouds and puffs observed is able to account for the increase in concentration peaks measured.

### Influence of pipe

Especially with larger pipes the wake formed behind the pipe had influence on the plume. The recirculation patterns of material could be observed when the plume was strongly bent over, but when the ZFE was near vertical the influence of the wake was very limited. Figure 7.8 shows the effect for the first test run in which the strongest ambient flow and the largest pipe were used. In the following three tests (up to number 4) the effect cannot be ignored, but the importance is decreasing. In later tests with smaller pipes the influences of the pipes were considered negligible.



Figure 7.8: Recirculation of material in wake of pipe



## Chapter 8: Discussion of stripping

Stripping of overflow plumes is defined as the removal of material from an overflow plume by a crossflow. Stripping is considered important because it would determine a source term for modelling of the passive phase of an overflow plume that also covers the upper part of the water column. The processes causing stripping as well as the quantification of stripping are not described in literature. The existence of stripping in practice is shown by passive material found in the upper part of the water column.

From the conducted experiments it can be concluded that stripping is not significant in small scale, continuous released, sediment-laden, buoyant jets in continuous crossflow. The breaking of vortices, the hypothesized stripping process in this M.Sc. thesis, is only rarely occurring in the modelled plumes. The cause of these unpredictable vortex break ups is not known, but is not thought to be due to the continuous crossflow the modelled plumes were released in. Probably the few vortex break ups seen in the experiments were caused by irregularities in the overflow concerning jet density, jet velocity or possibly even the presence of air bubbles. Also experiments with small variations of overflow density and velocity did not provide better insights. These experiments did however show that irregular overflowing might result in cloudy or puffy overflow plumes.

In the experiments it was seen that overflow plumes have the tendency to stabilize themselves as long as they are continuous. However, if material gets placed outside the dynamic plume for any reason, it will be advected from the plume and further spread passively. The focus on explaining the existence of passive material in the upper part of the water column in reality should therefore focus on possibilities for material to get placed outside the plume.

One of them still includes the stripping process. It is possible that the stripping process present in reality does not occur in the experiments due to scale effects. Due to the turbulent nature of the process, such dependence on length scale is possible if the process requires a minimum absolute length scale that needs to be relatively small compared to the overall length scale. However, the results of the experiment make it less likely that stripping is significant in overflow plumes.

Another possible mechanism to remove material from the plume is the existence of air in the overflow. Air bubbles create locally reversed buoyancy and therewith removal of (small) clouds of material from the plume seems logical. However, with the use of the Anti Turbidity Valve, the amount of air entrapped in the overflow can be reduced significantly.

A last mechanism that could explain the removal of material from the plume is the irregularity of the overflow discharge. Due to the influence of ship movements, waves, propeller suction and the characteristics of the overflow process itself large variations are occurring in jet density, jet velocity and local ambient velocity. It is well possible that during these variations overflow will occur with characteristics that temporarily cause passive behaviour of the plume. Then a short passive cloud might be created that is advected swiftly from the plume, as was seen in the experiments.

---

The results of the conducted experiments on stripping do not provide the right information to improve the modelling of overflow plumes. As it is not demonstrated that stripping is significant in overflow plumes, the possibilities to implement stripping in overflow plume models are not investigated. The experiments did furthermore not isolate or quantify a process that could explain the existence of passive material in the upper water column, so there is neither any desire nor a possibility to implement the creation of this material in (dynamic) plume models.

## Part 3: Vortex divergence



## Chapter 9: Vortex divergence experiment

*After the decision to stop with the stripping experiment, an experiment on vortex divergence was developed. Vortex divergence was observed in the earlier experiment, but the existence of bifurcation was speculated and therefore further investigated with this experiment. In this chapter the background of the experiment is presented.*

### 9.1 Basic idea of the experiment

*In paragraph 5.2 the objectives for the vortex divergence research were presented. In this paragraph it is stated first which of these objectives will be fulfilled by the experiment. After that the hypothesis of the outcome is presented, followed by the indication of the measuring need to verify the hypothesis.*

#### 9.1.1 Objectives

Vortex divergence is occurring when the two centres of the vortex pair cross profile are moving apart while the profile stays united, while vortex bifurcation means that the plume completely splits up into two parts. The experiments on vortex divergence should provide quantitative information on the diverging rate of overflow plumes and determine whether these plumes bifurcate or not. Next to that the influence of several parameters on vortex divergence and bifurcation needs to be determined. Mainly the dependency on the Richardson number and velocity scale has to be investigated.

#### 9.1.2 Hypotheses

Divergence was already observed in the model overflow plumes created in the experimental setup during the stripping experiments. In literature it is given that the diverging angle of buoyant jets in homogeneous surroundings is 8-10°, so values in this range are also expected in the experiments. It is also given that in homogeneous surroundings bifurcation does not occur; therefore bifurcation is not expected in the modelled overflow plumes.

The dependency of vortex divergence on the Richardson number and the velocity scale is hypothesized shortly here:

- Higher Richardson numbers are expected to increase the divergence rate. Since higher Richardson numbers indicated higher buoyancy rates it is expected that the vortex strength is increased so that the concentration profile will better follow the vortex pair velocity cross profile. The chance of bifurcation becomes higher.
- Higher velocity scales are thought decrease the divergence rate. Since higher ambient velocities are thought to produce more ambient turbulence it is thought that the concentration profile is smoothed more when the ambient velocity is increased. The possibility of bifurcation becomes therewith smaller. Also the relative vortex strength is smaller at higher velocity scales, which is thought to decrease the divergence rate.

### 9.1.3 Measurements needed

The divergence angle of the plume could be estimated from plan view observations of the whole plume, but this method is considered too crude. Therefore it was thought to determine the divergence angle by measuring and visualizing the concentration cross profile of the plume for several points downstream. For every point the position of the vortex centres is determined and the movement of these vortex centres between each measurement is a measure for the divergence rate. Whether vortex bifurcation is present in the plume could be investigated by looking whether ambient fluid has entered the original plume centreline.

Visualizing the (time-averaged) cross profile is done by measuring the time-averaged concentration of every point in a 5x5 to 8x8 grid in the cross direction of the plume. The distance between the gridlines is varying for each profile depending on the downstream distance from the orifice. From the visualization the vortex centre can be determined and the distance between the vortex centres is measured. Interpolation can be used to calculate the divergence-angle whereas extrapolation can be used to determine the (virtual) starting point of divergence. Two or three profiles will be measured per plume. The idea of determining the divergence with two measurements is sketched in figure 9.1.

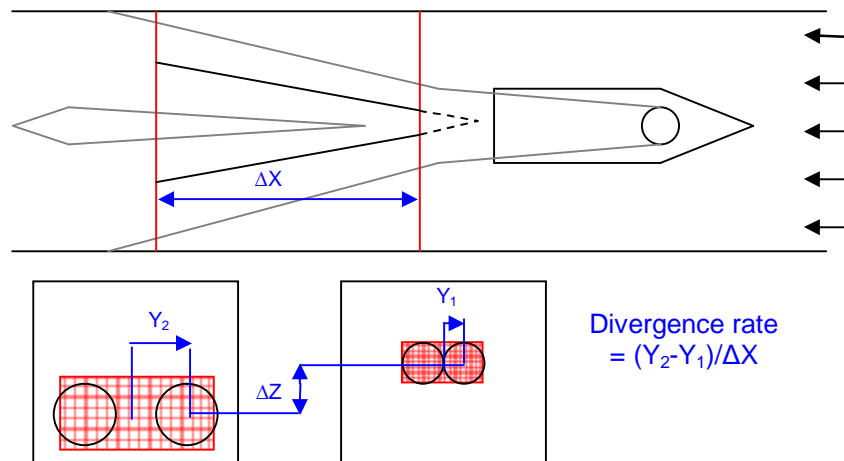


Figure 9.1: Sketch of the determination of divergence with two profile measurements

## 9.2 Experimental setup

In this paragraph the experimental setup of the vortex divergence experiment is shortly discussed. First the scaling of the vortex divergence experiment is discussed and the dimensions of the setup are described. After that the control of parameters is discussed. Further information on the working of the experimental setup is presented in Appendix E whereas more detailed information on several parts of the setup is presented in Appendix F, G and H.

### 9.2.1 Scaling

For the scaling of the vortex divergence the results of the parameters study in Appendix C are used. A Richardson scaling of 1:250 is adopted. The Reynolds numbers within the overflow pipes are with that scale smaller than the minimum Reynolds number recommended by Ettema *et al.* (2000) of about 4000 to 10000. But since the behaviour of the overflow plume directly after the orifice is observed to be sufficiently turbulent it has been assumed that the model can correctly predict the behaviour of the overflow plume.

Unlike the stripping experiment the scaling of the model does not have to be distorted, since the overflow pipe diameters are accepted. The grading of the material is more difficult to scale. There is no granular material available which size is sufficiently small to fulfil the scaling proposed. However, since overflow is thought to be a single phase fluid, the incorrect scaling of the material does not seem to hinder the near-field effects modelled. For that reason kaolinite is used in this experiment.

### 9.2.2 Dimensions

The dimensions used in this experiment are not directly determined by scaling all the parameters correctly with the mentioned 1:250 Froude scaling, but are adapted to be able to measure vortex divergence. Several test experiments were used to determine the combinations of parameter values that would deliver the best measurable diverging plumes. It turned out that higher discharge densities and a velocity scale of nearly one delivers the finest result.

In table 9.1 the magnitude of all parameters is presented for the typical overflow plume mentioned in paragraph 2.3 (called prototype here), for the 'correct' 1:250 Froude scale and for the experiment.

Parameter	Prototype	Correctly scaled	Experiment	Unit
$\rho$	1025	1000	1000	kg/m <sup>3</sup>
$\rho_{\text{mix}}$	1040-1060-1090	1015-1035-1065	1040-1050-1060	kg/m <sup>3</sup>
$u_{\text{amb}}$	0.0-1.0-4.0	0-0.063-0.253	0.04-0.05-0.06	m/s
$h$	20-35-80	0.05-0.14-0.32	0.35	m
$D_{\text{pipe}}$	1-3-4	0.004-0.012-0.016	0.004-0.01	m
$u_{\text{jet}}$	0.5-1.0-1.5	0.032-0.063-0.095	0.04-0.05-0.06	m/s
$g$	9.81	9.81	9.81	m/s <sup>2</sup>

Table 9.1: Magnitude of parameters in prototype, on scale and applied in the experiment.

### 9.2.3 Controlling the parameters

From the information above it can be derived that several parameters need to be controlled. In this part it is shortly explained how control is taken care of in the experimental setup for several parameters. Further comments on the working of the experimental setup are presented in Appendix E.

- The ambient velocity is the velocity to be set in the flume. It is determined by the discharges going in and out of the flume. For every combination of water depth and the incoming and outgoing discharge was calculated exactly. Since only a few predefined settings were to be made, the discharges needed to be set to several distinct valued. To control the discharge the frequency of the pump was adjusted and the discharge was checked by measuring it with a pipe discharge meter. During the building of the setup the flume velocity suffered from significant deviations. The cause and solutions for these deviations are discussed in Appendix H.
- The overflow velocity is controlled by adjusting the height difference over the siphon. The relation between the height difference and the resulting velocity was determined in calibration tests for each different siphon. The actual height difference was measured for every run.
- The overflow pipe diameter is varied by using several different siphons.
- The density of the mixture is created by adding kaolinite to clean water. The amounts of kaolinite and water needed were weighted to create the mixture with the wanted properties.
- The water depth in the flume is regulated by a weir at the end of the plume. Using weir overflow functions the water height above the weir can be calculated for the planned discharged. To set the wanted total water depth the weir height should be adjusted properly. The water depth is checked by a water height meter.

### 9.3 Measuring plan

To further confine the research work, only several parameter combinations were investigated. Experience from the stripping experiment had learned that it is better to reduce the measuring plan beforehand. The resulting plan is described here.

Since time was limited it the total amount of parameter combinations tested was reduced. For practical convenience the same overflow mixture was used for several tests, reducing the time needed to produce the mixture by making use of economies of scale. For each mixture it was planned to execute a series of tests in the same way.

First two tests are carried out to compare the two different pipe diameters. Since the Richardson number ( $Ri$ ) is very small in the smallest pipe, this comparison is made on a relatively small velocity scale ( $\zeta$ ). Next to that three tests with an increasing  $\zeta$  are made at an intermediate  $Ri$ . Due to the density differences between the three test series the  $Ri$  is increased for every series, but only with a relatively small amount.

The measuring plan for the vortex experiment is listed in table 9.2 and presented graphically in the  $Ri$ - $\zeta$  diagram in figure 9.4.

run nr	$\rho$ ( $kg/m^3$ )	$D$ ( $m$ )	$W$ ( $m/s$ )	$U$ ( $m/s$ )	$Ri$ (-)	$\zeta$ (-)
First test series						
1	1040	0.004	0.05	0.04	0.63	0.80
2	1040	0.01	0.05	0.04	1.57	0.80
3	1040	0.01	0.06	0.04	1.09	0.67
4	1040	0.01	0.06	0.05	1.09	0.83
5	1040	0.01	0.06	0.06	1.09	1.00
Second test series						
1	1050	0.004	0.05	0.04	0.78	0.80
2	1050	0.01	0.05	0.04	1.96	0.80
3	1050	0.01	0.06	0.04	1.36	0.67
4	1050	0.01	0.06	0.05	1.36	0.83
5	1050	0.01	0.06	0.06	1.36	1.00
Third test series						
1	1060	0.004	0.05	0.04	0.94	0.80
2	1060	0.01	0.05	0.04	2.35	0.80
3	1060	0.01	0.06	0.04	1.64	0.67
4	1060	0.01	0.06	0.05	1.64	0.83
5	1060	0.01	0.06	0.06	1.64	1.00

Table 9.2: Measuring plan vortex divergence experiment

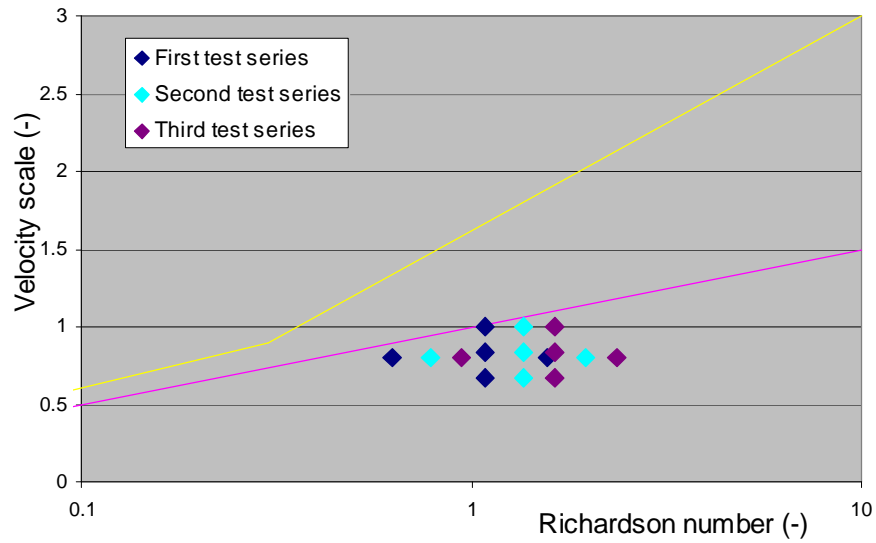


Figure 9.4: Measuring plan vortex divergence exp. presented graphically in  $Ri-\zeta$  diagram

## Chapter 10: Vortex divergence experiment results

*The results of the vortex divergence experiments are presented in this chapter. Due to practical problems not all tests planned for were carried out. The set of measurements that were carried out are presented in the first paragraph, the establishment of this set of measurements is discussed in Appendix J. The second paragraph presents the measured cross profile and the later paragraphs specify the results of the measurements for relevant parameters as the divergence angle, the plume path and the entrainment and dilution.*

### 10.1 Measurements

Due to problems with the siphons only few profile measurements were carried out. Also the amount of material discharged by the siphon might be different for several runs due to these problems. This makes comparison of the several measurement results complicated. To check whether profiles measured are indeed belonging to the same plume for every profile measurement the total amount of material ( $C_{tot}$ ) in the cross profile is determined. This information is added to the basic information on the plume which is presented in table 10.1.

Plume nr	Profile nr	Distance from orifice	$\rho$ ( $kg/m^3$ )	$D$ (m)	$W$ (m/s)	$U$ (m/s)	$C_{tot}$ ( $g/lcm^{-2}$ )
1	1	25 cm	1040	0.01	0.05	0.04	97
2	1	25 cm	1050	0.01	0.05	0.04	56
2	2	40 cm	1050	0.01	0.05	0.04	60
2	3	54 cm	1050	0.01	0.05	0.04	98
3	1	25 cm	1050	0.01	0.05	0.05	68
3	2	48 cm	1050	0.01	0.05	0.05	87

Table 10.1: Information on different profiles measured

From this table it can be concluded that only profiles 2.1 (plume nr.profile nr) and 2.2 can safely be compared since those two measurements are from the same plume, and the amount of material within the plume is also the same, indicating that the siphon was probably functioning in the same way. The profiles 3.1 and 3.2 might also be compared, but more care has to be taken due to the larger difference in amount of material discharged.

## 10.2 Cross profiles of every plume

For every plume the measured cross profiles are presented in this paragraph. To develop the cross profiles presented here, some processing of the results had to take place. The unprocessed results are presented in Appendix K. The figures presented here cover the whole flume cross profile and the concentration of material is indicated in red using the same scale for every figure. Some comments are made on the vortex divergence and bifurcation of the plume, taking the uncertainties caused by the malfunctioning of the experimental setup into consideration.

### Plume 1 ( $\rho=1040 \text{ kg/m}^3$ , $W=0.05 \text{ m/s}$ , $U=0.04 \text{ m/s}$ )

From the first plume only one profile has been measured. This profile is shown in figure 10.1. The cross profile indeed has the typical vortex pair shape described in literature. The total amount of material in this profile is  $97 \text{ g/lcm}^2$ , which is quite large if compared to the other tested plumes. Also the relatively high concentrations in the profile indicate that the total amount of material discharged is large. The two concentration centres are  $6.2 \text{ cm}$  apart and the plume is not (yet) fully bifurcated. Because only one profile is measured not much information on the plume can be presented.

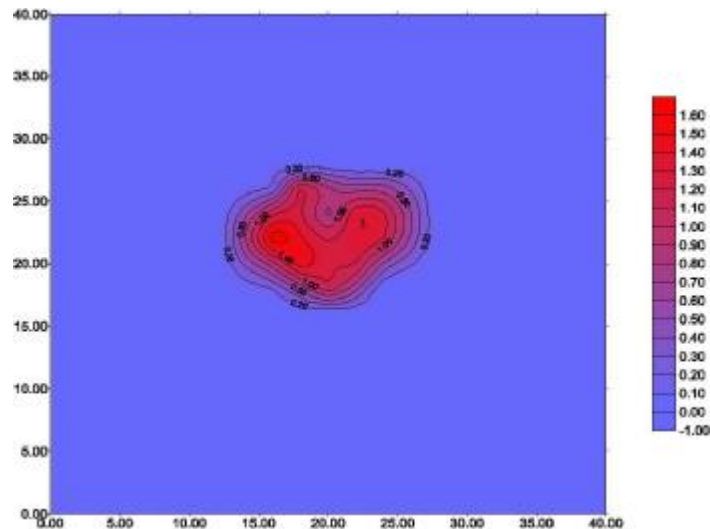


Figure 10.1: Concentration profile resulting for measurement 1.1  
(note different scale for concentrations)

### Plume 2 ( $\rho=1050 \text{ kg/m}^3$ , $W=0.05 \text{ m/s}$ , $U=0.04 \text{ m/s}$ )

The second plume was best documented. Not only three profiles were measured successfully, but also the amount of material discharged seemed constant for the first two measurements. The different profiles are shown in figure 10.2, 10.3 and 10.4 which show the processed result of measurement 2.1, 2.2 and 2.3 respectively.

Along the plume path the concentration peak within the cross profile is decreasing from about  $0.9 \text{ g/l}$  to  $0.6 \text{ g/l}$ . The fact that the concentration peak in the second (at  $40 \text{ cm}$  downstream) and third (at  $54 \text{ cm}$  downstream) cross profile is nearly the same can be explained by the difference in total material present in the cross profile. Probably the discharge of material was larger during the third measurement.

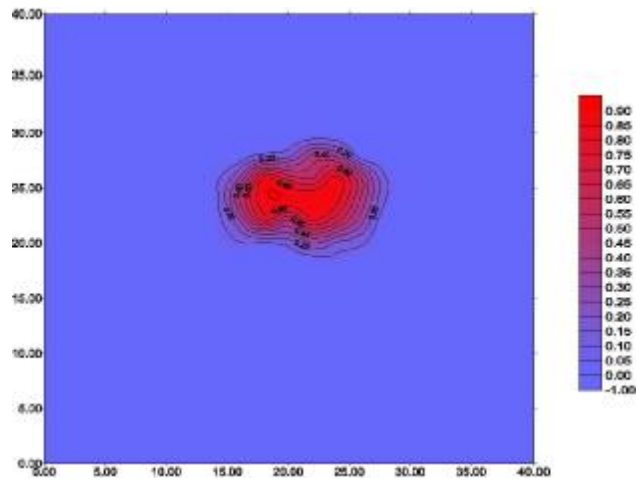


Figure 10.2: Concentration profile resulting for measurement 2.1

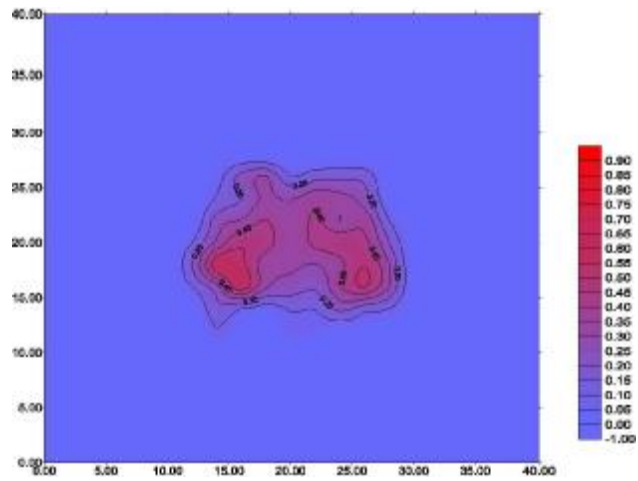


Figure 10.3 Concentration profile resulting for measurement 2.2

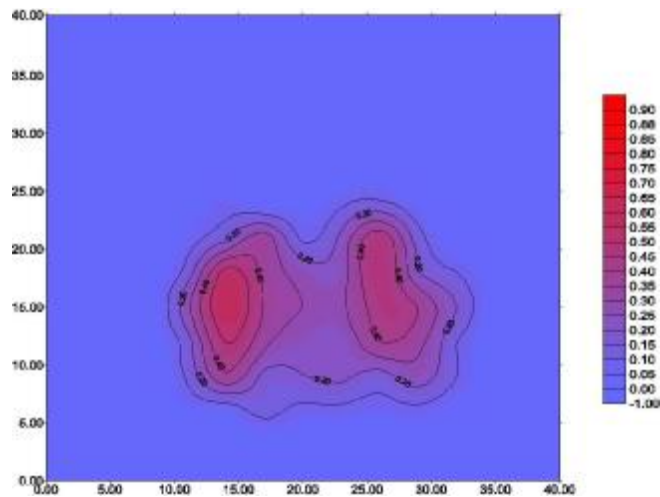


Figure 10.4: Concentration profile resulting for measurement 2.3

The vortices of the vortex pair are diverging, since the distance between the concentration centres is increasing, but the plume is not bifurcating. To quantify vortex divergence the distance between the concentration centres is estimated for every cross profile. The result is presented in table 10.2. The divergence rate seems to be decreasing with downstream distance as the increase in distance between profile 2.1 and 2.2 is larger than from 2.2 to 2.3. This is not in line with the expectation of a constant divergence rate over the whole developed plume as described in literature. Another cause for this observation may lay in the different amount of material discharged, that could have suppressed the divergence.

Profile nr.	Downstream distance of profile	Distance between vortex centres
2.1	25 cm	5.7 cm
2.2	40 cm	8.9 cm
2.3	54 cm	11.7 cm

Table 10.2: Distance between concentration centres in profiles 2.1, 2.2 and 2.3

**Plume 3 ( $\rho=1050 \text{ kg/m}^3$ ,  $W=0.05 \text{ m/s}$ ,  $U=0.05 \text{ m/s}$ )**

The quality of the measurements of the profiles of the third plume faced problems with the averaging time (which is equal to the time available for one point measurement) which was relatively short compared to the other plumes. For this reason the concentration profile showed several strange peaks. A peak levelling procedure was followed to obtain better looking results. The background of this procedure is presented in appendix K. The resulting profiles 3.1 and 3.2 are shown in figure 10.5 and 10.6 respectively.

Along the plume path the maximum concentration is again decreasing from about 0.85 g/l to 0.7 g/l, but it has to be taken into account that in the second profile more material is present. In both profiles it can be seen that the concentration maxima are not occurring in the vortex centres. This might also be due to the short averaging time problem described above.

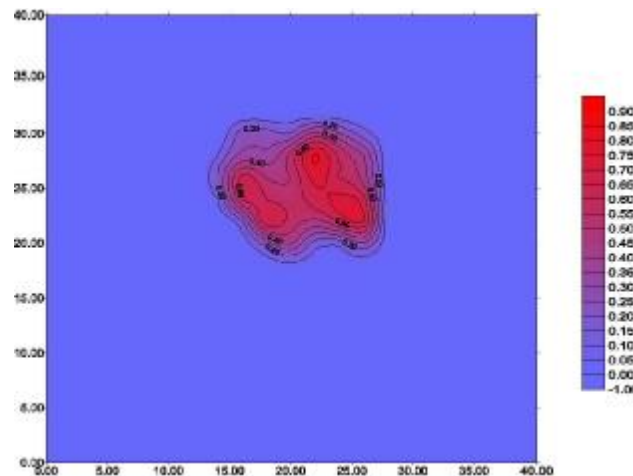


Figure 10.5: Concentration profile resulting for measurement 3.1

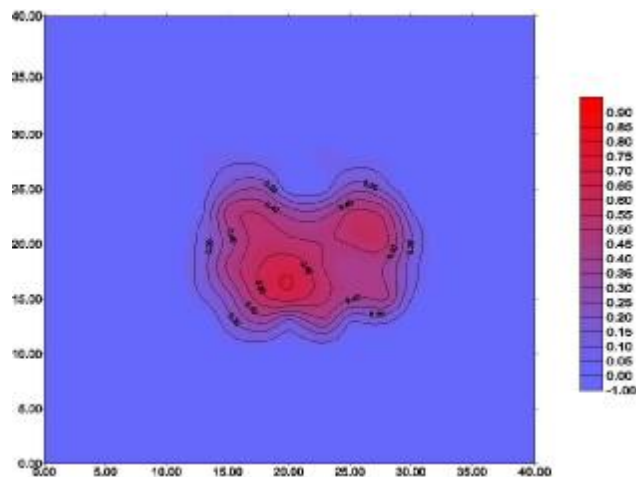


Figure 10.6: Concentration profile resulting for measurement 3.2

The vortices of the vortex pair are also diverging in this plume, but the divergence rate seems somewhat smaller than in the second plume. Again no bifurcation is present. The distance between the vortex centres was more difficult to estimate but is presented in table 10.3. Indeed the diverging rate for this plume is smaller than for the other.

Profile nr	Downstream distance of profile	Distance between vortex centres
3.1	25 cm	6.0 cm
3.2	48 cm	9.2 cm

Table 10.3: Distance between concentration centres in profiles 3.1 and 3.2

### 10.3 Vortex divergence rate

From the results of the distance between the vortex centres the divergence angle can be calculated. This is done first for plume 2 and 3 individually (for plume 1 this is impossible as only 1 data point is available). A divergence angle of  $9.8^\circ$  for plume 2 and  $10.8^\circ$  for plume 3 were found to give best data fit, but for both plumes it is seen that any divergence angle in the range of  $8-12^\circ$  would be well possible. To present the average vortex divergence rate in the experiment all results for the distance between vortex pairs are used. The result is presented in figure 10.7. An average divergence angle of  $10.2^\circ$  delivers best data fit but still any divergence angle in the range of  $8-12^\circ$  delivers acceptable results. These findings are in line with literature where the divergence angle is described to be in the range of  $8-10^\circ$ . The fact that the range observed in this experiment is larger and allows somewhat higher values might be due to the limited data set (giving a wide range of possible angles) consisting of plumes with relatively large vortex divergence (presenting a higher average angle).

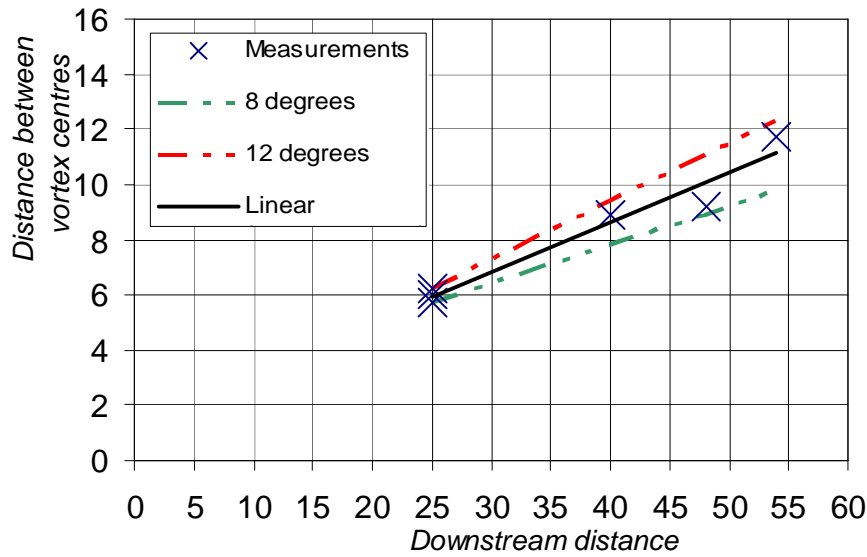


Figure 10.7: Vortex divergence observed in the experiments

### 10.4 Plume paths of tested plumes

The experiments also deliver information on the plume path of the tested plume. This information might be useful when the tests are compared with model results. For that reason the information on the plume path is only presented here in table 10.4. In the next chapter, the plume paths are presented graphically to compare it to the model results.

Profile nr	Downstream distance of profile	Vertical position of plume centre
1.1	25 cm	22.7 cm
2.1	25 cm	24.6 cm
2.2	40 cm	17.2 cm
2.3	54 cm	16.7 cm
3.1	25 cm	24.4 cm
3.2	48 cm	19.4 cm

Table 10.4: Vertical position of plume centre at every profile

### 10.5 Entrainment and dilution

Another interesting feature of the tested plumes is their entrainment rate. Entrainment is defined as the increase of volume flux per unit plume length, so if entrainment has to be measured the volume flux should be determined for several subsequent stages. With the present measurements this is not possible as volume flux is determined by multiplying the area of the plume cross profile ( $A$ ) by its mean velocity ( $W$ ). In the experiments it is possible to make an estimation of the area of the plume cross profile, but the velocity of the plume is not measured.

In order to give an idea about the entrainment and the mixing processes that play a role in the plumes, it is possible to look at their dilution. Dilution is defined as the ratio between the starting peak concentration and the local peak concentration at the measurement. The starting peak concentration is known for each plume and the local peak concentration can be determined in every profile measurement. The results for the dilution at every profile are presented in table 10.5.

Profile nr	Downstream distance of profile	Peak concentration	Dilution
1.1	25 cm	1.66 g/l	24.1
2.1	25 cm	0.89 g/l	56.2
2.2	40 cm	0.57 g/l	87.7
2.3	54 cm	0.60 g/l	83.3
3.1	25 cm	0.82 g/l	61.0
3.2	48 cm	0.67 g/l	74.6

Table 10.5: Dilution of plumes at every profile

The dilution figures show that the dilution increases with the plume length, which is logical as more clean water has entrained the plume, so the concentration in the plume drops. The results do show that measurement 1.1 and 2.3 probably have suffered problems with the siphon, as the peak concentration is higher (and subsequently the dilution is lower) than could be expected from the other measurements. The results for the dilution of the tested plumes will be used for comparison with model results in the next chapter.



## Chapter 11: CORMIX model results

*As a representative of dynamic plume models, the CORMIX model is used to model the plumes created in the experiments. The resulting model predictions for plume path, width and concentrations are presented here first. The results are compared with the measurements to investigate whether the CORMIX model delivers satisfying results for the tests carried out.*

### 11.1 Results for the tested plumes

The parameters for the laboratory situation of the tested plumes are put into the CORMIX model. The exact input values can be seen in appendix L, where the model input is presented. For the three plumes created the resulting trajectory ( $X$ ,  $Y$ ,  $Z$ ), peak dilution ( $S$ ), peak concentration ( $C$ ) and half width ( $b$ ) is presented in table 11.1, 11.2 and 11.3 respectively.

$X$ (m)	$Y$ (m)	$Z$ (m)	$S$ (-)	$C$ (mg/l)	$b$ (m)
0.00	0	0.38	1.0	4.00E+04	0.00
0.06	0	0.32	12.1	3.30E+03	0.01
0.14	0	0.28	31.6	1.26E+03	0.02
0.21	0	0.25	56.3	7.10E+02	0.03
0.29	0	0.22	85.3	4.69E+02	0.04
0.37	0	0.20	117.2	3.41E+02	0.05
0.45	0	0.17	151.7	2.64E+02	0.05
0.53	0	0.15	189.1	2.12E+02	0.06
0.61	0	0.12	228.1	1.75E+02	0.07
0.70	0	0.10	269.1	1.49E+02	0.07
0.78	0	0.08	311.8	1.28E+02	0.08

Table 11.1: CORMIX result for plume 1 ( $\rho=1040 \text{ kg/m}^3$ ,  $W=0.05 \text{ m/s}$ ,  $U=0.04 \text{ m/s}$ )

$X$ (m)	$Y$ (m)	$Z$ (m)	$S$ (-)	$C$ (mg/l)	$b$ (m)
0.00	0	0.38	1.0	5.00E+04	0.00
0.05	0	0.32	10.8	4.61E+03	0.01
0.12	0	0.29	29.0	1.72E+03	0.02
0.18	0	0.25	52.7	9.50E+02	0.03
0.25	0	0.22	80.4	6.22E+02	0.04
0.32	0	0.19	111.4	4.49E+02	0.05
0.40	0	0.17	145.3	3.44E+02	0.05
0.47	0	0.14	181.7	2.75E+02	0.06
0.54	0	0.12	220.3	2.27E+02	0.07
0.61	0	0.10	260.9	1.92E+02	0.07
0.69	0	0.08	303.4	1.65E+02	0.08

Table 11.2: CORMIX result for plume 2 ( $\rho=1050 \text{ kg/m}^3$ ,  $W=0.05 \text{ m/s}$ ,  $U=0.04 \text{ m/s}$ )

$X$ (m)	$Y$ (m)	$Z$ (m)	$S$ (-)	$C$ (mg/l)	$b$ (m)
0.00	0	0.38	1.0	5.00E+04	0.00
0.08	0	0.32	17.2	2.91E+03	0.02
0.18	0	0.28	43.9	1.14E+03	0.03
0.28	0	0.25	76.7	6.52E+02	0.03
0.38	0	0.22	114.1	4.38E+02	0.04
0.48	0	0.20	154.8	3.23E+02	0.05
0.58	0	0.17	199.1	2.51E+02	0.06
0.68	0	0.15	246.2	2.03E+02	0.06
0.78	0	0.12	295.8	1.69E+02	0.07
0.88	0	0.10	347.1	1.44E+02	0.08
0.98	0	0.08	400.8	1.25E+02	0.08

Table 11.3: CORMIX result for plume 3 ( $\rho=1050 \text{ kg/m}^3$ ,  $W=0.05 \text{ m/s}$ ,  $U=0.05 \text{ m/s}$ )

## 11.2 Comparison with test results

The results of the CORMIX model are compared with the measurements made in the experiment. For every measured cross profile the CORMIX results are determined (when necessary by interpolation) and compared to the measured results. This is done for the total amount of material, the plume path and the dilution of the plume. Due to the practical problems faced during the experiments not all cross profiles are suitable for comparison. The most promising cross profiles are also compared visually.

### Total amount of material

The most important factor in determining whether or not the plumes modelled in CORMIX are the same as the plume measured in the experiments is to see whether the amounts of material in the cross profiles are equal. The determination of amount of material measured was already mentioned in chapter 10, for the CORMIX result the cross profile is placed in a numerical grid with a grid size of  $1 \text{ cm}^2$  and the amount of material is determined via simple integration. The results are shown in table 11.4.

Profile nr	Material measured (g/lcm <sup>2</sup> )	Material CORMIX (g/lcm <sup>2</sup> )
1.1	97	42
2.1	56	42
2.2	60	35
2.3	98	35
3.1	68	18
3.2	87	25

Table 11.4: Total amount of material measured and calculated for each profile

The amount of material in the cross profile calculated by CORMIX is usually smaller than the amount of material measured. This might be due to the malfunctioning of the siphon, but can also be due to the crude method of calculation used in the

determination of material in the CORMIX cross profile, which is mainly due to the low significance of the CORMIX output (the width is only presented using one significant number, due to the fact that the CORMIX presents the results in meters, with two decimal places). Probably this problem also contributes to the variation in the given amount of material for the CORMIX prediction. It is thought that profile 2.1, 2.2 and 3.1 are the most promising profiles for comparison.

**Plume path**

As a first indication whether the plume path is modelled correctly, the position of the centre of the plume is compared for every cross profile. The centre positions for the measurements were already presented in paragraph 10.4, the position of the centre in the CORMIX predictions was given in the model output presented in paragraph 11.1. Linear interpolation was needed for profile 1.1 and 3.1. The results are presented in table 11.5.

Profile nr	$X$ (cm)	$Z_{measured}$ (cm)	$Z_{CORMIX}$ (cm)
1.1	25	22.7	23
2.1	25	24.6	22
2.2	40	17.2	17
2.3	54	16.7	12
3.1	25	24.4	26
3.2	48	19.4	20

Table 11.5: Plume centre positions measured and calculated

For the profiles that were considered suitable for comparison it is seen that the deviations of the CORMIX model are relatively small, taken into account the low significance of the numbers. The deviations of the other measurements are somewhat higher, but are also relatively low.

Another possibility to investigate whether the CORMIX prediction does correctly predict the plume path is plotting the CORMIX path in the same graph as the profile measurements. This is done in figure 11.1, 11.2 and 11.3 for plume 1, 2 and 3 respectively.

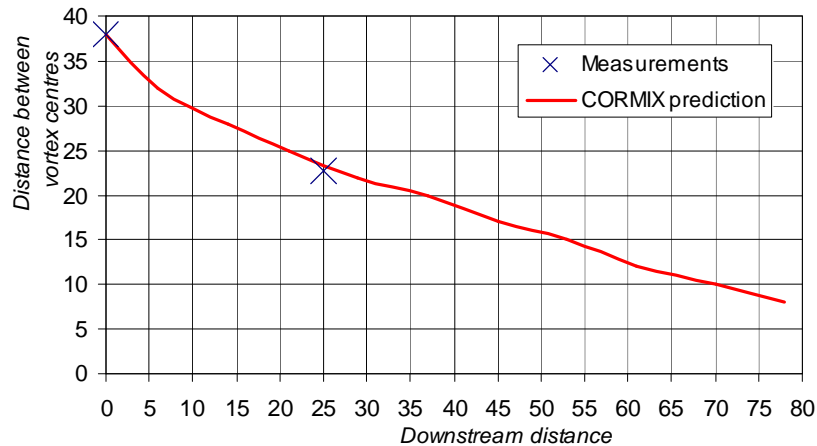


Figure 11.1: Plume path comparison plume 1 ( $\rho=1040 \text{ kg/m}^3$ ,  $W=0.05 \text{ m/s}$ ,  $U=0.04 \text{ m/s}$ )

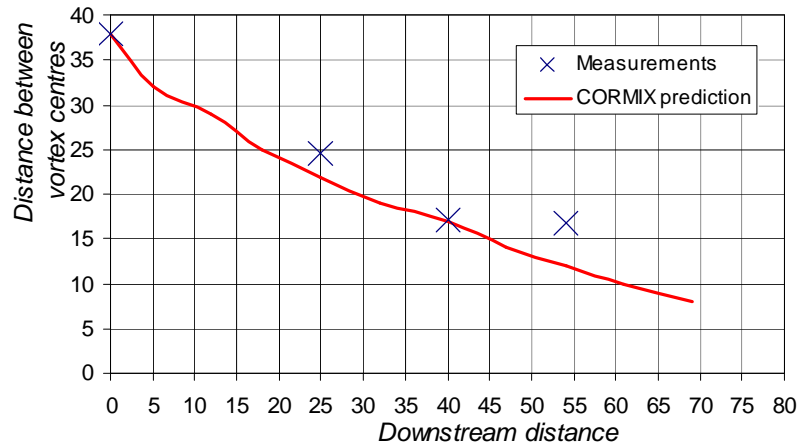


Figure 11.2: Plume path comparison plume 2 ( $\rho=1050 \text{ kg/m}^3$ ,  $W=0.05 \text{ m/s}$ ,  $U=0.04 \text{ m/s}$ )

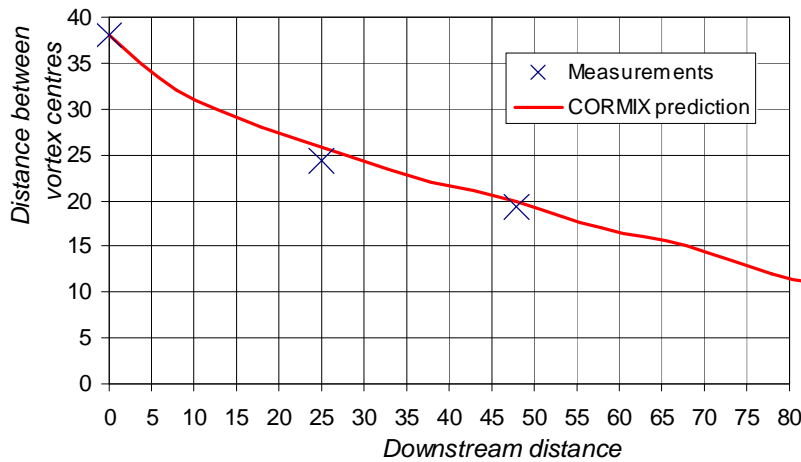


Figure 11.3: Plume path comparison plume 3 ( $\rho=1050 \text{ kg/m}^3$ ,  $W=0.05 \text{ m/s}$ ,  $U=0.04 \text{ m/s}$ )

Also from this comparison between the test results and model predictions it can be concluded that the plume path prediction of the model is sufficiently correct for all tested plumes.

**Peak concentration**

Also the dilution of the plume can be investigated. In paragraph 10.5 it was already presented that the dilution could be used to get an idea about the entrainment and mixing that takes place in the tested. For that reason it is interesting to compare the predicted dilution by the model with the measured dilution of the tested plumes. Table 11.6 presents this comparison, combining the information presented in paragraph 10.5 with the information presented in paragraph 11.1. For profile 1.1 and 3.1 linear interpolation of the data was needed.

It can be clearly seen in table 11.6 that the dilution predicted by CORMIX overestimates the dilution. This might be caused by the practical problems faced during the experiments, as the best comparable results show the least

overestimation of the dilution by CORMIX. In that case the index of the dilution is merely an index of the quality of the measurement.

Profile nr	Peak conc. measured (g/l)	Dilution measured (-)	Peak conc. CORMIX (g/l)	Dilution CORMIX (-)	Index dilution CORMIX (-)
1.1	1.66	24.10	0.60	67.11	279
2.1	0.89	56.18	0.62	80.39	143
2.2	0.57	87.72	0.34	145.35	166
2.3	0.60	83.33	0.23	220.26	264
3.1	0.82	60.98	0.80	62.66	103
3.2	0.67	74.63	0.32	154.80	207

Table 11.6: Peak concentrations measured and calculated

Another conclusion that might be drawn is the fact that the concentrations in the two vortex centres in reality are higher than the single peak in the Gaussian profile predicted by CORMIX. This might be possible if the peaks in reality are sharp and the Gaussian profile of the CORMIX prediction is relatively wide. That idea is sketched in figure 11.4, which shows two different distributions with the same material content (surface under the graph is equal). Whether that is valid in these measurements is investigated in the next section where the whole cross profile of the prediction is compared with the measured cross profiles.

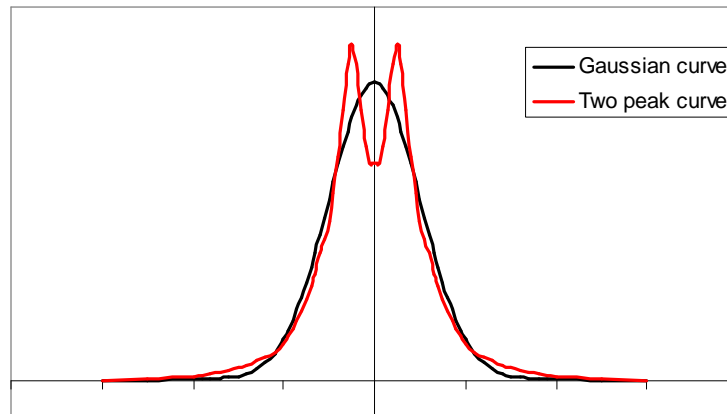


Figure 11.4: Different material distributions with the same material content

### Cross profile comparison

As a final investigation of the CORMIX prediction for the measured plumes, the full cross profiles of several measurements are compared. Due to the large discrepancies already seen in the previous sections, the profiles unsuitable for comparison (1.1, 2.3 and 3.2) are not reproduced here. The results for profile 2.1, 2.2 and 3.1 are presented in figure 11.5, 11.6 and 11.7 respectively.

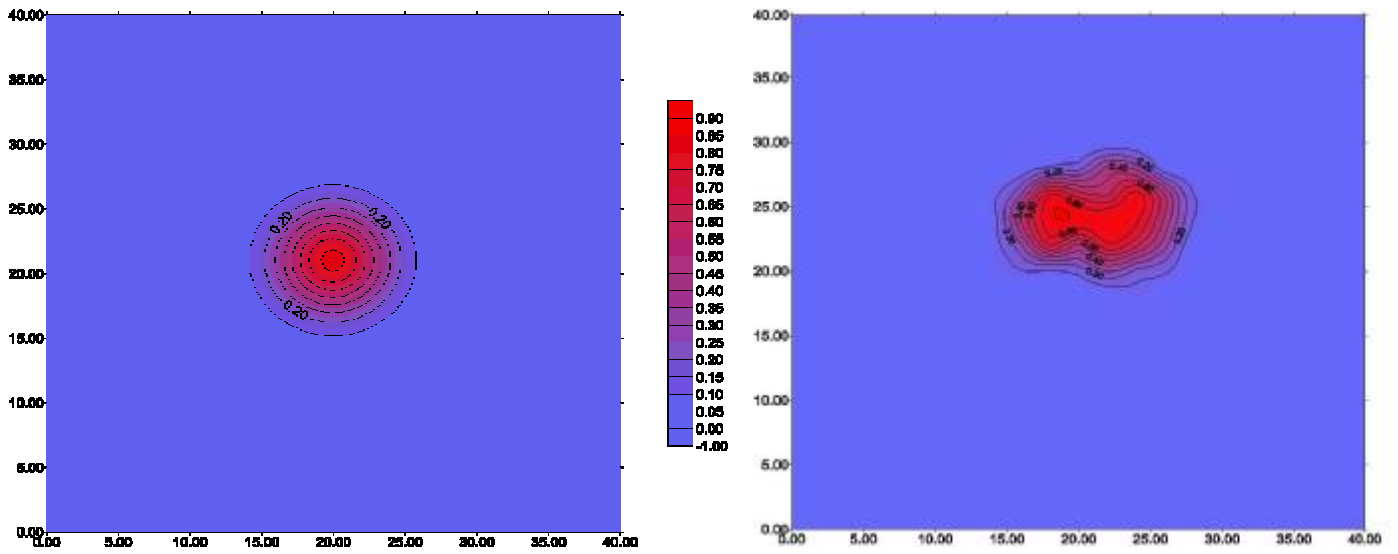


Figure 11.5: Comparison of model prediction (left) and measurement (right) of profile 2.1

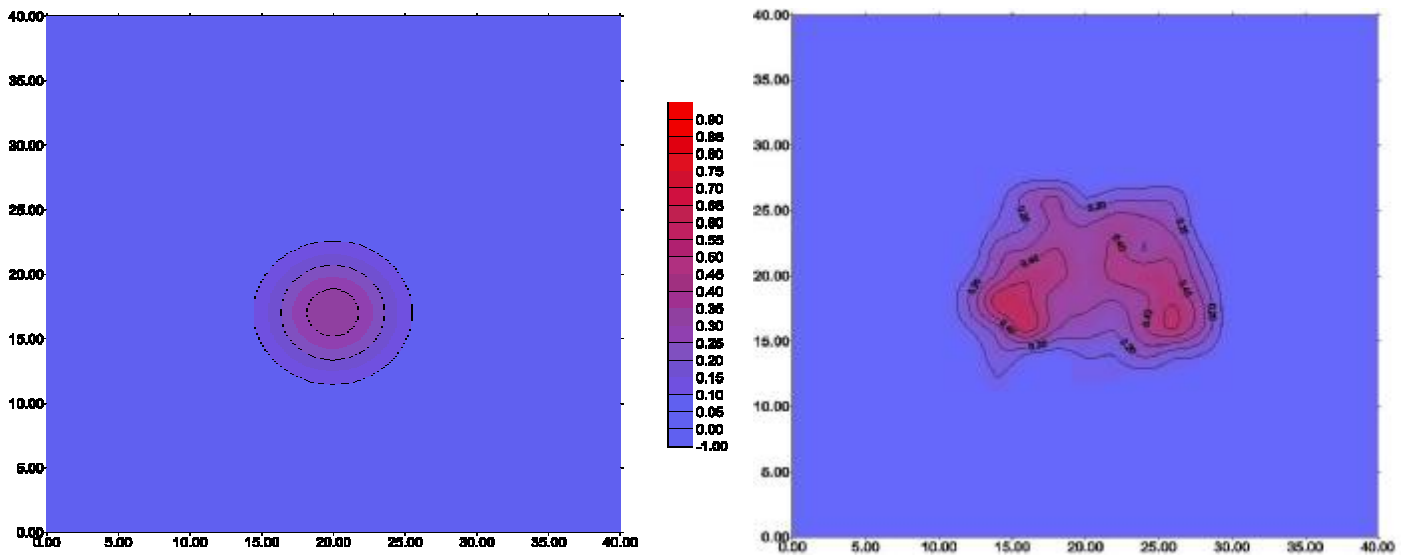


Figure 11.6: Comparison of model prediction (left) and measurement (right) of profile 2.2

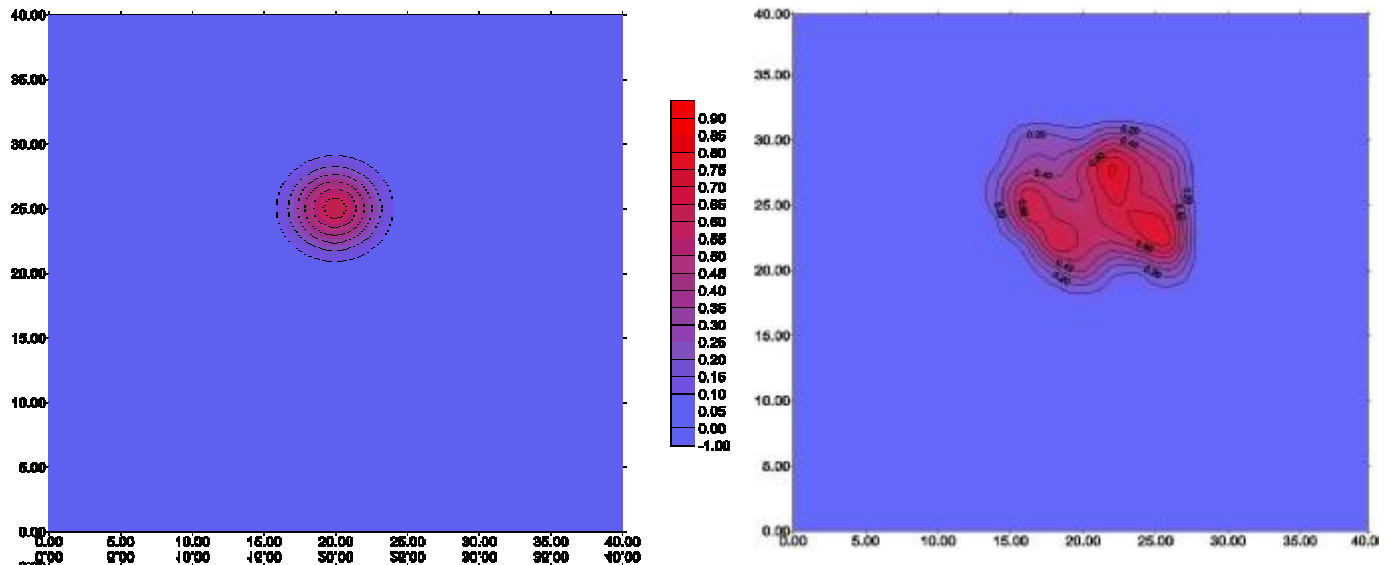


Figure 11.7: Comparison of model prediction (left) and measurement (right) of profile 3.1

From these results it can be concluded that the idea that the measured plume would have steeper peaks than the CORMIX prediction as sketched in figure 11.4, is unlikely to be true. The spread in the measured cross profiles is significantly larger than in the CORMIX prediction, and also the peaks are wider in the experiments than in the CORMIX prediction. Although this might be due to interpolation over the rough grid upon which the measurements have taken place, but that effect is not likely to completely account for the difference in peak spread. It is more likely that in the measurements continuously more material could be found than predicted by the CORMIX model, either because the experiment was malfunctioning or because the CORMIX model has the tendency to underpredict the amount of material and spreading. However, it is seen that for the plume path and too lesser extent also for the dilution this was not problematic, the CORMIX predictions corresponded quite well. Also the fact that the CORMIX model does not prescribe the vortex divergence present in these experiments seems to cause no hindrance.



## Chapter 12: Discussion of vortex divergence

### *12.1 Discussion of vortex divergence experiment*

During the earlier stripping experiments it was seen that the vortices of the vortex pair cross profile were diverging during the descent of the dynamic plume. Vortex bifurcation was however not observed. To investigate whether vortex divergence and bifurcation are important for overflow plumes an experiment to measure both was set up.

The results of the vortex divergence experiments are limited due to practical problems with the setup which are further explained in appendix J. Both the quantity and the quality of the data make that the obtained results should be treated with care.

In the experiments the plumes were not bifurcating; although the vortices were diverging, the time-averaged cross profile did show that there was always overflow material in between the vortices and that the profile remained united. The vortex divergence angle measured in the experiments was around  $10^\circ$  which lies just in the range described in literature ( $8-10^\circ$ ). However, within the data set obtained any vortex divergence angle between  $8-12^\circ$  would deliver acceptable results. The range of acceptable angles is considerable because of the limited data points. The mean of this range is somewhat higher than in literature, which is probably due to the focus of this experiment on plumes with considerable divergence. Any positive effect on vortex divergence caused by the limited width of the flume can only be speculated on and is by no means verifiable with the obtained data set.

Whether vortex divergence and bifurcation are relevant for overflow plumes in practice is questionable. The extra spreading due to these phenomena was limited during the experiments, especially when compared to other influences on spreading like bottom impingement for example. Bifurcation was not observed in the experiments. As bifurcation in homogeneous surroundings is also not discussed in literature, it is thought that in homogeneous environments bifurcation is not occurring in overflow plumes. The experiments did show considerable divergence and it is likely that also overflow plumes do show divergence to a more or lesser extent. This might increase the mixing rate and dilution of the dynamic plume. However, as the dilution in the dynamic phase is small compared to the dilution that takes place at the transition to the passive phase, it seems that this effect of vortex divergence can be considered irrelevant in the treatment of the spreading of overflow plume material in a broader sense. However, as the experiments carried out in this M.Sc. thesis did only look at the dynamic plume itself, they do not provide sufficient evidence to approve or disapprove this assumption.

## 12.2 Discussion on CORMIX applicability

As a representative of dynamic plume models, the applicability of CORMIX was investigated for the modelling of the dynamic plumes created in the vortex divergence experiments. As the vortex pairs are not represented in the model extra attention was paid to see whether CORMIX model was still appropriate in the description of the bent over phase of the dynamic plume.

The comparison of the test results with CORMIX model predictions was not able to provide a rigid conclusion on the applicability of the model. The measurement data set was limited in size and quality and also the CORMIX result was, due to the fact that dimensions were small, presented with limited significant numbers. Within the data set used it can however be concluded that the CORMIX model is likely to provide correct predictions for the plumes created in the experiment. The amount of material predicted was smaller than measured, which was probably due to the use of the malfunctioning siphons. The trajectory of the predicted plume did agree to large extent with the measurements. Finally the model was observed to overestimate the dilution and underestimate the size of the plume cross profile in the experiments. These problems could however also be connected to the deviations in the amount of discharged material during the experiments, as the model did show the least of these features at the measurements that were best comparable.

In order to discuss the CORMIX applicability with respect to vortex divergence more accurately, the underlying theory of the model was further looked at. As presented in paragraph 3.3 the CORMIX model uses the CorJet integral model for the prediction of overflow plumes. It was discussed that in this model the effect of the vortex pair formation is taken into account by an azimuthal shear process that causes extra entrainment. The entrainment rate for this extra entrainment is affected by the choice of the entrainment coefficient  $a_4$ . Since the value of this coefficient is set based on experimental data fit, global vortex divergence influences are included. As the actual diverging rate is influenced by the local vortex pair strength, as described in part 2.2.3, the influences of divergence will differ from these global influences for every specific case. The maxima of this difference are determined by the range of divergence angles possible. The presented divergence range of 8-10° seems to imply that this range is only small. It is therefore concluded in this M.Sc. thesis that the effects of vortex divergence are sufficiently taken into account in the CorJet model, especially when seen in the light of the amount of detail provided by this model.

Another, more fundamental, discussion on the applicability of the CORMIX model is the representation of the cross profile by a Gaussian profile altogether. This simplification is known to harm reality in the bent over phase, but is kept intact to keep the formulations simple. As the interest of the model is in predicting overall quantities (such as trajectory, size and dilution of the plume) this simplification is considered acceptable. In the treatment of the dynamic phase of overflow plumes for the determination of source terms for the passive phase the correct prediction of overall quantities is considered more important than the correct representation of details in the dynamic phase itself.

If more details of the dynamic phase of the plume are required, such as the description of the vortex structure within the cross profile for example, other more complex modelling techniques may be needed. Implementing parts of these complex descriptions in the CORMIX model would harm the simplicity of the model and therewith its functionality. This is considered undesirable for the modelling of the dynamic phase of overflow plumes.



## **Part 4: Conclusions & recommendations**



## Chapter 13: Conclusions

*To recapitulate the results obtained in this M.Sc. thesis, the conclusions of the work are summarized here. The conclusions of the stripping research are listed first, followed by those of the vortex divergence research. Although designing and building the experimental setup is discussed in the appendix, the conclusions drawn on the experimental setup are presented here too.*

### **13.1 Conclusions on stripping**

- The statement found in some literature that 3-5% of the total material in the dynamic plume would be stripped is not properly based and probably incorrect.
- In the small scale continuous overflow plumes created in a continuous ambient crossflow the existence of stripping was not demonstrated.
- The hypothesis that stripping is mainly caused by plume vortex breaking due to ambient crossflow was not supported by the tested plumes; vortex breaking only rarely occurred.
- It can not completely be excluded that stripping is present in dynamic plumes in reality. Due to its turbulent nature the existence of stripping might depend on length scale and therefore be absent in small-scale experiments but present in reality. This is however not likely.
- Continuous dynamic plumes have the tendency to stabilize themselves; any removal of material from the dynamic plume is due to external processes.
- In reality, these external processes might be the existence of entrapped air in the overflow or irregularities in overflow and ambient conditions.
- As no stripping of overflow plumes was quantified, implementing stripping in (dynamic) plume models is not investigated.

### **13.2 Conclusions on vortex divergence**

- The vortex divergence angle measured in the experiment was around  $10^\circ$  which falls within the range described in literature.
- Vortex bifurcation was not observed in the experiment, which makes it highly unlikely that overflow plumes in reality bifurcate in homogeneous environments.
- Although dynamic overflow plumes in reality probably do show divergence, the diluting effects of divergence on dynamic overflow plumes might be considered unimportant when seen in the light of overall spreading of plume material. The experiment results were however not able completely back this assumption.
- As the CORMIX model predetermines that the plume has a Gaussian cross profile, it does not reproduce any vortex creation, divergence or bifurcation.
- Although based on limited data, the CORMIX model is likely to provide correct predictions for the dynamic plumes tested.
- The most important effect of the vortex pair cross profile, extra entrainment, is taken into account in the CORMIX model by the azimuthal shear entrainment, that is quantified based on experimental data fit.

- Especially when considering the amount of detail the CORMIX model provides, the effects of vortex divergence are sufficiently taken into account in the model.
- The CORMIX model is thought to be suitable for the prediction of dynamic overflow plumes as for the determination of the source terms for far-field models the overall quantities, rather than the detailed structure of the plume, are important.
- Extending the CORMIX model to be able to reproduce details of the dynamic plume, such as the vortex pair cross profile, is thought to be unnecessarily complicating and affecting the functionality of the model.

### *13.3 Conclusions on the experimental setup*

- Building an experimental setup to carry out experimental research on overflow plumes was a major undertaking, but carried out successfully.
- The current flume in the Fluid Mechanics Laboratory of Delft University of Technology is suitable for creating plumes, but its dimensions are too limited for experiments at optimal scale.
- In the current flume, the velocity variations are relatively large. They are probably caused by the use of a pump in the experimental setup, since turbulence turned out not to be the origin of these deviations. This did however not seem to hinder the experiments.
- The siphons originally designed for the stripping experiment did function correctly, but the influence of the flexible hoses on the overall accuracy might be discussed, even when measures against effects such as swirling are taken. The adapted siphons for small scale test did functioned as well, but were less reliable. The large scale flexible hoses used as well as the rough finishing of the siphons made that the reliability and reproducibility were not sufficient.

## Chapter 14: Recommendations for further research

*With the results of this M.Sc. thesis some information on dynamic overflow plumes is gathered. However, still some questions concerning overflow plumes are unanswered and the results of this work even created new questions to be answered in further research. In this chapter some recommendations for this further research are presented. First the recommendations for (dynamic) overflow plume research are presented, followed by the possibilities of the experimental setup created.*

### 14.1 Recommendations for overflow plume research

*In this M.Sc. thesis only two aspects of the dynamic overflow plume, being stripping and vortex divergence, were studied in detail. Other aspects were investigated to a lesser extent. Therefore the recommendations on these two aspects are far more detailed than on the other.*

#### 14.1.1 General overflow plume research

In chapter 4 several possibilities for experimental research were listed. Several aspects of overflow plumes were said to be more important or relevant for experimental research. Only two of those aspects are investigated in this thesis. Therefore focussing on one of the other aspects mentioned there would in my opinion be a good idea to extend the knowledge on overflow plumes.

During the tests and analyses carried out other important knowledge gaps could be identified. Here the most important of those gaps are listed and commented.

- The classification of plumes proposed by Winterwerp (2002) still raises questions on its global applicability and the influence of other parameters. Further research might be aimed at creating a larger data set that contains more parameters. Furthermore it might be interesting to investigate the behaviour at the transitions between dynamic, transitional and passive plumes in more detail to obtain an idea on the stability of the types of behaviour.
- The magnitude and effects of ships movements should be considered in more detail. Perhaps the ship movements and corresponding irregularities of overflowing might be superimposed on overflow velocity and density and ambient velocity for the determination of the velocity scale and Richardson numbers. These variations might then produce a probability distribution for the stochastic values of the velocity scale and Richardson number of a plume instead of one single combination. In my opinion a numerical study to these effects might be optimal to create insights in the importance of ship movements, but it could also be studied in scale experiments.
- More generally, the resemblance between overflow plumes in laboratory tests and in reality is a major point of interest. The simplifications adopted in laboratory tests do create deviations from the behaviour in reality. Furthermore scale effects might hinder applicability of laboratory test results. Literature research might investigate the magnitude of these deviations and the possibilities to reduce them. Also experiments at larger scale (for example in the dredging flume of WL Delft Hydraulics) might provide extra information on this.

- The propeller influence is in literature only confined to wake forming behind the ship. However, the large amount of water that is brought into movement to the screw of the vessel also has to enter the screw. It is well known that this screw suction increases the velocity close to the ship. Perhaps this also has influence on the plume. This might be investigated experimentally or in prototype tests in reality.
- The bottom impingement of an overflow plume is very interesting for the further passive spread of material. It is unknown to what extent bottom impingement is investigated. To improve the understanding of it, carrying out experiments with the correct assumptions on the experimental (flume) velocities are recommended. Also the effect of vortex divergence at the moment of impingement might be taken into account in this research.

### 14.1.2 Stripping research

The experiment implemented in this M.Sc. thesis yielded no results for stripping in the created overflow plumes. The conclusion is that stripping is not a process occurring in continuous released small scale overflow plumes in a continuous ambient crossflow. That raises questions about the existence stripping in reality. In this M.Sc. thesis it is only speculated that stripping is unlikely to exist and be significant for overflow plumes in reality. Further research has to provide data to approve or disapprove this speculation.

A first approach to get to know more about stripping is carrying out tests with overflow plumes in practice. If, in some way, the dynamic phase of a plume in reality could be visualized a lot of information on the process and the amount of stripping would become available. However, this option is not very realistic, since the results of plume tests in reality are confined to profile measurements at some distance of the ship.

The existence of possibilities to obtain more information on stripping in other scale models is difficult to assess. There is always the possibility that the employed scaling hindered the processes and carrying out experiments on larger scale might reduce that hindrance. Increasing the scale also improves the measurability of the stripped material. If a small part of a larger plume is stripped, the concentrations will be better detectable with concentration meters.

Enlarging the scale is most probably not enough to create stripping plumes in laboratory experiments. The laboratory conditions should be extended with more overflow plume characteristics like waves, ship movements etc. to make sure the (unknown) driving force for stripping or, more in general, the creation of passive clouds of material outside of the plume is added to the experiment.

### 14.1.3 Vortex divergence research

The experiments carried out in this M.Sc. thesis showed that the vortex pair created in the bent over phase of dynamic overflow plumes is diverging. The vortex divergence research aimed at providing insights in the magnitude and relevance of this divergence, but was unsuccessful in giving clear predictions on that. The idea

was raised that vortex divergence is not important in dynamic overflow plumes, since the dilution created by it is small compared to the dilution created by the transition to the passive phase.

To check whether these ideas are true more research is needed on both the dilution effects of vortex divergence itself as on the effect of vortex divergence on the transition process from dynamic to passive phase. Especially the bottom impingement might be altered by the fact that the plume is more or less diverging, since bifurcation might occur to more or lesser extent.

Important for this research is the creation of a large data set on the divergence rate, spreading and dilution of (modelled) overflow plumes. This M.Sc. thesis made a start with that, but as these tests were partially unsuccessful, the quality of the resulting data set is not sufficient for further research purposes. The set should be extended with more and better measurements. It is advised to either pick a smaller scale (taken into account the scale effects) or to choose a larger (especially wider) flume for those measurements.

## 14.2 Advice for further research with the experimental setup

*Since an experimental setup is built in which not only plume modelling, but any sediment-water interaction process might be investigated, here some advice is given on the use of the experimental setup. First for plume research some comments are presented, next to that a few more general ideas are presented.*

### 14.2.1 Plume research in the experimental setup

In this M.Sc. thesis plumes were created in the experimental setup but the experiments were not completely successful. In further research in the experimental setup, the creation of plumes is certainly possible, but with several limitations. Here those limitations are listed and some advice is provided to help making further plume research in the experimental setup a success.

- The scale of the experiment should be equal to or smaller than the 1:250 scale adopted in the vortex divergence experiment. In this way the effects of the limited width of the flume are negligible in the dynamic phase of the plume.
- When the bottom impingement is also investigated in the experiment, the scale should either be reduced further to make the experimental setup suitable for the experiment. After bottom impingement the radial spreading of material makes the width already earlier insufficient. Circulations are then created in the flume. This means that it is probably best to turn to another setup when bottom impingement is to be investigated.
- The siphons to be used require extra attention. Self regulating systems like the ones adopted in this M.Sc. thesis must be implemented with sufficiently large controlled friction, to make the influences of variable friction of movable parts of the system become negligible. If one wants to avoid the use of such systems a measuring and control system should be implemented. However, these systems usually have their own instabilities that should not be underestimated.
- The use of a dividing plate should be investigated and reconsidered. The working of the dividing plate is much depending on the spreading of the plume. In the experiments the plume rests had mostly spread already to the upper part of the water column, so that the measurement had to be stopped. The reduction in waste water created by the dividing plate did not weigh out the amount of problems created by the discontinuous testing possibilities. The discharge of all water to the waste water reservoir can easily be implemented by placing the end weir just before the division in upper and lower part. This also makes it possible to regulate waste discharging without any influence on the flume velocity.
- The use of the pump is also a main concern of this experimental setup. The possibilities to reduce the pump influence on the discharge and therewith the flume velocity should be further investigated. But as the current velocity deviations are known, the effects of these velocity deviations can also be taken into account when interpreting the measurement results.
- Extensions of the setup are possible in various ways. Mounting a moving ship on the flume as well as other extensions discussed and proposed should be possible in principle.

### 14.2.2 Other research in the experimental setup

As stated above, in principle all sorts of sediment-water interactions might be investigated in the experimental setup. Since the setup is a stand-alone system within the Fluid Mechanics Laboratory of Delft University of Technology all sorts of sediment may be released in the setup, without any harm for the rest of the laboratory. Also testing of the interaction of water with different qualities and properties is for that reason possible. A few ideas that are thought of are listed here:

- The investigation of density currents.  
During the stripping tests it was observed that when large amounts of material were dumped in the flume a density current was formed which travelled against the flume velocity. Typical features of that density current such as its nose and the Kelvin-Helmholtz instabilities were seen. Also the sedimentation and erosion could be observed.
- The investigation of salt wedges.  
In nearly the same manner as density currents salt wedges might be investigated.
- Scour around structures.  
Since suspended sediment can safely be removed from this setup, the scour occurring around structures (like poles for wind energy) might be modelled in this flume. However, most probably the scale of the flume is somewhat too limited for this purpose.
- The working of silt screens and bubble screens.  
As any source of sediment can easily be created and removed from this setup the working of silt screens and bubble screens could also be tested. Placing a silt screen or bubble screen should not provide any problems and its effectiveness could be indicated both qualitatively and quantitatively.



## References

- ABDELWAHED, M.S.T. AND CHU, V.H. 1978. *Bifurcation of Buoyant Jets in Cross Flow*. Department of Civil Engineering and Applied Mechanics, McGill University, Montreal, Quebec; Technical Report nr 78-1.
- BATTJES, J.A. 2002. *Vloeistofmechanica*, Dictaat CT 2100, Delft University of Technology.
- BADLOO, P. 1998. *Milieuvriendelijke Zandwinning: 'Minimaliseren van de pluimvorming tijdens de zandwinning met een sleepopperzuiger deel I&II'* M.Sc. thesis, Delft University of Technology
- BAIRD, W.F. 2004. *Development of the MMS Dredge Plume Model.*, W.F. Baird & Associated LTD, Madison, Wisconsin.
- BLAAUWENDRAAD, J. 2006. *Dynamica van systemen*, Dictaat CT 2022, Delft University of Technology.
- BLOKLAND, T. 1988. 'Determination of dredging induced turbidity' *Terra et Aqua*, 38, pp 3-12
- BOOT, M. 2000. *Near-field verspreiding van het overvloeiverlies van een sleepopperzuiger*. M.Sc. thesis, Delft University of Technology, the Netherlands.
- BRAY, R.N., BATES, A.D., & LAND, J.M. 1997. *Dredging: a handbook for engineers, second edition*, London: Arnold.
- BURT, T.N. & HAYES, D.F. 2005. 'Framework for Research Leading to Improved Assessment of Dredge Generated Plumes' *Terra et Aqua*, 98, pp 20-31
- CHEUNG, V. 1991. *Mixing of a round buoyant jet in a current*. Ph.D. thesis, University of Hong Kong, Hong Kong.
- CORTELEZZI, L. AND KARAGOZIAN, A.R. 2001. 'On the formation of the counter-rotating vortex pair in transverse jets' *Journal of Fluid Mechanics*, 446, pp 347-373
- DANKERS, P.J.T. 2002. *The behaviour of fines released due to dredging: A literature review*. Delft University of Technology, the Netherlands.
- DELVIGNE, G.A.L. 1977. *Spreading and mixing of buoyant discharges in an ambient flow*. WL Delft Hydraulics, report on investigation R 880-III.
- DEMAS, 1995. *Suspended solids concentration in dredging, final report*. Geotechnical Engineering Office, Civil Engineering Department.
- DEMUREN, A.O. 1994. *Modelling Jets in Crossflow*, NASA Contract No. NAS1-19480.
- DIMOTAKIS, P.E. 1986. 'Two-dimensional shear-layer entrainment' *AIAA Journal*, 24 (11), pp 1791-1796

- DONEKER, R.L. AND JIRKA, G.H. 1991. 'Hydrodynamic classification of submerged single-port discharges' *Journal of Hydraulic Engineering*, 117 (9), pp 1095-1112
- DONEKER, R.L. AND JIRKA, G.H. 1997. *D-CORMIX continuous dredge disposal mixing zone water quality model laboratory and field data validation study* Oregon Graduate Institute Portland, Oregon, 44.
- DONEKER, R.L., JIRKA, G.H. AND HINTON S.W. 2007. *CORMIX User Manual Draft v2.0* from <http://www.mixzon.com/downloads/>
- ETTEMA, R., ARNDT, R., ROBERTS, P. & WAHL, T. 2000. *DHydraulic modeling – Concepts and practice*, Reston: ASCE.
- FANNELÖP, T.K. 1994. *Fluid mechanics for industrial safety and environmental protection*, Amsterdam: Elsevier Science.
- FISCHER, H.B., IMBERGER, J., LIST, E.J., KOH, R.C.Y. AND BROOKS, N.H. 1979. *Mixing in inland and coastal waters*, New York: Academic Press.
- FRIC, T.F. 1990. *Structure in the near-field of a transverse jet*. Ph.D. thesis, California Institute of Technology, United States of America.
- GERRITSEN, H., TATMAN, S., DIRKS, W., HESSELMANS, G., NOORBERGEN, H. 2005. 'Feasibility of using remote sensing as a tool for scheduling and control of dredging' *Proceedings of the 31<sup>st</sup> IAHR congress*.
- GUNTER, G., MACKIN, J.G., AND INGLE, R.M. 1964. *A report to the district engineer on the effect of the disposal of spoil from the inland waterway, Chesapeake and Delaware Canal, in Upper Chesapeake Bay*, U.S. Army Corps of Engineers, District Philadelphia.
- HINZE, J.O. 1975. *Turbulence*, New York: McGray-Hill
- HODGSON, J.E., RAJARATNAM, N. AND MOAWAD, A.K. 1999. 'Circular jets in crossflows of finite depth' *Proceedings of the Institution of Civil Engineers. Water, Maritime and Engineering*, 136, pp 35-42
- JANSEN, E. 1999. 'Introduction to spill, spill monitoring and spill management' *Proceedings Øresund Link Dredging & Reclamation Conference, may 1999, Copenhagen, Denmark*, pp 175-184
- JIRKA, G.H. AND FONG, H.L.M 1981. 'Vortex dynamics and bifurcation of buoyant jets in crossflow' *Journal of the Engineering Mechanics Deivision*, 107 (3), pp 479-499
- JIRKA, G.H. 2004. 'Integral model for turbulent buoyant jets in unbounded stratified flows. Part I: Single Round Jet' *Environmental Fluid Mechanics*, 4, pp 1-56
- JOHN, S.A., CHALLINOR, S.L., SIMPSON, M., BURT, T.N. AND SPEARMAN, J. 2000. *Scoping the assessment of sediment plumes arising from dredging*, London: CIRIA.

- JONES, G.R., NASH, J.D. AND JIRKA, G.H. 1996. *CORMIX3: An expert system for mixing zone analysis and prediction of buoyant surface discharges* Technical Report, DeFrees Hydraulics Laboratory, Cornell University, Portland, Oregon.
- KEFFER, J.F. AND BAINES, W.D. 1963. 'The round turbulent jet in a cross-wind' *Journal of Fluid Mechanics*, 15 (4), pp 481-496
- KELSO, R.M., LIM, T.T. AND PERRY, A.E. 1996. 'An experimental study of round jets in cross-flow' *Journal of Fluid Mechanics*, 306, pp 111-144
- KURIMA, J., KASUGI, N. AND HIRATA, M. 1983 Image on: <http://www.thtlab.t.u-tokyo.ac.jp/Visual/AxiSymJet.gif> (as visited on 01-12-2006)
- LEE, J.H.W. AND CHEUNG, V. 1990. 'Generalized Lagrangian model for buoyant jets in a current' *Journal of Environmental Engineering*, 116 (6), pp 1085-1116
- LEE, J.H.W. AND CHU, V.H. 2003. *Turbulent jets and plumes: a Lagrangian approach*, Boston: Kluwer Academic Publishers.
- MORTON, B.R. AND IBBETSON, A. 1996. 'Jets deflected in a crossflow' *Experimental Thermal and Fluid Science*, 12, pp 112-133
- MORTON, B.R., TAYLOR, G. AND TURNER, J.S. 1956. 'Turbulent Gravitational Convection from Maintained and Instantaneous Sources' *Proceedings of the Royal Society of London. Series A*, 234, pp 1-23
- MOUSSA, Z.M., TRISCHKA, J.W. AND ESKINAZI, S. 1977. 'The near field in the mixing of a round jet with a cross-stream' *Journal of Fluid Mechanics*, 80 (1), pp 49-80
- NIEUWAAL, M. 2001. *Requirements for sediment plumes caused by dredging*. M.Sc. thesis, Delft University of Technology, the Netherlands.
- PAPANICOLAOU, P.N. AND LIST, E.J. 1988. 'Investigations of round vertical turbulent jet buoyant jets' *Journal of Fluid Mechanics*, 195, pp 341-391
- PENNEKAMP, J.G.S., EPSKAMP, R.J.C., ROSENBRAND, W.F., MULLIÉ, A., WESSEL, G.L., ARTS, T. AND DEIBEL, I.K. 1996. 'Turbidity caused by dredging; viewed in perspective' *Terra et Aqua*, 64, pp 10-17
- RAJARATNAM, N. 1976. *Turbulent jets*, Amsterdam: Elsevier Scientific Publishing Company.
- RICHARDS, J.M. 1963. 'Experiments on the motions of isolated cylindrical thermals through unstratified surroundings' *Int. Journal of Air and Water Pollution*, 7, pp 17-34
- RODI, W. 1982. *Turbulent buoyant jets and plumes*, Oxford: Pergamon Press.
- RODI, W. 1993. *Turbulence models and their application in hydraulics: a state of the are review*, Rotterdam: Balkema.

- SCORER, R.S. 1959. 'The behaviour of chimney plumes' *Int. Journal of Air Pollution*, 1, pp 198-220
- SREENIVAS, K.R., PRASAD, A.K. 2000. 'Vortex-dynamics model for entrainment in jets and plumes' *Physics of Fluids*, 12 (8), pp 2101-2107
- VAN RHEE, C. 2002. *On the sedimentation process in a Trailing Suction Hopper Dredger*, Ph.D. Thesis, Delft University of Technology, the Netherlands.
- VAN DER SALM, R. 1998. *Milieuvriendelijke zandwinning: De verspreiding van overvloeiverlies*, M.Sc. Thesis, Delft University of Technology.
- VAN DER SCHRIECK, G.L.M. 2000. *Baggertechniek – Snijkopzuiger & Sleephopperzuiger*, Dictaat CT 5300, Delft University of Technology.
- SMITS, J. 1998. *Environmental aspects of dredging, Guide 4: Machines, Methods and Mitigation*, The Hague: IADC & CEDA.
- SU, L.K. AND MUNGAL, M.G. 2004. 'Simultaneous measurements of scalar and velocity field evolution in turbulent crossflowing jets.' *Journal of Fluid Mechanics*, 513, pp 1-45
- THEVENOT, M.M., PRICKETT, T.L. AND KRAUS N.C. 1992. *Tylers beach Virginia, dredge material plume monitoring project – September, 27 to October 4, 1991*. U.S. Army Corps of Engineers, Waterways Experimental Station, Vicksburg, Mississippi.
- WHITESIDE, P.G.D., OOMS, K. AND POSTMA, G.M. 1995. 'Generation and decay of sediment plumes from sand dredging overflow.' *Proceedings of the 14<sup>th</sup> World Dredging Congress, November 1995, Amsterdam*, pp 877-892.
- WINTERWERP, J.C. 2002. 'Near field behaviour of dredging spill in shallow water.' *Journal of Waterway, Port, Coastal and Ocean Engineering*, 128(2), pp 96-98.
- WOOD, I.R., BELL, R.G. AND WILKINSON, D.L. 1993. *Ocean disposal of wastewater*, Singapore: World Scientific Publishing.

## List of used symbols

### Roman symbols used:

$b$	Gaussian half width
$B$	specific buoyancy flux
$c$	local mean concentration
$C_D$	drag coefficient
$D_{pipe}$	diameter of overflow pipe
$E$	entrainment rate
$F_D$	ambient drag force
$Fr$	Froude number
$g$	acceleration of gravity
$h$	water depth
$L$	statistical parameter representing concentration separation
$L_b$	plume penetration in crossflow length scale
$L_b'$	plume to stratification length scale
$I_M / L_M$	jet-plume transition length scale
$L_m$	jet penetration in crossflow length scale
$L_m'$	jet to stratification length scale
$l_Q$	jet development length scale
$L_{ZFE}$	length of Zone of Flow Establishment
$M$	specific momentum flux
$Q$	specific volume flux
$Q_c$	flux of tracer mass
$Q_{xi}$	flux of excess state parameter
$\hat{r}$	characteristic impulse width
$r$	radius
$R$	crossflow parameter
$Re$	Reynolds number
$Ri$	Richardson number
$s$	plume length
$\dot{u}$	vectorial impulse velocity
$U / U_{amb}$	ambient velocity
$W$	plume velocity
$x$	global horizontal direction in direction of the ambient flow
$X_i$	local excess state parameter
$y$	global horizontal direction in direction perpendicular to the ambient flow
$z$	global vertical direction
$z_B$	plume to crossflow vertical length scale
$z_C$	bent over plume vertical length scale
$z_M$	jet to crossflow vertical length scale
$Z_{ZFE}$	vertical length of Zone of Flow Establishment
$ZEF$	Zone of Established Flow
$ZFE$	Zone of Flow Establishment

**Greek symbols used:**

$a_n$	(shear) entrainment coefficient
$\beta_n$	forced entrainment coefficient
$\gamma$	transverse angle relative to ambient current
$\delta$	transverse angle to horizontal plane
$\epsilon$	relative excess density
$\zeta$	velocity scale/ratio
$\theta$	angle to horizontal plane
$\mu$	local specific mass flux
$\rho_{amb}$	density of ambient fluid
$\rho_{mix}$	density of mixture
$\sigma$	angle relative to ambient current

## List of figures and tables

### List of figures (main text)

Figure 1.1: Picture of an overflow plume in practice (Hong Kong East Lamma Marine Borrow Area, December 2000) .....	1
Figure 1.2: Monitoring setup at Øresund link project (Jansen, 1999) .....	4
Figure 1.3: Sketch of dredge plume including processes. (free after: Baird, 2004)....	6
Figure 1.4: Sketch of a passive plume with relevant processes (Dankers, 2002) .....	6
Figure 1.5: Classification of overflow plumes in shallow water (Winterwerp, 2002) ...	8
Figure 1.6: Diagram of the outline of the report. ....	13
Figure 2.1: Sketch of a vertical downward released negatively buoyant jet in a stagnant fluid (free after: Fannelöp. 1994) .....	18
Figure 2.2: Schematic figure of the transitions in behaviour of the buoyant jet. ....	20
Figure 2.3: The transition from a Gaussian profile (near field) to a vortex-pair profile (far field) of a buoyant jet in a crossflow (Lee and Chu, 1993) .....	21
Figure 2.4: Normalized jet trajectory when $z_M < z_B$ (Fischer et al., 1979) .....	22
Figure 2.5: Normalized jet trajectory when $z_M > z_B$ (Fischer et al., 1979) .....	22
Figure 2.6: Flow visualization of an axi-symmetric turbulent jet. (Kurima <i>et al.</i> , 1983).....	26
Figure 2.7: Illustration of different types of entrainment .....	27
Figure 2.8: Development of vortex pair cross section due to shear forcing at the plume edge and its resulting torque.....	29
Figure 2.9: Mechanism of azimuthal shear (Jirka, 2004).....	30
Figure 2.10: Correlation of $L$ with $\dot{u}/U$ (Cheung, 1991).....	31
Figure 2.11: Top and side view of vortex bifurcation due to influence boundary (in this case water surface approach).....	32
Figure 2.13: Sketch of bottom influences possible (left: bifurcation, right convergence) .....	33
Figure 2.14: Relative magnitude of length scales determines the behaviour type....	37
Figure 2.15: Plot of Richardson numbers and velocity scales of data points. ....	38
Figure 2.16: Sketch of a dynamic overflow plume (free after: Su and Mungal, 2006) .....	40
Figure 2.17: Visualizations of degrees of freedom of ships.....	41
Figure 2.18: Cloud formation in overflow plumes containing air (Dankers, 2002)....	42
Figure 2.19: Influence of ship's propeller mixing effects (free after: Dankers, 2002) .....	43
Figure 3.1: CORMIX elements and conceptual linkages .....	51
Figure 3.2: Overview of CORMIX GUI.....	52
Figure 3.3: Vertical part of flow classification diagram for negative buoyant jets released in a homogenous ambient.....	53
Figure 4.1: Sketch of wave influence experimental setup .....	66
Figure 4.2: Sketch of the moving measurement frame method applied in a moving ship experimental setup .....	67
Figure 4.3: Principal of stripping experiment.....	68

Figure 4.4: Top view of the vortex divergence experimental idea .....	68
Figure 6.1: Sketch of the measuring plan for stripping. (Left: side view, Right: frontal view with projected surface marked).....	76
Figure 6.3: Graphical presentation of measuring plan .....	79
Figure 7.1: No material found outside the plume edges.....	82
Figure 7.2: Series of subsequent pictures showing a vortex breaking from a plume	83
Figure 7.3: Clouds formed directly downstream of a starting plume.....	84
Figure 7.4: Series of subsequent pictures showing the results of a pipe displacement .....	84
Figure 7.5: Development of a dynamic plume of heavy material in the passive plume rests of preceding lighter mixture. ....	85
Figure 7.6: Overflow pipe with funnel constructed for variable overflow creation ....	85
Figure 7.7: Plumes with varying overflow parameters behaving as separate clouds and puffs.....	86
Figure 7.8: Recirculation of material in wake of pipe.....	87
Figure 9.1: Sketch of the determination of divergence with two profile measurements .....	94
Figure 9.4: Measuring plan vortex divergence exp. presented graphically in $Ri-\zeta$ diagram .....	98
Figure 10.1: Concentration profile resulting for measurement 1.1 (note different scale for concentrations) .....	100
Figure 10.2: Concentration profile resulting for measurement 2.1 .....	101
Figure 10.3 Concentration profile resulting for measurement 2.2.....	101
Figure 10.4: Concentration profile resulting for measurement 2.3 .....	101
Figure 10.5: Concentration profile resulting for measurement 3.1 .....	102
Figure 10.6: Concentration profile resulting for measurement 3.2 .....	103
Figure 10.7: Vortex divergence observed in the experiments.....	104
Figure 11.1: Plume path comparison plume 1 ( $\rho=1040 \text{ kg/m}^3$ , $W=0.05 \text{ m/s}$ , $U=0.04 \text{ m/s}$ ) .....	109
Figure 11.2: Plume path comparison plume 2 ( $\rho=1050 \text{ kg/m}^3$ , $W=0.05 \text{ m/s}$ , $U=0.04 \text{ m/s}$ ) .....	110
Figure 11.3: Plume path comparison plume 3 ( $\rho=1050 \text{ kg/m}^3$ , $W=0.05 \text{ m/s}$ , $U=0.04 \text{ m/s}$ ) .....	110
Figure 11.4: Different material distributions with the same material content.....	111
Figure 11.5: Comparison of model prediction (left) and measurement (right) of profile 2.1.....	112
Figure 11.6: Comparison of model prediction (left) and measurement (right) of profile 2.2.....	112
Figure 11.7: Comparison of model prediction (left) and measurement (right) of profile 3.1.....	113

List of figures (appendix)

Figure A.1: Geometry for a vertical jet in a crossflow. (Fischer *et al.*, 1979) ..... 143

Figure D.1: Definition of all parameters in stripping experiment ..... 151

Figure E.1: Plan view of experimental setup as built in the Fluid Mechanics Laboratory..... 157

Figure E.2: Flow diagram of one measurement run..... 159

Figure E.3: Plan view of the adapted experiment setup with all objects indicated. 161

Figure E.4: Picture of the model ship used to prevent wake forming behind the pipe ..... 162

Figure E.5: Flow diagram of measurement run in vortex bifurcation experiment... 164

Figure F.1: Discharge meters clamp-on sensors and transmitter as found in experimental setup..... 165

Figure F.2: EMS probe and control unit as found in experimental setup..... 166

Figure F.3: Time series of velocities measured with EMS with indicated velocity deviations..... 167

Figure F.4: Measuring setup including Vectrino and cathode of electrolysis apparatus. .... 168

Figure F.5: Principle sketch of the measurement method of the Temposonics Magnetostrictive Position Sensor ..... 169

Figure F.6: Height meter as placed in experimental setup (turned 90° clockwise). 169

Figure F.7: OPCON concentration meter: probe, detail of probe and control units. 170

Figure F.8: Calibration setup to calibrate concentration meters, right: detail of the measuring bin ..... 171

Figure F.9: Calibration curve of one of the OPCON devices during the experiments ..... 172

Figure F.10: OSLIM used to measure the outgoing water concentration ..... 173

Figure F.11: OSLIM used to measure incoming water concentration detail: pipe water sampler..... 173

Figure G.1: Sketch of the idea of the siphon used ..... 174

Figure G.2: Placing of the siphon in the experimental setup..... 175

Figure G.3: Idea of calibration setup..... 175

Figure G.4: Pictures of the calibration setup: overview, front view and detail ..... 176

Figure G.5: Calibration graph of 6 cm siphon to be used in stripping experiment.. 176

Figure G.6: Different flanges used in experiment, the dark one is already placed in the basis that was reused for every flange..... 177

Figure G.7: Straws implemented in the 6 cm pipe ..... 178

Figure G.8: Smaller siphons created for the experiments..... 179

Figure H.1: Meandering in the flume visualized by dye..... 180

Figure H.2: Packs of corrugated sheets placed into the flume to prevent meandering. .... 181

Figure H.3: Setup of pump and frequency converter ..... 182

Figure H.4: Measures to increase the stiffness of the flume construction. .... 183

Figure H.5: Spectra of Vectrino signal before and after increasing the stiffness of the flume..... 183

Figure H.6: Setup for Vectrino apparatus loaded with concrete blocks and lead bars .....	184
Figure H.7: Spectra of Vectrino signal before and after loading its setup .....	184
Figure H8: Spectrum for the Vectrino at a flume velocity of 10 cm/s for the investigation of the Kolmogorov spectrum law (shown in black) .....	186
Figure I.1: Possible reduction of the plume raising by changing the bottom profile. ....	189
Figure I.2: Sketches of multiple passing setups.....	190
Figure J.1: Base case plume in experimental flume.....	195
Figure J.2: Plume with halved flume velocity and increased density. ....	196
Figure J.3: Initial phase of small plume.....	196
Figure J.4: Circulation process in the cross-section of the flume .....	197
Figure J.5: Stripping tests carried out presented in $Ri-\zeta$ diagram .....	198
Figure K.1: Unprocessed results measurement 1.1 .....	200
Figure K.2: Unprocessed results measurement 2.1 .....	201
Figure K.3: Unprocessed results measurement 2.2 .....	201
Figure K.4: Unprocessed results measurement 2.3 .....	201
Figure K.5: Unprocessed results measurement 3.1 .....	202
Figure K.6: Unprocessed results measurement 3.2 .....	202
Figure N.1: Main calibration OPCON1\.....	207
Figure N.2: Main calibration OPCON2 .....	207
Figure N.3: First re-calibration OPCON1 .....	208
Figure N.4: Second re-calibration OPCON1 .....	208
Figure N.5: First re-calibration OPCON2 .....	208
Figure N.6: Second re-calibration OPCON2 .....	209
Figure N.7: Calibration OPCON vortex divergence (20-4).....	209
Figure N.8: Calibration OPCON vortex divergence (15-5).....	210
Figure N.9: Calibration OPCON vortex divergence (16-5).....	210
Figure N.10: Calibration OPCON vortex divergence (21-5) .....	211
Figure O.1: Main calibration OSLIM1 .....	212
Figure O.2: Re-calibration OSLIM1 .....	212
Figure O.3: Main calibration OSLIM2.....	213
Figure O.4: Re-calibration OSLIM2 .....	213
Figure P.1: Calibration graph siphon with diameter of 3 cm .....	214
Figure P.2: Calibration graph siphon with diameter of 4 cm .....	215
Figure P.3: Calibration graph siphon with diameter of 5 cm .....	215
Figure P.4: Calibration graph siphon with diameter of 6 cm .....	216
Figure P.5: Calibration graph of siphon with diameter of 0.4 cm.....	216
Figure P.6: Calibration graph of siphon with diameter of 1.0 cm.....	217

List of tables (main text)

Table 2.1: Vertical velocity, buoyant jet trajectory and dilution formulations for the four limiting cases of a buoyant jet.....22

Table 2.2: Experimentally determined coefficients used in asymptotic trajectory and dilution formulations. (Fischer *et al.*, 1979)..... 23

Table 2.3: Model formulations for the shear entrainment factor  $\alpha$ .....28

Table 2.4: Model formulations for the forced entrainment factor  $\beta$ .....28

Table 2.5: Typical value range for parameters in overflow plumes..... 35

Table 2.6: Values for relevant parameters in three cases. .... 36

Table 2.7: Range of values for governing parameters in overflow plumes..... 37

Table 2.8: CorJet model prediction of typical overflow plume extended with entrainment and specific volume flux. .... 41

Table 3.1: Length scales used in CORMIX relevant for overflow plumes..... 52

Table 3.2: Standard values entrainment coefficients used in CorJet ..... 58

Table 4.1: List of important knowledge gaps in theory with comments ..... 62

Table 4.2: List of important information needs in modelling with comments..... 63

Table 6.1: Dimensions of parameters in experiment ..... 78

Table 7.1: Stripping tests carried out in the experimental setup..... 81

Table 9.1: Magnitude of parameters in prototype, on scale and applied in the experiment. .... 95

Table 9.2: Measuring plan vortex divergence experiment ..... 97

Table 10.1: Information on different profiles measured ..... 99

Table 10.2: Distance between concentration centres in profiles 2.1, 2.2 and 2.3 .. 102

Table 10.3: Distance between concentration centres in profiles 3.1 and 3.2..... 103

Table 10.4: Vertical position of plume centre at every profile..... 104

Table 10.5: Dilution of plumes at every profile..... 105

Table 11.1: CORMIX result for plume 1 ( $\rho=1040 \text{ kg/m}^3$ ,  $W=0.05 \text{ m/s}$ ,  $U=0.04 \text{ m/s}$ ) ..... 107

Table 11.2: CORMIX result for plume 2 ( $\rho=1050 \text{ kg/m}^3$ ,  $W=0.05 \text{ m/s}$ ,  $U=0.04 \text{ m/s}$ ) ..... 107

Table 11.3: CORMIX result for plume 3 ( $\rho=1050 \text{ kg/m}^3$ ,  $W=0.05 \text{ m/s}$ ,  $U=0.05 \text{ m/s}$ ) ..... 108

Table 11.4: Total amount of material measured and calculated for each profile.... 108

Table 11.5: Plume centre positions measured and calculated ..... 109

Table 11.6: Peak concentrations measured and calculated..... 111

## List of tables (appendix)

Table B.1: Combination of parameter values and the resulting values for governing parameters and length scales.....	150
Table D.1: Grouping of parameters and dimensions.....	152
Table D.2: Presentation of the k-values in dimensionless $\Pi$ -parameters .....	152
Table D.3: List of dimensionless $\Pi$ -parameters.....	153
Table D.1: Legend of colour coding used in Table F.2.....	155
Table D.2: Listing of all stripping tests originally planned .....	156
Table E.1: Legend of numbered parts in figure E.1 .....	158
Table E.2: Legend of numbered parts in figure E.2 .....	162
Table I.1: Mean values for the parameters to be adopted.....	189
Table I.2: Amount of buffer needed before each cycle.....	191
Table I.3: Time needed for several items in a measurement run. ....	193
Table I.4: Calculation of buffer need.....	194
Table J.1: Parameter values of the stripping tests that are carried out with comments .....	197
Table J.2: Vortex bifurcation tests carried out.....	198
Table K.1: Information on different profiles measured .....	200
Table L.1: All input parameters used in the CORMIX model .....	204
Table M.1: Head fall for different pipe diameters possible.....	205

## Appendices



## Appendix A: Deduction of asymptotic results

The deduction of the asymptotic solutions presented in table 2.1 is presented in this appendix. To come to these solutions the equations of motion are reworked by the use of similarity solutions. The jet is for that reason specified by figure A.1 below and two regions are considered. The first region specified by flow through the plane  $A(z)$ , the second by flow through the plane  $A(x)$ .

This deduction is copied with editing from Fischer et al., 1979 (page 347-353).

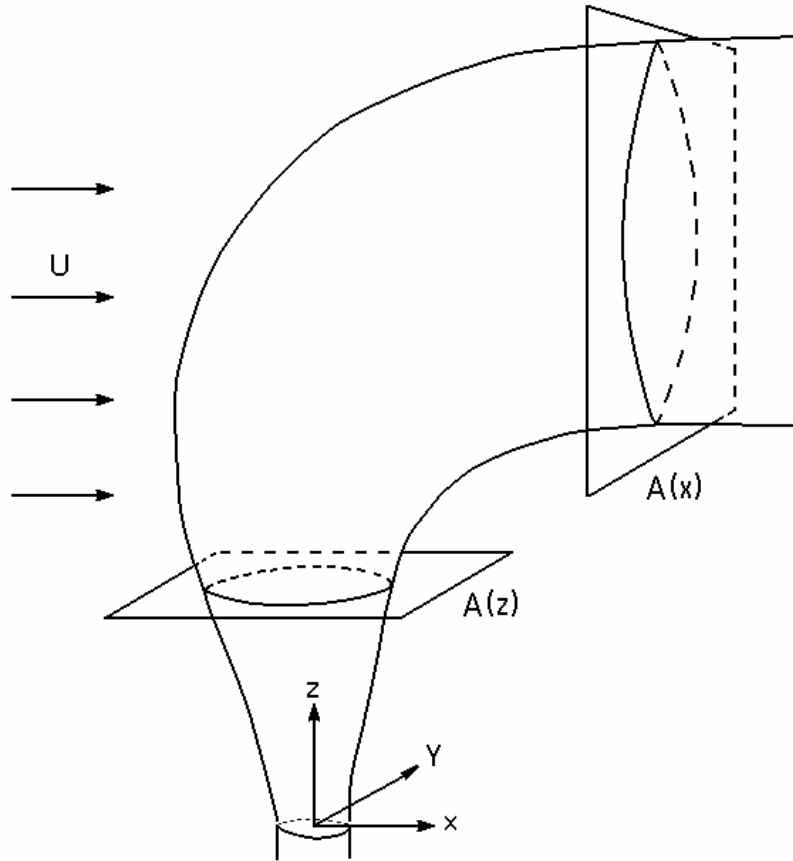


Figure A.1: Geometry for a vertical jet in a crossflow. (Fischer *et al.*, 1979)

Motion is described by the following two time-averaged momentum equations

$$\frac{\partial}{\partial x} \left( \overline{u^2} + \overline{u'^2} + \frac{\overline{p}}{r_0} \right) + \frac{\partial}{\partial y} (\overline{u'v'}) + \frac{\partial}{\partial z} (\overline{uw} + \overline{u'w'}) = 0 \quad (\text{A.1})$$

$$\frac{\partial}{\partial x} (\overline{uw} + \overline{u'w'}) + \frac{\partial}{\partial y} (\overline{w'v'}) + \frac{\partial}{\partial z} \left( \overline{w^2} + \overline{w'^2} + \frac{\overline{p}}{r_0} \right) = \left( \frac{r_a - \overline{r}}{r_0} \right) g \quad (\text{A.2})$$

where overbars denote time-average values of velocities, primes the deviations from these time averages and  $p$  includes the hydrostatic pressure distribution.  $\rho_a$  is the ambient fluid density and  $\rho_0$  a reference density. The Boussinesq approximation

holds that  $\rho_0 \approx \rho_a \approx \rho$ . Furthermore it is assumed that viscous stresses are negligible.

The conservation of volume and mass require that

$$\frac{\partial \bar{u}}{\partial x} + \frac{\partial \bar{w}}{\partial z} = 0 \quad (\text{A.3})$$

and that (provided  $\rho_a$  is independent of  $z$ )

$$\frac{\partial}{\partial x} (\bar{u}(\bar{r} - r_a) + \overline{u'r'}) + \frac{\partial \overline{v'r'}}{\partial y} + \frac{\partial}{\partial z} (\bar{w}(\bar{r} - r_a) + \overline{w'r'}) = 0 \quad (\text{A.4})$$

where  $\rho'$  is the deviation of the fluid density from its time-averaged value and molecular diffusive transport is ignored.

Now the sections  $A(z)$ , where the jet is in a predominantly vertical motion, and  $A(x)$ , where the jet is in a predominantly horizontal motion are considered and the equations are averaged over these planes.

For example, integrating equation (A.2) across the jet cross section  $A(z)$  delivers

$$\int_{A(z)} \frac{\partial}{\partial x} (\bar{u}(\bar{r} - r_a) + \overline{u'r'}) dx dy + \int_{A(z)} \frac{\partial}{\partial y} (\overline{w'r'}) dx dy + \int_{A(z)} \frac{\partial}{\partial z} \left( \bar{w}^2 + \overline{w'^2} + \frac{\bar{p}}{r_0} \right) dx dy = \int_{A(z)} \left( \frac{r_a - \bar{r}}{r_0} \right) g dx dy \quad (\text{A.5})$$

It is possible to define the boundary of the jet cross section in a variety of ways. For example it could be selected as the perimeter of the jet beyond which jet-induced turbulent stress vanish. Alternatively it could be chosen as the boundary beyond which mean vertical velocities vanish. These two boundaries do not necessarily coincide, but as far as this analysis is concerned it makes no difference. This being so, then it is relatively easy to see that equation (A.5) reduces to

$$\int_{A(z)} \frac{\partial}{\partial z} \left( \bar{w}^2 + \overline{w'^2} + \frac{\bar{p}}{r_0} \right) dx dy = \int_{A(z)} \left( \frac{r_a - \bar{r}}{r_0} \right) g dx dy \quad (\text{A.6})$$

similarly equation (A.4) becomes

$$\int_{A(z)} \frac{\partial}{\partial z} (\bar{w}(\bar{r} - r_a) + \overline{w'r'}) dx dy = 0 \quad (\text{A.7})$$

when integrated over the same cross section.

Equations (A.6) and (A.7) form the basis of the analysis of buoyant jets in the vertical flow regime. Equation (A.6) in effect states that the rate of change of vertical flow force in a vertical direction is equal to the buoyancy force.

It is assumed that the contributions to the flow force from  $\overline{w'r'}$  and  $p/\rho_0$  are small and opposite in sign, so that they can be ignored. Equation (A.6) can then be rewritten as

$$\int_{A(z)} \frac{\partial}{\partial z} \bar{w}^2 dx dy = \int_{A(z)} \left( \frac{r_a - \bar{r}}{r_0} \right) g dx dy \quad (\text{A.8})$$

Similarly, in equation (A.7) the turbulent transport term  $w'\rho'$ , although it is shown in some research works that this is a poor assumption in buoyancy-driven flows. Nevertheless, the zero order description of the flow should not be compromised, so equation (A.7) is rewritten into

$$\int_{A(z)} \frac{\partial}{\partial z} (\bar{w}(\bar{r} - r_a)) dx dy = 0 \quad (\text{A.9})$$

Equations (A.8) and (A.9) are the equations that are used for the description of predominantly vertical flows. The equations (A.2) and (A.4) are considered in the same manner across the vertical plane  $A(x)$ . Making the same simplifications as above in the integration across the horizontal plane, the resulting formulas are

$$\int_{A(x)} \frac{\partial}{\partial x} (\bar{u}\bar{w}) dy dz = \int_{A(x)} \left( \frac{r_a - \bar{r}}{r_0} \right) g dy dz \quad (\text{A.10})$$

$$\int_{A(x)} \frac{\partial}{\partial x} (\bar{u}(\bar{r} - r_a)) dy dz = 0 \quad (\text{A.11})$$

Equations (A.10) and (A.11) will be used to define the horizontal flow regimes. Equation (A.10) states that the rate of change of horizontal flux of vertical momentum is equal to the buoyancy force acting in a vertical plane. Equation (A.11) merely states that the horizontal flux of buoyancy is conserved.

First a jet without buoyancy is considered as a source of volume flux  $Q$  and momentum flux  $M$ , and at first the vertical flow regime is considered so that equations (A.8) and (A.9) are appropriate. Since the jet has no buoyancy the right-hand side of equation (A.8) will be zero and in equation (A.9)  $\rho_a - \rho$  is thought to be the excess concentration of some tracer material in the jet.

The flow is imagined to be fully developed, that is  $z \gg l_0$ , and self-similarity of the velocity and tracer profiles is thought to be correct. Then it is written

$$\bar{w}(x, y, z) = w_m(\bar{z}) f\left(\frac{x}{z}, \frac{y}{z}\right) \quad (\text{A.12})$$

$$\frac{r_a - \bar{r}}{r_0} = q(\bar{z}) Y\left(\frac{x}{z}, \frac{y}{z}\right) \quad (\text{A.13})$$

where  $z$  is the  $z$  coordinate of the jet axis and is function of  $x$ ;  $\varphi$  and  $\psi$  are undefined functions describing the lateral distribution of velocity and tracer. Substituting equations (A.12) and (A.13) into equations (A.8) and (A.9) and remembering that the right hand side of equation (A.8) will be zero gives

$$\frac{d}{dz} \int_{A(z)} \bar{z}^2 w_m^2(\bar{z}) f^2 d\left(\frac{x}{z}\right) d\left(\frac{y}{z}\right) = 0 \quad (\text{A.14})$$

$$\frac{d}{dz} \int_{A(z)} \bar{z}^2 w_m(\bar{z}) q(\bar{z}) f y d\left(\frac{x}{z}\right) d\left(\frac{y}{z}\right) = 0 \quad (\text{A.15})$$

where the differentiation can be moved outside the integral because  $\varphi$  and  $\psi$  are assumed to vanish at the perimeter of the cross section of integration. These two equations imply that

$$\bar{z}^2 w_m^2(\bar{z}) \sim M \quad (\text{A.16})$$

$$\bar{z}^2 w_m(\bar{z}) q(\bar{z}) \sim B/g \quad (\text{A.17})$$

because the integrals are independent on  $z$  by virtue of the fact that the integrands vanish outside  $A(z)$  and the actual value of the integrals is irrelevant provided that there is only interest in proportionalities. The parameter on the right-hand side of equation (A.17) must be  $B/g$  since the left-hand side is proportional to flux of excess tracer mass in the jet.

From equations (A.16) and (A.17) it can be seen that

$$w_m(\bar{z})/U \sim M^{1/2}/(\bar{z}U) \quad (\text{A.18})$$

$$q(\bar{z}) \sim B/(gM^{1/2}\bar{z}) \quad (\text{A.19})$$

or, after rewriting

$$w_m(\bar{z})/U \sim (z_M/\bar{z}) \quad (\text{A.20})$$

$$Mgq(\bar{z})/UB = D_1(z_M/\bar{z}) \quad (\text{A.21})$$

where  $z_M = M^{1/2}/U$  and  $D_1$  is a constant of proportionality. These solutions are valid where  $w_m(z) \gg U$  or equivalently,  $z \ll z_M$ . It is apparent that  $z_M$  is the vertical height at which the vertical velocity in the jet has decayed to the order of the crossflow velocity.

For a jet in a crossflow it seems reasonable that the slope of the jet trajectory is specified by

$$w_m(\bar{z})/U = d\bar{z}/dx \quad (\text{A.22})$$

Then equation (A.20) implies that the jet trajectory is given by

$$\bar{z}/z_M = C_1(x/z_M)^{1/2}, \bar{z} \ll z_M \quad (\text{A.23})$$

for some 'constant'  $C_1$  which may be a function of the ratio  $z_M/l_0$ . Thus, for a momentum-dominated jet with a 'weak' crossflow solutions are obtained for the maximum vertical velocity, tracer concentration and jet trajectory, plus a criterion for their application.

Now the case is considered when the jet is in a bent-over region and equations (A.10) and (A.11) are appropriate. Self-similarity is expected again and in this case giving

$$\bar{w}(x, y, z) = w_m(\bar{z}) f\left(\frac{z-\bar{z}}{z}, \frac{y}{z}\right) \quad (\text{A.24})$$

$$\frac{r_a - \bar{r}}{r_0} = q(\bar{z}) y \left(\frac{z-\bar{z}}{z}, \frac{y}{z}\right) \quad (\text{A.25})$$

$$\bar{u} \approx U \quad (\text{A.26})$$

because the similar profile will be centered on  $z$ . Then, provided  $\varphi$  and  $\psi$  vanish outside the perimeter of the jet, it can be derived that

$$\frac{d}{dx} \int_{A(x)} \bar{z}^2 U w_m(\bar{z}) f d\left(\frac{z-\bar{z}}{z}\right) d\left(\frac{y}{z}\right) = 0 \quad (\text{A.27})$$

$$\frac{d}{dx} \int_{A(x)} \bar{z}^2 U q(\bar{z}) y d\left(\frac{z-\bar{z}}{z}\right) d\left(\frac{y}{z}\right) = 0 \quad (\text{A.28})$$

which imply that

$$w_m(\bar{z})/U \sim (z_M/\bar{z})^2, \bar{z} \gg z_M \quad (\text{A.29})$$

$$Mgq(\bar{z})/UB = D_2 (z_M/\bar{z})^2, \bar{z} \gg z_M \quad (\text{A.30})$$

in which  $D_2$  is an empirical constant. These solutions will only apply in the bent-over region where  $w_m(z) \ll U$  or equivalently,  $z \gg z_M$ . Again the trajectory can be deduced from equations (A.22) and (A.29) to be

$$\bar{z}/z_M = C_2 (x/z_M)^{1/3}, \bar{z} \gg z_M \quad (\text{A.31})$$

for some constant  $C_2$ . It is again apparent that  $z_M$  is the vertical height at which the jet will begin to appear appreciably bent.

Next to consider is the pure plume in a crossflow. For that is assumed that the flow is produced solely by a source of buoyancy flux  $B$  and that a 'vertical' and 'horizontal' flow region occurs as before. This time because of the buoyancy it is not possible to ignore the right-hand side of equation (A.8) and (A.9), so that assuming self-similarity in the 'vertical' region leads to the results

$$(d/dz) [\bar{z}^2 w_m^2(\bar{z})] \sim g \bar{z}^2 q(\bar{z}) \quad (\text{A.32})$$

$$(d/dz) [\bar{z}^2 w_m(\bar{z}) q(\bar{z})] = 0 \quad (\text{A.33})$$

From these two results and using equation (A.22) it may be easily shown that if  $dz \approx dz$ , which seems reasonable, then

$$w_m(\bar{z})/U \sim (z_B/\bar{z})^{1/3}, \bar{z} \ll z_B \quad (\text{A.34})$$

$$\left(\frac{z_B}{z_M}\right)^2 \frac{gMq(\bar{z})}{UB} = D_3 \left(\frac{z_B}{\bar{z}}\right)^{5/3}, \bar{z} \ll z_B \quad (\text{A.35})$$

$$\bar{z}/z_B = C_3 (x/z_B)^{3/4}, \bar{z} \ll z_B \quad (\text{A.36})$$

where  $C_3$  and  $D_3$  are proportionality constants to be determined empirically and  $z_B = B/U^3$  is the characteristic length scale for this problem. These solution are only valid if the plume is not bent over, which numerically is determined by  $\bar{z} \ll z_B$ .  $z_B$  is the vertical distance along the jet trajectory where the vertical velocity of the plume decays to the order of the cross-flow velocity.

Last asymptotic to consider is the plume in a bent-over flow. In this region equations (A.10) and (A.11), and similarity forms such as equations (A.24) and (A.25), imply that

$$(d/dx) [\bar{z}^2 U w_m(\bar{z})] \sim g \bar{z}^2 q(\bar{z}) \quad (\text{A.37})$$

$$(d/dx) [\bar{z}^2 U q(\bar{z})] = 0 \quad (\text{A.38})$$

Again using equation (A.22) it may be shown, with some algebra, that

$$w_m(\bar{z})/U : (z_B/\bar{z})^{1/2}, \bar{z} \gg z_B \quad (\text{A.39})$$

$$\left(\frac{z_B}{z_M}\right)^2 \frac{gMq(\bar{z})}{UB} = D_4 \left(\frac{z_B}{\bar{z}}\right)^2, \bar{z} \gg z_B \quad (\text{A.40})$$

$$\bar{z}/z_B = C_4 (x/z_B)^{2/3}, \bar{z} \gg z_B \quad (\text{A.41})$$

---

with  $C_4$  and  $D_4$  as constants of proportionality.

All the four situations mentioned have their own row in table 2.2, with for every row three columns giving the three formulas for velocity ratio (A.20, A.29, A.34 and A.39), trajectory (A.23, A.31, A.36 and A.41) and dilution (A.21, A.30, A.35 and A.40).

## Appendix B: All combinations of parameter values

*In the last part of chapter 2 the possibilities for overflow plumes are determined. Important part of that is the determination of the governing parameters. Four of the needed input parameters are varied in three steps, minimum, typical and maximum. This leads to  $3^4 = 81$  possible combinations. To be complete, all combinations are listed here in table B.1. The values for the governing parameters as well as the length scales are added too.*

	$D_{pipe}$	$W$	$U_{amb}$	$\rho_{amb}$	$\rho_{mix}$	$g$	$Q$	$M$	$B$	$Ri$	$\zeta$	$l_Q$	$l_M$	$z_M$	$z_B$
Nr	m	m/s	m/s	kg/m <sup>3</sup>	kg/m <sup>3</sup>	m/s <sup>2</sup>	m <sup>3</sup> /s	m <sup>4</sup> /s <sup>2</sup>	m <sup>4</sup> /s <sup>3</sup>	-	-	m	m	m	m
1	4.00	0.50	4.00	1025	1090	9.81	6.283	3.142	3.909	9.954	8.000	3.545	1.194	0.443	0.061
2	3.00	0.50	4.00	1025	1090	9.81	3.534	1.767	2.199	7.465	8.000	2.659	1.034	0.332	0.034
3	1.50	0.50	4.00	1025	1090	9.81	0.884	0.442	0.550	3.733	8.000	1.329	0.731	0.166	0.009
4	4.00	1.00	4.00	1025	1090	9.81	12.566	12.566	7.818	2.488	4.000	3.545	2.387	0.886	0.122
5	3.00	1.00	4.00	1025	1090	9.81	7.069	7.069	4.397	1.866	4.000	2.659	2.067	0.665	0.069
6	1.50	1.00	4.00	1025	1090	9.81	1.767	1.767	1.099	0.933	4.000	1.329	1.462	0.332	0.017
7	4.00	1.50	4.00	1025	1090	9.81	18.850	28.274	11.726	1.106	2.667	3.545	3.581	1.329	0.183
8	3.00	1.50	4.00	1025	1090	9.81	10.603	15.904	6.596	0.829	2.667	2.659	3.101	0.997	0.103
9	1.50	1.50	4.00	1025	1090	9.81	2.651	3.976	1.649	0.415	2.667	1.329	2.193	0.499	0.026
10	4.00	0.50	1.00	1025	1090	9.81	6.283	3.142	3.909	9.954	2.000	3.545	1.194	1.772	3.909
11	3.00	0.50	1.00	1025	1090	9.81	3.534	1.767	2.199	7.465	2.000	2.659	1.034	1.329	2.199
12	1.50	0.50	1.00	1025	1090	9.81	0.884	0.442	0.550	3.733	2.000	1.329	0.731	0.665	0.550
13	4.00	1.00	1.00	1025	1090	9.81	12.566	12.566	7.818	2.488	1.000	3.545	2.387	3.545	7.818
14	3.00	1.00	1.00	1025	1090	9.81	7.069	7.069	4.397	1.866	1.000	2.659	2.067	2.659	4.397
15	1.50	1.00	1.00	1025	1090	9.81	1.767	1.767	1.099	0.933	1.000	1.329	1.462	1.329	1.099
16	4.00	1.50	1.00	1025	1090	9.81	18.850	28.274	11.726	1.106	0.667	3.545	3.581	5.317	11.726
17	3.00	1.50	1.00	1025	1090	9.81	10.603	15.904	6.596	0.829	0.667	2.659	3.101	3.988	6.596
18	1.50	1.50	1.00	1025	1090	9.81	2.651	3.976	1.649	0.415	0.667	1.329	2.193	1.994	1.649
19	4.00	0.50	0.00	1025	1090	9.81	6.283	3.142	3.909	9.954	0.000	3.545	1.194	-	-
20	3.00	0.50	0.00	1025	1090	9.81	3.534	1.767	2.199	7.465	0.000	2.659	1.034	-	-
21	1.50	0.50	0.00	1025	1090	9.81	0.884	0.442	0.550	3.733	0.000	1.329	0.731	-	-
22	4.00	1.00	0.00	1025	1090	9.81	12.566	12.566	7.818	2.488	0.000	3.545	2.387	-	-
23	3.00	1.00	0.00	1025	1090	9.81	7.069	7.069	4.397	1.866	0.000	2.659	2.067	-	-
24	1.50	1.00	0.00	1025	1090	9.81	1.767	1.767	1.099	0.933	0.000	1.329	1.462	-	-
25	4.00	1.50	0.00	1025	1090	9.81	18.850	28.274	11.726	1.106	0.000	3.545	3.581	-	-
26	3.00	1.50	0.00	1025	1090	9.81	10.603	15.904	6.596	0.829	0.000	2.659	3.101	-	-
27	1.50	1.50	0.00	1025	1090	9.81	2.651	3.976	1.649	0.415	0.000	1.329	2.193	-	-
28	4.00	0.50	4.00	1025	1060	9.81	6.283	3.142	2.105	5.360	8.000	3.545	1.627	0.443	0.033
29	3.00	0.50	4.00	1025	1060	9.81	3.534	1.767	1.184	4.020	8.000	2.659	1.409	0.332	0.018
30	1.50	0.50	4.00	1025	1060	9.81	0.884	0.442	0.296	2.010	8.000	1.329	0.996	0.166	0.005
31	4.00	1.00	4.00	1025	1060	9.81	12.566	12.566	4.209	1.340	4.000	3.545	3.253	0.886	0.066
32	3.00	1.00	4.00	1025	1060	9.81	7.069	7.069	2.368	1.005	4.000	2.659	2.817	0.665	0.037
33	1.50	1.00	4.00	1025	1060	9.81	1.767	1.767	0.592	0.502	4.000	1.329	1.992	0.332	0.009
34	4.00	1.50	4.00	1025	1060	9.81	18.850	28.274	6.314	0.596	2.667	3.545	4.880	1.329	0.099
35	3.00	1.50	4.00	1025	1060	9.81	10.603	15.904	3.552	0.447	2.667	2.659	4.226	0.997	0.055
36	1.50	1.50	4.00	1025	1060	9.81	2.651	3.976	0.888	0.223	2.667	1.329	2.988	0.499	0.014
37	4.00	0.50	1.00	1025	1060	9.81	6.283	3.142	2.105	5.360	2.000	3.545	1.627	1.772	2.105
38	3.00	0.50	1.00	1025	1060	9.81	3.534	1.767	1.184	4.020	2.000	2.659	1.409	1.329	1.184
39	1.50	0.50	1.00	1025	1060	9.81	0.884	0.442	0.296	2.010	2.000	1.329	0.996	0.665	0.296
40	4.00	1.00	1.00	1025	1060	9.81	12.566	12.566	4.209	1.340	1.000	3.545	3.253	3.545	4.209
41	3.00	1.00	1.00	1025	1060	9.81	7.069	7.069	2.368	1.005	1.000	2.659	2.817	2.659	2.368
42	1.50	1.00	1.00	1025	1060	9.81	1.767	1.767	0.592	0.502	1.000	1.329	1.992	1.329	0.592
43	4.00	1.50	1.00	1025	1060	9.81	18.850	28.274	6.314	0.596	0.667	3.545	4.880	5.317	6.314

44	3.00	1.50	1.00	1025	1060	9.81	10.603	15.904	3.552	0.447	0.667	2.659	4.226	3.988	3.552
45	1.50	1.50	1.00	1025	1060	9.81	2.651	3.976	0.888	0.223	0.667	1.329	2.988	1.994	0.888
46	4.00	0.50	0.00	1025	1060	9.81	6.283	3.142	2.105	5.360	0.000	3.545	1.627	-	-
47	3.00	0.50	0.00	1025	1060	9.81	3.534	1.767	1.184	4.020	0.000	2.659	1.409	-	-
48	1.50	0.50	0.00	1025	1060	9.81	0.884	0.442	0.296	2.010	0.000	1.329	0.996	-	-
49	4.00	1.00	0.00	1025	1060	9.81	12.566	12.566	4.209	1.340	0.000	3.545	3.253	-	-
50	3.00	1.00	0.00	1025	1060	9.81	7.069	7.069	2.368	1.005	0.000	2.659	2.817	-	-
51	1.50	1.00	0.00	1025	1060	9.81	1.767	1.767	0.592	0.502	0.000	1.329	1.992	-	-
52	4.00	1.50	0.00	1025	1060	9.81	18.850	28.274	6.314	0.596	0.000	3.545	4.880	-	-
53	3.00	1.50	0.00	1025	1060	9.81	10.603	15.904	3.552	0.447	0.000	2.659	4.226	-	-
54	1.50	1.50	0.00	1025	1060	9.81	2.651	3.976	0.888	0.223	0.000	1.329	2.988	-	-
55	4.00	0.50	4.00	1025	1040	9.81	6.283	3.142	0.902	2.297	8.000	3.545	2.485	0.443	0.014
56	3.00	0.50	4.00	1025	1040	9.81	3.534	1.767	0.507	1.723	8.000	2.659	2.152	0.332	0.008
57	1.50	0.50	4.00	1025	1040	9.81	0.884	0.442	0.127	0.861	8.000	1.329	1.521	0.166	0.002
58	4.00	1.00	4.00	1025	1040	9.81	12.566	12.566	1.804	0.574	4.000	3.545	4.969	0.886	0.028
59	3.00	1.00	4.00	1025	1040	9.81	7.069	7.069	1.015	0.431	4.000	2.659	4.303	0.665	0.016
60	1.50	1.00	4.00	1025	1040	9.81	1.767	1.767	0.254	0.215	4.000	1.329	3.043	0.332	0.004
61	4.00	1.50	4.00	1025	1040	9.81	18.850	28.274	2.706	0.255	2.667	3.545	7.454	1.329	0.042
62	3.00	1.50	4.00	1025	1040	9.81	10.603	15.904	1.522	0.191	2.667	2.659	6.455	0.997	0.024
63	1.50	1.50	4.00	1025	1040	9.81	2.651	3.976	0.381	0.096	2.667	1.329	4.564	0.499	0.006
64	4.00	0.50	1.00	1025	1040	9.81	6.283	3.142	0.902	2.297	2.000	3.545	2.485	1.772	0.902
65	3.00	0.50	1.00	1025	1040	9.81	3.534	1.767	0.507	1.723	2.000	2.659	2.152	1.329	0.507
66	1.50	0.50	1.00	1025	1040	9.81	0.884	0.442	0.127	0.861	2.000	1.329	1.521	0.665	0.127
67	4.00	1.00	1.00	1025	1040	9.81	12.566	12.566	1.804	0.574	1.000	3.545	4.969	3.545	1.804
68	3.00	1.00	1.00	1025	1040	9.81	7.069	7.069	1.015	0.431	1.000	2.659	4.303	2.659	1.015
69	1.50	1.00	1.00	1025	1040	9.81	1.767	1.767	0.254	0.215	1.000	1.329	3.043	1.329	0.254
70	4.00	1.50	1.00	1025	1040	9.81	18.850	28.274	2.706	0.255	0.667	3.545	7.454	5.317	2.706
71	3.00	1.50	1.00	1025	1040	9.81	10.603	15.904	1.522	0.191	0.667	2.659	6.455	3.988	1.522

Table B.1: Combination of parameter values and the resulting values for governing parameters and length scales.

## Appendix C: Parameter study for scaling

*In chapter 5 & 6 the dimensions of several parameters are determined. Scaling is used based on the mutual relations of these parameters. First all the various (n) parameters are summed up, then following the  $\Pi$ -theorem, there are (n-3) dimensionless parameters, since it is thought that there are three fundamental dimension (M, L, T). Those are investigated, regrouped and modified to get a meaningful set of parameters explaining the process. After that the scale parameters are determined.*

### Inventory of parameters

In figure D.1 all changeable and unchangeable parameters of the experiment are summed up.

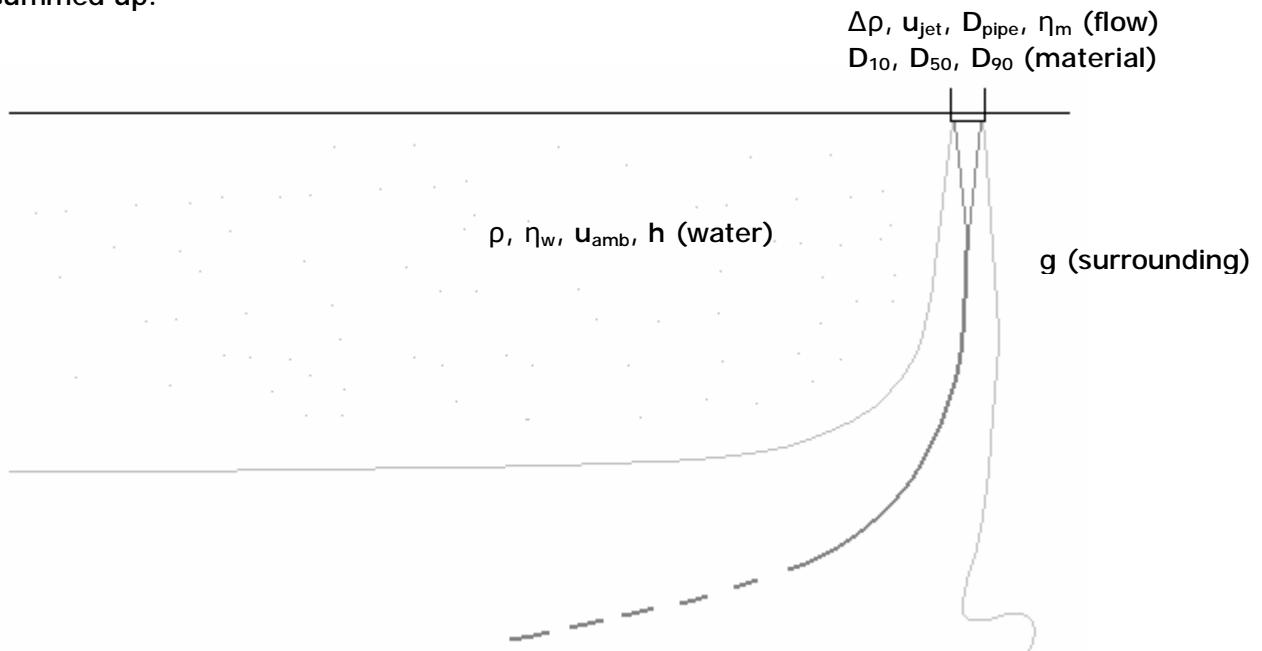


Figure D.1: Definition of all parameters in stripping experiment

The dependent variable is the volume flux of stripping ( $Q_{stripping}$ ) and the widening of the plume ( $\Delta D_{plume}$ ) at specified length from the pipe end ( $l_{plume}$ ).

### Applying $\Pi$ -theorem

In table D.1 these parameters are ordered systematically and the dimensions are shown by giving the power which should be used for each of the three fundamental dimensions.

Group	Dependent		Changeable											Unchangeable	
Parameter	$Q_{strip}$	$\Delta D_{plu}$	$\rho$	$u_{amb}$	$h$	$\Delta\rho$	$u_{jet}$	$D_{pipe}$	$D_{10}$	$D_{50}$	$D_{90}$	$\eta_m$	$l_{plume}$	$\eta_w$	$g$
M	0	0	1	0	0	1	0	0	0	0	0	1	0	1	0
L	3	1	-3	1	1	-3	1	1	1	1	1	-1	1	-1	1
T	-1	0	0	-1	0	0	-1	0	0	0	0	-1	0	-1	-2

Table D.1: Grouping of parameters and dimensions

The  $\Pi$ -theorem states that in this case there are  $15-3=12$  dimensionless parameters, which can be composed with:

$$\Pi = p_1^{k_1} p_2^{k_2} p_3^{k_3} \dots p_{15}^{k_{15}} \quad (D.1)$$

Since every parameter has the dimensions  $[M^\alpha L^\beta T^\gamma]$  and every  $\alpha$ ,  $\beta$  and  $\gamma$  is given in the previous table, it can be stated that  $\Pi$  can only be dimensionless if the following functions are to be fulfilled:

		$+k_3$			$+k_6$						$+k_{12}$		$+k_{14}$		$= 0$
$3k_1$	$+k_2$	$-3k_3$	$+k_4$	$+k_5$	$-3k_6$	$+k_7$	$+k_8$	$+k_9$	$+k_{10}$	$+k_{11}$	$-k_{12}$	$+k_{13}$	$-k_{14}$	$+k_{15}$	$= 0$
$-k_1$			$-k_4$			$-k_7$					$-k_{12}$		$-k_{14}$	$-2k_{15}$	$= 0$

Elimination of  $k_{13}$ ,  $k_{14}$  and  $k_{15}$  yields:

$$k_{13} = -2\frac{1}{2}k_1 - k_2 + 1\frac{1}{2}k_3 - \frac{1}{2}k_4 - k_5 + 1\frac{1}{2}k_6 - \frac{1}{2}k_7 - k_8 - k_9 - k_{10} - k_{11}$$

$$k_{14} = -k_3 - k_6 - k_{12}$$

$$k_{15} = \frac{1}{2} (-k_1 + k_3 - k_4 + k_6 - k_7)$$

Then table D.2 can be composed giving the k-values for each parameter in each dimensionless  $\Pi$ .

	$k_1$	$k_2$	$k_3$	$k_4$	$k_5$	$k_6$	$k_7$	$k_8$	$k_9$	$k_{10}$	$k_{11}$	$k_{12}$	$k_{13}$	$k_{14}$	$k_{15}$
parameter	$Q_{strip}$	$\Delta D_{plu}$	$\rho$	$u_{amb}$	$h$	$\Delta\rho$	$u_{jet}$	$D_{pipe}$	$D_{10}$	$D_{50}$	$D_{90}$	$\eta_m$	$l_{plume}$	$\eta_w$	$g$
$\Pi_1$	1	0	0	0	0	0	0	0	0	0	0	0	$-2\frac{1}{2}$	0	$-\frac{1}{2}$
$\Pi_2$	0	1	0	0	0	0	0	0	0	0	0	0	-1	0	0
$\Pi_3$	0	0	1	0	0	0	0	0	0	0	0	0	$1\frac{1}{2}$	-1	$\frac{1}{2}$
$\Pi_4$	0	0	0	1	0	0	0	0	0	0	0	0	$-\frac{1}{2}$	0	$-\frac{1}{2}$
$\Pi_5$	0	0	0	0	1	0	0	0	0	0	0	0	-1	0	0
$\Pi_6$	0	0	0	0	0	1	0	0	0	0	0	0	$1\frac{1}{2}$	-1	$\frac{1}{2}$
$\Pi_7$	0	0	0	0	0	0	1	0	0	0	0	0	$-\frac{1}{2}$	0	$-\frac{1}{2}$
$\Pi_8$	0	0	0	0	0	0	0	1	0	0	0	0	-1	0	0
$\Pi_9$	0	0	0	0	0	0	0	0	1	0	0	0	-1	0	0
$\Pi_{10}$	0	0	0	0	0	0	0	0	0	1	0	0	-1	0	0
$\Pi_{11}$	0	0	0	0	0	0	0	0	0	0	1	0	-1	0	0
$\Pi_{12}$	0	0	0	0	0	0	0	0	0	0	0	1	0	-1	0

Table D.2: Presentation of the k-values in dimensionless  $\Pi$ -parameters

The twelve dimensionless parameters obtained are listed in table D.3.

$\Pi_1$	=	$Q_{strip} * I_{plume}^{-2,5} * g^{-0,5}$
$\Pi_2$	=	$\Delta D_{plume} / I_{plume}$
$\Pi_3$	=	$\rho * I_{plume}^{1,5} * \eta_w^{-1} * g^{0,5}$
$\Pi_4$	=	$u_{amb} * I_{plume}^{-0,5} * g^{-0,5}$
$\Pi_5$	=	$h / I_{plume}$
$\Pi_6$	=	$\Delta \rho * I_{plume}^{1,5} * g^{0,5} / \eta_w$
$\Pi_7$	=	$u_{jet} * I_{plume}^{-0,5} * g^{-0,5}$
$\Pi_8$	=	$D_{pipe} / I_{plume}$
$\Pi_9$	=	$D_{10} / I_{plume}$
$\Pi_{10}$	=	$D_{50} / I_{plume}$
$\Pi_{11}$	=	$D_{90} / I_{plume}$
$\Pi_{12}$	=	$\eta_m / \eta_w$

Table D.3: List of dimensionless  $\Pi$ -parameters

## Regrouping and analyzing parameters

It is clear that the parameters just obtained can be regrouped and reworked to come up with more meaningful dimensionless parameters.

The first one that can be obtained is an overall Froude number, since:

$$\Pi_4 * \Pi_5^{-1/2} = u_{amb} * h^{-0,5} * g^{-0,5}$$

Another important one is the Richardson number:

$$\Pi_6 / \Pi_3 * \Pi_8 / \Pi_7^2 = (\Delta \rho / \rho * g * D_{pipe}) / u_{jet}^2$$

However the jet densimetric Froude number which is the inverse of the square root of it is more commonly used:  $u_{jet} / (g * \Delta \rho / \rho * D_{pipe})^{1/2}$

Furthermore a Reynolds number of the ambient flow can be obtained:

$$\Pi_3 * \Pi_4 * \Pi_5 = u_{amb} * h / \nu$$

Similar to the jet Froude number, the jet Reynolds number is also present:

$$\Pi_3 * \Pi_7 * \Pi_8 = u_{jet} * D_{pipe} / \nu$$

The combinations of  $\Pi_6$  instead of  $\Pi_3$  seems to give a Reynolds-like parameter in dimensions, but since that is associated with a density difference this doesn't have a physical meaning.

More meaningful is the dimensionless relative excess density:

$$\Pi_6 / \Pi_3 = \Delta \rho / \rho$$

The mixture grading characteristics are embedded in  $\Pi_9$ ,  $\Pi_{10}$  and  $\Pi_{11}$ , whereas the relative size of the particles is given by:

$$\Pi_{10} / \Pi_8 = D_{50} / D_{pipe}$$

Since lengths are now being related it should also be stated that the relative diameter size of the pipe is important:

$$\Pi_8 / \Pi_5 = D_{pipe} / h$$

Finally a velocity scale ( $\zeta$ ) can be determined by:

$$\Pi_4 / \Pi_7 = u_{amb} / u_{jet}$$

The relevance of  $\Pi_{12}$  can be discussed, but it should be kept in this form.

For the dimensionless dependent of  $Q_{strip}$  it might be nice to rewrite:

$$\Pi_1 * (\Pi_5)^2 / \Pi_4 = Q_{strip} / (h^2 * u_{amb})$$

The dimensionless dependent of  $\Delta D_{plume}$  is correctly given by  $\Pi_2$

## Scaling parameters

The water motion around the discharge point is correctly scaled if both the (jet densimetric) Froude number and the Reynolds number is the same in the experiment as in reality. The scale, denoted by subscript  $r$ , should be equal to one.

To reproduce the plume behaviour in the model correctly the density difference should be the same (the scale  $(\Delta\rho/\rho)_r$  should be one).

Furthermore it should be stated that all length scales will be equal as well as all velocity scales, since problems with a distorted model should be avoided.

For the Froude number this results in:

$$(u_{\text{jet}})_r = (\Delta\rho/\rho)_r * g_r * (D_{\text{pipe}})_r^{1/2}, \text{ with } g_r=1 \text{ and } (\Delta\rho/\rho)_r=1, (u_{\text{jet}})_r = \sqrt{(D_{\text{pipe}})_r}$$

velocity scale =  $\sqrt{(\text{length scale})}$

For the Reynolds number this results in:

$$u_r = v_r/h_r, \text{ with } v_r=1, u_r=1/h_r$$

$$\text{velocity scale} = 1/(\text{length scale})$$

This gives that  $(\text{length scale})^{1.5} = 1$ , which only has a trivial solution.

Since fulfilling both conditions is impossible, one should be dropped. There is general agreement in the literature that that should be the Reynolds number (Hecker, 1990; Roberts and Snyder, 1993; both in Ettema et al., 2000). When the flow is turbulent in the prototype, it is sufficient to have turbulent flow in the model as well, with minimum Reynolds numbers in the order of 4,000 to 10,000.

Another problem is the scaling of the sediment properties. Most probably scaling with the length scale will deliver grain size diameters that are too small. Therefore it is thought to scale the sediment diameters in such way that the Navier-Stokes particle fall velocity ( $w_s$ ) is scaled correctly by the velocity scale.

Finally the role of viscosity can be discussed. It is thought that the viscosity is the same in the model as in the prototype. So both  $(\eta_m)_r$  as  $(\eta_w)_r$  are equal to 1, to have no hindrance by the dimensionless parameter  $\Pi_{12}$ . It is thought that the influence of the differences in the model compared to the prototype is minor, and therefore the parameters are from now on left out of the discussion.

## Appendix D: Measuring plan stripping experiment

In chapter 6 part 6.3 the original measuring plan of the stripping experiment is discussed and presented graphically. The table listing of all measurements is presented in this appendix in table D.2. The legend of the colour coding used is given in table D.1.

First base case					
Checking the influence of one parameter	$\rho$	$D$	$W$	$U$	$h$
High Richardson number	high $\zeta$			low $\zeta$	
Low Richardson number	high $\zeta$			low $\zeta$	
Smaller overflow pipe diameter					
Grading influence investigation					

Table D.1: Legend of colour coding used in Table F.2

run nr	$\rho$ ( $\text{kg}/\text{m}^3$ )	$D$ (m)	$W$ (m/s)	$U$ (m/s)	$h$ (m)	$Ri$ (-)	$\zeta$ (-)
1	1035	0.05	0.11	0.1	0.3	1.42	0.91
2	1020	0.05	0.11	0.1	0.3	0.81	0.91
3	1035	0.05	0.11	0.1	0.3	1.42	0.91
4	1050	0.05	0.11	0.1	0.3	2.03	0.91
5	1035	0.04	0.11	0.1	0.3	1.14	0.91
6	1035	0.05	0.11	0.1	0.3	1.42	0.91
7	1035	0.06	0.11	0.1	0.3	1.70	0.91
8	1035	0.05	0.07	0.1	0.3	3.50	1.43
9	1035	0.05	0.11	0.1	0.3	1.42	0.91
10	1035	0.05	0.15	0.1	0.3	0.76	0.67
11	1035	0.05	0.11	0.05	0.3	1.42	0.45
12	1035	0.05	0.11	0.1	0.3	1.42	0.91
13	1035	0.05	0.11	0.15	0.3	1.42	1.36
14	1035	0.05	0.11	0.1	0.2	1.42	0.91
15	1035	0.05	0.11	0.1	0.3	1.42	0.91
16	1035	0.05	0.11	0.1	0.4	1.42	0.91
17	1050	0.06	0.07	0.1	0.4	6.01	1.43
18	1050	0.05	0.07	0.1	0.3	5.01	1.43
19	1050	0.04	0.07	0.1	0.2	4.00	1.43
20	1035	0.05	0.11	0.1	0.3	1.42	0.91
21	1050	0.06	0.07	0.05	0.4	6.01	0.71
22	1050	0.05	0.07	0.05	0.3	5.01	0.71
23	1050	0.04	0.07	0.05	0.2	4.00	0.71
24	1035	0.05	0.11	0.1	0.3	1.42	0.91
25	1020	0.04	0.15	0.05	0.4	0.35	0.33
26	1020	0.05	0.15	0.05	0.3	0.44	0.33
27	1020	0.06	0.15	0.05	0.2	0.52	0.33

---

28	1035	0.05	0.11	0.1	0.3	1.42	0.91
29	1020	0.04	0.15	0.1	0.2	0.35	0.67
30	1020	0.05	0.15	0.1	0.3	0.44	0.67
31	1020	0.06	0.15	0.1	0.4	0.52	0.67
32	1035	0.05	0.11	0.1	0.3	1.42	0.91
33	1035	0.03	0.15	0.1	0.3	0.46	0.67
34	1035	0.03	0.15	0.15	0.3	0.46	1.00
35	1050	0.03	0.11	0.15	0.3	1.22	1.36
36	1035	0.03	0.11	0.1	0.3	0.85	0.91
37	1035	0.05	0.11	0.1	0.3	1.42	0.91
38	1035	0.05	0.11	0.1	0.3	1.42	0.91
39	1035	0.05	0.11	0.1	0.3	1.42	0.91
40	1035	0.05	0.11	0.1	0.3	1.42	0.91

Table D.2: Listing of all stripping tests originally planned

## Appendix E: Working and use experimental setup

*In both chapters 6 and 9 information is presented on the experiments carried out in this M.Sc. thesis. The experimental setup is one of the important parts of those experiments. In this appendix the working and use of the experimental setup is discussed. In the first paragraph the stripping experimental setup is discussed as well as the experimental procedure followed in the stripping experiment. In the next paragraph the vortex divergence experimental setup is presented and the adjustments to the stripping experimental setup are discussed next to the procedure followed in the vortex divergence experiment.*

### E.1 Stripping experimental setup

*The measurements needed and the way to control the parameters in the stripping experiment is shortly discussed in chapter 6. In this paragraph a plan view of the experimental setup as built is given first followed by a short description of its working and the separate parts used. After that the method of making one run of measurements is discussed*

#### E.1.1 Plan view

A plan view of the experimental setup as it is built with all the objects placed in and around it is given in figure E.1. The different parts that are numbered in the figure are listed in table E.1.

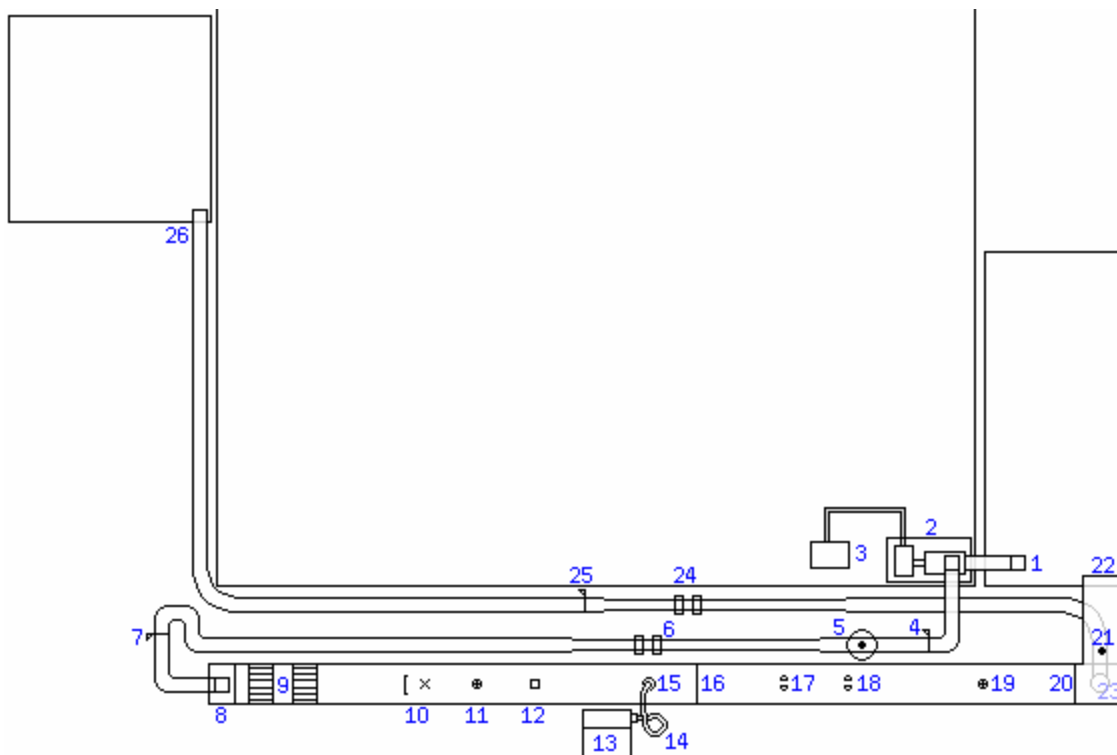


Figure E.1: Plan view of experimental setup as built in the Fluid Mechanics Laboratory

Nr	Part	Nr	Part
1	Intake from reservoir	14	Calibrated siphon
2	Pump	15	Overflow orifice
3	Frequency converter	16	Start dividing plate
4	Valve	17	Concentration measurement (OPCON)
5	Concentration measurement (OSLIM)	18	Concentration measurement (OPCON)
6	Discharge meter	19	Velocity meter (EMS)
7	Valve	20	End weir
8	Flume intake tower	21	Concentration measurement (OSLIM)
9	Straight lining sheets	22	Clean water recycled in reservoir
10	Velocity meter (Vectrino)	23	Waste water bottom outlet
11	Velocity meter (EMS)	24	Discharge meter
12	Water level meter	25	Valve
13	Well mixed reservoir	26	Waste water dumped in reservoir

Table E.1: Legend of numbered parts in figure E.1

### E.1.2 Working of the setup

The frequency converter (3) controls the frequency of the electric motor of the pump (2) such that the discharge through the incoming pipe can be controlled. By adjusting a valve (4) the dependency of the discharge on the frequency can be controlled. The incoming discharge will be measured with a pipe discharge meter (6). An extra valve (7) is placed to open and close the incoming pipe without adjusting the controls. The concentration of the incoming material is measured with an OSLIM (5), which continuously taps water from the pipe. The tapped water is collected to be able to check the concentration further after testing.

The flume has a tendency to create meandering flow. To prevent the development of those meanders straight lining sheets (9) are placed in the beginning of the flume. After that the velocity in the flume is measured with both Vectrino (10) and EMS (11) and the water depth is measured (12). The working principles of the measurement instruments are explained in appendix F as well as the reasons for using several instruments.

The overflow is brought into the flume by a calibrated siphon (14), from a well-mixed reservoir (13) with a constant head difference with the flume. The siphon is mounted with a special orifice (15) with the desired diameter and straight lining straws. For each overflow pipe diameter another siphon and orifice is used. The working of this siphon and the special orifice as well as the calibration of the siphon is further discussed in appendix G.

The overflow plume waste flows under the dividing plate as is described in paragraph 6.1. In the upper water column concentration measurements are carried out with two OPCON concentration meters (17&18). They are used to see whether stripping is continuous or patchy. Again the velocity is measured with an EMS (19). In the end of the flume a weir (20) is placed to control the wanted water depth. For each velocity a different weir is used, to keep the total water level always at a level of about 40 cm. The depth variations proposed for the overflow can be created by adjusting the depth of release of the overflow. After the end weir, the concentration of the overflowing water is measured as an indication for the averaged concentration in the

flume above the second bottom. Again this is done with an OSLIM (21) and again the tapped water is stored for onward confirmation of measured concentrations.

At the end of the part under the dividing plate, an outlet (23) is created that connects to the waste water pipe. The driving force of the waste water pipe is the head fall over the pipe. When designing the setup it had to be calculated whether the height difference present would be sufficient to create the wanted discharge, that calculation is put in Appendix M. A valve (25) controls the discharge which is measured with a pipe discharge meter (24).

### E.1.3 Experimental procedure

Taking a measurement in the experimental setup requires some preparation. The flume has to be clean, the overflow mixture should be prepared at the right density and all other settings have to be verified. After the measurements have been taken the setup has to be turned off in several steps. The total set of preparations, measurements and conclusion processes is called a run. This part describes the subsequent operations that should be carried out in one run. A flow diagram is presented in figure E.2. The operations can be grouped into 6 groups. The actions taken in every group are further discussed.

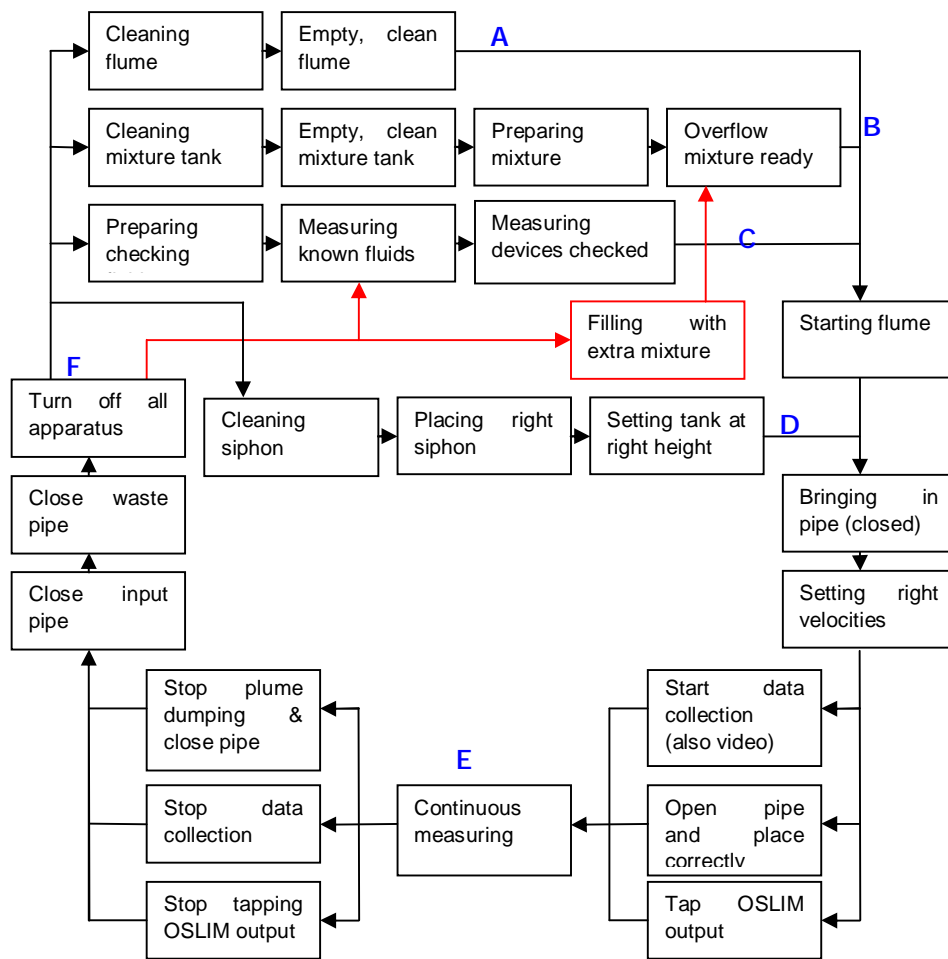


Figure E.2: Flow diagram of one measurement run

A. Cleaning the flume.

During the discharge through the flume low concentrations of plume material can come anywhere in the setup. When the flow is stopped, this material can settle in any place. When the flume is not cleaned correctly before running a new test the resuspension of that settled material can alter concentration measurements. Cleaning the flume consist of the removal of the water and the flushing of the pipes. After flushing the bottom of the flume will be washed with a damp cloth.

B. Preparing the mixture.

The mixture in the reservoir of tank has to be of the correct density. Therefore first all material from previous tests have to be removed. After that the amount of water and kaolinite needed is weighted. The kaolinite is after that brought in suspension with a small amount of water before all material is mixed in the tank. The pump in the tank has to be turned on to make sure the water level within the tank is at the correct height.

C. Calibrating the measuring equipment.

To check that the measuring equipment is working right they should be calibrated before the experiment is started. The EMS should be held in a standing bucket of water and set to zero. All concentration meters should measure two samples before they can be used: one with clean water and one with a known concentration.

D. Checking the siphon.

For separate overflow pipe diameters separate siphons are to be used. For setting the right jet velocity, the water level within the tank should have the correct head difference with respect to the flume. Finally the siphon must also be filled with material and not stand to long in a closed position. When the overflow is not running material within the siphon will settle and the siphon will not function properly.

E. Measuring.

Sampling is usually started just before the stopper on the overflow pipe is removed. The video is running continuously and data is collected by the computer. When the plume is in steady state tapping the water measured in the OSLIM devices can be started. After some time of continuous measuring (usually about 3 minutes) the tapping will be stopped, the overflow will be stopped and the measurement equipment is stopped.

F. Stopping the experiment.

When the measurement equipment is stopped first the incoming discharge will be stopped by closing the valve. The water depth in the flume starts to decrease then. The waste discharge might be increased to remove the last plume rests quicker. When the last plume rests are removed the waste discharge can be closed and all apparatus can be turned off. The flume can also be kept moving and then the next test can directly start if there is enough mixture ready and if the measuring equipment is checked.

## E.2 Vortex divergence experimental setup

For the experiments on vortex bifurcation the experimental setup built for the stripping experiment was slightly adjusted. The working of the majority of the setup is the same. Therefore here only the adjustments are described in detail. First the plan view of the total setup is presented, then the working of the adjustments are explained. Finally the measuring procedure is explained.

### E.2.1 Overview

The main system built in the laboratory around the flume for the stripping experiment is kept intact. The false bottom system in the flume is shortened, and the amount of concentration measurements is reduced. An overview of the total setup is presented in figure E.3, the numbered parts of the setup are listed in table E.2.

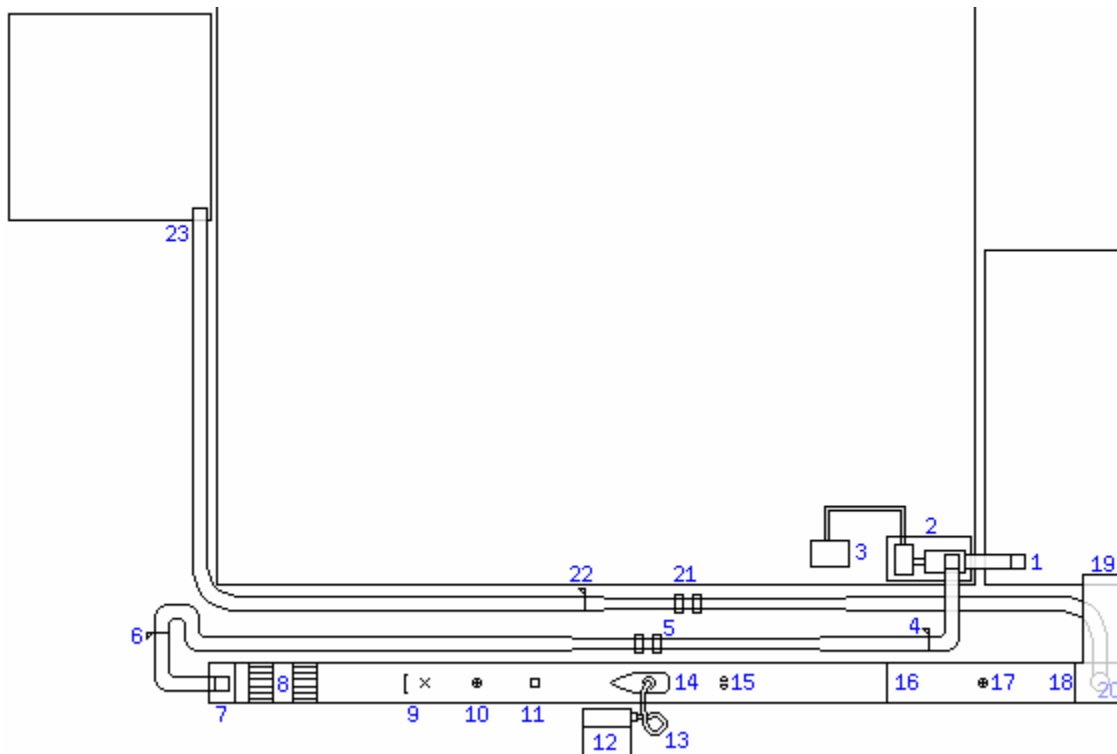


Figure E.3: Plan view of the adapted experiment setup with all objects indicated.

Nr	Part	Nr	Part
1	Intake from reservoir	13	Calibrated siphon
2	Pump	14	Ship overflow pipe orifice
3	Frequency converter	15	Concentration measurement (OPCON)
4	Valve	16	Start dividing plate
5	Discharge meter	17	Velocity meter (EMS)
6	Valve	18	End weir
7	Flume intake tower	19	Clean water recycled in reservoir
8	Straight lining sheets	20	Waste water bottom outlet
9	Velocity meter (Vectrino)	21	Discharge meter
10	Velocity meter (EMS)	22	Valve
11	Water level meter	22	Waste water dumped in reservoir
12	Well mixed reservoir		

Table E.2: Legend of numbered parts in figure E.2

### E.2.2 Working of the adapted parts

Here the adjustments made with respect to the stripping experimental setup are discussed. For more details the reader is referred to the previous chapter on the stripping experimental setup.

The length of the dividing plate is shortened. This is done to make sure the plume has more time to sink to the bottom. Whether that indeed works will depend on the density of the overflow mixture. Removing a part of the dividing plate creates also more space to take the concentration measurements with the OPCON.

The OSLIM concentration meters were removed. They were used to measure an overall concentration increase, and in this setup that is not needed anymore.

One of the OPCON devices is also removed, since it is handier to handle only one measurement apparatus in one time.

New smaller siphons are used. They are also and calibrated to obtain a relation between the jet velocity and the height difference. The orifice of the pipe is placed in a model of a ship (not on scale) to prevent wake forming behind the pipe exit. A picture of that ship is presented in figure E.4.



Figure E.4: Picture of the model ship used to prevent wake forming behind the pipe

As discussed in part 9.1.3 of the main text the concentration profile of the plume behind the ship is measured by taking several point measurements of the concentration with the OPCON concentration meter. Depending on the shape of the cross profile of the plume a 5x5 to 8x8 matrix of point measurements is made. Also the distances between the point measurements is depending on the shape of the cross profile and is about 2-3 cm. Time-averaged measurements are taken averaging over 10-20 s, depending on the downstream location of the measurement. It is thought that further downstream the length and time scales of the variation are larger, meaning that distances between the point measurements can become larger but that averaging has to take place over more time.

### E.2.3 Experimental procedure

Measuring one cross profile of a plume contains a number of actions. What actions have to be carried out is depending on the plume. When the plume mainly sinks to the bottom and is completely removed under the dividing plate a continuous plume can be created and all point measurements can be taken in one sequence. However, if the plume tends to stay above the dividing plate, the plume discharge has to be stopped after each vertical line of measurement points to make sure the clean water tank does not get polluted. In figure E.5 a flow diagram is presented which shows both options. The actions to be taken in both cases and the actions to be taken per case are discussed next.

#### A. Preparation.

The preparation of the experiment consists of making sure that the flume itself is clean, that the correct overflow mixture is prepared, the OPCON is checked for calibration and that the right siphon is placed and prepared. After that the ship is placed in the flume with a closed pipe and the velocities of the flume are correctly installed.

A detailed discussion of each of those parts is given in the previous chapter.

#### B. Continuous measurements.

If the plume does not pollute the water above the second bottom, the plume can be measured continuous. The concentration profiles can be measured in one row. Each time the OPCON has to be placed correctly and then the measurement can be taken.

It is important that during these tests the velocities, the water depth and the incoming and waste discharge are checked regularly. Also the plume behaviour should be inspected regularly to be constant, since there are always possibilities for irregularities in time.

#### C. Discontinuous measurements.

If the plume tends to pollute the water above the dividing plate, the discharge of material should be stopped regularly in order to prevent the material from entering the clean water tank. Normally one series contains enough time to measure one vertical row of points. Depending on the cross-profile measured 5 to 7 series are needed to measure one profile.

It is important to make sure that the siphons are not influenced by the stopping and starting procedures of the discharge. When the discharge is stopped, material tends to settle within the siphon. The siphon therefore needs to be taken out of the flume regularly for flushing, after that several series can be ran.

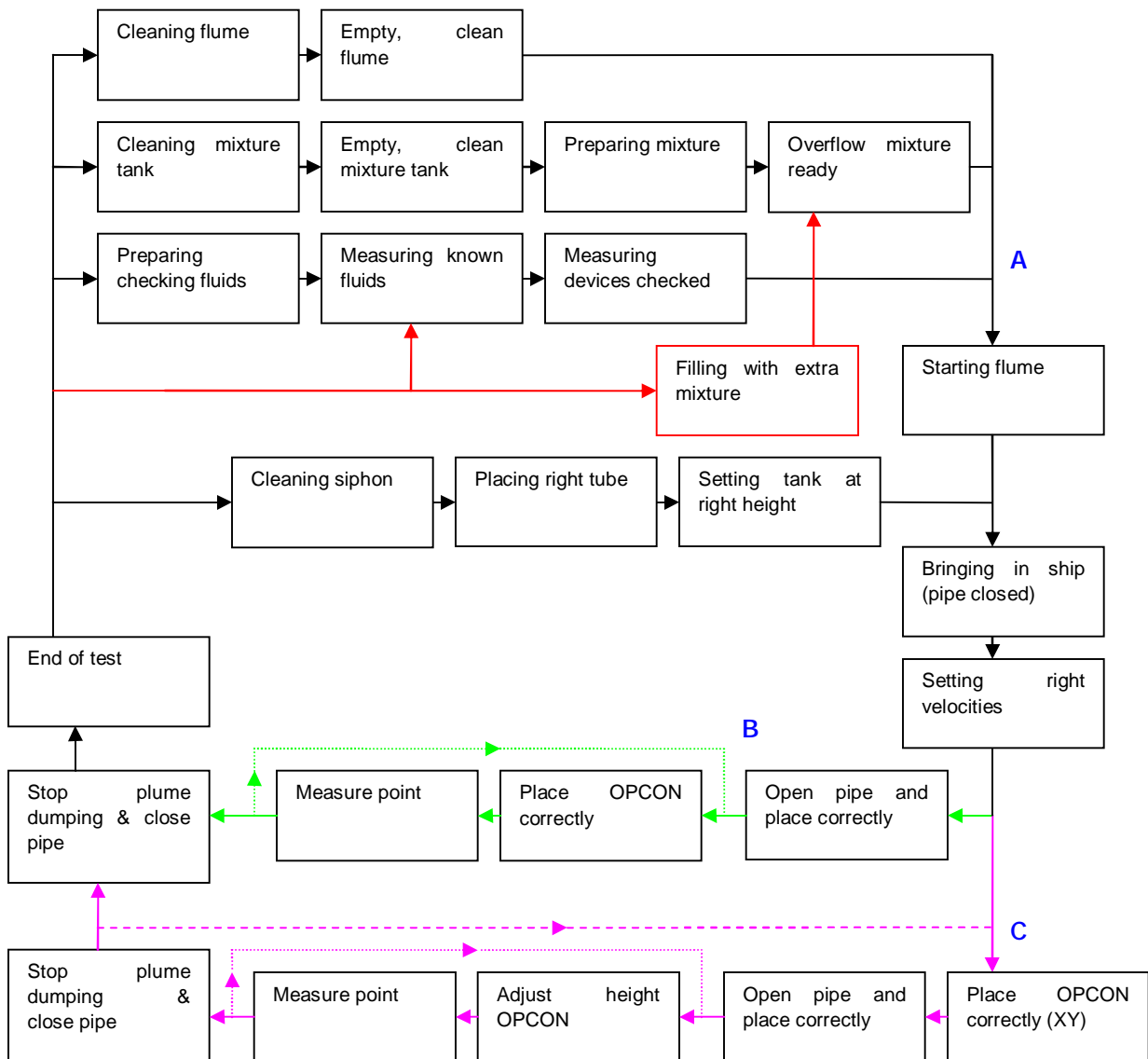


Figure E.5: Flow diagram of measurement run in vortex bifurcation experiment

## Appendix F: Instruments used in experimental setup

*The success of measurements taken in an experimental setup is mainly depending on the type of equipment used and its correct functioning. Getting to know the specific features of the equipment used is essential in that. Here all equipment used is shortly discussed presenting the main features, accuracy and operational characteristics. If problems were faced during the experiments carried in this M.Sc. thesis those are discussed too.*

### F.1 Discharge meters

The discharge meters used in the experimental setup are Proline Prosonic Flow meters type 91W. They consist of two clamp-on sensors to be mounted on the pipe and a transmitter for the input and output of data. Figure F.1 shows the mounted clamp-on sensors and the transmitter as they can be found in the experimental setup.

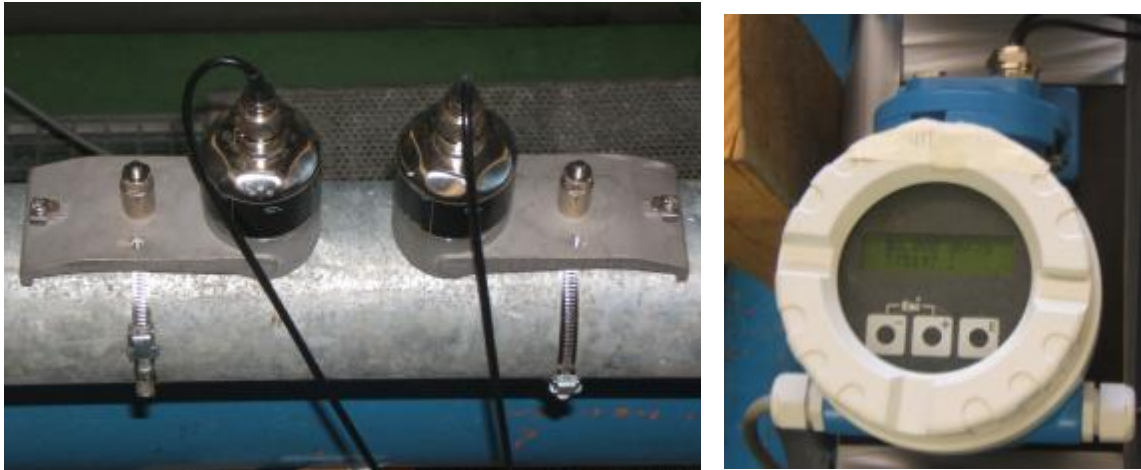


Figure F.1: Discharge meters clamp-on sensors and transmitter as found in experimental setup

The discharge meters operate on the principle of transit time difference. An acoustic (ultrasonic) signal is sent from one measuring sensor to another in both directions. A transit time difference arises because the signal propagation velocity of the sound waves is greater in the direction of flow than against the direction of flow. This difference is directly proportional to the flow velocity. The flow is calculated from the pipe cross-sectional area and the measured transit time difference. To obtain reliable measurement results the flow velocity must be higher than 0.3 m/s in order to make the time difference recognizable. For that reason the pipe diameter had to be reduced at the place of the sensors. An inlet run length of 10 times the pipe diameter and an outlet run length of 5 times the pipe diameter is minimally needed in order to keep the measurements correct, so therefore the lengths of the small pipes are more than 15 times the pipe diameter.

After setting the required input for the meters about the pipe and fluid characteristics, the discharge meters were directly operational and no calibration was

needed. The performance characteristics of the supplier guarantees that the error limit of the discharge meters for this setup is about 2% of the reading plus about 0.1% of the full scale used, which is set at 25 m<sup>3</sup>/s.

More information on the Proline Prosonic Flow meters can be found on [www.endress.com](http://www.endress.com).

## F.2 EMS velocity meters

Several methods were used to measure the velocity. One of them were EMS (or in English EMF = ElectroMagnetic Flow) velocity meters. An EMS velocity meter consists of a probe and a control unit for signal processing. The principle behind this method lies in the fact that in an electrical conductor (water) moving through a magnetic field a voltage is induced. For a given field strength, the magnitude of the induced voltage is proportional to the velocity. EMS velocity meters create a magnetic field and measure the induced voltage.

For that reason the sensor of the probe is placed in the flume. The magnetic field created has a cylindrical shape with a height of 5 mm and a diameter of 50 mm. As the magnetic field may not be interrupted, the sensor probe should be placed at some distance from physical boundaries. The placement of the probes in the experimental setup is presented in figure F.2 as is the control unit used.

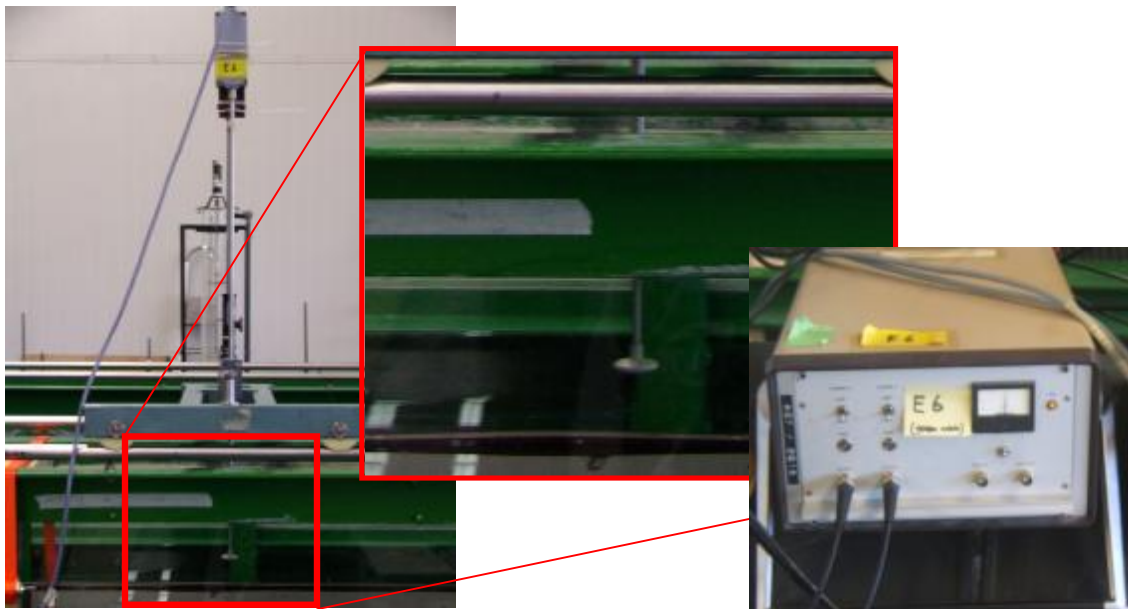


Figure F.2: EMS probe and control unit as found in experimental setup

The installation of the EMS velocity meters is relatively straightforward, but the meters have to be calibrated before each run. The accuracy of the instruments is about 0.01 m/s plus 1% of the measured value. The flume velocities that will be generated are of the order of 0.05 m/s, so the deviations is about 20% of the generated velocity. This would lead to the conclusion that the EMS velocity meters are in principal unsuitable for measuring the velocities in the experiment. However, application of the EMS velocity meters showed that the deviations due to the system inaccuracy can be visually distinguished from real velocity changes. That makes the

EMS velocity meters suitable for qualitative investigations of the velocities in the flume, like verifying that no wave pattern exists in the velocity in the flume. This is illustrated in figure F.3 which shows a time series of velocity measurements with the EMS velocity meter. The velocity is measured during the start-up of the flume. At the beginning the velocity was zero and the signal of the EMS velocity meter indicates a mean velocity of about -0.005 m/s and has a bandwidth of about 0.01 m/s (as indicated by the accuracy of the apparatus). This situation is shown in the yellow ellipse in figure F.3. Then the flume was started up and a wave started travelling through the flume. Still the instrument has an accuracy of 0.01 m/s, but the starting waves can clearly be observed. Those waves are indicated in the blue ellipse in figure F.3. Due to the accuracy of the apparatus it is difficult to estimate where the waves end and the situation with continuous velocity starts, but after about 1050 timesteps the deviations in velocity observed are thought to be due only to the inaccuracy of the apparatus. That is indicated in the red ellipse in figure F.3.

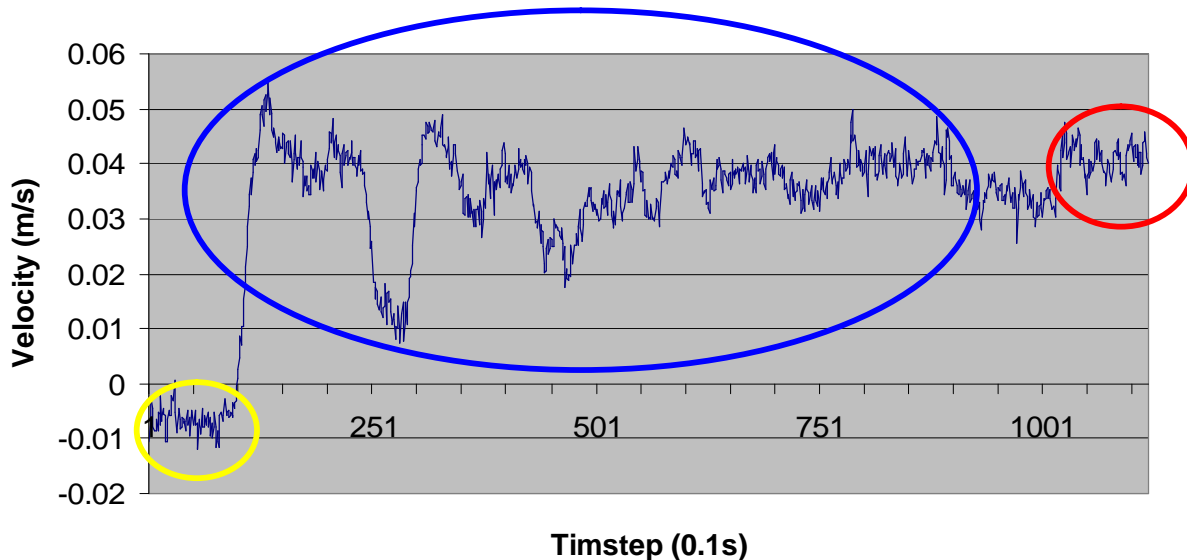


Figure F.3: Time series of velocities measured with EMS with indicated velocity deviations

### F.3 Vectrino velocity meter

Another apparatus that was used to measure the velocity in the flume was the Vectrino ADV (Acoustic Doppler Velocity meter). Its measuring principle is based on measuring the Doppler shift in frequency between sent and reflected sound pulses. The reflection of the sound originates from particles suspended in the water. However, if clean water is used, the amount of reflected beams is small, which give rise to accuracy problems of the system. For that reason the measuring setup including a Vectrino in the flume also consists of an apparatus to create H<sub>2</sub>-bubbles via electrolysis. The negatively charged cathode is designed as a long string wire tightened to a frame, so that the creation of H<sub>2</sub>-bubbles is spread over some area. Somewhat downstream the Vectrino is placed and its sound pulses are reflected on the H<sub>2</sub>-bubbles. The setup is shown in figure F.4.



Figure F.4: Measuring setup including Vectrino and cathode of electrolysis apparatus.

The data collected by the Vectrino apparatus is handled by an accompanied software program. In this program not only the mean velocity is presented, but also the reliability of the apparatus is presented, based on the number of pings (reflected sound pulses) measured. With that information the optimal setup of measuring apparatus and electrolysis apparatus was determined.

#### *F.4 Water height meter*

The measurement device to measure the water height in the flume is the Temposonics Magnetostrictive Position Sensor. The method used to determine the position of the floating ring, which in fact is a permanent magnet, is quite complex and schematically shown in figure F.5. A sensor current is sent along a magnetostrictive sensing element called waveguide, creating a magnetic field in radial direction. In the position magnet area, the waveguide is distorted elastically. Due to the time curve of the current pulse, this distortion is a highly dynamic process which produces a torsion wave in the effective field of the permanent magnet. Detection of this torsion wave is ensured by a special pulse converting system at the upper end of the waveguide, consisting of a magnetostrictive metal strip connected to the waveguide, an inductive detector coil and a fixed permanent magnet. In this torsion pulse converting system, the ultrasonic wave of the magnetic field distortion causes a permeability change of the metal strip. The resulting time change of the permanent magnetic field induces an electric current signal in the sensing coil, which is processed in the sensor electronics. The position of the permanent magnet (float) is determined accurately by travel time measurement, measuring the time between the current pulse start and the arrival of the electric reply signal, since both the speed of the current pulse and the speed of the ultrasonic torsion wave are constant.

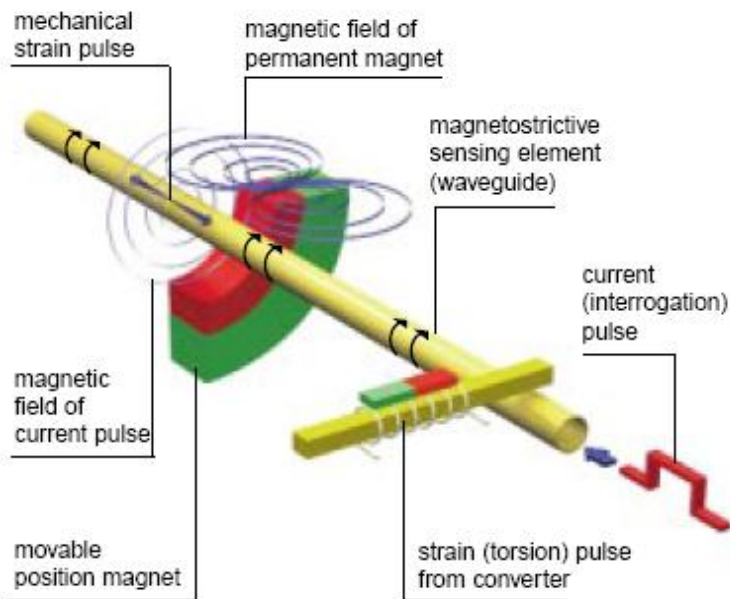


Figure F.5: Principle sketch of the measurement method of the Temposonics Magnetostrictive Position Sensor

This displacement measurement principle seems complicated but ensures high accuracy, long-term stability and insensibility for external influences like vibrations. The measurement has an accuracy of about 0.1 mm and calibration has to take place only once. The placement of the height meter in the experimental setup is shown in figure F.6.

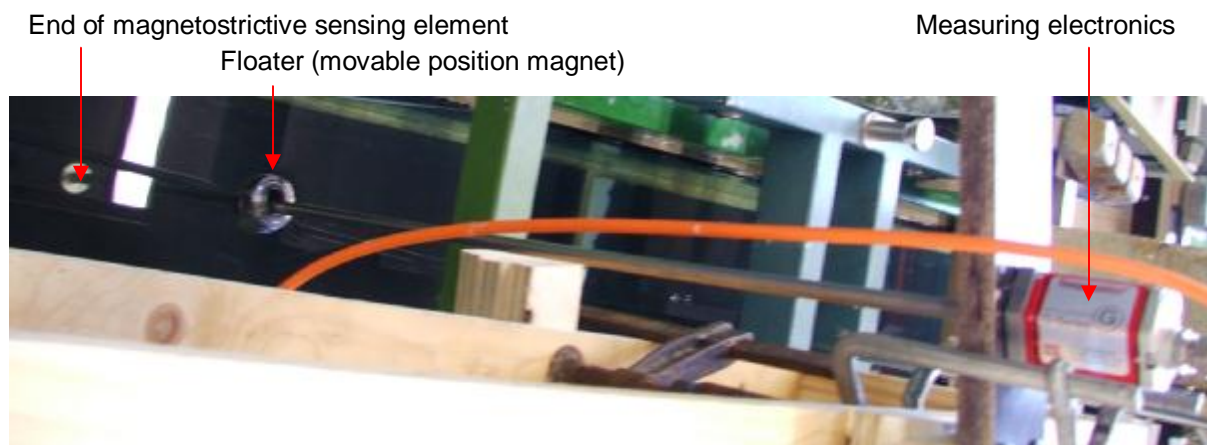


Figure F.6: Height meter as placed in experimental setup (turned 90° clockwise)

### F.5 OPCON concentration meters

To take point-measurements of the concentration of material, OPCON concentration meters were used. The OPCON concentration meter uses the principle of extinction of near infrared radiation by sediment particles. Infrared light is emitted from the probe and a sensing volume of 2.5 mm x 2.6 mm x 30 mm is exposed. The extinction of light is compared to a reference system and is the measure for the concentration. The control unit is used for power supply, amplification and post-processing. The probe and control unit as placed in the experimental setup is shown in figure F.7.



Figure F.7: OPCON concentration meter: probe, detail of probe and control units

Important feature of an optical extinction meter such as the OPCON is the saturation of the instrument. Above a certain threshold, the output is constant for every concentration. The cause for the saturation can either be physical or due to the tuning of the instrument.

Physical saturation occurs above the minimum concentration that extinguishes all radiation emitted. If the concentration is higher than that minimum concentration still all radiation is extinguished and the apparatus still represents the minimum concentration value of extinction. The exact value of that minimum concentration is depending on the magnitude of the sensing volume, the light source strength and the type of material.

When the instrument is tuned to measure low concentrations, saturation can occur already at lower concentrations. Fine-tuning causes the concentration increase needed for the same output voltage increase becomes smaller. Since the maximum voltage output is limited the maximum concentration corresponding to that output becomes smaller. Shifting the output signal can to some extent prevent this, but will transpose saturation effects to the low concentration side. Saturation caused by

tuning can be spotted quite easily, since the output signal of the measurement devices will be maximal.

In the experiments saturation was reached for several times. In the stripping experiment tuning saturation was observed several times when clouds of material were removed from the plume, while the apparatus was set at highest sensibility to see whether the downstream water normally stayed clean. In the vortex bifurcation experiment, saturation had to be removed since levelling down high concentration disturbs the correct prediction of time-averaged profile. It turned out that too close to the orifice peak concentrations did cause physical saturation, which takes place at about 2,6 g/l. Moving the equipment further downstream ensured that peak concentrations were lower than the saturation threshold.

Another important feature of concentration measurement is the conversion from output voltage to concentration. This conversion has to be based on calibration of the equipment using the exact same settings as used in the measurements. A calibration setup was used in which the OPCON concentration meter had to measure known concentrations which were increased stepwise. By making several of these calibration measurements, the conversion relationship between output voltage and concentration could be obtained. The calibration setup is shown in figure F.8 and an example of a resulting calibration curve is presented in figure F.9. All calibration curves used in the experiments are presented in Appendix N.



Figure F.8: Calibration setup to calibrate concentration meters, right: detail of the measuring bin

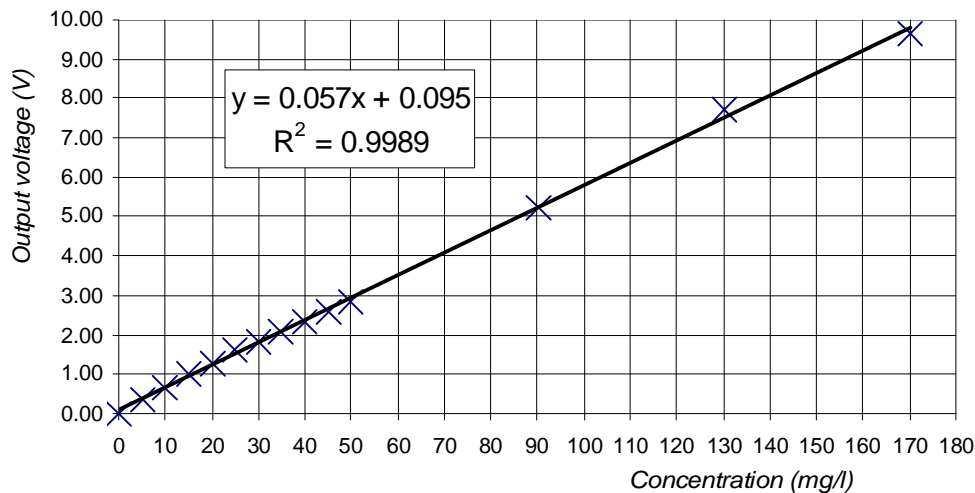


Figure F.9: Calibration curve of one of the OPCON devices during the experiments

Before a new measurement is made two mixtures have to be measured, one with a concentration of 0 mg/l and another with a known (measurable) concentration. The results can be used to check whether the conversion still holds. If not, another calibration series in the calibration setup has to take place.

## F.6 OSLIM concentration meters

During the stripping experiment next to OPCON concentration meters OSLIM concentration meters were used to measure water samples taken as a measurement of the mean concentration. The OSLIM concentration measuring method is based on the attenuation of the intensity of a light beam, due to the light absorption and scattering of particles suspended in a liquid. The method is optical, just like the OPCON. Main difference is the fact that the OSLIM 'probe' is placed outside the water so that samples to be analyzed have to be pumped through via various hoses. The system therefore consists of an intake, several hoses to the OSLIM 'probe', an OSLIM control unit and power supply, a pump and a spill of the hose. During tests the spill water is preserved for further research. Figure F.10 and F.11 show how the OSLIM concentration meters were installed in the stripping experimental setup.

Also the OSLIM concentration meters needed calibration in the way described in the previous paragraph for the OPCON. The results of this calibration are presented in Appendix O. It turned out that the sensitivity of the OSLIM was lower than the OPCON but that the noise of the signal was significantly smaller. Besides that the saturation concentration was lower, which made that saturation was not an issue with the use of the OSLIM. The system of sampling makes the OSLIM concentration meters impracticable in taking point measurements. Therefore they are used to give time-averaged concentrations. To do so the measuring should only start when the process is at steady state. Due to the malfunctioning of the experimental setup the steady state situation for stripping never occurred. The results of the OSLIM measurement were therefore never used.

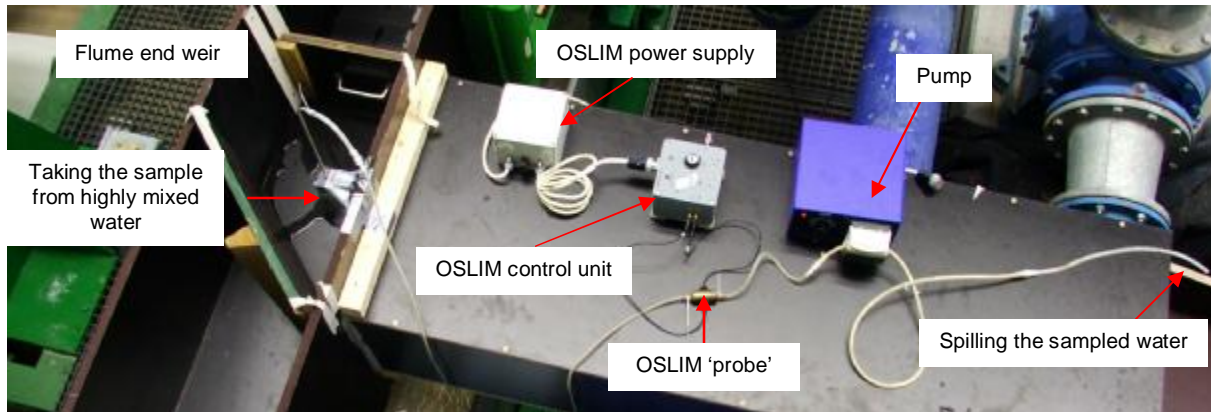


Figure F.10: OSLIM used to measure the outgoing water concentration

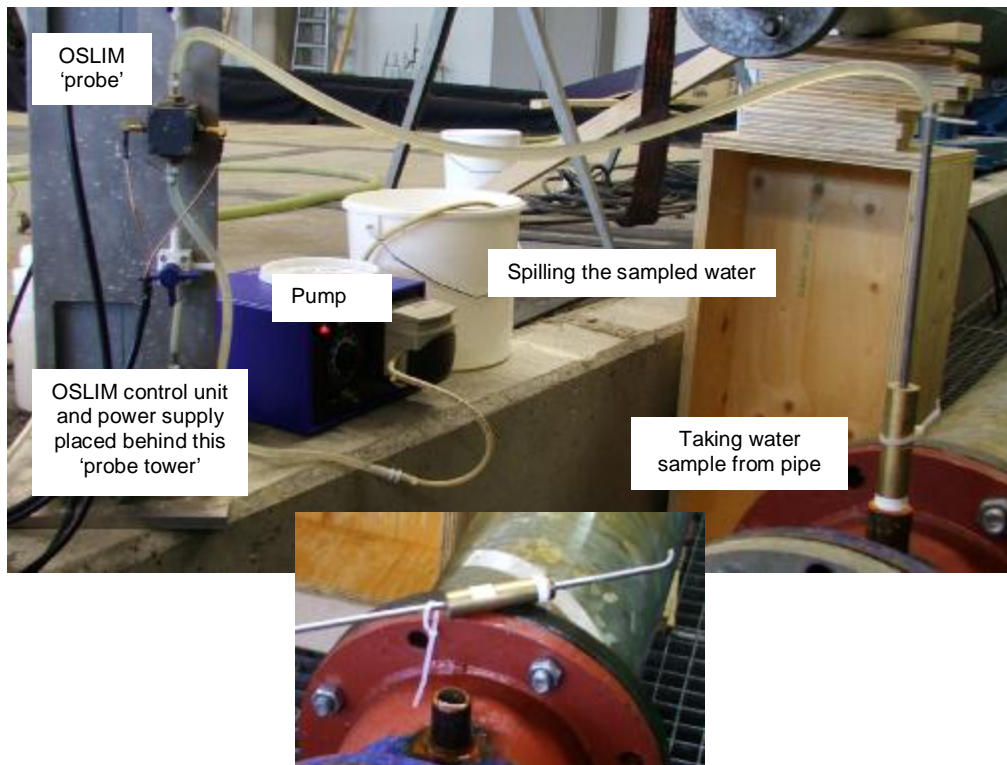


Figure F.11: OSLIM used to measure incoming water concentration  
detail: pipe water sampler

## Appendix G: Siphons used in experimental setup

*In both the experimental setups material had to be discharged through the modelled overflow pipe. The discharge had to be regulated to control the overflow velocity. A calibrated siphon was used to discharge the material. In this appendix the working of that siphon and the method of calibration used is explained. First the general idea is presented, followed by the method of calibration. After that two major adjustments made are discussed: the increase of the frictional resistance in order to create more head difference needed and the streamlining implemented in the overflow pipe to reduce hose effects such as swirl. Finally the use of the smaller siphons in the vortex divergence experiment is evaluated shortly.*

### G.1 General idea of siphon

In general a siphon is used to transport liquid from a reservoir with a higher water level to a reservoir with a lower water level. The velocity in a siphon without resistance is given by Torricelli's equation (Battjes, 2002):

$$u = \sqrt{(2g\Delta h)} \quad (\text{G.1})$$

In which  $u$  represents the outgoing velocity,  $g$  the gravitational acceleration and  $\Delta h$  is the head differences between the two reservoirs. However, in normal conditions friction losses will cause that this velocity is not reached. In small head differences and siphon diameters, friction will be dominant. However, the velocity  $u$  will always depend linearly on the square root of the head difference  $\Delta h$ .

For discharging the overflow mixture this principle of siphons is used. The head difference between the flume (which has a constant water level) and reservoir is made adjustable by placing a lift under the reservoir. The height in the reservoir is kept constant by continuously pumping extra mixture into the reservoir for overflowing over a weir. That is also advantageous in keeping the material in the reservoir mixed.

The relationship between the head difference in the reservoir and flume and the velocity of the overflow is investigated and calibrated for. The idea is sketched in figure G.1 and figure G.2 shows the siphon as it is placed at the experimental setup.

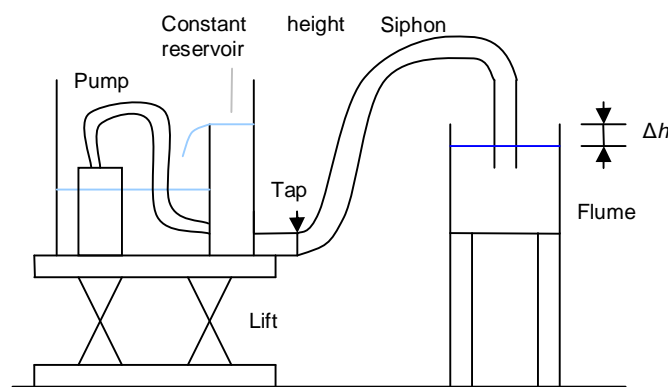


Figure G.1: Sketch of the idea of the siphon used



Figure G.2: Placing of the siphon in the experimental setup

### G.2 Calibrating siphon

To calibrate the siphons used in the experiment a setup was built to measure the discharge of the siphon at various head differences. On the reservoir-side nothing is changed. On the other side, the flume is exchanged for a tank, placed inside a larger reservoir. When the siphon is discharging, the tank overflows into the reservoir. The water level of the reservoir is measured and the relationship between the water level and volume is used to calculate back the discharge. The idea is sketched in figure G.3 and the calibration setup in reality is shown in figure G.4.

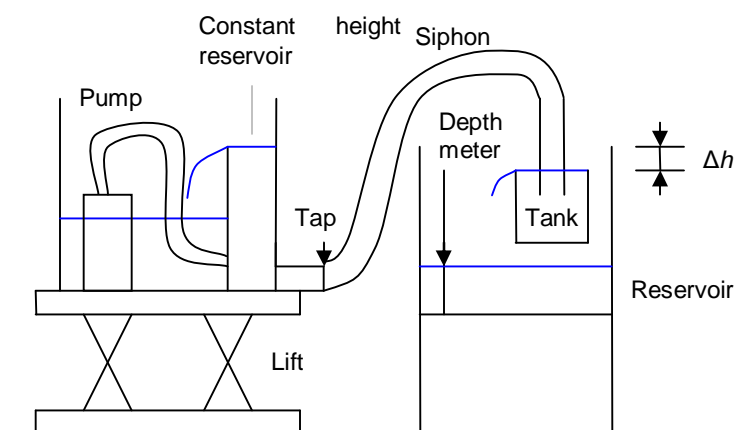


Figure G.3: Idea of calibration setup

The result of the measurements in the calibration setup is a graph that indicates the velocity in the overflow pipe at different height differences. When the square root of the height differences are set out on the horizontal axis and the corresponding

velocities on the vertical axis a straight line evolves which is typical for each siphon. As an example, that calibration graph is presented in figure G.5 for the 6 cm siphon used in the stripping experiment. The calibration graphs for all siphons used are presented in appendix P.



Figure G.4: Pictures of the calibration setup: overview, front view and detail

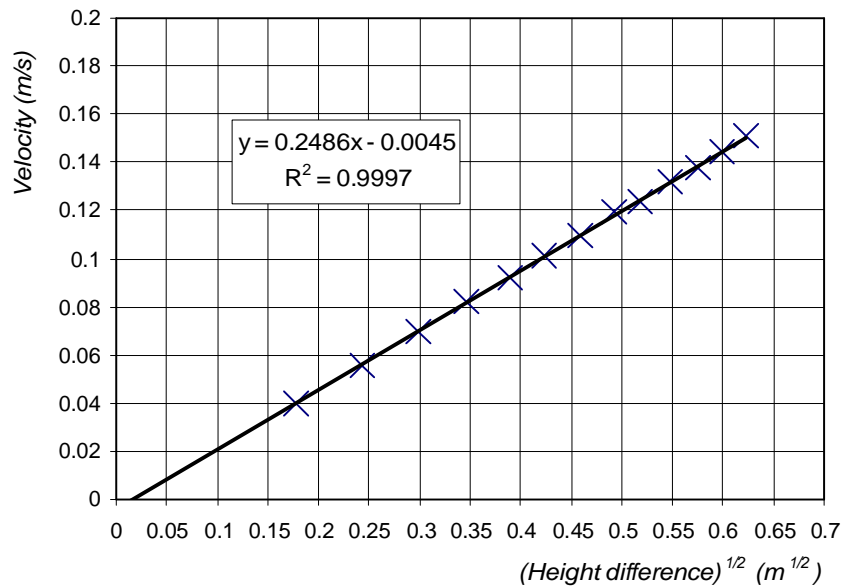


Figure G.5: Calibration graph of 6 cm siphon to be used in stripping experiment

### G.3 Increasing the frictional resistance

In the first calibration runs using the siphons proposed it turned out that the height difference needed to obtain the wanted velocities were no more than a few centimetres. Since setting the height of the elevating table is rather rough, the velocity could not be regulated as precisely as needed. To overcome that problem the frictional resistance in the pipe had to be increased. Since the height difference needed to create the wanted velocity is only small, the final height difference is mostly determined by the head loss created by increasing the resistance. The resistance was increased by bringing in a flange (a metal disc with a small opening) in the opening from the constant head reservoir to the siphon. The several different flanges used in the experiment are shown in figure 7.17.



Figure G.6: Different flanges used in experiment, the dark one is already placed in the basis that was reused for every flange.

The abrupt change in the profile of the pipeline caused by the flange creates a retardation head loss. Since this head loss is approximately proportional with the velocity squared, local retardation head losses are written in the form:

$$\Delta H_v = x \frac{U^2}{2g} \quad (\text{G.2})$$

For the widening of the flow after a flange, the value of  $\Delta H_v$  is given by the rule of Carnot which yields that (Battjes, 2002):

$$\Delta H_v = \frac{(U_1 - U_2)^2}{2g} = \left(1 - \frac{A_1}{A_2}\right)^2 \frac{U_1^2}{2g} \quad (\text{G.3})$$

When the flange is installed also an intake head loss will be created by it. This head loss is determined by amount of the contraction of the flow (Battjes, 2002). Due to the fact that the opening is slightly rounded, this contraction is thought to be negligible. Also other friction head losses are considered negligible when compared to this retardation head loss. Therefore the total head loss in the siphon can be estimated by applying equation (G.3).

It followed that for every siphon diameter then proposed (being 3, 4, 5 and 6 cm) it was best to use a separate flange. The height difference (to overcome the head loss) of every siphon, would than range from 8 to 35 cm for the wanted variation in jet velocities. The flanges used had a diameter of 9, 12, 15 and 18 mm respectively.

### *G.4 Streamlining the outflow*

From the first tests of the siphons it was concluded that swirling effects of the flexible hoses could be seen in the discharges of the pipes. Those swirling effects are dependent on the way the hoses hang, how they are bended etcetera. Since the height difference is varied during the tests, these swirling effects will not continuously be the same. To improve reproducibility the swirling effects could best be removed. This is done by implementing two compartments of straws in the overflow pipes. The straws, having an inner diameter of about 0.4 cm have a length of about 4 cm (10 times their diameter). Placing two of these compartments is proven in practice to be most useful in streamlining the flow. Figure G.7 shows the straws as they are implemented in the 6 cm pipe.

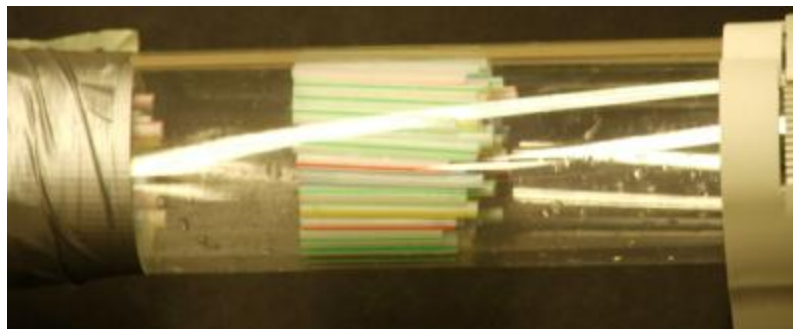


Figure G.7: Straws implemented in the 6 cm pipe

### *G.5 Smaller siphons created*

During the stripping experiment it was seen that the large siphons used brought too much material into the flume. For that reason a smaller overflow pipe mouth had to be mounted on the siphon. First a pipe with a diameter of 1.2 cm was created to finish the stripping experiments. For this pipe a mouth was made which could be slide over the end of the 3 cm pipe used before, by gluing rings with several increasingly smaller diameters together the transition from 3 cm to 1.2 cm was created. For the vortex bifurcation experiments later the final pipe diameter was made 1 cm in the same manner, as told before, also a ship model was mounted on the pipe end. This adapted siphon is shown in figure G.8.

When this adapted siphon was calibrated it turned out that the head loss of the siphon was too small. The variation in height needed for the wanted set of jet velocities was limited to about 10 cm. For that reason an extra head loss had to be created, similarly to the flanges used before. It was chosen to put a small pipe in the hose of the siphon, which would be pinched in the siphon start. This 'friction pipe' is taken out of hose and shown on the white cloth in figure G.8.

For the other small siphon used in the vortex bifurcation experiment a completely new system was adopted. A small laboratory hose of 0.4 cm was mounted on a wooden slat so that the opening could be placed about 30 cm below reservoir level, at the other end, the hose ended directly in the ship orifice, without the use of any pipe. Since the length of the hose determined the friction losses, a nicely working range of height difference could be adopted. This small siphon is also shown in figure G.8.



Figure G.8: Smaller siphons created for the experiments.

The working of the smaller siphons was not as successful as the earlier larger siphons. As discussed before the siphons turned out to be unreliable.

The adapted siphon got obstructed several times by sediment particles. Normally flushing the siphon regularly (in between every test) was needed to make sure the siphon continuously discharged the same amount of material. After some time it was needed to disassemble the siphon and clean it totally. In the final week of testing the obstruction lasted even after that. Most probably the 'friction pipe' was assembled differently from before the disassembling, creating different frictional behaviour.

If the working of the siphon is indeed influenced by the way it is assembled, it is not guaranteed that the siphon was working in the same way in both the experiment as in the calibration. This also makes the measurement runs carried out unreliable.

The small hose siphon faced different problems. First the orifice of the hose was not straight and flat, which had a large influence on the vorticity distribution in the plume. Next to that problems with swirl in the hose are suspected. In the large pipes straws were placed to straighten the streamlines after a flexible hose, here this could not be done. Finally the connection between the hose and the ship broke down. The hose was withdrawn for about 1 cm. As a result the plume was first dumped in the ship and then via the ship orifice in the flume. Of course that yielded different plume behaviour.

## Appendix H: Velocity deviations in the flume

*One of the major problems faced in building the experimental setup was the control and measurement of the flume velocity. After completion of the setup, flume velocity measurements showed that the velocity was deviating much from its mean, more than was expected based on turbulence and measurement noise. It turned out that the whole flume was vibrating. Here the process of recognition and solving that problem is discussed, mostly on chronological order.*

### *H.1 Air in the pipelines*

When the experimental setup was designed, some problems were foreseen on the velocity created in the system. Due to the use of a pump, discontinuities in the velocity might arise because of the stroke of the pump or the entrainment of air bubbles. Furthermore the pump itself might be vibrating. After the first instalment of the pump and the pipeline, the pump indeed was heavily vibrating. The discharge delivered was not constant and getting the pump started was very difficult. All this was due to presence of air in the pipeline. Vacuum connectors were installed to remove the air from the pipeline. That reduced the discharge variations but could not make it disappear. The vibrations of the pump and the pipeline were not stopped and also the velocities and the watershed in the flume were still irregular.

Small adjustments in the setup were implemented such as replacing the underflow end weir by an overflowing one, closing the entrance by a few centimetres to make the intake tower of the flume act as a buffer and placing an extra valve into the pipeline. The reduction of the variations in the measured flume velocity by these adjustments was only small.

### *H.2 Meandering*

One hypothesis on the source of velocity variations was that the flow in the flume was meandering. Bringing in dye on one side of the flume did show that meandering indeed took place as can be seen in figure H.1 in which the dye released at the right side of the flume was (partly) moved to the middle of the flume.

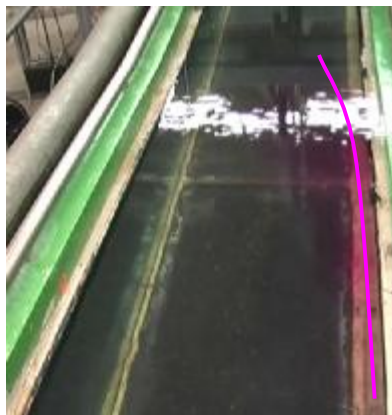


Figure H.1: Meandering in the flume visualized by dye

The most common solution to meandering in laboratory flumes is placing two packs of corrugated sheets that are fixed together to make a series of tubes into the flume. From earlier investigations in flumes it is known that the length of each pack should be about the width of the flume and the packs should be placed about 30 cm apart. Figure H.2 shows how the packs are placed in the experimental setup. The effects of these sheets were acceptable: meandering of dye clouds could no longer be observed, and the variations in the velocity in cross-direction were reduced to negligible proportions. However, the variations of the velocity in longitudinal direction were still too large.



Figure H.2: Packs of corrugated sheets placed into the flume to prevent meandering.

### *H.3 Frequency converter*

Another hypothesis on the cause of the velocity variations, especially of those in longitudinal direction, was the fact that the pump was delivering much more head than needed. The head was dissipated by nearly closing the valve. This gave possibly rise to an accumulation of air behind the pump, that makes the pump pressure fluctuating.

To resolve the air accumulation either the head created by the pump should be lowered or the air should be removed, for example by discharge system for (part of) the water. It was chosen to control the head created by the pump by using a frequency converter to regulate the frequency of the electrical motor. By regulating the frequency of the electrical motor the pump frequency and therewith the created head could be adjusted. The frequency converter was regulated directly by the measuring computer used. The setup is shown in figure H.3.

The velocity variations indeed reduced by applying this setup, with about 30-50% depending on the flume velocity installed. A drawback of applying this method was that the pump discharge was more affected by the clean water basin level. During testing this water level decreases as water is moved from the clean water basin via the flume to the waste water basin. That problem could be sorted out by slowly increasing the frequency of the pump over time.

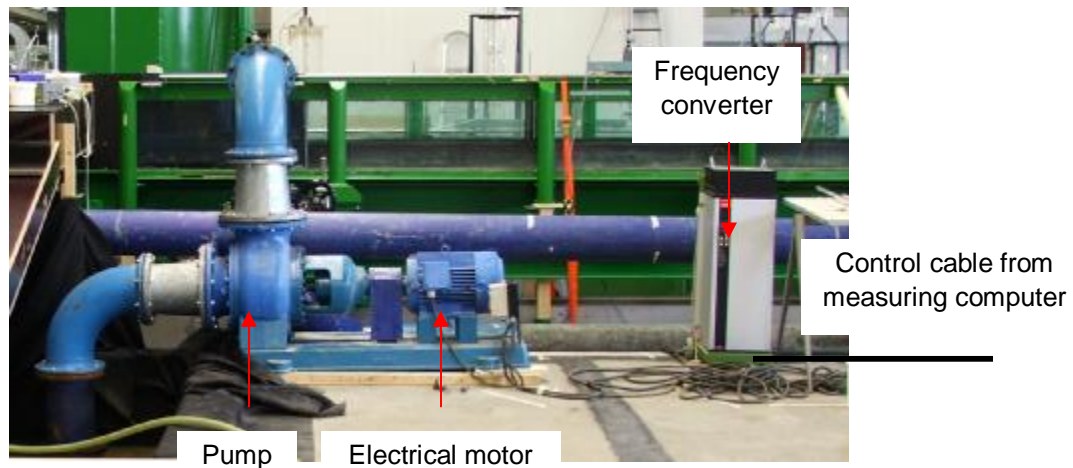


Figure H.3: Setup of pump and frequency converter

#### *H.4 Spectral analysis*

Despite the successful implementation of the frequency converter and the packs of corrugated sheets the velocity variations in the flume velocity are still more than about 15% of the mean velocity, which is more than can be accounted for by turbulence, which is in laboratory flumes usually about 10% (as checked by laser measurements in other flumes).

Analyzing the data gave rise to the idea that variations due to waves or vibrations in one or more frequencies were the cause of the problem. These frequencies might be correlated with the resonance frequency of the flume, resonance of some of the measurement equipment or perhaps the frequency with which the pump is controlled.

The resonance frequency of the flume is determined by its mass and stiffness. Visual observations showed that the resonance frequency for the whole flume during tests was about 4 Hz. To reduce the resonance present either the mass might be increased or the stiffness of the whole construction might be increased. By altering those both the resonance frequency is shifted and the resonance amplitude is reduced (Blaauwendraad, 2006).

For the flume it was thought that it was easier to significantly alter the stiffness than the mass. The stiffness of the tilting flume construction is very low since the flume only stands on eight rollers on metal wedges in order to make it possible to tilt the flume. Furthermore the height of the flume construction is large when compared to its width, which makes the construction vulnerable for lateral movements, especially since most of the mass can be found at considerable height above the foundation.

Since tilting was not used in the experiments, extra supports were supplied to improve the stiffness of the construction. To make sure that the flume was resting on all of these supports, cleats were used to fix all supports. To increase the stiffness of the construction further the flume was pressed down towards its foundation supports by two tension straps. Both measures are shown in figure H.4.

To prevent lateral movements at the top of the flume, lateral support was provided by placing slanting brackets that are well founded. Again cleats were used to make sure these brackets were fixed correctly. The brackets also are shown in figure H.4.

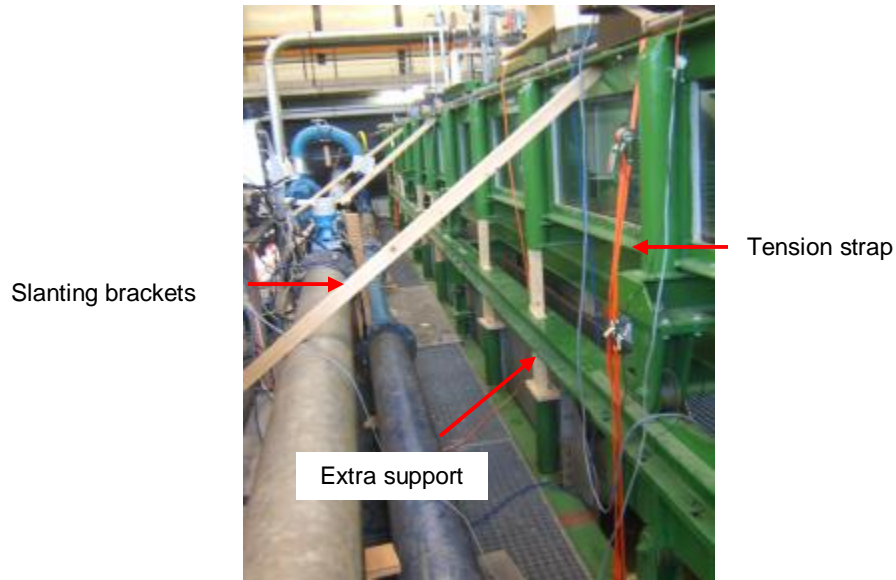


Figure H.4: Measures to increase the stiffness of the flume construction.

To check whether the amendments to the flume construction helped to reduce the velocity variations measured in the flume spectral analysis is carried to see which frequencies were causing the velocity variations and whether these variations are decreased. Two resulting spectra are shown in figure H.5. Despite the scale differences between the two graphs it can be seen that increasing the stiffness indeed had a positive influence on the variations present. Several peaks corresponding to resonance frequencies of the flume diminished in the new situation.

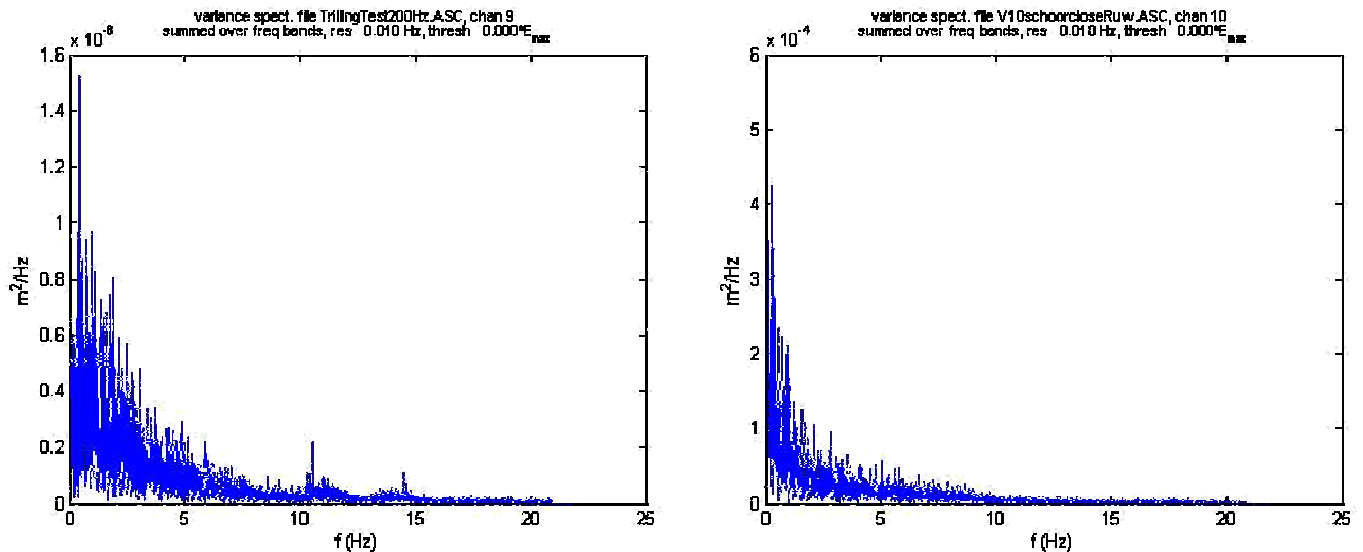


Figure H.5: Spectra of Vectrino signal before and after increasing the stiffness of the flume.

To tackle the resonance of the measurement instruments the stiffness of their attachment to the flume was increased and their weight was increased by placing blocks of concrete and bars of lead. Especially for the Vectrino velocity meter this turned out to be necessary. The resulting setup for the Vectrino apparatus is shown in figure H.6.



Figure H.6: Setup for Vectrino apparatus loaded with concrete blocks and lead bars

The differences in spectrum before and after placing the extra weight are shown in figure H.7. It can be seen that especially for low frequencies the variance is reduced considerable but that in overall the reduction is not significant.

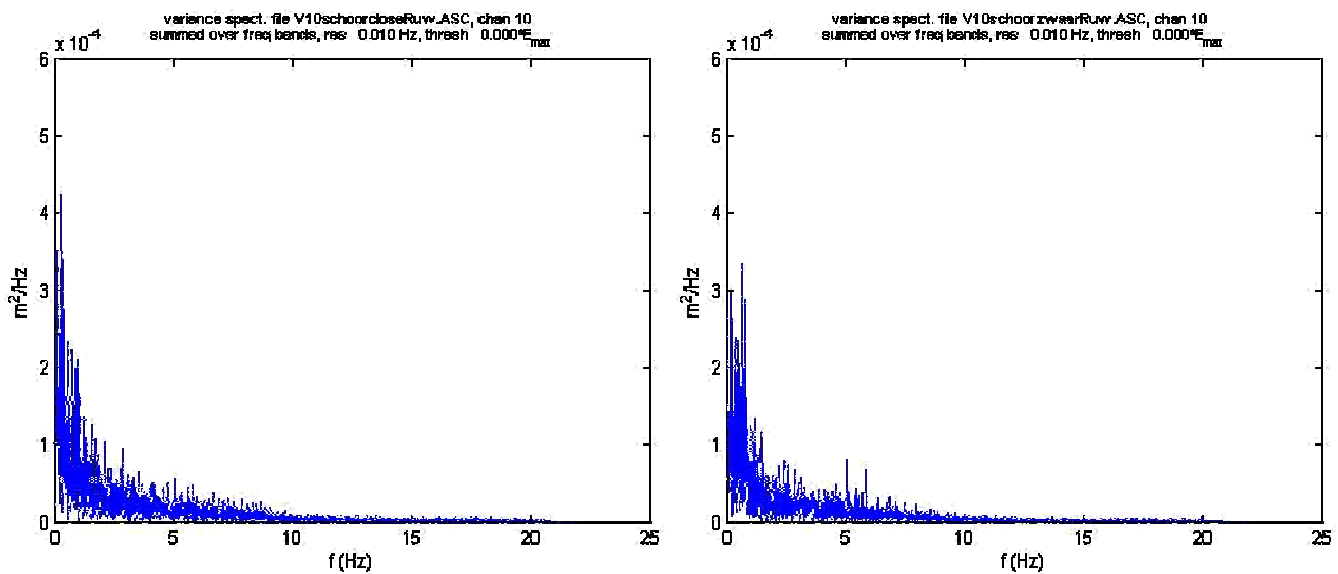


Figure H.7: Spectra of Vectrino signal before and after loading its setup

## H.5 Spectral analysis of turbulence properties

In order to investigate whether the origin of the velocity deviations lay in turbulence properties, the spectrum of the velocity signal can be investigated for obeying the so-called Kolmogorov spectrum law.

Turbulence is known to transfer kinetic energy from large eddies to smaller eddies through non-linear interactions. Finally the smallest eddies lose their energy by viscous dissipation into heat. Kolmogorov hypothesized that at sufficiently high Reynolds numbers, there is a range of high wave numbers where the turbulence is statistically in equilibrium and is determined by dissipation ( $\varepsilon$ ) and viscosity ( $\nu$ ) (Hinze, 1975). This self-similarity in the process allows predicting this part of the spectrum, most commonly referred to as the inertial (sub)range. Kolmogorov stated that the same amount of energy coming into this range (at large scales) should be equal to the amount of energy leaving this range (via dissipation). Since at (infinitively) high Reynolds-numbers the viscosity is not important, the energy at each length scale ( $E(k)$ ) should be depending only on the dissipation ( $\varepsilon$ ). Considering the dimensions of  $E(k)$ , [ $\text{m}^3/\text{s}^2$ ] and  $\varepsilon$ , [ $\text{m}^2/\text{s}^3$ ], the energy distribution in this range is given by (Hinze, 1975):

$$E(k) = a_c \varepsilon^{2/3} k^{-5/3} \quad (\text{H.1})$$

In which  $a_c$  is a dimensionless constant.

To investigate whether the current energy distribution indeed shows this behaviour in the inertial range of the spectrum, it has to be translated from a time (frequency,  $f$ ) scale to a length (wavenumber,  $k$ ) scale. Since the flow has a large mean velocity component in the direction of the flume, the Taylor hypothesis of frozen turbulence might be used, which means that the wave length is directly linked to their timescale via the mean velocity ( $U$ ). For the wavenumber this yields:

$$k = \frac{2\pi f}{U} \quad (\text{H.2})$$

To investigate the Kolmogorov spectrum law, it is convenient to plot the spectrum using logarithmic axis, since then a straight line with  $-5/3$  slope should show up. Any influence of resonance should become visible in single peaks.

For different flume velocities and different measuring devices the  $E(k)$ -spectrum is created on logarithmic scales. As an example figure H.8 shows the spectrum of the Vectrino velocity meter at a flume velocity of 10 cm/s in which the  $-5/3$  law is indicated in black.

For laboratory circumstances, in which the limited length scales for eddies and relatively low Reynolds numbers hinders the development of equilibrium turbulence, the results are quite reasonable. However, large deviations from this  $-5/3$  slope are found beyond wave numbers of about  $10^3$  to  $10^4$ . The corresponding frequencies of those wave numbers are about 25 to 30 Hz, which are the frequencies at which the pump is fed.

Since in this setup a pump is indispensable, it is thought that the velocity deviations in the setup cannot be resolved further. This is most probably only problematic in

detailed analysis of turbulent properties of the flow. As in the experiments proposed those are not needed, the velocity determined is thought sufficiently accurate.

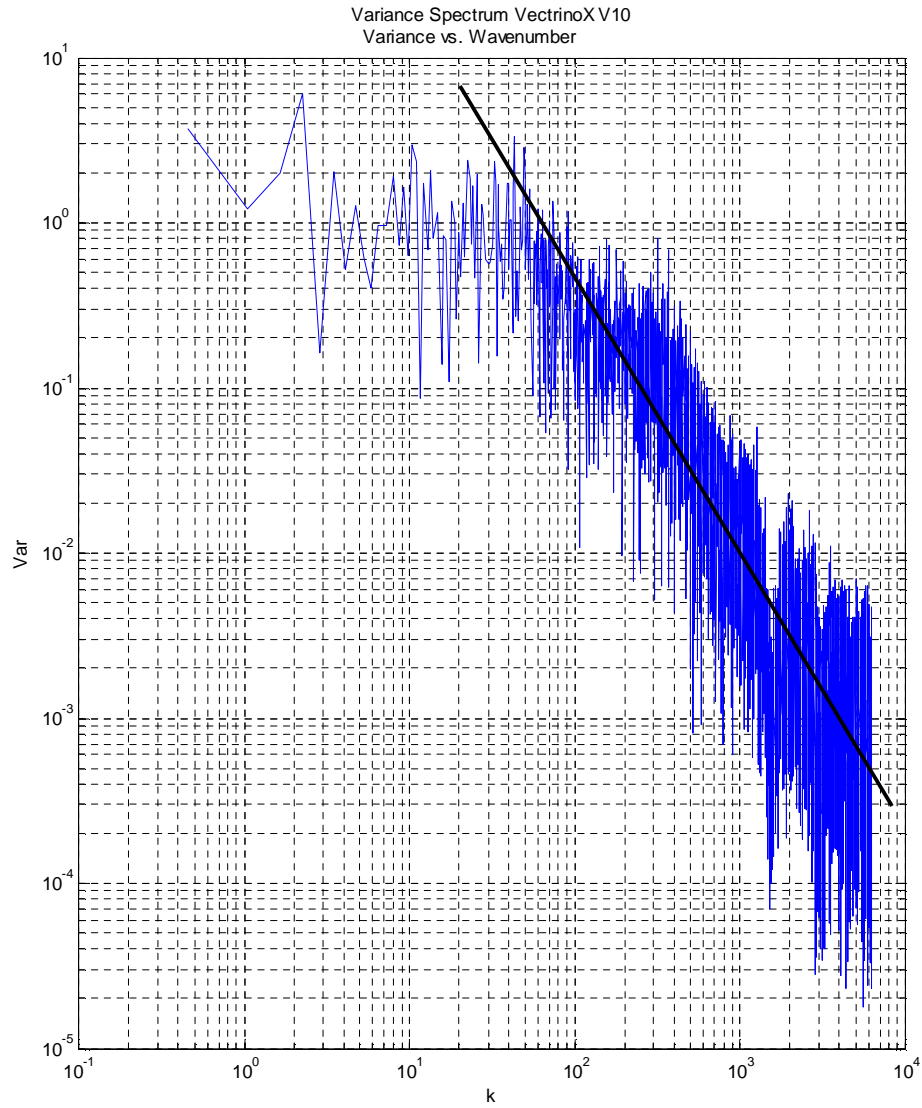


Figure H8: Spectrum for the Vectrino at a flume velocity of 10 cm/s for the investigation of the Kolmogorov spectrum law (shown in black)

## Appendix I: Development history of exp. setup

*In chapter 6 and appendix E the experimental setup to measure stripping was discussed. Before that experimental setup was built, several options and ideas were investigated. Here those ideas are presented chronologically. Also several optimization calculations are presented during the discussion.*

*This appendix is a merger of several documents written during the developments of the experimental setup.*

### *1.1 Principle idea*

The principle was already was already sketched in chapter 4. It is the idea to measure the average concentration difference between the water before the plume and after the plume above the dividing plate. It has to be determined whether and on what scale the experiment has to take place, what the dimensions have to be and what the possible measuring equipment is. Furthermore practical problems expected will steer the development of the experimental setup.

### *1.2 Scale experiment*

The first idea was to build a scale experiment. The scale of the experiment should be large to have less scale problems on the one hand, but should also be small to fit in the flumes of the Fluid Mechanics Laboratory. Looking at the possibilities in the Fluid Mechanics Laboratory, the water depth is the most influencing parameter for the research, but also limited width can become a problem. For the main experiment a Froude scale of 1:50 might be possible in one of the sediment flumes.

Important in scaling is the turbulence level of the flow. That can be checked by calculating the Reynolds numbers.

For an experiment in the sediment flume the velocities are scaled by  $\sqrt{(1/50)}$  and the length scales by  $(1/50)$ . Also the kinematic viscosity is slightly different. This results in a (flume) Reynolds number ranging from  $1.41 \cdot 10^4$  to  $2.47 \cdot 10^5$  with a mean of  $8.49 \cdot 10^4$  and a jet Reynolds number ranging from  $1.70 \cdot 10^3$  to  $2.04 \cdot 10^4$  with a mean of  $8.49 \cdot 10^3$ .

These jet Reynolds numbers are too low, especially at the minimum case. Adjustments should be made to make sure that the minimum case has a  $Re_{jet}$  above 4,000 and the normal case a  $Re_{jet}$  above 10000. Also at the analyzing of the data the low Reynolds number should be bared in mind.

The average concentration of sediment in the water column to be measured by the concentration meters is estimated by determining the amount of solids in the modelled overflow mixture, calculating the amount of mixing that will take place in the flume and estimating the amount of material stripped from the plume.

The amount of sediment in the modelled overflow mixture is as much to make the density difference the same as in the prototype say at the mean value 1055-1025= 30 kg/m<sup>3</sup>. Given that the density of the fines is 2650 kg/m<sup>3</sup> the volume percentage

(v) can be determined by:  $(1-v) * 1000 \text{ kg/m}^3 + v * 2650 \text{ kg/m}^3 = 1030 \text{ kg/m}^3$ . The volume percentage will then be 1.82 %. This means a concentration of 48.2 g/l.

The mixing occurring in the flume will be depending on the ratio of the discharge of the flume over the discharge of the overflow, which is in the mean conditions  $(1.5 * 0.7 * 0.8) / (1 * 1/4 * \pi * 0.06^2) \approx 300$ .

When the stripped material is guessed to be 1-5 % of the overflow mixture this means that 1-5 % of 1.82% will be mixed by a factor 300. This yields a volume percentage of 0.00006-0.0003 %, being 0.0016-0.0080 g/l. This might be too low to be measured, especially since there is no certainty about the figures (especially not on the amount of stripping). If those are a factor of say ten off, the concentration is too low to give accurate measurements.

It is clear that making a scale experiment with scale 1:50 give rise to many problems, not only concerning the magnitude of the involved features but also with the large amounts of water used (and polluted). Furthermore, the large amount of water used makes that the concentrations of the stripped material are very low and immeasurable. To reduce that amount of water, the dimensions of the flume and therewith the scale should be reduced.

However, making the scale smaller to say 1:100, problems will occur with the overflow jet, which will not be turbulent anymore. It might be argued that the demands for scale should be dropped for the overflow jet but that the rest of the experiment will be put to 1:100. This can only be done if it is thought that the diameter of the pipe does not give principal changes to the processes investigated. It is thought that that is the case here, meaning that only the magnitude but not the process of stripping and entrainment is influenced by overflow jet diameters. This assumption implies that when the influence of the diameter on the measured values is determined in this region this influence can be extrapolated to more realistic diameter values.

### *1.3 Distorted scale experiment*

If a 1:100 scale with distortion is adopted, the values assigned to all the parameters can be determined. For the density and the density differences nothing changes, important notice still is the fact that the water in the experiment is fresh and not salt. The velocities are now scaled 1:10 following the square root given by the Froude-scaling. The diameter of the pipe is kept at 1:50 scale, a distortion needed to keep the Reynolds number high enough. The material in the mixture is determined to be kaolinite, since the diameter of this material (1-10  $\mu\text{m}$ ) falls in the range of the proper scaled (via the Stokes fall velocity)  $D_n$ 's. However making a mixture with a defined  $D_{10}$ ,  $D_{50}$  and  $D_{90}$  seems unnecessary since the mixture can be interpreted a single phase fluid.

Segregation effects are, especially when scaled down, of minor importance at least for stripping and entrainment processes. This results in table I.1 showing the mean values for the parameters.

Parameter	Prototype	Experiment	Comments
$\rho$	1025 kg/m <sup>3</sup>	1000 kg/m <sup>3</sup>	fresh water
$\rho_{\text{mix}}$	1060 kg/m <sup>3</sup>	1035 kg/m <sup>3</sup>	density difference equal
$u_{\text{amb}}$	1,5 m/s	0,15 m/s	
$h$	30 m	0,30 m	
$D_{\text{pipe}}$	3 m	0,05 m	distorted to keep turbulent
$u_{\text{jet}}$	1 m/s	0,1 m/s	
$D_{10}$	1-15 $\mu\text{m}$	-	no specific parameter
$D_{50}$	55-85 $\mu\text{m}$	-	no specific parameter
$D_{90}$	105-135 $\mu\text{m}$	-	no specific parameter
$g$	9.81 m/s <sup>2</sup>	9.81 m/s <sup>2</sup>	

Table I.1: Mean values for the parameters to be adopted

The dimensions of the experiment means that it might be possible to do the experiment in a long tilting flume, which has a width of 40 cm and a maximum height of also 40 cm. In order to determine whether the width of the flume is sufficient, the spreading of the plume has to be estimated using earlier investigations by Papanicolaou and List (1988) and Fischer et al. (1979) stating that  $b_w/z$ , in which  $b_w$  is the width of the plume and  $z$  is the length of the trajectory, gives a value of 0,105. The width of the plume is preferably kept lower then 2/3 of the total flume width, being about 25 cm. With a starting width of 6 cm, this means that the trajectory must be smaller than  $19/0,105 \approx 180$  cm. This is more than four times the water depth and is therefore unrealistic. It can safely be stated that before the impact of the plume on the bottom, the width is far sufficient.

The extent of shortcoming of the width at the impact should be checked experimentally. Main concern is the raising up of the plume rests against the side of the flume. Perhaps that problem can be reduced by changing the bottom profile. The effects of that are shown in figure I.1. Trial experiments should look what is necessary, what is possible and what is optimal with this.

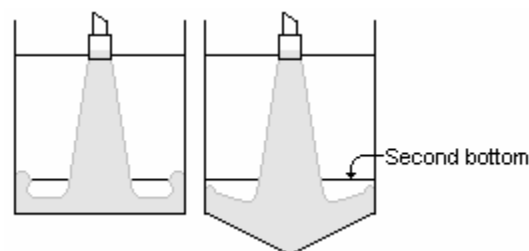


Figure I.1: Possible reduction of the plume raising by changing the bottom profile.

The concentration calculation can now start over again to check whether measurability indeed is improved. The mixing factor is now lowered because of the smaller flume dimensions, so the ratio of the discharge of the flume over the discharge of the overflow, in the mean conditions now becomes  $(1.5 \cdot 0.35 \cdot 0.4) / (1 \cdot 1/4 \cdot \pi \cdot 0.06^2) \approx 75$ . The stripped material can then be estimated to be 1-5% of 1.82% divided by 75 being 0.0002-0.0012%, meaning 0.0064-0.0321

g/l. The improvement of the concentration is a factor 4, originating from the fact that the flume width and height are 2 times smaller, while the amount of material put into the flume is the same, since the overflow dimensions are the same. The concentrations of stripped material now come in a measurable range, even if the amount of stripped material is overestimated.

#### 1.4 Multiple passing

If the concentration after one run would still be insufficient (because for example the amount of stripping is too far less than the expected 1-5%) the possibilities to use the water with stripped material again as an input for the experiment and let this water pass the plume another time. This batch process will require a large buffer. Another option is to design an experimental setup which will allow continuous multiple passing of a plume. The advantage of multiple passing of material is of course that the amount of stripped material becomes so much larger as the number of passing. The experimental setups for both options are sketched in figure 1.2, the top sketch for single passing or batch multiple passing and the lower sketch for continuous multiple passing.

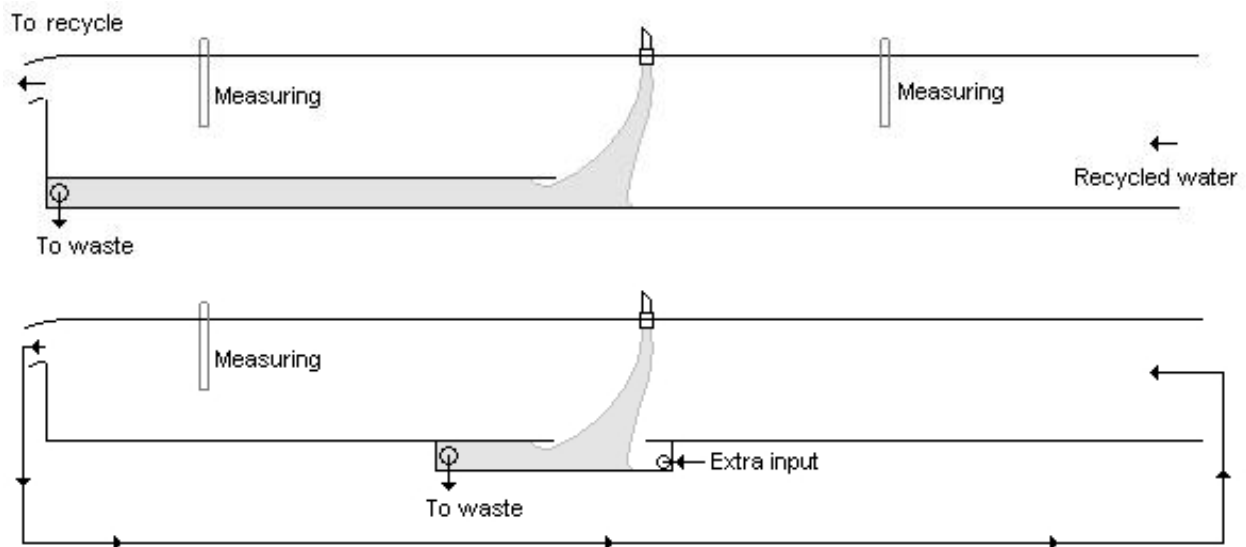


Figure 1.2: Sketches of multiple passing setups

The differences in both options shall be further discussed here. In the single passing or batch multiple passing experimental set up, the waste collecting part will be large (to cope with variations in waste) and will be built in the flume, extending all the way to the flume end. This means that the water coming out of the flume, which can be recycled, is less than the water that came in the flume. Therefore the concentration of material is unknown in the beginning of the experiment, so that concentration should be measured twice: before and after passing the plume, this should both be done at the same (high) accuracy, to make an accurate measure of the difference.

In the continuous multiple passing experiments the water that leaves the flume must re-enter it, so it is not allowed that there is any difference. However, to get rid of the waste material, this should be pumped out. For that reason the waste collecting part

will be put under the flume. The created underlying space should have an extra input to make sure that the amount of water in the flume before and after the plume stays the same. The discharge of this extra input should together with the discharge of the overflow be equal to the discharge to the waste siphon, which is equal to the ambient velocity times the dimensions of the underlying waste collecting space profile. The problems arising from making the extra space under the flume and the design of the extra input system are the reason that in my opinion multiple passing in a batch system is preferable.

In both cases the material that is removed as waste can be re-used as new overflow fluid, after adding some extra kaolinite, or draining of excess water.

The amount of buffer needed can now be estimated. Say that for the measurability it is needed to let the water pass the plume 5 times (to obtain a 5 times larger signal). Furthermore it is conservatively assumed that the second bottom will take away 1/6 of the depth. To be safe it is also thought that each run 10 % of the material is lost by the sampling time differences. The maximum needed run time is 3 minutes, water depth is maximum 40 cm and the velocity is maximum 0.25 m/s.

The amount of water needed for the fifth cycle is  $0.4\text{m} \times 0.4\text{m} \times 0.25\text{m/s} \times 180\text{s} = 7.2\text{m}^3$ , the amount of water in the fourth cycle should then be  $7.2\text{m}^3 \times 1.1 \times 6/5 \approx 9.5\text{m}^3$ . For all cycles, the result is presented in table I.2.

Cycle nr.	Amount needed
5	7,2 m <sup>3</sup>
4	9,5 m <sup>3</sup>
3	12,5 m <sup>3</sup>
2	16,6 m <sup>3</sup>
1	21,8 m <sup>3</sup>

Table I.2: Amount of buffer needed before each cycle

Of course only after the first cycle the material needs to be buffered, so about 17 m<sup>3</sup> is the maximum volume of buffer needed. Of course, when fewer cycles can be carried the volume of buffer goes down, following the figures in table C.2. Creating more than 5 cycles is highly unfavourable. On the other hand lower second bottom placement, smaller water depth and smaller water velocity as well as shorter measurement time will lower the volume of buffer needed.

### 1.5 Measurement equipment

In the setup two concentration measurement points are to be placed, the first one before passing the plume, the other one after the passing of the plume above the dividing plate. Furthermore during the runs the width of the plume will be measured by in situ measurements of the density profile

The idea of the measuring points in the flume is to measure the average concentration of the water flowing through that profile. Since concentration measuring devices are usually not made to measure whole profiles, but to measure points, it is wise to measure the concentration at several points (at several depths) simultaneously and to interpolate the value of the concentration of the whole profile.

For that reason it is thought that at each measuring point, three measuring devices will be installed, one close to the bottom, one close to the water surface and one exactly in between.

The accuracy of the concentration measuring devices needed follows from the concentration calculations made above. When devices are present that can accurately measure concentrations in the range from 0,0050 to 0,1000 g/l with an accuracy of say 0,5-1 mg/l it is thought that the experiment can be carried out in a single run, although it is not sure that this is the correct range. If less accurate measuring devices are available, the use of (up to five) cycles can increase the workability to concentrations in the range of 0,030 to 0,500 g/l with an accuracy need of about 2,5-5 mg/l.

The exact placement in the trajectory is another point of discussion. The first measuring point is quite easy since it should be placed as close to the plume, but far enough upstream that anything concerned with the plume (equipment, measuring devices for plume width, camera views) is not hindered. This is done to be sure that the incoming water is well mixed and that the circumstances that are going into the plume are correctly reproduced by the measurements. For the second measuring point it is more difficult. At one hand one should opt that the device should be placed as close to the plume as possible, to directly measure what is coming from the plume, so that the values reproduce exactly what is happening. On the other hand, the patchiness of the stripping that is expected, do not allow for taking measurements if only three points are measured. This patchiness needs to be dissolved and mixed a bit before three point measurements will reproduce profile measurements, to maximize this a place to the far end of the flume is better. One should however not measure too close to the end since there the flow pattern is not longer homogeneous. Since it is thought that this mixing is most important, the measuring point is placed near the end of the flume.

For the measurements of the width of the plume at different heights (to measure entrainment) it is thought to measure the profile of the plume by moving an OSLIM concentration meter through the plume. It should however be checked that this OSLIM meter does not influence the stripping of the plume. In that case there are also possibilities to determine the width of the plume visually or by using camera.

## 1.6 Buffer problems

The need for the normal water buffer should be further investigated since the buffer volume is limited and it is not possible to build a larger buffer. The need for the normal water buffer originated from the batch process for multiple passing. However, since the continuous approach is adopted, this is no longer valid. Also the need for a normal water buffer when no multiple passing is necessary is unclear: if the concentration differences are measurable it is unnecessary to have a large buffer.

The only reason that a normal buffer is still needed is the fact that part of the water that went into the experiment does not come out as clean water, but as waste water. The amount of water lost was estimated before to be 0.009 m<sup>3</sup>/s, but for safety and ease it is said that it is 10 l/s. This means that the amount of buffer needed is only depending on the time that one measurement set can take place, or in case of multiple passing the time needed for say 5 or 10 passings of the plume.

As said the material that is needed to buffer in the beginning will be dumped in the waste water buffer afterwards, so it should also be checked that that one is large enough.

To determine the time needed a detailed investigation of a run should take place, especially focusing on the time needed.

For each item of a run the time needed and the comments for both buffers are gathered in the table I.3.

Nr.	Item	Time	Comments
1	Filling flume	5 minutes	Either clean water from the system or water from the normal buffer
2	Starting flume	5 minutes	In the time the velocity profiles are build up no losses are made
3	Waste starts	2 minutes	Clean water is wasted to establish the straight stream lines around the beginning of the dividing plate
4	Overflow starts	0.5 minute	Some time is needed to make sure the overflow plume goes under the second bottom
5	Measuring time	3 minutes	With a sampling time of 3 seconds, 60 samples can be made during the measurement cycle
6	Overflow stops	1.5 minute	Instantaneous stop, but some time needed to measure the overflow plume dimensions
7	Waste stops	3 minutes	Only after all plume rests are wasted the waste can stop, so this is travelling time for plume rests
8	Measuring devices off	instant	
9	Flume off	instant	
10	Emptying flume	5 minutes	Emptying the flume means top water to normal buffer, low water to waste water buffer

Table I.3: Time needed for several items in a measurement run.

This means that the time water is taken out of the normal water system into the waste water system is about 10 minutes. So in this time  $600 \text{ s} * 10 \text{ l/s} = 6000 \text{ l}$  is taken away in a measurement were the differences can be measured, so when no multiple passing is needed. This will only just fit in the largest normal buffer possible, since for pumping there is always a layer of water in the buffer needed.

When multiple passing is needed the cycle time of a water particle through the experimental setup becomes important. The velocity in the pipe to the flume is estimated to be the same as the flume velocity and the length is also estimated to be equal: 15 m. The velocity back to the buffer from the flume is estimated at 0.10 m/s and that distance is said to be 5 meters maximum.

The corresponding cycle times can then be calculated. From that the time needed for a measurement with 5 passings and the time needed for a 10 passings experiment are calculated from that, since the cycle time replaces the measurement time from the table above. For each velocity the value of lost material is also different, so the amount of buffer needed for 5 and 10 cycle experiment differs per flume velocity. The results of all these calculations are given in table I.4.

Flume velocity	Cycle time	5 passing time	10 passing time	Waste discharge	5 passing waste	10 passing waste
0.05 m/s	650 s	3670 s	6920 s	0.003 m <sup>3</sup> /s	11.01 m <sup>3</sup>	20.76 m <sup>3</sup>
0.10 m/s	350 s	2170 s	3920 s	0.006 m <sup>3</sup> /s	13.02 m <sup>3</sup>	23.52 m <sup>3</sup>
0.15 m/s	250 s	1670 s	2920 s	0.009 m <sup>3</sup> /s	15.03 m <sup>3</sup>	26.28 m <sup>3</sup>

Table I.4: Calculation of buffer need.

Again it becomes clear that 10 times passing is highly unfavourable, but also the 5 times passing figures are problematic for the normal water buffer. The waste water buffer, being 6 m \* 5 m \* 0.55 m = 16.5 m<sup>3</sup> can just handle this. The conclusion is that when multiple passing stays problematic from the point of view of buffering. When needed solutions might be found in continuously adding clean water to the normal water buffer with a given discharge.

The conclusion is that the large buffer option should be build and that all possibilities to increase the buffer, or decrease the buffer need should be investigated. It is thought that with this buffer capacity the experiment could be carried although the margins are small.

Furthermore it can be concluded that the buffer capacity might become problematic: only two experiments can be carried out in a row and then the waste water buffer is nearly full. However, in a full waste water buffer it takes 46 hours for the material to settle out. This would mean that after doing 2 experiments the campaign has to be halted for two days. Since a lot of measurements has to be carried out this is unacceptable.

However if this is not successful enough it is wise to create another waste water buffer of about the same size. That will mean that measurements can take place every other day, leaving the in between time to clean up the setup and to do investigate the results.

It is needed to already start to investigate where this buffer (or separate buffers) might be placed so that when necessary quick action can be taken to build them.

## Appendix J: Course of experiments

*In chapter 7 and chapter 10 it was mentioned that the experiments that were carried out had not followed the measuring plan. In these chapter a list is given of the tests that are carried out. This appendix describes how the experiments got round to that. First the course of the stripping experiments is treated, followed by the course of the vortex divergence experiments*

### *J.1 Course of the stripping experiments*

As indicated in the measuring plan the first test that was carried out was the 'base case'. The plume looked as shown in figure J.1. It was impossible to lift the pipe further to increase the water depth used, since then large parts of the plume would pass above the dividing plate.



Figure J.1: Base case plume in experimental flume.

Apparently the velocity scale is not strong enough to make the plume passive, but the trajectory of the plume edge is near horizontal. As a result, the descent of the plume takes a long time in which the plume dilutes. This makes the available width of the flume insufficient. This means that at relatively high velocity scales (but still showing dynamic plumes) the experimental setup does not operate properly.

As a solution, the flume velocity was halved, to make sure that the plume starts more vertical. This did not provide sufficient improvements, since the bending of the plume took place very soon. For that reason the density of the material was also increased. The resulting plume was no longer bent over too soon and steadily sank to the bottom. However in this configuration too much material was discharged in the flume and a density current could establish over the bottom travelling in the opposite direction of the flume velocity. Since that density current was constantly eroding, the dividing plate was of no more use (See figure J.2). It can be concluded that the amount of material discharged had to be reduced.



Figure J.2: Plume with halved flume velocity and increased density.

To reduce the amount of discharged material the smallest pipe present with a diameter of 3 cm was used. Since the reduction of discharged material was too small another pipe, with even a smaller diameter of 1.2 cm, was built. Using that pipe was a real improvement and the experiment did almost function correctly. That can be seen in figure J.3 which shows the initial phase of that plume.



Figure J.3: Initial phase of small plume

What also can be seen in figure J.3 is that the bottom impingement of the plume generates a circulation. Near-bottom water is pushed radially outwards, impinges the glass plate and moves further upwards. That is the reason that the woollen strings that indicate the streamlines near the glass plates not inline with horizontal flow in figure J.3. This circulation eventually causes that material moves above the false bottom. That process is indicated in figure J.4.

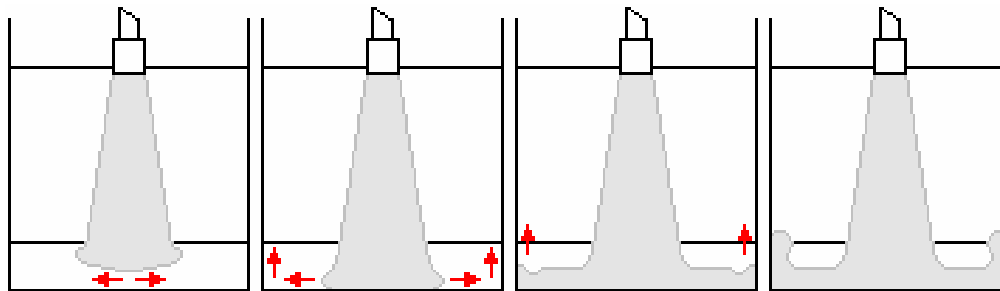


Figure J.4: Circulation process in the cross-section of the flume

Several adjustments to the flume and jet velocity and density of the overflow material could not prevent that either this circulation process or the strong bending of the plume was hindering the functioning of the setup. If this problem had to be resolved some major changes would have to be implemented in the setup.

On the other hand, observations and measurements near the plumes up to this point did not yield a significant concentration increase close to the near-vertical descent phase of the dynamic plume. There does not seem to be any stripping. The study of those results and the discussion of them are put forward in chapters 7 and 8. The measurements were put to a hold, and later several tests were carried out that specifically focussed on enhancing stripping by making the density of the material and the vertical velocity discontinuous. Furthermore the overflow pipe was shaken and moved to create extra stripping.

To conclude this paragraph all tests that are carried out in the experimental setup are listed in table J.1 and presented in the  $Ri$ - $\zeta$  diagram in figure J.5.

Run nr	$\rho$ ( $kg/m^3$ )	$D$ ( $m$ )	$W$ ( $m/s$ )	$U$ ( $m/s$ )	Comments	$Ri$ (-)	$\zeta$ (-)
1	1035	0.05	0.11	0.10	Base case (fig 5.6)	1.42	0.91
2	1050	0.05	0.11	0.05	Velocity halved, density increased	2.03	0.45
3	1050	0.04	0.11	0.05	As (2) but smaller pipe (fig 5.7)	1.62	0.45
4	1050	0.03	0.11	0.05	Smallest pipe used	1.22	0.45
5	1050	0.012	0.11	0.05	New smaller pipe made (fig 5.8)	0.49	0.45
6	1030 – 1070	0.012	0.10 – 0.15	0.04 – 0.10	Trying to stop circulation	0.30 – 0.80	0.25 – 1.00
7	varying	0.01	varying	0.05	Varying input to stimulate stripping	-	-

Table J.1: Parameter values of the stripping tests that are carried out with comments

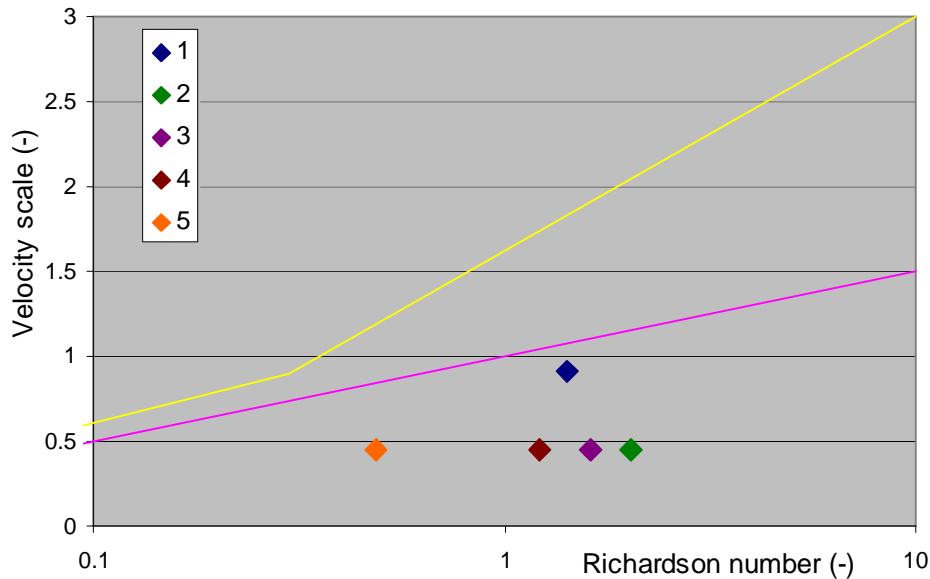


Figure J.5: Stripping tests carried out presented in  $Ri$ - $\zeta$  diagram

### J.2 Course of the vortex divergence experiments

In three weeks time, three cross profile of 15 plumes had to be measured. After the first few measurements it was shown that this measuring of 3 profiles per day would be the maximum measuring rate, not the normal. It was thought to stick to measuring 3 profiles per plume and to see for every week how much plumes could be measured. Several practical problems as well as the two day closure of the laboratory due to Ascension Day caused that in the end only 1 plume was indeed measured three times, 1 plume was measured 2 times and another plume was measured 1 time. They are listed below in table J.2.

Test nr	Number of profiles	$\rho$ ( $kg/m^3$ )	$D$ (m)	$W$ (m/s)	$U$ (m/s)	$Ri$ (-)	$\zeta$ (-)
1	1	1040	0.01	0.05	0.04	1.57	0.80
2	3	1050	0.01	0.05	0.04	1.96	0.80
3	2	1050	0.01	0.05	0.05	1.96	1.00

Table J.2: Vortex bifurcation tests carried out

The practical problems causing this pitiful result are the observed saturation effects of the OPCON concentration meter, problems with the pump intake and irregularity of the siphon discharge followed by the breakdown of the siphons. Each of these problems is shortly discussed next.

#### Saturation effects of the OPCON concentration meter

During the first week of measurements it was observed that the OPCON concentration meter had limitations to the concentration to be measured and that these limitations were exceeded in the first few measurements. Finding the correct settings of the OPCON to overcome this problem took several days, and all

intermediate measurements turned out to be useless. Finally the correct settings were achieved and one correct profile of the plume investigated in this week was obtained.

In Appendix F, part F.5 saturation of the OPCON concentration meter is described in further detail.

#### **Pump intake problems**

After the first week, the pump used in the experimental setup was needed for three weeks in the setup of another student. After these weeks, the pump was put back in place, but the intake pipe was altered. This showed up during the first test of the day. Adjusting the intake took half a day and as a result, only half a profile could be measured that day.

#### **Siphon problems**

During the third week, when the third profile of the third plume was measured, the siphon started to discharge a smaller amount of material. Normally, flushing the siphon for some time ensures that the amount of material discharged is constant, but this time extensive flushing did not help in getting the discharge back to a 'normal' rate. For that reason the siphon was disassembled and cleaned. After assembling the discharge rate was different, but still smaller than normal.

What the siphon discharge rate was was unknown now. It was thought best not to use the siphon further before it was newly calibrated. There was however no time available to carry out a new calibration.

After that the smaller siphon with a diameter of 0.4 cm was used, but during the first test series the connection between the hose and the ship broke down. Repair was thought of, but that required the installation of a new connection between hose and ship. If that connection had to be installed, the siphon had to be recalibrated.

Since there was no time available for siphon calibration, the experiments were stopped completely.

## Appendix K: Raw results of vortex divergence exp.

In chapter 10, the results of the vortex divergence experiments are discussed. In paragraph 10.2 the processed results are presented. Here the unprocessed results are shown and the processing method is shortly discussed.

### Presentation of unprocessed results

The tests which have been carried out with the experimental setup to measure vortex bifurcation are listed in table 10.1 in chapter 10. Here that table is repeated as table L.1 in summarized form. Also the figures of the raw results that are associated with the profiles are indicated.

Test nr	Profile nr	Distance from orifice	$\rho$	$D$	$W$	$U$	Figure nr
1	1	25 cm	1040	0.01	0.05	0.04	L.1
2	1	25 cm	1050	0.01	0.05	0.04	L.2
2	2	41 cm	1050	0.01	0.05	0.04	L.3
2	3	54 cm	1050	0.01	0.05	0.04	L.4
3	1	25 cm	1050	0.01	0.05	0.05	L.5
3	2	42 cm	1050	0.01	0.05	0.05	L.6

Table K.1: Information on different profiles measured

↓Z X→	16	18	20	22	24
28	0.000	0.000	0.000	0.000	0.000
26	0.168	1.180	0.794	0.700	0.682
24	1.032	1.207	0.713	1.322	1.198
22	1.561	1.421	1.132	1.350	1.168
20	0.805	1.470	1.164	1.175	0.552
18	0.115	0.640	1.057	0.652	0.009

Measurement

Distance from orifice: 25 cm.

Averaging time: ± 12.5 s

Total amount of material measured: 97 mg/cm

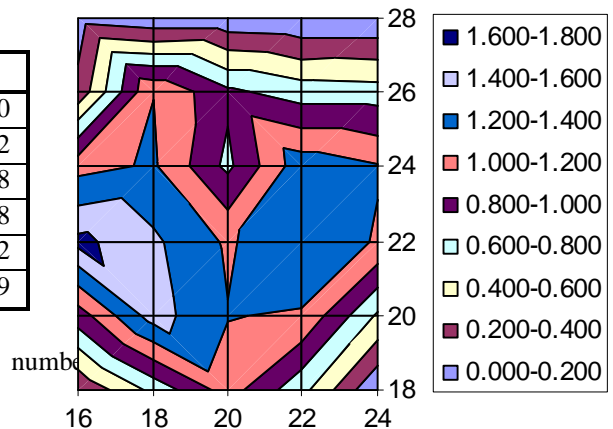
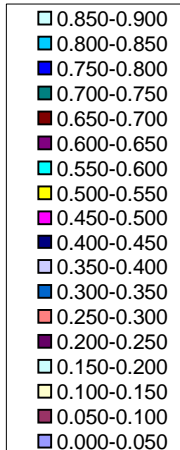
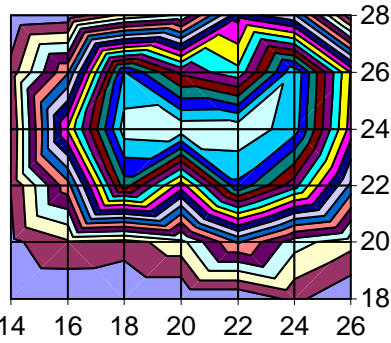


Figure K.1: Unprocessed results measurement 1.1

↓Z X→	14	16	18	20	22	24	26
18	0,000	0,000	0,000	0,000	0,000	0,064	0,000
20	0,037	0,094	0,075	0,133	0,306	0,170	0,119
22	0,052	0,280	0,725	0,472	0,789	0,618	0,337
24	0,050	0,506	0,875	0,884	0,888	0,823	0,476
26	0,072	0,295	0,803	0,637	0,565	0,840	0,496
28	0,000	0,016	0,115	0,157	0,432	0,356	0,014
30				0,007			



Measurement

number: 14 16 18 20 22 24 26

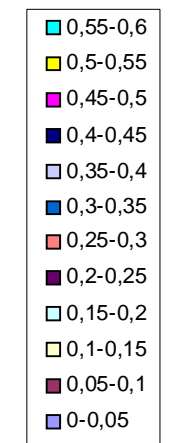
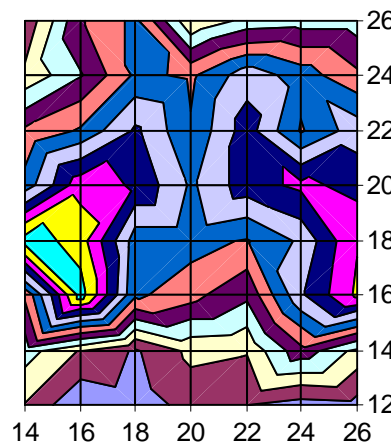
Distance from orifice: 25 cm.

Averaging time: ± 11 s

Total amount of material measured: 56 mg/cm

Figure K.2: Unprocessed results measurement 2.1

↓Z X→	14	16	18	20	22	24	26
12	0,096	0,006	0,024	0,067	0,052	0,023	0,029
14	0,171	0,096	0,043	0,113	0,104	0,232	0,135
16	0,26	0,573	0,311	0,268	0,209	0,392	0,509
18	0,581	0,527	0,322	0,321	0,295	0,361	0,496
20	0,32	0,485	0,442	0,342	0,426	0,462	0,433
22	0,26	0,307	0,409	0,305	0,426	0,293	0,378
24	0,111	0,196	0,312	0,291	0,378	0,327	0,26
26	0,061	0,245	0,313	0,1	0,165	0,173	0,172



Measurement

number:

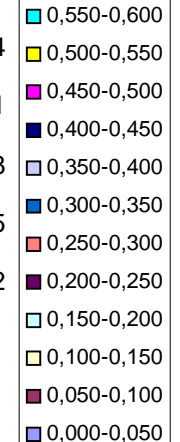
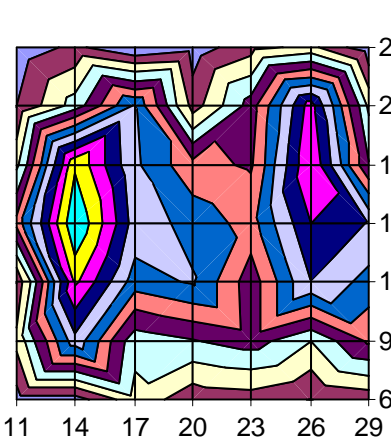
Distance from orifice: 40 cm.

Averaging time: ± 13 s

Total amount of material measured: 60 mg/cm

Figure K.3: Unprocessed results measurement 2.2

↓Z X→	11	14	17	20	23	26	29
6	0,031	0,025	0,134	0,067	0,072	0,049	0,071
9	0,115	0,384	0,167	0,196	0,224	0,150	0,259
12	0,048	0,508	0,326	0,356	0,221	0,400	0,331
15	0,268	0,600	0,383	0,330	0,281	0,450	0,396
18	0,138	0,541	0,359	0,266	0,244	0,500	0,204
21	0,049	0,173	0,354	0,077	0,224	0,475	0,141
24	0,017	0,063	0,001	0,026	0,080	0,117	0,012



Measurement

number:

Distance from orifice: 54 cm.

Averaging time: ± 15 s

Total amount of material measured: 98 mg/cm

Figure K.4: Unprocessed results measurement 2.3

↓Z X→	16	18	20	22	24	26
30	0,246	0,243	0,208	0,438	0,302	0,141
28	0,332	0,316	0,538	1,022	0,568	0,401
26	0,795	0,282	0,832	0,923	0,595	0,454
24	0,257	0,24	0,681	0,82	0,723	0,789
22	0,178	0,854	0,561	0,475	0,775	0,701
20	0,026	0,248	0,415	0,148	0,134	0,292
18	0,025	0,022	0,072	0,033	0,039	0,027

Measurement  
 Distance from orifice: 25 cm  
 Averaging time: ± 10 s  
 Total amount of material measured: 68 mg/cm

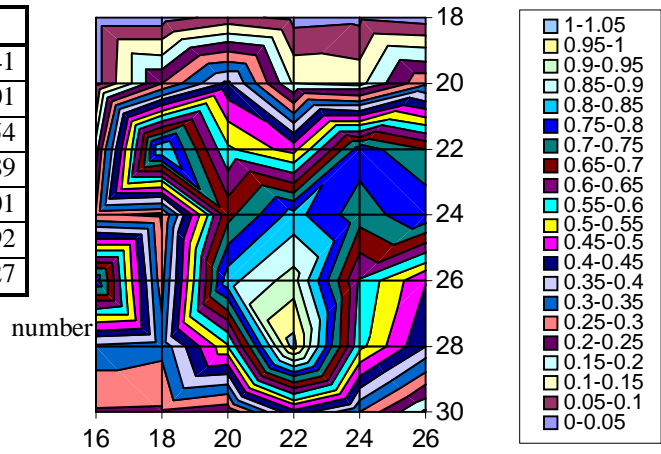


Figure K.5: Unprocessed results measurement 3.1

↓Z X→	12,5	15	17,5	20	22,5	25	27,5
12,5	0	0,158	0,338	0,165	0,38	0,103	0,119
15	0,101	0,24	0,574	0,642	0,515	0,167	0,408
17,5	0,158	0,424	0,615	0,674	0,507	0,275	0,384
20	0,147	0,335	0,551	0,533	0,497	0,317	0,515
22,5	0,088	0,442	0,476	0,346	0,346	0,506	0,431
25	0,056	0,221	0,281	0,051	0,065	0,26	0,154
27,5	0,056	0,067	0,051	0,041	0,089	0,045	0,046

Measurement  
 Distance from orifice: 48 cm  
 Averaging time: ± 12 s  
 Total amount of material measured: 87 mg/cm

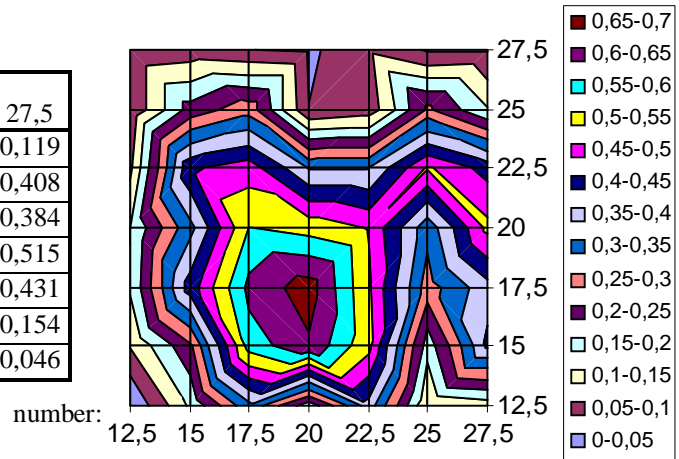


Figure K.6: Unprocessed results measurement 3.2

**Comments on the measurement results**

In the unprocessed results shown in the previous part do show several familiarities but also have striking differences.

In all profiles the counter-rotating vortex pair (CVP) can be seen. In measurements 3.2 and 3.3 the CVP is not totally crystallized, probably due to insufficient averaging time, but also here it is clearly seen that the concentration profile is not Gaussian-like. On the exact shape of the CVP and the mean and maximum concentrations in it cannot be said very much with this limited data set available. It is striking that the (time-averaged) concentration peaks observed here vary widely in concentration from 0.5 g/l to 1.6 g/l. However, from the indication of the total amount of material in the cross profile follows that this might also follow from the ‘incorrectness’ of the plume. Especially the variation between plume number 1 (measurement 1.1) and plume number 2 (measurement 2.1 and 2.2) can be fully accounted to that effect.

**Processing of the measurement results**

For the further analysis presented in chapter 10, each plume cross-profile was shown with respect to the flume. Furthermore notoriously bad data points were kept out of the analysis. Sometimes extra data points had to be imposed at the edge of the plume to make the picture more complete and to prevent steep the formation of steep slopes. For example in measurement 2.2 some data points in column 28 had to be estimated. Finally averaging took place using a smoothing, least curvature averaging function used in SURFER software.

**Peak levelling procedure**

In measurements 3.1 and 3.2 strange peaks were occurring. These peaks were due to insufficient averaging time. Because that time is insufficient very high and very low values are too dominant in the determination of the average concentration. By taking different averaging periods within the maximum period available the variation of the average values could be determined. Based on that variation a new value is imposed. Best examples are point (18,26) and (18,24) which have typically low values points because of the inclusion of several zero values in the beginning and end of the measuring period. If those are removed the profile is smoothed as can be seen in figure 10.5.

## Appendix L: CORMIX input data

In chapter 11, the results of the CORMIX model are presented. In paragraph 11.1 it is stated that the parameter values of the laboratory situation are put into the CORMIX model. The three varied parameters are specified for every plume. Here all the input parameters used in the experiment are listed in table L.1.

AMBIENT PARAMETERS:	
Cross-section	= bounded
Width	BS = 0.4 m
Channel regularity	ICHREG = 1
Ambient flowrate	QA = 0.01 m <sup>3</sup> /s
Average depth	HA = 0.4 m
Depth at discharge	HD = 0.4 m
Ambient velocity	UA = 0.04 m/s      0.05 m/s
Darcy-Weisbach friction factor	F = 0.0106
Calculated from Manning's n	= 0.01
Wind velocity	UW = 0 m/s
Stratification Type	STRCND = U
Surface density	RHOAS = 1000 kg/m <sup>3</sup>
Bottom density	RHOAB = 1000 kg/m <sup>3</sup>
DISCHARGE PARAMETERS: Single Port Discharge	
Nearest bank	= left
Distance to bank	DISTB = 0.2 m
Port diameter	D0 = 0.01 m
Port cross-sectional area	A0 = 0.0001 m <sup>2</sup>
Discharge velocity	U0 = 0.05 m/s
Discharge flowrate	Q0 = 0.000004 m <sup>3</sup> /s
Discharge port height	H0 = 0.38 m
Vertical discharge angle	THETA = -90 deg
Horizontal discharge angle	SIGMA = 0 deg
Discharge density	RHO0 = 1040 kg/m <sup>3</sup> 1050 kg/m <sup>3</sup>
Density difference	DRHO = -40 kg/m <sup>3</sup>
Buoyant acceleration	GP0 = -0.3923 m/s <sup>2</sup>
Discharge concentration	C0 = 40000 mg/l      50000 mg/l
Surface heat exchange coeff.	KS = 0 m/s
Coefficient of decay	KD = 0 /s

Table L.1: All input parameters used in the CORMIX model

## Appendix M: Head fall calculation waste water pipe

In Appendix E, part E.1.3 it is said that the waste water pipe is driven by the head fall over the pipe. Whether the available head fall would be sufficient the wanted discharges is calculated here.

The head fall needed in a pipe is given by:

$$\Delta h_{needed} = \left( \frac{l}{L} + \xi_{in} + \xi_{curve} + \xi_{vertical} + \xi_{tap} + 1 \right) \frac{u^2}{2g} \quad (J-1)$$

In which  $\lambda$  is the roughness factor and  $\xi_{in}$ ,  $\xi_{curve}$ ,  $\xi_{vertical}$  and  $\xi_{tap}$  are hindrance coefficients,  $L$  is the length of the pipe and  $u$  is the velocity in the pipe.

To determine  $u$  the maximum discharge is determined to be  $0.15 \text{ m/s} * 0.15 \text{ m} * 0.4 \text{ m} = 0.009 \text{ m}^3/\text{s}$ . The pipe should thus be dimensioned to discharge at least 15 l/s, to have quite some spare capacity. The pipe diameter is to be chosen, based on availability in the laboratory and the head fall created. The Re-number becomes  $7.07 * 10^4$ , so the flow is highly turbulent, and it is said that the flow is hydraulic rough. The roughness factor  $\lambda$  is determined iteratively using the formula of Colebrook and White to be 0.020 using of pipe material roughness ( $k$ ) of 0.25 for steal pipes. The length of the pipe is estimated to be 15 m (along the flume) + 10 m (along the pathway) + 5 m (extra safety) = 30 m.

The hindrance coefficients are determined using the recommendations by Battjes (2002). The entry coefficient  $\xi_{in}$  is estimated to be 1, since the entry is not only straight (meaning a coefficient of 0.5) but also perpendicular to the flow direction. The two curves of ninety degrees each have a hindrance coefficient  $\xi_{curve}$  of 1.265. The curvature from the vertical inlet to the horizontal pipe has an estimated hindrance coefficient  $\xi_{vertical}$  of also 1.265. Finally the tap hindrance coefficient is more difficult to prescribe but is estimated to be 1.9.

Imposing these parameter values table M.1 is produced presenting the head fall for different pipe diameters possible.

Pipe diameter (mm)	Head fall (m)
120	1.15
150	0.43
180	0.20
200	0.13
250	0.05
280	0.03

Table M.1: Head fall for different pipe diameters possible

The available height difference is about 0.5 m, so up to pipe with a diameter of 150 mm no problems are expected.

---

Finally the decision was taken to implement a pipe of 280 mm, which is the same as the incoming water pipe. For the discharge measurement, the pipe had to be decreased locally in diameter, in order to obtain a velocity high enough to guarantee correct working of the discharge meter. This imposed some extra head fall, but since the head loss calculated was far from the available height difference, this was not thought to raise any problems.

## Appendix N: OPCON calibration curves

In appendix F, part F.5 the calibration of the OPCON concentration meters is discussed. Here all the calibration curves of the OPCON are presented. First the calibrations for the stripping experiments are presented, followed by the calibrations for the vortex divergence experiment.

### Stripping experiment

In the stripping experiment 2 OPCON concentration meters were used. Before the experiments started the main calibration was carried out for each of them. During the test series the meters have been re-calibrated twice in order to check the calibration line for shifting. Before each of those re-calibrations, the zero of the instrument was changed.

The main calibrations are presented in figure N.1 and N.2 for OPCON1 and OPCON2 respectively. After that figure N.3 and N.4 present the re-calibrations of OPCON1 and figure N.5 and N.6 present the re-calibrations of OPCON2.

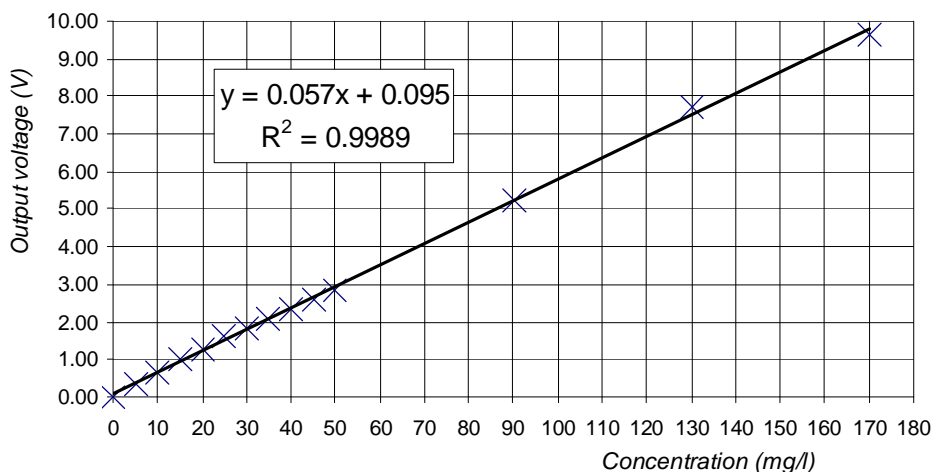


Figure N.1: Main calibration OPCON1\

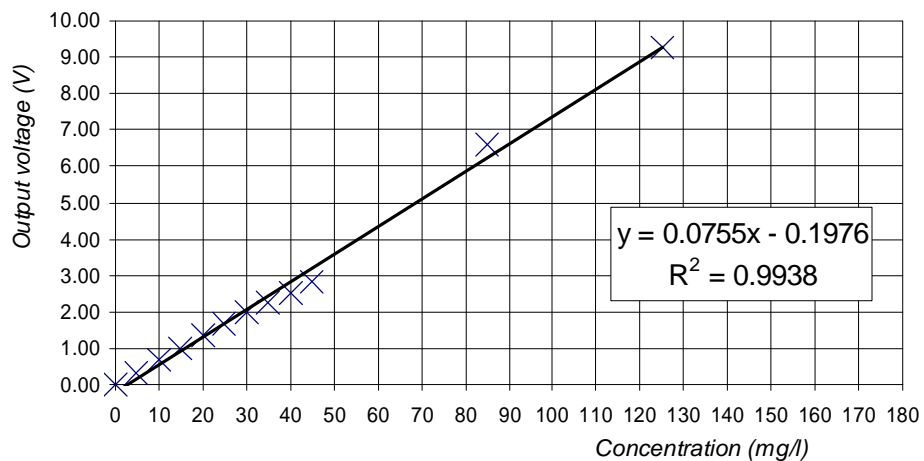


Figure N.2: Main calibration OPCON2

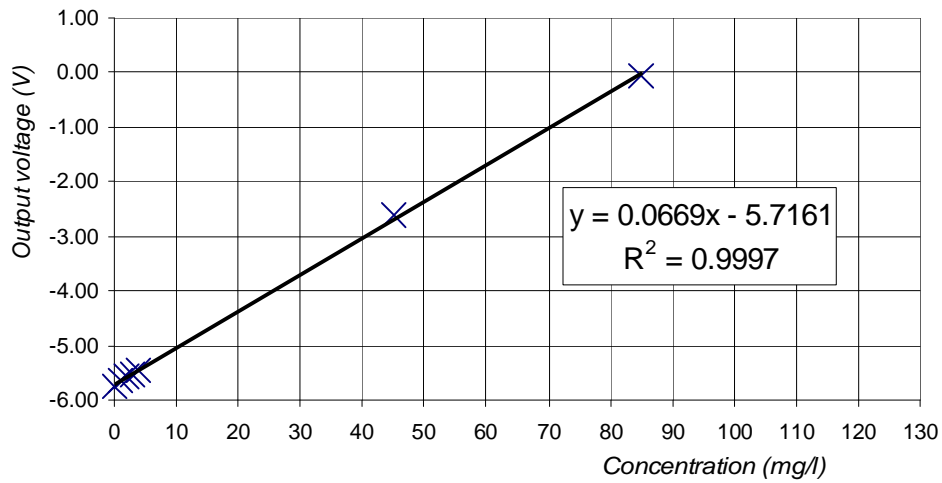


Figure N.3: First re-calibration OPCON1

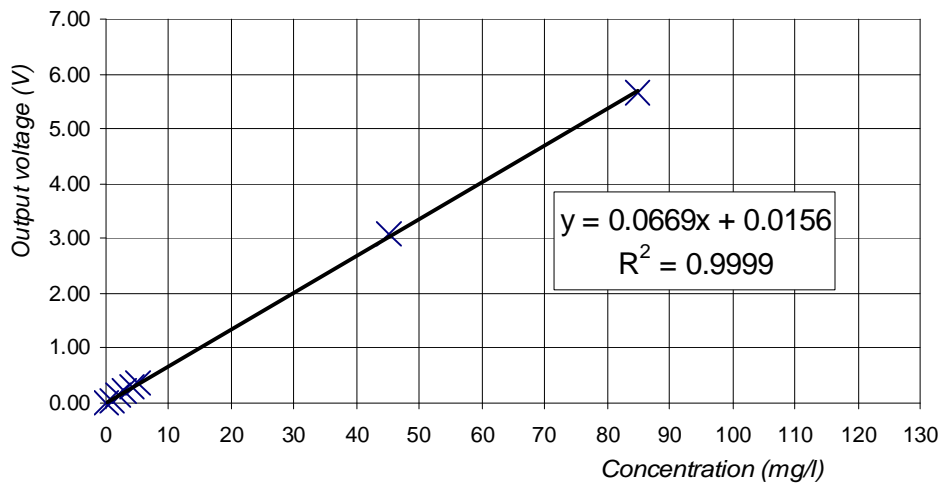


Figure N.4: Second re-calibration OPCON1

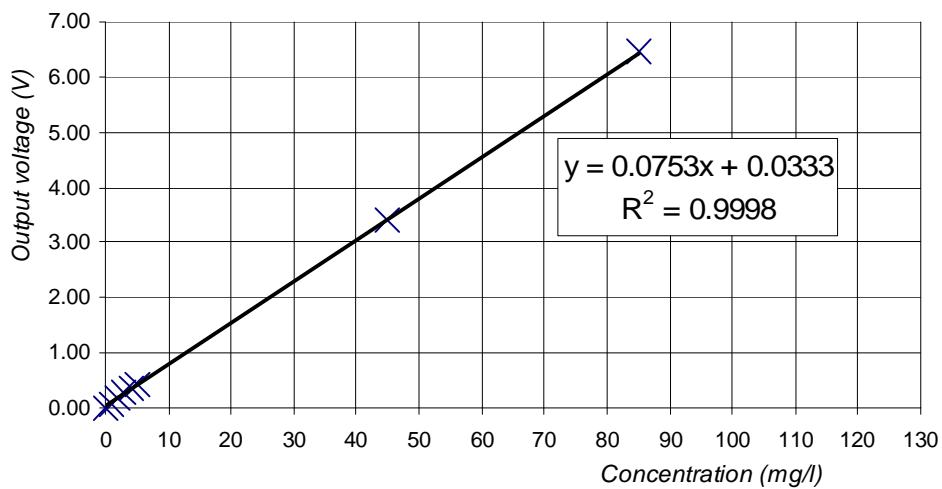


Figure N.5: First re-calibration OPCON2

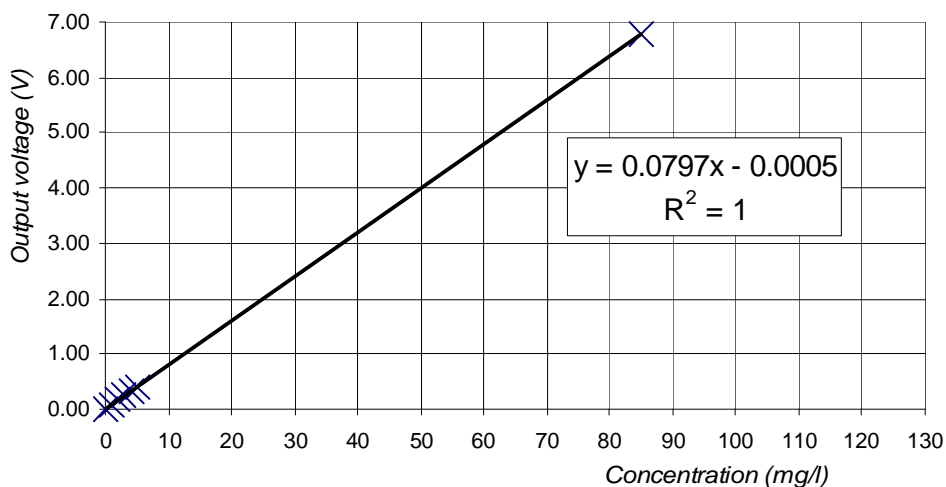


Figure N.6: Second re-calibration OPCON2

### Vortex divergence experiment

During the vortex divergence experiments only one OPCON (OPCON1) was used. Once a day the measurement apparatus was recalibrated, to make sure the measurements would not deviate. However, not every day suitable measurements could be taken, therefore only the calibrations of the days with correct measurements are represented here. It should be mentioned that the settings of the apparatus were different for the first calibration (20-4) compared to the others. Figure N.7 presents the calibration at 20-4, whereas N.8, N.9 and N.10 represent the calibration on 15-5, 16-5 and 21-5 respectively.

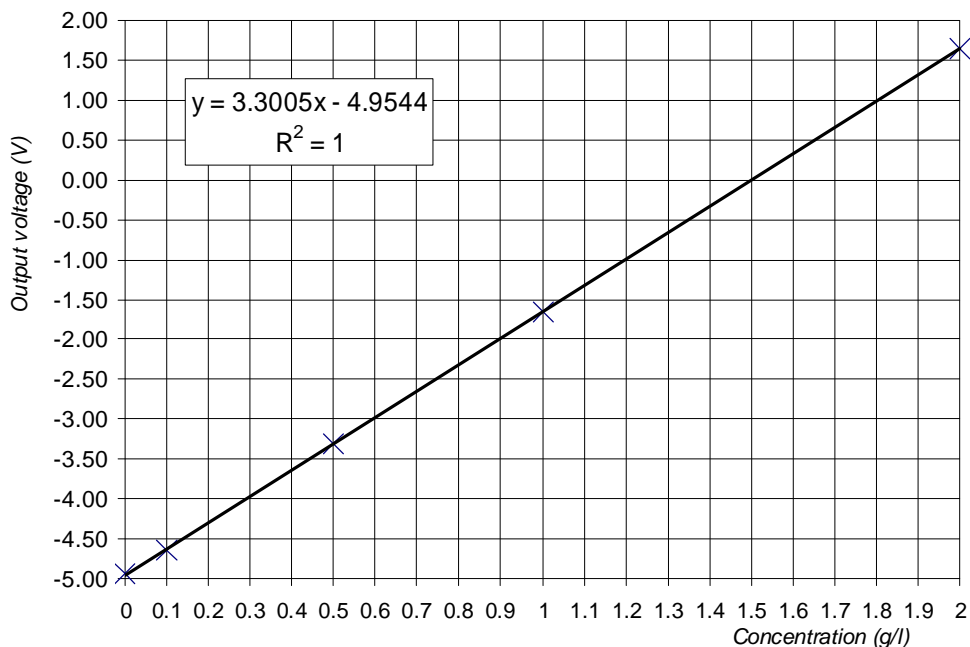


Figure N.7: Calibration OPCON vortex divergence (20-4)

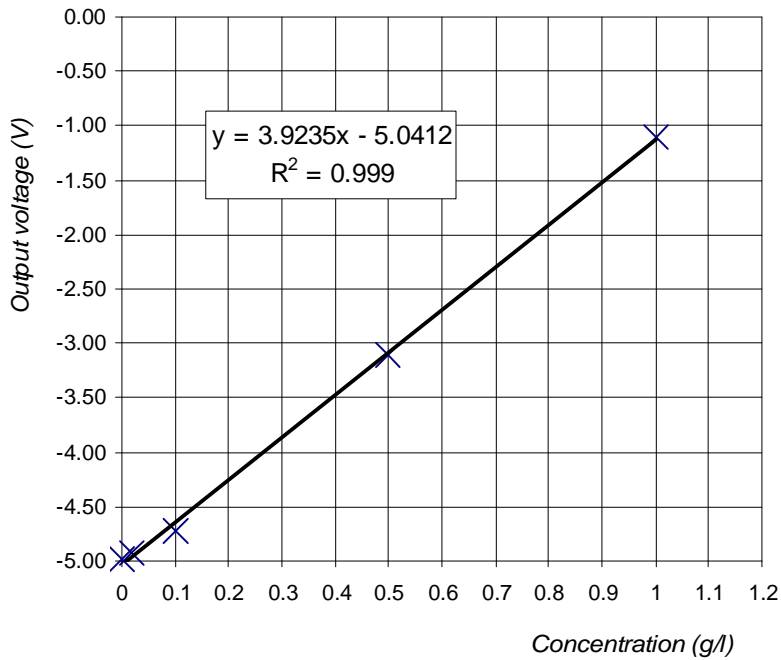


Figure N.8: Calibration OPCON vortex divergence (15-5)

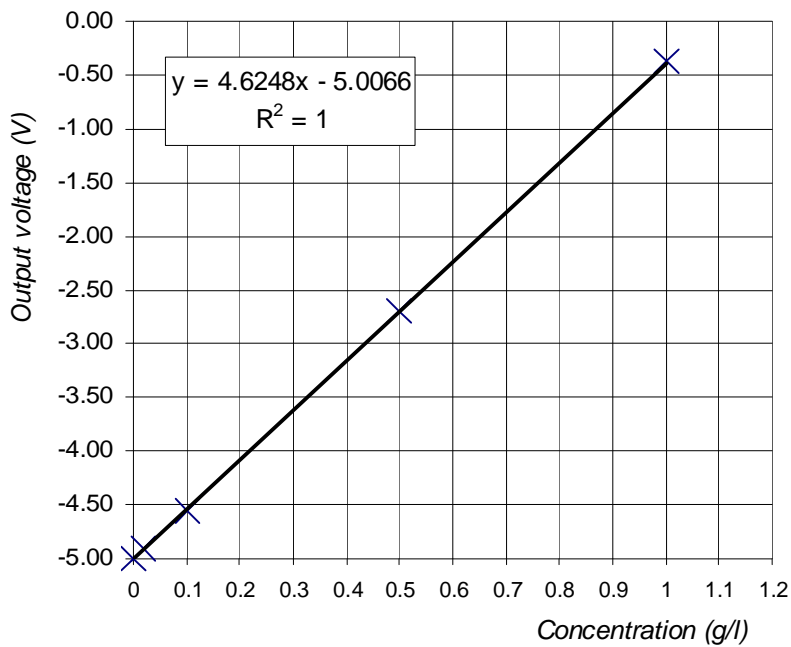


Figure N.9: Calibration OPCON vortex divergence (16-5)

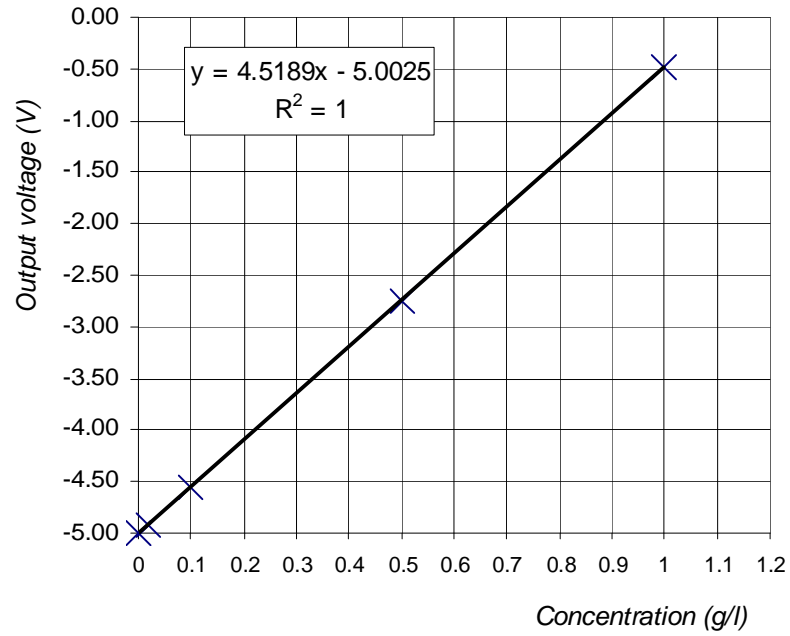


Figure N.10: Calibration OPCON vortex divergence (21-5)

## Appendix O: OSLIM calibration curves

In chapter F, part F.6 the calibration of the OSLIM concentration meters is discussed. Here all the calibration curves of the OSLIM are presented. The OSLIM concentration meters were only used in the stripping experiment and after a few tests it was known that their results would not be used further. Therefore only the main calibration and one re-calibration are carried out. In figure O.1 and O.2 the results are presented for OSLIM1 and in figure O.3 and O.4 the results of OSLIM2 are presented.

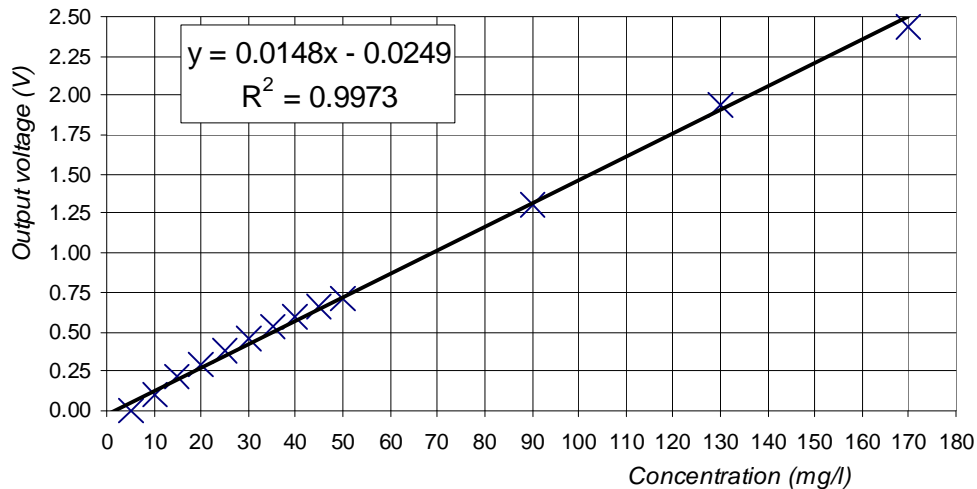


Figure O.1: Main calibration OSLIM1

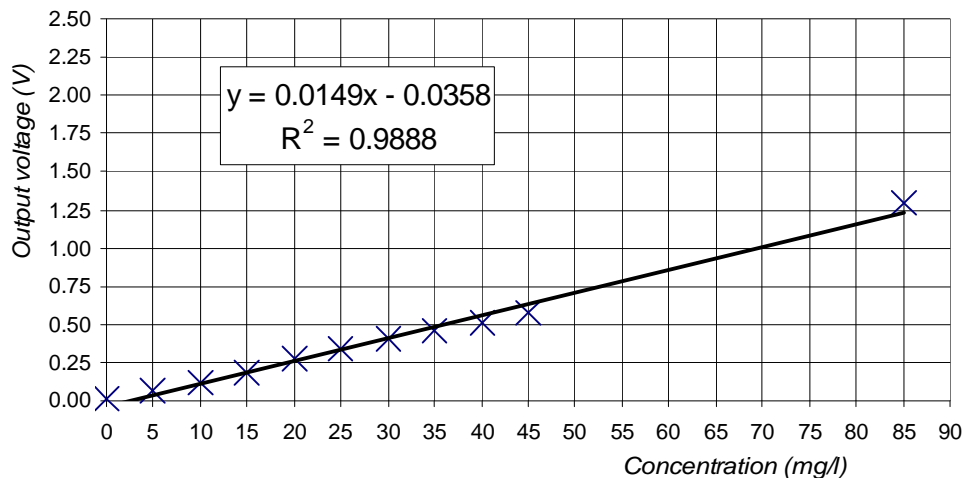


Figure O.2: Re-calibration OSLIM1

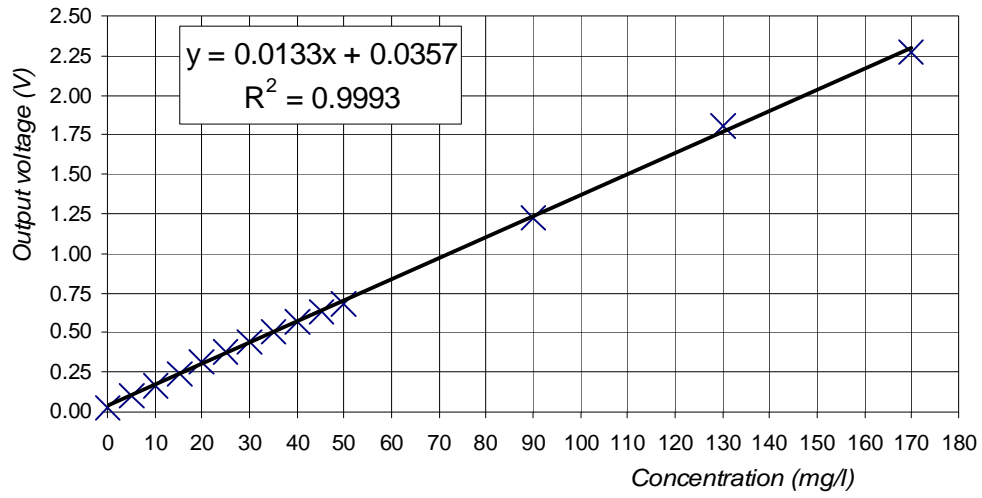


Figure O.3: Main calibration OSLIM2

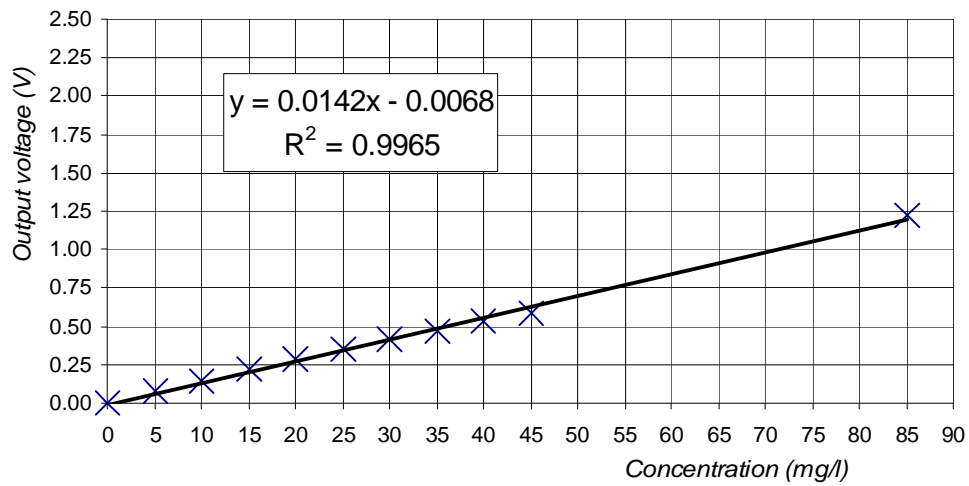


Figure O.4: Re-calibration OSLIM2

## Appendix P: Siphon calibration graphs

In Appendix G, part G.2 the calibration of the siphons used in the experiment is discussed. Due to the fact that the siphons were adapted regularly, the siphons were also calibrated several times. Other siphons were used in the stripping experiment and in the vortex divergence experiment. Therefore these two experiments are treated separately

### Stripping experiment

In the stripping experiment it was thought to use 4 siphons with a diameter of 3, 4, 5 and 6 cm respectively. These pipes were calibrated four times: after building the siphon, after implementing the flanges, after implementing the flanges with mixture and after implementing the straight-lining straws. Since only the last design with straight-lining straws was used in the experiment, only these calibration graphs are presented here as figure P.1, P.2, P.3 and P.4 for the siphons with a diameter of 3, 4, 5 and 6 cm respectively.

Since these siphons were too large for the experimental setup in the flume (see chapter 5, part 3.2), another siphon with a diameter of 1.2 cm was designed. This siphon was however never calibrated.

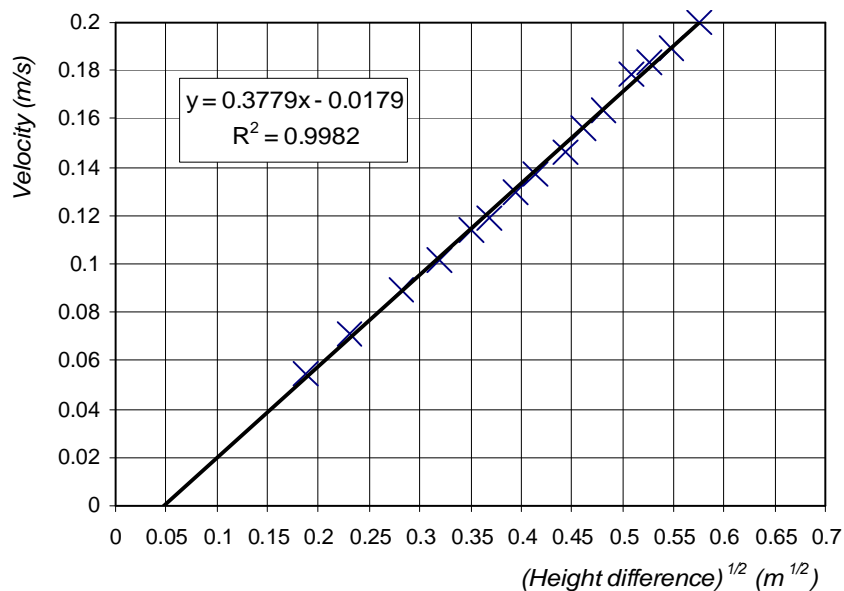


Figure P.1: Calibration graph siphon with diameter of 3 cm

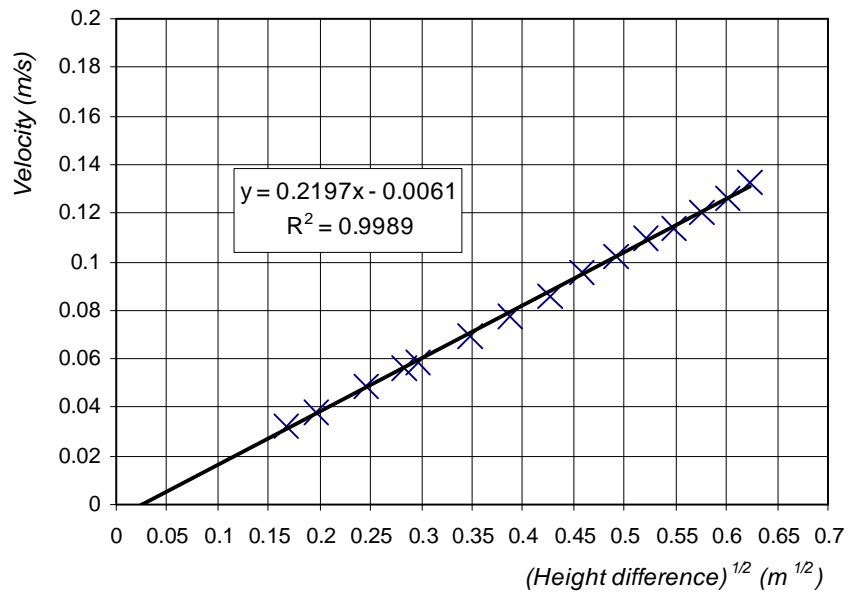


Figure P.2: Calibration graph siphon with diameter of 4 cm

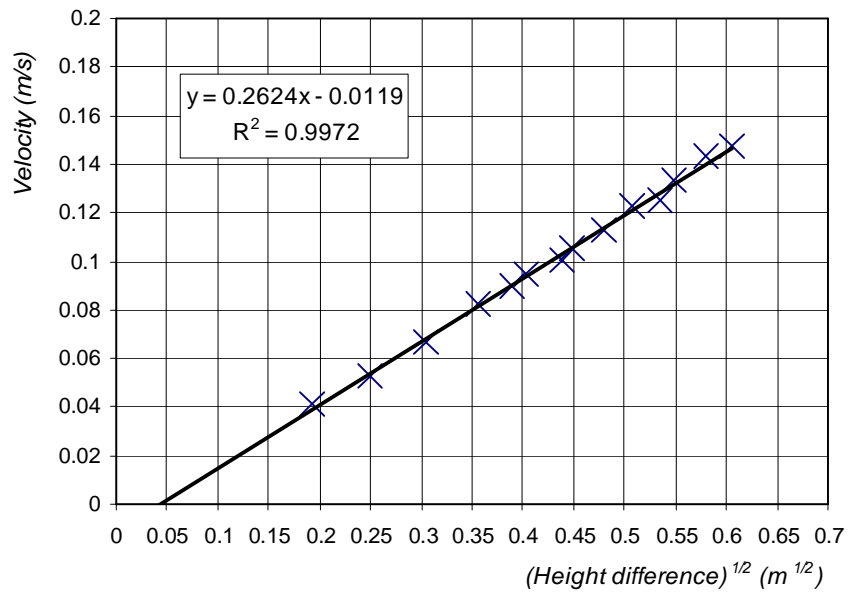


Figure P.3: Calibration graph siphon with diameter of 5 cm

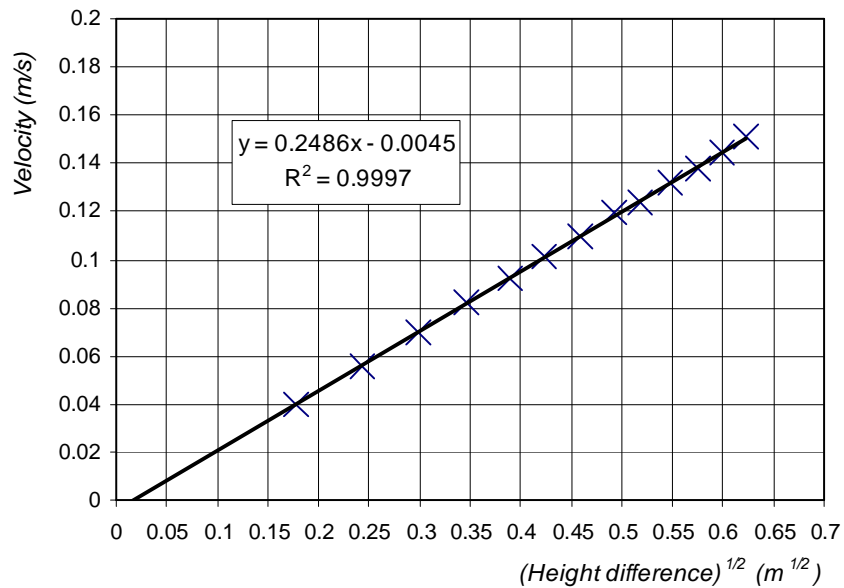


Figure P.4: Calibration graph siphon with diameter of 6 cm

### Vortex divergence experiment

In the vortex divergence experiment, only two siphons were used, which were both mounted on a boat. During calibration several adjustments were made to the siphons, to make sure a well functioning height-velocity relation was acquainted. Only one calibration graph for each siphon was worked out completely and is presented here in figure P.5 and P.6 for the siphon with a diameter of 0.4 cm and 1.0 cm respectively.

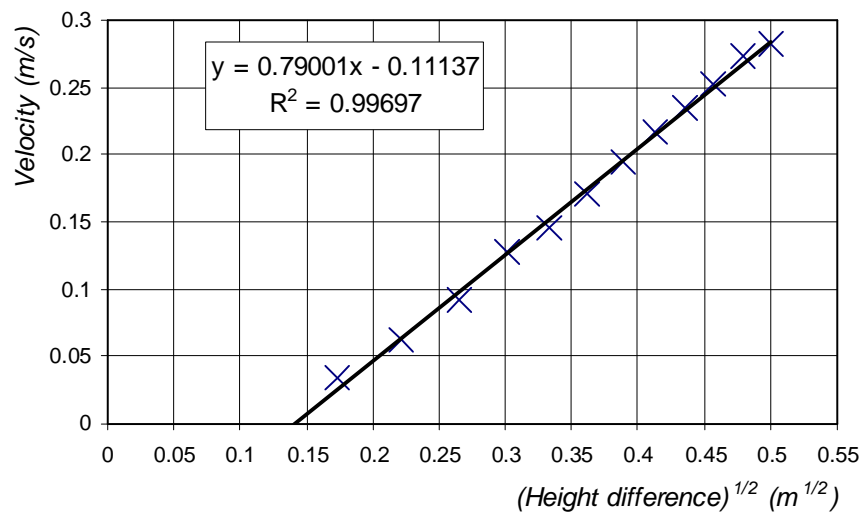


Figure P.5: Calibration graph of siphon with diameter of 0.4 cm

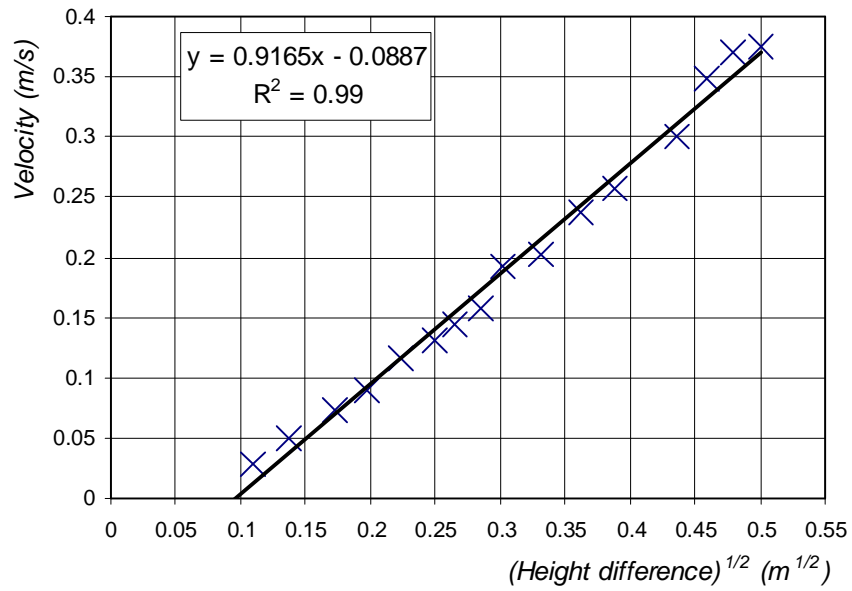


Figure P.6: Calibration graph of siphon with diameter of 1.0 cm